The analysis of oxysterols by capillary liquid chromatography tandem mass spectrometry

A thesis submitted in partial fulfilments of the requirements for the degree of

Doctor of Philosophy

KERSTI KARU

Department of Pharmaceutical and Biological Chemistry

The School of Pharmacy

University of London

April 2009

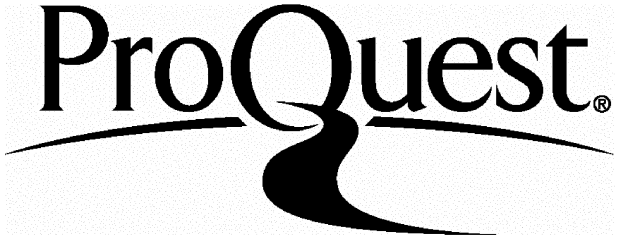

Plagiarism Statement in Thesis

This thesis describes research conducted in the School of Pharmacy, University of London between November 2003 and March 2009 under the supervision of Professor William J Griffiths and Dr. Mire Zloh. I certify that the research described is original and that any parts of the work that have been conducted by collaboration are clearly indicated. I also certify that I have written all the text herein and have clearly indicated by suitable citation any part of this dissertation that has already appeared in publication.

Kersti Karu — 06/04/2009

Signature — Date

Abstract

Oxysterols are oxygenated metabolites of cholesterol. They are present in very low concentrations in mammalian systems, always accompanied by high excess of cholesterol. Therefore, their analysis can be challenging. The traditional method for the analysis of sterols is by gas-chromatography (GC)-mass spectrometry (MS), however the absence of molecular ions in GC-MS spectra, can make the identification of novel oxysterols difficult. A capillary liquid chromatography multi-stage fragmentation mass spectrometry (cap-LC-MS^n) methodology has been developed for the identification, with high sensitivity (0.8 pg on-column) and specificity of oxysterols in mammalian central nervous system (CNS), and cortical neurons. Oxysterols were extracted with ethanol, separated from cholesterol by straight-phase chromatography, 3β-hydroxysterols were oxidised with cholesterol oxidase to their corresponding 3-ketones, which were then derivatised with Girard P (GP) hydrazine. The oxidised/GP-derivatised oxysterols were separated by reversed-phase LC, and ES-MS, -MS^2, -MS^3 were recorded to allow their characterisation. Forty authentic reference sterols were oxidised, GP-derivatised, and analysed by cap-LC-MS^n. The identification of sterols in tissues/cells was based on comparison of their retention time, MS^2, MS^3 spectra with authentic standards. Twenty four sterols were identified in rat brain. 24S-Hydroxycholesterol was confirmed as a major oxysterol (17-24 μg/g). 24S-Hydroxycholesterol is biosynthesised exclusively in brain by the action of CYP46A1, other oxysterols identified in brain tissue included 24,25-, 24,27-, 25,27-, 6,24-, 7α,25-, and 7α,27-dihydroxycholesterols. Nineteen sterols were identified in three regions of embryonic (E11) mouse CNS. Hydroxycholesterols were expressed at low levels (estimated 4-165 ng/g) in the developing CNS, including 24S-hydroxycholesterol. 24S,25-Epoxycholesterol was present at relatively high levels, suggesting that the mevalonate pathway is significantly active at E11. Seventeen sterols were identified in rat cortical neurons, including 24S,25-epoxycholesterol. The methodology was further evaluated for the prenatal diagnosis of Smith-Lemli-Opitz syndrome (SLOS) by measuring sterols in amniotic fluids and blood spots from SLOS affected patients. In conclusion, the profiling of oxysterol/sterol levels may offer important information for a better understanding of neurodegenerative disorders and to diagnose disease.

Dedicated to All My Teachers

Acknowledgments

This work could not have been done without all the support and encouragement from family, my supervisors and colleagues over the years, and I would like to express my sincere gratitude to them. I have been extremely fortunate to have excellent supervisors, outstanding scientists. I would like to thank Professor William J Griffiths for accepting me as a student and sharing his great knowledge in chemistry and mass spectrometry, teaching how to solve biological problems using mass spectrometry. Thank you for all fascinating talks on mass spectrometry, and all your kindness and patience over the years. Your endless good spirits made the mass spectrometry group at the SOP a great working place. Thank you for providing excellent working facilities and instrumentation. Professor Laurence H Patterson and Professor David Thurston I would like to thank for accepting me for the PhD training, for their encouragement and support over my part-time PhD training. I am highly indebted to Dr. Yuqin Wang for teaching all aspect of scientific research especially on mass spectrometry and LC, for passing her practical skills and for all the advices, ideas and suggestions. Special thanks to Dr. Gary Woffedin and Dr. Martin Hornshaw at ThermoScientific for analyses of brain samples on Orbitrap, and Dave Sectrett for LCQ advice. Dr. Mire Zloh. Thank you for giving freely of your time and passing knowledge in analytical chemistry. Above all thank you for being the one to ask and taking an interest in all matters. Sincere thanks to Dr. Andrew F Wilderspin for letting me use his laboratory for the extraction of lipids and helpful advice. Thank you to Emmanuel Samuel for getting me started on LC-MS and for all help and support; to Dr. Sonia Nisar & Dr. Catherine Lane for the introduction to the LCQ. Thank you to Dr. John Turton for providing brain samples, Gunvor Alvélius for introducing me to the lipid extraction, Dr. Colin James for all the help with computers, and to all the members of Prof. Ann Stephenson laboratory for letting me share the centrifuge facility and being so friendly to me. Thank you to Mazlina, Shilbe, Christina, Marina, Ahmed, Amar and Andrea for being always supportive and for contributing to the nice atmosphere in the lab. Everyone else in the lab past and present members that interacted with me and had the pleasure and the pain to spend together the PhD-time: Sybille, Cathrin, Richard. **A Big Thank you to All at the School of Pharmacy.**

Table of Contents

List of Figures

List of Tables

List of Abbreviations

7-DHC	7-dehydrocholesterol
8-DHC	8-dehydrocholesterol
Aβ	amyloid beta
ac	alternating current
ACAT	acylCoA:cholesterol acyltransferase
APCI	atmospheric pressure ionization
BBB	blood brain barrier
BPI	base peak chromatogram
°C	degrees Celsius
Cap-LC	capillary liquid chromatography
Cap-LC-MS	capillary liquid chromatography coupled to mass spectrometer
C_{18}	reversed phase
CID	collision induced dissociation
cm	centimeter
CHO	treatment with cholesterol oxidase
CNS	central nervous system
CYP	cytochrome P-450
CYP27A1	sterol 27-hydroxylase
CYP46A1	cholesterol 24-hydroxylase
CYP7A1	cholesterol 7α-hydroxylase
CYP7B1	oxysterol 7α-hydroxylase
Da	Dalton
DHCs	dehydrocholesterols
dc	direct current
DNA	deoxyribonucleic acid
E11	embryonic stage of the development day 11
EI	electron ionisation
ES	electrospray
ER	endoplasmic reticulum
f	femto (10^{-15})
g	grams
GC	gas chromatography
GC-MS	gas chromatography mass spectrometry
GP	Girard P
h	hour
HDL	high density lipoproteins
HMG-CoA	3-hydroxy-3-methylglutaryl coenzyme A
HPLC	high performance liquid chromatography
Hz	hertz (cycles per second)
Insig	insulin-induced gene

id	inner diameter
L	liter
LDL	low density lipoproteins
LC-MS	liquid chromatography mass spectrometry
LIPID MAPS	lipid metabolites and pathways strategy
LXR	liver X receptor
MALDI	matrix assisted laser desorption ionisation
m	milli (10^{-3})
mL	milliter
µ	micro (10^{-6})
MS^n	tandem mass spectrometry or multi-stage fragmentation mass spectrometry
MS^2	MS/MS
MS^3	MS/MS/MS
m/z	mass-to-charge ratio
Nano	nano (10^{-9})
Nano-ES	nano electrospray
Nano-ES-MS	nano electrospray mass spectrum
p	pico (10^{-12})
ppm	parts per million
RA	relative abundance
RF	radio frequency
RIC	reconstructed ion chromatogram
RRT	relative retention time
RP-HPLC	reversed phase HPLC
P-450	cytochrome P450
s	second
SCAP	SREBP-escort binding protein
SIM	selected ion monitoring
SREBP	sterol regulatory element binding protein
SRM	selected reaction monitoring
SLOS	Smith-Lemli-Opitz syndrome
SPE	solid phase extraction
TIC	total ion chromatogram
TOF	time of flight
TOF-MS	time of flight mass spectrometry
TLC	thin layer chromatography

Chapter 1

Introduction

1.1 Global and targeted metabolomics

Sequencing of the human genome has provided the possibility of building a comprehensive picture of the cell. There has been significant development in the fields of genomics, transcriptomics, proteomics and metabolomics. Genomics looks at the genome that is the entire collection of the genes of an organism. Similarly transcriptomics looks at the transcriptome that is the complete set of mRNA transcripts, and proteomics looks at the proteome that is the expressed set of proteins that are encoded by the genome [1,2]. In the same manner, the metabolome can be defined as the complete set of small molecules (non-polymeric compounds with a molecular weight <1,000 Da) that are involved in general metabolic reactions and that are biosynthesised by a cell, tissue, or organism. The transcriptome, proteome and metabolome are characterised by dynamic changes because of their sensitivity to genetic or environmental changes [3]. In summary the genome is what might be expressed, and the proteome is what is actually expressed, the metabolome is what is done and represents the current status of biological system.

The elucidation of the metabolome is particularly challenging because of the diverse chemical nature of the small molecules. The metabolome is based on small molecules that are very diverse in their structures and properties. There are two conceptually different branches to metabolomic research [4]. The first often referred to as "global metabolomics", can be defined as the dynamic, qualitative and quantitative analysis of the metabolome under a given set conditions [4,5]. To compile a complete metabolome is still an important challenge. The second concept is "targeted metabolomics", where analytical methods are designed to identify and quantify small molecules of a particular class in an unbiased fashion [4]. In the field of lipid analysis, this approach was adapted by the Lipid Metabolites And Pathways Strategy (LIPID MAPS) consortium in the USA [6], The European Lipidomics Initiative (ELIfe) [7] and the LipidBank in Japan [8]. Lipids are broadly defined as any fat-soluble molecules which include a wide range of molecular structures. Lipids can be broadly classified in eight classes: fatty acyls, sterol lipids, prenol lipids, saccharolipids, polyketides, sphingolipids, glycerolipids, and

glycerophospholipids [9,10]. Due to the structural diversity in lipid classes, it is not possible to accommodate all classes with a common method of extraction, chromatography and detection. The full identification of species in these classes therefore remains a challenging task, especially considering the fact that some lipid species are present in low abundance [4,11]. An alternative term for "targeted metabolomics" is "metabolite profiling" [4], and this approach was adapted for the profiling of oxysterols in biological matrices in this work.

Mass spectrometry (MS) is the most widely used technique for metabolite profiling [12,13]. The main advantages of MS are its abilities to separate and characterise charged ionised analytes in the gas phase according to their mass-to-charge ratios (*m/z*). It can also provide structural information by fragmenting the analyte ions. The various techniques used to record these fragmentation reactions are called tandem MS, or MS/MS or MS^n, and are described later in this chapter. These features lead to unparalleled selectivity, sensitivity and the ability to provide structural information for components in complex mixtures. This tool is utilised in this work for characterisation of novel, and identification of known cholesterol metabolites in biological material. The fundamental metabolomic work-flow includes:- sampling, an extraction step, followed by some form of separation, then analysis by mass spectrometry (MS) [by direct infusion MS and liquid chromatography (LC)-MS], and the final step is data analysis (see Figure 1.1).

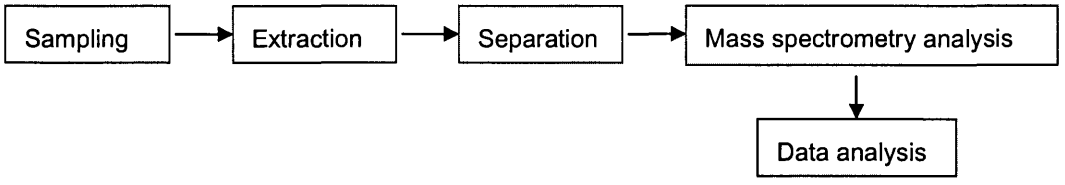

Figure 1.1 Work-flow in metabolomic approach for the analysis of sterols from biological samples.

1.2 Sample preparation

The detection and analysis of sterols in cells, tissues and biofluids poses a significant technical challenge due to their often low concentrations, varied polarity and presence in complex mixtures. Therefore, analysis of complex mixtures is simplified by appropriate isolation procedures. These procedures involve an extraction of lipids, and fractionation into lipid classes.

This brings sterols into a format that is compatible with liquid chromatography and mass spectrometry analyses. In terms of "targeted metabolomics", the sample preparation described in this work is tailored for oxysterols [14]. The first step in all analytical methods is organic solvent extraction of sterols. Deuterated internal standards can be used to monitor the extraction procedure. Traditionally steroids are analysed, after extraction and fractionation, by gas chromatography (GC) [15-17], high performance liquid chromatography (HPLC) [18], gas chromatography/mass spectrometry (GC/MS) [12,14,19-24], and electrospray ionisation (ES) liquid chromatography/mass spectrometry (LC/MS) [25-30]. The following section briefly reviews sample preparation procedures prior to mass spectrometry analysis.

1.2.1 Extraction of lipids from tissues

Most methods of lipid isolation from biological samples exploit their solubility in organic solvents [6,13,14,31,32]. The two main structural features of lipids controlling their solubility in organic solvents are hydrophobic hydrocarbon chains or other aliphatic moieties and any polar functional groups, such as hydroxyl groups, which are markedly hydrophilic. For example, cholesteryl esters are very soluble in hydrocarbons such as hexane, and also in moderately polar solvents such as chloroform, whereas oxysterols dissolve readily in ethanol.

Oxysterols are present in low abundance amongst a matrix of other lipids, including phospholipids and cholesterol in mammalian systems [31,33-37]. In order to extract lipids, it is necessary to use solvents that not only dissolve the lipids readily, but also overcome interactions between the lipids and the tissue matrix. It is essential to disrupt both the hydrophobic and polar interactions at the same time. Ethanol is considered as a good solvent for sterols because it readily penetrates cell membranes [4,14,31,38]. Alcohols are used either alone or in combination with other less polar organic solvents like acetone or chloroform. One of the more common methods for lipid extraction involves the addition of chloroform-methanol solution (2:1; v/v) to a biological tissue. The crude extract is then shaken and equilibrated with one fourth the volume of water [31], or better a dilute aqueous salt solution (e.g. 0.88% potassium chloride) as described in the classic paper by Folch, Lees and Stanley [39]. It is essential that the final ratio

of chloroform, methanol and saline solution be close to 8:4:3, by volume, to achieve most efficient transfer of lipids into the organic phase. The solvents then partition into two layers or phases, the lower consisting of chloroform-methanol-water in the ratio 86:14:1 (by volume) with an upper phase in which the proportions are respectively 3:48:47 [39]. The lipids remain in the chloroform-rich lower phase, while non-lipid components are in the upper layer. More than one extraction may be required but with most tissues the lipids are removed almost completely after two or three treatments [13,14,31,40]. The Bligh/Dyer method is a successful adaption of the above method that is especially suited to large samples with a high water content [40]. Bligh and Dyer [40] took into account the water already present in the samples when adding further water in the washing step. The Bligh/Dyer procedure is particularly suitable for lipid extraction of incubation media, tissue homogenates or cell suspensions. Modifications to these procedures have been made to maximise the ability to extract lipids of particular interest with high efficiency [10,31,32,41,42]. McDonald *et al.* in 2007 [41] has modified the extraction specifically for sterols. In this procedure ethanol is substituted for methanol, the tissue is homogenised in ethanol, following addition of chloroform and saline solution, and the water-chloroform-ethanol ratio is maintained as above. The disadvantage of this method it requires a precise separation of two immiscible layers. Lipid extraction with organic solvents is usually the first step toward sterol analysis, but a standard method for lipid extraction from biological samples has not been established yet. Therefore, results between research laboratories using different methods for lipid extraction may vary.

1.2.2 Saponification of lipid extracts

In biological tissues cholesterol and oxysterols exist free or esterified to long-chain fatty acids [34,41]. Sterols in human circulation are esterified to 70-75% [34], while essentially probably all sterol in the Central Nervous System (CNS) is unesterified cholesterol and is believed to reside in two pools: one is represented by the myelin sheaths and the other by the plasma membranes of astrocytes and neurons [33,43]. In order to estimate the total oxysterols it is therefore necessary to hydrolyse the esterified oxysterols during the sample preparation.

Several methods have been proposed: alkaline hydrolysis (saponification), enzymatic hydrolysis and transesterifcation [31,34]. Saponification is probably the most common procedure. In this work, the aim was to identify the oxysteryl esters. Our saponification procedure was as follows:- after homogenation of brain in ethanol, cholesterol and sterols of similar polarity were separated from oxysterols using a straight phase column, where cholesterol and more hydrophobic sterols elute with hexane-dichloromethane (Fraction U1), while oxysterols elute in ethyl acetate (Fraction U2). Fraction U1 was dried down, and hydrolysis solution was added. Hydrolysis reagents were prepared immediately prior to use. Now free sterols were subjected to further purification steps before LC-MS analysis as shown in Figure 2.4, the route UB1.

1.2.3 Preliminary fractionation of lipid extract. Purification by solid phase extraction (SPE).

Solid phase extraction (SPE) is used to extract sterols from crude lipid mixtures prior to LC-MS analysis in this work. Crude lipid extract contains steryl esterss, mono-, di-, and triacylglycerols, phospholipids, all of which are all strongly retained on reversed phase HPLC columns, and accumulation of these compounds on the LC column can lead to changes in retention time, decreased resolution, and increased back pressures.

From a general point of view, the principles of SPE are the same as HPLC. Generally, chromatographic methods utilise differential solubility and adsorption of compounds at the interface of a stationary and mobile phase. It exploits differences in the polarity of the matrix components and analytes to facilitate separation. The extractive solid phase consists of small porous particles of silica which in the reversed phase mode have a bonded organic outer layer. Sterols can be isolated from other classes of lipids with the appropriate stationary phases and solvents. Oxysterols containing hydroxyl-, oxo-, or epoxy-groups can be separated from cholesterol, steryl esters and phospholipids by normal (or straight phase) chromatography. Cholesteryl esters are the least polar, phospholipids the most polar, and cholesterol and oxysterols have intermediate polarity. Sterols that have been retained by the solid phase particles can then be eluted by washing with an appropriate mobile phase.

Since the cholesterol concentration is several orders of magnitude higher than oxysterol levels in mammals [37,44], it is important to separate oxysterols from cholesterol early in the sample preparation procedure. This reduces the risk of artifactual oxysterol formation by autoxidation. Oxysterols are more polar than cholesterol (Figure 1.13). The separation of the bulk of cholesterol from oxysterols might be achieved by choosing conditions so that oxysterols are retained on a normal (straight) phase SPE column while the bulk of cholesterol passes straight through, or conversely by allowing oxysterols to elute through a reversed phase column while the bulk of cholesterol is retained. The separation can be achieved by choosing appropriate solvents for washing and elution of oxysterols from the stationary phase.

In SPE or HPLC of lipids, normal- and reversed phase modes are primarily used. Separation in the reversed-phase mode is mainly by partition chromatography, whereas separation in the normal phase mode is primarily by adsorption chromatography [13,14,45,46]. Normal phase SPE or HPLC is used for the separation of the lipids into their respective classes. Reversed phase SPE or HPLC, on the other hand, is mainly used to separate each lipid class into individual species [46]. Reversed phase SPE consists of a non-polar stationary phase (e.g. ODS or C_{18}), and an aqueous, moderately polar eluting mobile phase (e.g. water-methanol). In reversed phase chromatography of lipids, the lipophilic interaction between the octadecyl chains of the column and the hydrophobic site of the analyte determines the retention, the more polar the sterol analyte, the lower the retention. Elution of analytes is accomplished by choosing a solvent that will distrupt the van der Waals forces retaining the molecules on the stationary phase. Sample application is made in high aqueous organic solution.

The aim of this project was the development of selective and sensitive methods for the lipidomic profiling of oxysterols in the brain. The brain extract contains large amounts of various phospholipids and other non-polar components, which are fat-soluble compound. The formation of micelles or lipid aggregates is very likely to occur in a high aqueous solution. However, a SPE method with reversed phase columns can be used for the extraction of sterols from crude extracts of lipids by two approaches.

In the first approach, a crude ethanol brain extract is diluted with water to a 70% ethanol solution. This is desirable to ensure that oxysterols are dissolved in solution. The resulting solution is passed through the C_{18} SPE column. The non-polar lipids such as cholesteryl esters, triacylglycerols and cholesterol are retained on the stationary phase, while polar or conjugated sterols are found in the effluent. Griffiths *et al.* [47] used this first approach for the separation of oxysterols from cholesterol (and other lipids of lower polarity/hydrophobicity) present in plasma. Liu *et al.* [48] used this approach for the extracton of neurosteroids from brain extract.

The second approach is a "recycling" SPE method; by this method it is possible to apply oxysterols on SPE C_{18} columns in a solution of high organic content (70%). Liere *et al.* in 2004 [49] and Schumacker *et al.* in 2008 [50] showed in their work, on the measurement of pregnenolone and dehydroepiandrosterone in the brain, that when the lipid extract was deposited in 40% methanol on SPE C_{18} columns, lipids were only poorly dissolved and retained by the non-polar stationary phase. Therefore, they deposited lipid extract in 100% methanol, and used a "recycling" method, where steroids were successively retained on the C_{18} SPE columns in methanol-water mixtures of increasing polarity. After these sequential recycling, the different fractions were then stepwise eluted with solvent mixtures of increasing concentrations of methanol (decreasing polarity) [50]. Griffiths *et al.* [14,38] used an aqueous 70% methanol solution, and the "recycling" SPE method to deposit these oxysterols on the SPE C_{18} column. This novel recycling/elution procedure had been carefully validated by Griffiths *et al.* [38] using ^{14}C-labelled cholesterol. Radioactivity was found to be exclusively retained on the C_{18} SPE column, and then completely eluted with methanol [38]. In this work, brain (100 mg) was homogenised in ethanol (1 mL), centrifuged, the supernatant retained, and the residue extracted further with methanol-dichloromethane (1:1, v/v, 1 mL). The supernatants were combined and dried down, the residue was reconstituted in hexane-dichloromethane (2:8, v/v, 2 mL). This solution was applied to a Unisil (activated silicic acid) column (8 x 0.8 cm). Cholesterol and sterols of similar polarity were eluted with 80 mL of hexane-dichloromethane (2:8, v/v) Fraction U1 (see Figure 2.4, the route U1B), and oxysterols with 10 mL ethyl acetate, Fraction

U2 (see Figure 2.4, the route U2C). Oxysterols were then oxidised with cholesterol oxidase from *Streptomyces sp.* to convert 3β-hydroxy-5-ene and 3β-hydroxy-5α-hydrogen sterols to their 3-oxo-4-ene and 3-oxo equivalents, which were subsequently derivatised with Girard P (GP) hydrazine to sterol GP hydrazones. This resulting reaction mixture was in a solution of 70% methanol content, and was passed through a SPE C_{18} column using a recycling method. When more polar GP derivatised oxysterols were present in the mixture, they were eluted in the effluent. The effluent was collected, then diluted with water and was redeposited again on the same C_{18} SPE column. This process was repeated three times with stepwise increment of the water content until all oxysterols were deposited on the same SPE C_{18} column. After these sequential recycling, GP derivatised oxysterols were then eluted twice with 1 mL methanol, and the most hydrophobic sterols were eluted in a further 1 mL of chloroform-methanol (1:1, v/v) [38,51,52].

The separation of lipids according to their polarity can also be achieved by using a normal (or straight) phase SPE chromatography. The normal phase SPE chromatography utilises a polar stationary phase, and a non-polar mobile phase. Use of more polar solvents in the mobile phase will decrease the retention time of the analytes (e.g. sterols), while more hydrophobic solvents tend to increase retention times of the same analytes. Unmodified silica is the sorbent of choice for lipid fractionation, because a sample of lipid extract is applied to and eluted with organic solvents. Silicic acid (Unisil) is used in this work. The polar silanol groups present at the surface of the silica sorbent will more strongly absorb polar compounds such as phospholipids, rather than neutral lipids such as sterols. The retention of sterols and their elution times will depend on solvent polarity. A mixture of a non-polar solvent (e.g. hexane) with a polar modifier (e.g. dichloromethane) is used to control solvent strength and selectivity. The mechanism of retention is that analyte (e.g. sterols) and solvent molecules (e.g. hexane-dichloromethane, 8:2, v/v) compete for the adsorption "sites" on the silicic acid (Unisil) SPE column, the sterol molecules must first displace a solvent molecule. Sterol molecules with polar

functional groups or which are capable of hydrogen bonding, or polarisable molecules have a strong affinity for the silicic acid stationary phase (Unisil), and will be strongly retained.

Lund and Diczfalusy in 2003 [53] had resolved sterols containing more than one hydroxyl group from cholesterol using a 100-mg Insolute silica cartridge. The SPE column was pre-washed and loaded with lipids. Steryl esters were eluted from the column with 1 mL of hexane. Cholesterol and other mono-hydroxycholesterols were eluted with 8 mL of 0.5% isopropanol in hexane. Oxysterols were eluted next with 5 mL of 30% isopropanol in hexane. Eluates from each chromatographic step were dried under nitrogen, and reconstituted in 95% methanol in water for LC-MS analysis.

1.3 Mass spectrometry

Typically, a mass spectrometer is composed of four major sections: (i) an inlet (for sample introduction), (ii) an ion-source, (iii) a mass analyser, and (iv) a detector and a data system (Figure 1.2) [54-56]. Sample molecules from the inlet device are admitted to the ion source where they become ionised, then the ions are transported to the mass analyser, where they are separated according to their mass-to-charge ratio (*m/z*). The sample ions are then detected by an ion detection system that produces a signal proportional to the number of ions detected. The signal from the ion detection system is received, and amplified by the system electronics, and is then passed on to the data system for further processing, and a plot of relative ion abundances (the ion current or the number of ions) against *m/z* corresponds to a mass spectrum.

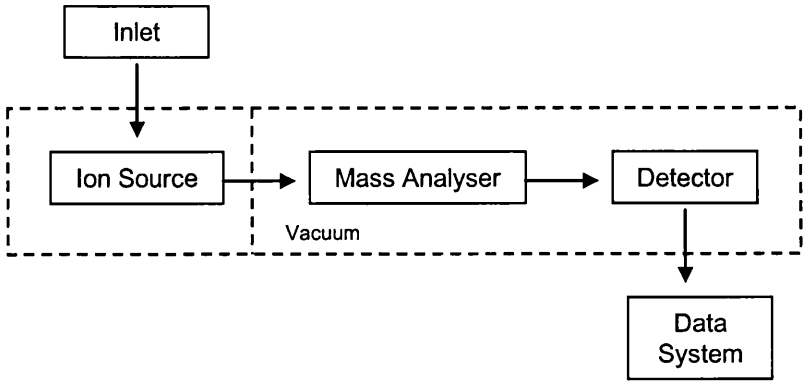

Figure 1.2. Schematic diagram of a mass spectrometer. The ion source may be under vacuum or at atmospheric pressure. The mass analyser and detector are always under vacuum.

A separating inlet device precedes the ion source in many cases. Therefore, complex mixtures can be separated prior to admission to the mass spectrometer. Today, the separating inlet device is usually either a capillary gas chromatography (GC) column or a high-performance liquid chromatography (HPLC) column, although capillary electrophoresis and thin-layer chromatography can be interfaced with mass spectrometry.

In the late 1980s, two "soft" ionisation techniques were developed for generating ions of intact biomolecules {electrospray ionisation (ES) and matrix-assisted laser desorption ionisation (MALDI)}. ES produces gas-phase ions from molecules in a solution, and is easily directly coupled to liquid chromatography (LC-MS). The theory of ES formation is described below. MALDI mass spectrometry, conversely, is a laser-based method mostly used for analysis of large proteins, but has been used successfully for sterols [14,57]. The sterol derivatised with Girard P reagent to introduce a charge to the analyte is mixed with a matrix, such as 2,5-dihydroxybenzoic acid, and applied to a sample holder as a small spot. A laser is fired at the spot, and the matrix absorbs the light energy with the result that analyte, and matrix become are ionised and vaporised.

The mass analyser is the main part of the mass spectrometer. The important characteristics of mass analysers are mass resolution, mass accuracy, mass range, sensitivity, linear dynamic range, speed and capability for MS/MS or MS^n, (n=2,3,4,...). MS/MS and MS^n are also called tandem mass spectrometry, where "tandem mass spectra" of fragment ions are generated from selected precursor ions. Instrument resolution (resolving power) dictates the ability to distinguish between two adjacent ions of closely different *m/z* [58,59]. Speed is the number of spectra acquired per unit time. Sensitivity can be expressed as abundance or detection sensitivity. Abundance sensitivity is the inverse of a quantity obtained by dividing the abundance of a large peak by the abundance of a background peak, whereas detection sensitivity is the smallest amount of an analyte that can be detected at a certain defined confidence level [54].

1.4. *The electrospray (ES) process*

An ES is produced by applying a strong electric field to a liquid passing through a capillary (Figure 1.3) [60-62]. The ES source forms an electrical circuit consisting of two electrodes. The first electrode is the capillary. The second electrode is the sample orifice of the mass spectrometer, also called the counter-electrode [54,61,63]. The capillary and the counter-electrode are separated by 0.3 - 1 cm (Figure 1.3) [63].

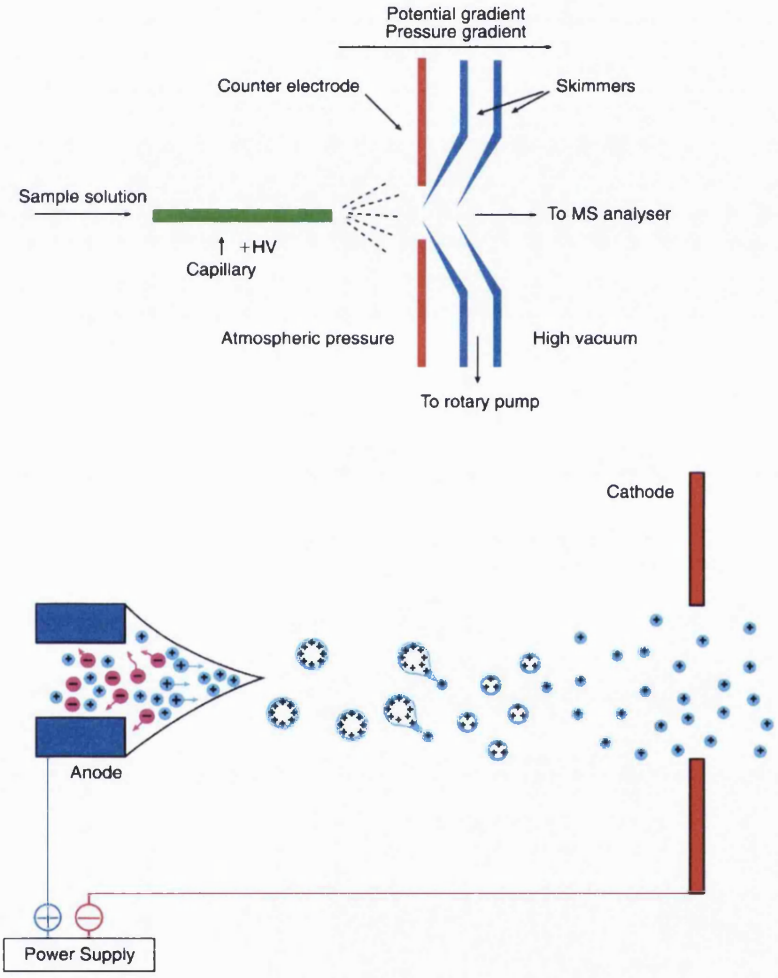

Figure 1.3. Schematic presentation of the ES process. In the positive-ion mode, a high positive potential is applied to the capillary, causing positive ions in solution to move towards the meniscus. Destabilisation of the meniscus occurs, leading to the formation of the Taylor cone and a fine jet, emitting droplets with excess positive charge [55,60,63]. Gas-phase ions are formed from the charged droplets by solvent evaporation and Coulomb fission cycles. With the continual emission of positively charged droplets from the capillary, to maintain charge balance, oxidation occurs within the capillary [60,63]. If the capillary is metal, oxidation of metal may occur at the liquid/metal interface: $M_{(s)} \rightarrow M^{n+}_{(g)} + ne^-$ (in metal); and negative ions may be removed from the solution by electrochemical oxidation: $4OH^-_{(aq)} \rightarrow O_{2(g)} + 2H_2O_{(l)} + 4e^-$(in metal) [63]. Reproduced from ref. [55].

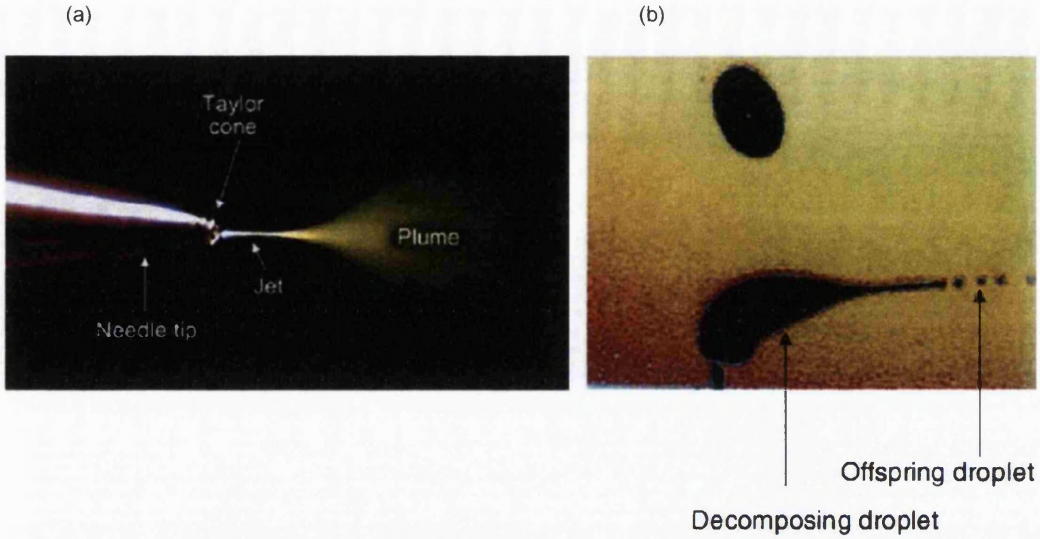

Figure 1.4. (a), and (b) The ES process, viewed through a high-powered microscope (left panel). In the positive-ion mode, a high positive potential is applied to the capillary (anode), and as the liquid exits the capillary it becomes charged and assumes a conical shape, known as the Taylor cone [60]. At the tip of the cone, the liquid is drawn into a filament, which then becomes unstable, breaking up into a mist of charged droplets. Since the droplets are charged they repel each other and fly apart. Gas-phase ions are formed from charged droplets in a series of solvent evaporation-Coulomb fission cycles. The droplet distorts, creating a miniature Taylor cone, and when the parent droplet reaches the Rayleigh limit, fission occurs. This leads to a string of multiple, small, highly charged offspring droplets. The critical point at which the surface tension of the droplet is overcome by the electrostatic repulsion of the surface charges is known as the Rayleigh stability limit. (a) is reproduced from ref. [55], and (b) from www.newobjective.com/electrospray/

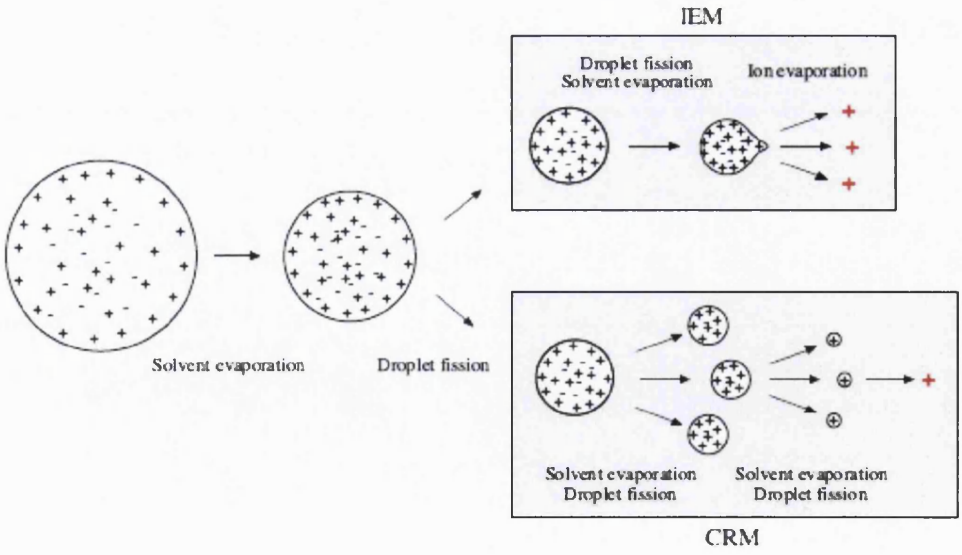

Figure 1.5. The two models for gas phase ions generation by ES process: the ion evaporation model (IEM) and the charge residual model (CRM). Reproduced from ref. [64].

To start the ES, a potential difference of a few kV is applied between the two electrodes. The optimal voltage depends on source geometry, sample flow rate, solvent, sprayer dimensions and position [62]. When a positive potential is applied to the capillary (anode), charge separation takes place in the capillary and negative counter-ions become discharged on the inner walls of the capillary, while the positive ions are repelled from the walls. The positive ions will start to drift towards the outlet of the capillary [63]. The repulsion between the positive ions on the liquid surface overcomes the surface tension of the liquid and the surface begins to expand allowing the positive charges and liquid to move downfield forming the Taylor cone (Figures 1.3 and 1.4a). If the applied field is sufficiently high, a fine jet emerges from the cone tip which breaks up into small charged droplets [63]. This happens at the Rayleigh stability limit, when electrostatic repulsion of the surface charge is equal to the surface tension of the solution [54,55,60,63]. The droplets are positively charged due to excess of positive ions on the surface of the liquid cone and the cone jet. The resulting charged droplets drift downfield through the air and travel down a pressure and potential gradient towards an orifice in the mass spectrometer's high-vacuum system (Figure 1.4). The counter electrode is held at a low potential. As droplets travel towards the counter electrode, they may pass through a heated capillary (180^0- 270^0) to allow solvent to evaporate as on a Thermo Finnigan LCQ^{duo} instrument [65]. The electrical charge density at the surface of the droplets increases as the droplet size decreases. Fission of the droplets occurs at the Rayleigh limit. The unstable droplet distorts into a teardrop shape and the resulting point of the drop emits a fine jet of very small offspring droplets (Figure 1.4b). These offspring droplets carry away only approximately 2% of the parents mass but some 15% of the parent charge [63].

Droplet fission followed by repeated evaporation and repeated droplet fission leads ultimately to gas phase ions by presumed two models (Figure 1.5). The charge residual (CRM) and the ion evaporation (IEM) models, both assume that gas phase ions are formed only from very small droplets [54,63]. The CRM proposes that gas phase ions result from a continuation of the Rayleigh explosions due to solvent evaporation causing large droplets to divide into many

smaller droplets until droplets containing only one analyte ion remain [54,63]. The IEM model assumes that the increased charge density that results from solvent evaporation causes Coulombic repulsion to overcome the surface tension of a droplet (Rayleigh stability limit), resulting in a fission of ions from droplet surfaces. The debate over which mechanism gas phase ions are formed is still an unresolved issue.

1.5. Mass analysis

Sample molecules are ionised by ES, and during this process, the analyte acquires a charge (unless it is pre-charged). The ion optics focuses and accelerates the ions into the mass analyser, where they are analysed and sorted according to their *m/z* ratios. Ions can be separated by electric fields, magnetic fields, or by measuring the time it takes an ion to travel a fixed distance in the mass analyser. Therefore, there are a number of different mass analysers used in lipidomic research, including the ion trap, quadrupole, time-of-flight (TOF), Fourier transform (FT) ion cyclotron resonance (ICR) and Orbitrap. They are diverse in terms of design and performance, and can be used as stand-alone instruments, or they can be coupled to form complex multi-stage instruments. The commonly coupled instruments include:- the quadrupole-ion trap [55,66,67], the quadrupole-time of flight (Q-TOF) and linear ion trap-Orbitrap [4,52,68-71]. The quadrupole-ion trap mass analyser used in this work and its operation is described in more detail below.

1.5.1 Scan modes in the ion trap mass analyser

The quadrupole-ion trap mass analyser is the site of mass analysis. The ion storage, ion isolation, collision induced dissociation (CID) steps are all performed in the ion trap [72-74]. Ions that are produced in the ion source can be mass analysed to produce a mass spectrum. Alternatively, by varying the voltages on the trap, the trap can first eject all ions except for the selected precursor ions, and then collide these ions with background gas that is present in the trap. The collisions of the selected precursor ions with the background gas can cause them to fragment into fragment ions. This process is called collision induced dissociation (CID). The fragment ions can then be mass analysed [54,65,72-74].

Each sequence of loading the ion trap with ions followed by mass analysis of ions is called a scan [72,75]. The ion trap can be run in different scan modes and different scan types to load, fragment, and eject ions from the mass analyser.

The number of stages of mass analysis is represented as multi-stage fragmentation (MS^n), where n is the scan power (each stage of mass analysis includes an ion selection step, n=2,3,4...). The following scan modes are utilised MS and MS^n in our work. The MS scan mode corresponds to a single stage of mass analysis (that is, a scan power of n=1). The MS scan mode involves only precursor ions, and no fragmentation of the precursor ions takes place. The MS scan mode can be a full scan experiment or a selected ion monitoring (SIM) experiment, see below for details on SIM. In the MS^n, for example, in an MS^2 scan, precursor ions are fragmented into fragment ions. A MS^2 scan can be a full scan experiment or a selected reaction monitoring (SRM) experiment, see details on SRM below.

1.5.2 Scan types in the ion trap mass analyser

The ion trap mass analyser can be operated in the following scan types: (i) full scan, (ii) selected ion monitoring (SIM), (iii) MS^n, (iv) selected reaction monitoring (SRM), and (v) zoom scan [65,74].

The full scan type provides a full mass spectrum of each analyte or precursor ion. With full scan, in the last step of mass analysis (the ion scan-out step) the mass analyser is scanned from the first mass to the last mass without interruption to generate a mass spectrum. Full scan type provides more information about the analyte than does SIM or SRM, however full scan does not provide the sensitivity that can be achieved by the other scan types. The full scan type includes:- (i) single-stage full scan, and (ii) multi-stage full scan [65,74].

The single-stage (MS) scan has one stage of mass analysis (n=1). With single-stage full scan type, the ions formed in the ion source are stored in the mass analyser. Then, these ions are sequentially scanned out of the mass analyser to produce a full mass spectrum. The single-stage MS scan is used to determine the molecular weights of sterols or the molecular weight of each component in a mixture in this work.

To use the SIM and SRM scan type the ions of interest should be known, and this type of scan is mostly used for quantitative analysis of compounds.

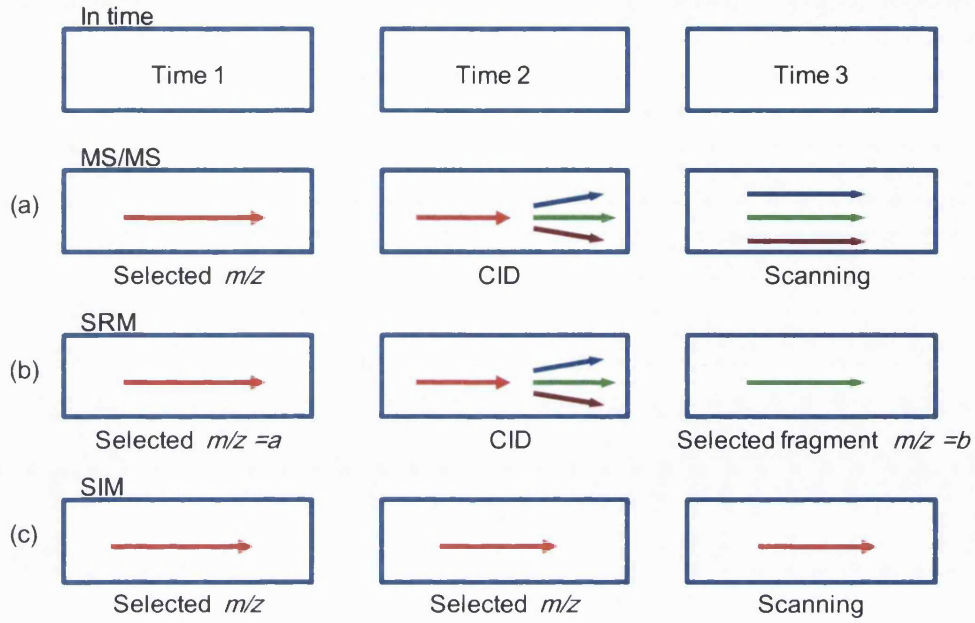

Figure 1.6 Main scan types performed by an ion-trap instrument.

The multi-stage fragmentation (MS^n) scans is used in this work to determine structural information about known and/or unknown sterols. In this type of scan, a packet of ions generated in the ion source is confined in the trap, the ion of interest is then held in the trap while all others are scanned out. The ion of interest is then activated by collision with helium gas present in the ion-trap. When sample ions and gas molecules collide with sufficient energy, the sample molecules start to fragment to produce one or more fragment ions. In the second stage of mass analysis, the fragment ions are stored in the mass analyser. Then they are sequentially scanned out of the ion trap to generate a full MS^2 (MS/MS) mass spectrum [4,55,65,68,74]. Figure 1.6a represents a simple MS^2 product ion scan performed, where the ion trap instrument consists of two mass separating events (MS_1 and MS_2) arranged in series in-time. MS/MS is usually taken to mean a product-ion scan. This specific experiment known as a MS^2 event and can be indicated as precursor mass → e.g. 534→. If necessary, one of the fragment-ions can be held in the ion trap, further activated, and its fragment-ions scanned out of the trap to generate a (MS^3) MS/MS/MS spectrum. This experiment is known as a MS^3 scan and can be written

precursor mass → fragment mass → e.g. 534→455→. Using appropriate collision energies, it is possible to fragment an ion to generate MS^2 and MS^3 spectra which provide detailed structural information. Therefore, the MS^n experiment offers the ability to compare acquired mass spectra to reference libraries for possible identification of unknowns.

The multi-stage full scan type gives more information about a compound than does SRM, but provides lower scan speed than SRM, as more time is spent monitoring a range of different fragment ions than in SRM. SRM is a two-stage (n=2) technique in which precursor ion, and fragment ion pairs are monitored (Figure 1.6b). In the first stage of mass analysis, the ions formed in the ion source are stored in the mass analyser. Ions of one *m/z* ratio (the precursor ions) are selected, and all other ions are ejected from the mass analyser [65]. Then, the selected ions are oscillated, and then collide with background gas that is present in the mass analyser. The collisions of the precursor ions cause them to fragment to produce one or more fragment ions. In the second stage of mass analysis, the fragment ions are stored in the mass analyser. Ions of one or more *m/z* ratios are selected, and all other ions are ejected from the mass analyser. Then, the selected ions are sequentially scanned out of the mass analyser to produce a SRM mass spectrum. Similar to SIM, SRM allows for the very sensitive analysis of trace components in complex mixtures. However, much structural information is lost, but because pairs of ions are only monitored (one fragment ion for each precursor ion), the specificity obtained in SRM can be much greater than that obtained in SIM.

Selected ion monitoring (SIM) is a single stage (n=1) technique, in which a particular ion or set of ions is monitored (Figure 1.6c). In the SIM scan type, the ions formed in the ion source are stored in the mass analyser. Ions of one or more *m/z* ratios are selected and all other ions are ejected from the mass analyser. Then, the selected ions are sequentially scanned out to generate a SIM mass spectrum [65,74]. SIM can improve the detection limit, but it can also reduce specificity, as only specific ions are monitored. Zoom scan is an enhanced resolution MS scan type which offer resolutions of 10,000 (FWHM) by scanning a short *m/z* range slowly. This type of scan allows the determination of the charge state and molecular weight of an ion [55].

1.5.3 The operation of the quadrupole ion trap mass analyser during mass analysis

The mass analyser consists of three stainless steel electrodes: the entrance and exit endcap electrode and one "donut-shaped" ring electrode [55,72,73]. The endcap electrodes are virtually identical and have hyperbolical geometry (Figure 1.7a). The ring electrode is located halfway between the two endcap electrodes and is also of hyperbolical geometry. Figure 1.7b shows a cross-section the ion trap [65,72-74].

Together, the electrodes form a cavity in which mass analysis occurs. Ions produced in the ES source enter the mass analyser cavity through the entrance endcap electrode. The exit endcap electrode is the closest to the ion detection system, and has a small hole in its centre, and ions can be ejected through the exit endcap electrode during mass analysis. Helium gas enters the mass analyser cavity through a nipple on the exit endcap electrode, and is present in the trap as a damping gas, and a collision activation partner [65,72,73,75].

A low direct current (dc) voltage is applied to the mass analyser electrodes to draw in ions from the ion optics. Ions of all *m/z* values enter the ion trap at the same time. Various alternating current (ac) voltages are applied to the electrodes to trap, fragment, and eject ions according to their *m/z* ratios [73]. These ac voltages are called RF voltage, waveform voltage, resonance excitation RF voltage, and resonance ejection RF voltage [65,73]. An ac voltage of constant frequency (0.76 MHz) and variable amplitude is applied on the ring electrode. The frequency of the ac voltage is in the radio-frequency (RF) range, and this voltage is referred to as the ring electrode RF voltage. The application of an RF voltage to the ring electrode produces a three-dimensional quadrupole field within the ion trap cavity. This time-varying field drives ionic motion in both the axial (toward the endcaps) and radial (from the ring electrode toward the centre) directions. Ionic motion must be stable in both the axial and radial directions for an ion to remain trapped and is related to *m/z* value of ions in the ion trap.

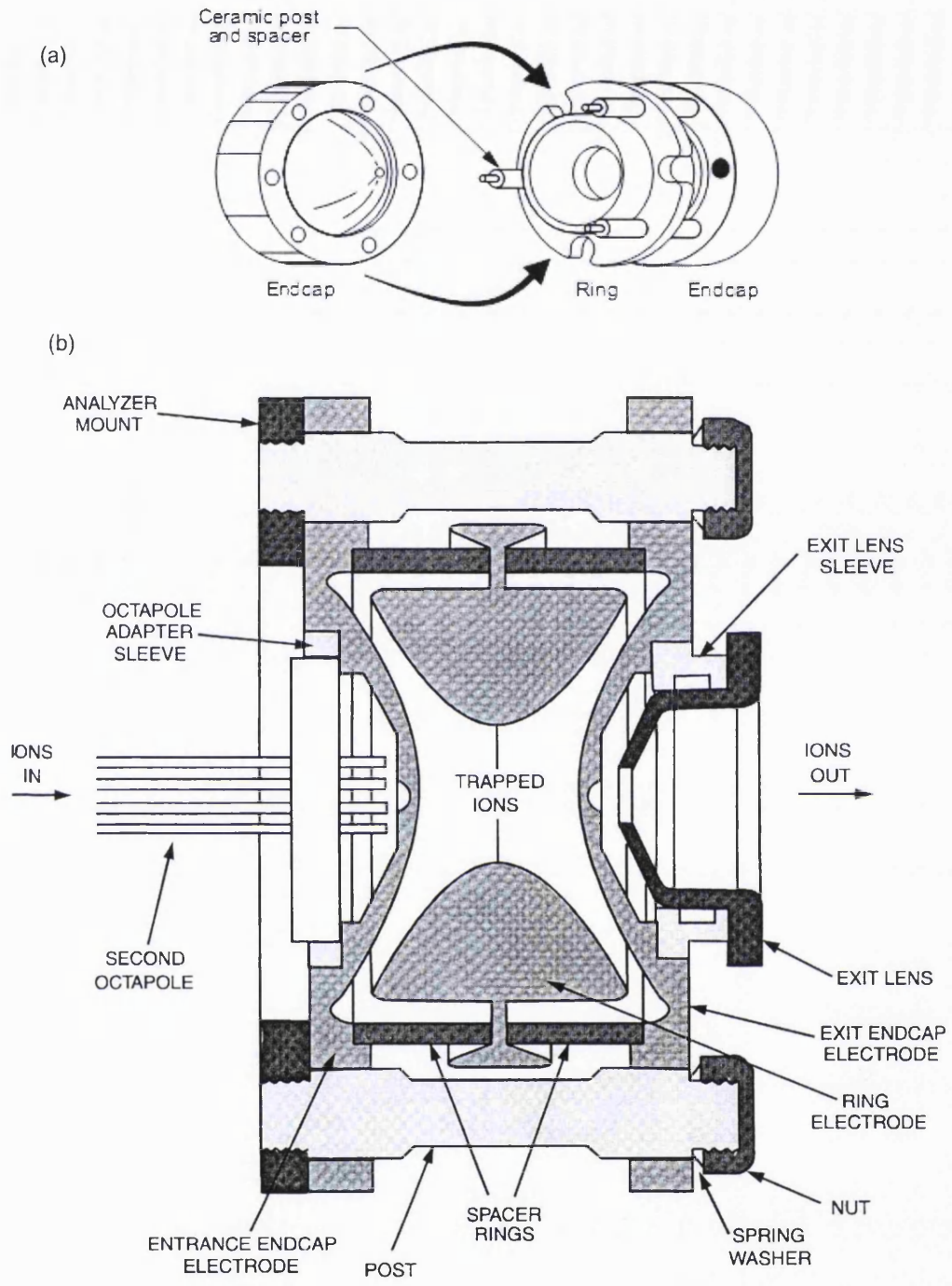

Figure 1.7 Schematic diagram of the LCQ^{duo} ion trap manufactured by Thermo Finnigan (now Thermo Fisher Scientific). (a) The ion trap consists of three electrodes with hyperbolic surfaces, the central ring electrode, and two adjacent end-cap electrodes. The schematic of the assembly shows how the electrodes are aligned and isolated using ceramic spaces and posts. The device is radially symmetrical, taken from [72]. (b) Cross section view of the LCQ^{duo} ion trap manufactured by Thermo Scientific. Reproduced from ref. [65].

Figure 1.8 shows a stable oscillatory trajectory of ions confined within the ion trap [58]. The collisions of the ions entering the ion trap with helium slow the ions so that they can be trapped by the RF field in the ion trap. These collisions reduce the kinetic energy of the ions, thereby damping the amplitude of their oscillations [72,73,75]. As a result, the ions are focused into the centre of the cavity rather than being allowed to spread throughout the cavity. During ion scan out, the system produces a mass-dependent instability to eject ions from the ion trap in the axial direction [65,72,73,75].

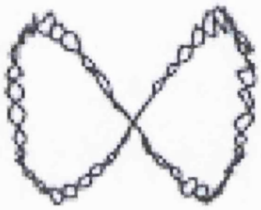

Figure 1.8 Oscillating figure of trajectory confined by ions in the ion trap. Reproduced from ref. [58].

When the amplitude of the ring RF electrode is low, all ions above a minimum *m/z* ratio are trapped. During the ion scan out, the ring electrode RF voltage is ramped at a constant rate. Ions of increasing *m/z* ratio become successively unstable in the axial direction as the ring electrode RF voltage increases, and are ejected from the ion trap. The voltage at which an ion is ejected from the ion trap is defined as its resonance voltage. Since the oscillating frequencies of the ions are a function of their mass, ions of different *m/z* values will exit the ion trap at different voltages and times [73].

The ion isolation waveform voltage, resonance excitation RF voltage, and resonance ejection RF voltage are ac voltages that are applied to the endcap electrodes to stimulate the motion of the ions in the axial direction [65]. The voltages applied to the endcap electrodes are equal in amplitude, but are 180° out of phase to one another. When the RF frequency applied to the endcaps is equal to the resonance frequency of a trapped ion, which depends on its *m/z* value, the ion gains kinetic energy. If the magnitude of the applied voltage is large enough, the ion is ejected from the ion trap in the axial direction [65].

The waveform voltage consists of a distribution of frequencies containing all resonance frequencies except for those corresponding to the ions to be trapped, and is defined as the ion

isolation waveform voltage [65]. This voltage acts during the ion isolation step of SIM, SRM and MS^n full scan applications. The ion isolation waveform voltage, in combination with the ring electrode RF voltage, ejects all ions except those of a selected *m/z* ratio.

During the collision induced dissociation step of SRM, and MS^n full scan applications, the resonance excitation RF voltage is applied to the endcap electrodes to fragment precursor ions into fragment ions. The resonance excitation RF voltage is not strong enough to eject an ion from the ion trap. Nevertheless, ion motion in the axial direction is enhanced and the ion gains kinetic energy. After many collisions with the helium damping gas, which is present in the ion trap, the ions gain enough internal energy to cause it dissociate into fragment ions. The fragment ions have different resonating frequencies from the precursor ion and therefore are dampened into the centre of the ion trap by the helium gas [65,73]. The fragment ions are then mass analysed. It is important to note that the minimum storage mass during collision induced dissociation is typically set to one quarter of the precursor ion *m/z* ratio.

During the scan out, the resonance ejection RF voltage facilitates the ejection of ions from the mass analyser and therefore improves mass resolution. The resonance ejection RF voltage is applied at a fixed frequency and increasing amplitude during the ramp of the ring electrode RF voltage. Only when an ion is about to be ejected from the ion trap cavity by the ring electrode RF voltage it is in resonance with the resonance ejection RF voltage [65,72,73]. When an ion approaches resonance, it moves further away from the centre of the ion trap, where the field generated by the ring electrode RF voltage is zero (and space-charge effects are strong), into a region where the field produced by the ring electrode RF voltage is strong (and space-charge effects are small). As a result, the ejection of the ion is facilitated.

Ion traps are fast scanning (1000 *m/z* units/s) mass analysers. A disadvantage of ion traps is their relatively low mass accuracy (100 ppm) in full scan, which is considerably lower than that achievable on beam instruments [55]. This is due to space charge effects, defined as changes in ion motion which result from the mutual Coulombic interactions of ions [72].

1.6. Direct infusion nano-electrospray mass spectrometry (nano-ES-MS) analysis

The proteomics community has demonstrated [56] that maximum sensitivity is achieved by combining low-flow-rate LC with nano-electrospray (nano-ES) MS [76,77]. For this application, nano-ES sources are designed to allow flow rates of less than 1 µL/min. These so-called nano-ES experiments can be performed on-line, coupled to nano-LC, or off-line, by spraying liquids from capillaries. The nano-ES-MS analysis without chromatographic separation is also called direct infusion nano-ES-MS. In this type of experiment, the spray capillary is loaded with approximately 1 µL of analyte solution, and the flow rate is maintained by the electrospray process without the need for a delivery device such as syringe pump. The capillary is coated with a conducting material to allow the supply of the high voltage to the tip. The spraying orifice of the capillary is about 5 µm internal diameter (i.d.) in this work, and is able to produce a stable electrospray signal with flow rates in the low nL/min range. There are several advantages of nano-ES-MS, which are:- compatibility with nano-LC, low sample and solvent consumption, increased sensitivity and spray stability. Because, low-flow ES capillaries will emit small droplets, which possess a higher surface-to-volume ratio, this enhances the desorption of ions into the gas phase.

After extraction, fractionation and enrichment steps samples can be analysed by direct infusion nano-ES-MS. However, mass spectrometers are incapable of separating isomers, and a single peak in the full mass spectrum can represent several isobaric sterols. In addition, MS/MS of precursor ions can generate a mixture of fragmentation patterns of several sterols making the identification process extremely difficult or impossible. Consequently, only a few sterols can be identified by direct infusion ES-MS. Therefore, online or offline separation of sterols prior to the mass spectrometry analysis is often used to reduce the complexity of sterol mixture.

1.7 LC-MS analysis

High performance liquid chromatography (LC) is a form of chromatography in which the mobile phase is forced under controlled high pressure through a relatively narrow bore column

containing a stationary phase. In general, liquid chromatography (LC) can separate cholesterol metabolites in a time dimension, potentially allows isomer separation, and provides additional information on the physico-chemical properties of eluting sterols. The development of technologies to couple LC and MS started in the early 1970s by the group of Tal'roze [46]. LC is performed with various size columns that range from 0.1 to 4.6 mm internal diameter [78]. The common types of columns and their characteristics are given in Table 1.1.

There are several ES interfaces which match with flow rates of the order of 5 - 100 µL/min, and which are most compatible with narrow bore or micro-bore columns [78-80]. It is possible to interface wide- or normal-bore LC columns to such ES interfaces, but with the requirement of a post-column split. A new generation of nano-ES or micro-ES interface has been developed, which perform optimally at low-flow-rates (< 1 µL/min). The benefit of ES is that this ionisation technique is a concentration rather than a mass dependent process, which effectively means that maximum sensitivity is achieved with high concentration, low volume samples, analysed at low flow rates (e.g. 1 pmol/µL, 1 µL, 1 µL/min) rather than with dilute, high volume samples, analysed at high flow rates (cf. 0.02 pmol/µL, 50 µL, 50 µL/min) [81]. This dictates that the combination of low-flow-rate LC with nano-ES-MS offers maximum sensitivity of analysis. Therefore, the combination of low-flow-rate LC with nano-ES-MS is the preferred method for sterol analysis [4,14,38,47,51,52,81-83].

Table 1.1 Classification of LC columns by column internal diameter.

Column	Dimensions (i.d, mm)	Flow rate, µL/min
Wide-bore (preparative)	>4.6	>3000
Conventional:		
Normal-bore (analytical)	3 – 4.6	500 - 2000
Narrow bore	1 -2	20 – 300
Capillary:		
Micro-bore	0.15 – 0.80	2 -20
Nano-bore	0.02 – 0.10	0.1 - 1

The chromatographic column packed with stationary phase constitutes the most critical component of the chromatography system. The key characteristics of the stationary phase include the support matrix (material, particle structure and pore structure) and the surface chemistry. The support matrix forms a skeleton of the stationary phase. The support matrix

provides the surface upon which functional groups may be attached which provide the chemical binding interactions enabling a separation to occur. The partical structure is a critical parameter for the chromatographic efficiency, and thus the resolution attainable in a given separation. Chromatographic media of spherical shape are greatly preferred. The two key characteristics of the particle structure are the average particle diameter and the particle size distribution. The pore structure of the stationary phase affects capacity. The pore diameter must be large enough to allow free access to all the internal surface area by molecular diffusion. In chromatographic packings, pores in the range of 60-150 ångströms (Å) are optimal for small molecules [46].

Reversed phase LC (RP-LC) is a widely used LC-MS method for the separation of molecular species of lipids within a single lipid class [13,14,31,45], and because mobile phases used in RP-LC are compatible with ES mass spectrometry analysis. By far the most widely used stationary phase consists of octadecylsilyl (C_{18}) groups, linked to a silanol surface by covalent bond, i.e (surface-Si)-O-$(CH_2)_{17}CH_3$. Other stationary phases of this type include bonded octanyl (C_8), ethyl (C_2) and phenyl groups [31]. These stationary phases are used in combination with aqueous-organic solvent mixtures (e.g. water mixed with a polar organic modifier, such as methanol, isopropanol, or acetonitrile). The chromatographic mechanism involves partitioning of sterols from the polar mobile phase to a non-polar stationary phase. High proportions of organic solvents are used for sterols separation on the RP-column, as sterols are hydrophobic by nature, they will interact strongly with the stationary phase. Increasing the strength of the eluting solvent enables elution of the more retained hydrophobic sterols.

A capillary LC system fitted with an analytical column consisting of C_{18} packing material of 180 µm internal diameter (i.d.), 3 µm particles, and 100 Å pore size interfaced through fused silica to a nano-ES source of a LCQ^{duo} ion trap mass spectrometer has been used in this work. The column is pumped with a mixture of two mobile phases of different polarities, which carry the sample into the column, and effect controlled partition/elution of different sample components at different times. During binding and elution, molecules from the sample move through the spaces between the packing particles at the same rate as the mobile phase.

However, the sterols also freely diffuse in and out of the packing particle pores, gaining access to the bonded phase surface. Some of the sterols will bind to the surface with greater or lesser strength. While inside the particles or bound to the surface, the sterols will not move down the column, or move more slowly. However, the mobile phase conditions can be changed, for example gradually (gradient elution) to weaken the binding interaction for the very tightly binding sterols, by increasing organic solvent in the mobile phase.

During a LC-MS (or direct infusion nano-ES-MS) analysis, the mass spectrometer could be programmed to scan, repetitively, over a specific mass range and a specified chromatographic time. The scan can be wide, as in the full scan type or can be selective as MS^2 or MS^3 scans. In this work, several different scans were programmed during the LC-MS run. At the end of each scan, the sum of the ion current intensities across the specified mass range, is computed and stored. Many scans are acquired during LC-MS analysis, in which all ions from each scan are summed and plotted as a function of time or the scan number, producing total-ion-current (TIC) chromatogram [65]. When, the mass spectrometer is programmed to acquire MS^2 (for example 534→) and MS^3 (534→455→) scans, at the end of LC-MS run, it is also possible to generate a total-ion-chromatograms (TIC) for a programmed transition (for example specific TIC for the transition 534→455→). A mass spectrum can be retrieved for any chosen scan number in the TIC chromatogram to provide qualitative identification of a compound. Therefore, RIC chromatogram shows the variation, with time, of a single ion with a chosen *m/z* value or a specific transition. These chromatograms are generated post-acquisition from the TIC trace.

Data-dependent acquisition can be performed during sterol LC-MS analysis, as the sterol enters into the mass spectrometer [65]. The mass spectrometer is programmed to acquire a scan over a specified mass range, with the incorporation of an inclusion list for expected sterols. A full-scan spectrum is acquired first, the precursor ion is selected automatically, and its MS/MS spectrum is acquired. This cycle repeats several times as long as the preselected intensity remains above threshold. The MS/MS spectra of all components present in a single

eluting LC peak can thus be acquired provided that their intensity is above the preselected threshold.

1.8 LC-MS analysis of sterols

LC-MS/MS has been used to identify, quantify and determine the structures of steroids [25-30,48,84-86], and sterols [4,14,38,41,47,51,52,68,82,83,87,88]. Burkard and colleagues [89] developed a LC-MS method for the quantification of 24S-hydroxycholesterol and 27-hydroxycholesterol in human plasma. After saponification, solid-phase extraction, oxysterols were separated using a 125 mm x 2 mm (i.d), 5 µm particle size, C_{18} column with a linear gradient, and analysed by positive ion atmospheric pressure chemical ionisation (APCI) mass spectrometry. 24S- and 27-Hydroxycholesterol do not give $[M+H]^+$ ions, they fragment in the ion-source to give $[M+H-H_2O]^+$ and $[M+H-2H_2O]^+$ ions. A significant disadvantage of this LC-MS method is that molecular weight information and structural information are not available. The isomeric nature of oxysterols requires LC separation, and identification of 24S- and 27-hydroxycholesterols is then based on retention time. Burkard *et al.* [89] achieved a quantification limit for plasma samples of 0.5 mL of 40 µg/L (8 ng on-column) and 25 µg/L (5 ng on-column) for 24S- and 27-hydroxycholesterol, respectively by using selected ion monitoring (SIM) of $[M+H-H_2O]^+$ and $[M+H-2H_2O]^+$ ions. This limit of detection is not sufficient for identification of the oxysterols in a small amount of biological sample. Razzari-Fazeli *et al.* [90] achieved the separation of 7α-hydroxycholesterol, 7β-hydroxycholesterol, and 25-hydroxycholesterol online using a 250 mm x 4.6 mm (i.d.), 3 µm particle size C_{18} column under isocratic conditions with acetonitrile-water (60:40, v/v) at 1 mL/min, and performed analysis by positive-ion APCI-MS. 7-Oxocholesterol and 25-hydroxycholesterol co-eluted under this experimental condition, however they were distinguish by using SIM, the $[M+H]^+$ ions were monitored for the identification of 7-oxocholesterol, and $[M+H-2H_2O]^+$ ions for 25-hydroxycholesterol [90]. Alternatively, oxysterols can be analysed as $[M+NH_4]^+$ ions, but their MS/MS spectra are dominated by $[M+H-H_2O]^+$ and $[M+H-2(H_2O)]^+$ fragment-ions providing little structural information [41,91].

Above studies shows that sterols analysis by ES and APCI suffer from their poor ionisation, and the loss of molecular weight information as molecular ions are not usually observed, and little structural information is generated from MS/MS experiments. This reduces the selectivity of LC-MS method. Also, the physiological endogenous concentrations for several sterols are very low, and the sensitivity of tandem mass spectrometry is not adequate [21,33,36,92]. Derivatisation of sterols can enhance the ionisation efficiencies, by introducing a pre-charged group onto the sterol structure [30,93-95]. This leads to higher sensitivity, and specific detection. Honda *et al.* [30] derivatised monohydroxysterols into picolinyl esters and analysed by LC-MS/MS with positive-ion ES. Sterol picolinyl esters isolated from human serum were separated on a Hypersil GOLD column (150 x 2.1 mm, 3 µm) using an isocratic mode with acetonitrile-methanol-water (45:45:10, v/v/v) containing 0.1% acetic acid, at flow rate of 300 µL/min. The detection limits of the picolinyl esters of sterols were 2 - 10 fg on-column. An alternative design of derivative involves the incorporation of a pre-charged group such as a quaternary nitrogen [29,96,97]. Steroids containing an oxo group can be readily derivatised with commercially available Girard T reagent [(hydrazinocarbonylmethyl)trimethylammonium chloride, $(CH_3)_3N^+CH_2CONHNH_2Cl^-$] or Girard P reagents (Figure 3.1) [96,98,99]. The resulting product is water-soluble and compatible with reversed-phase chromatography. Shackleton *et al.* in 1997 [96] obtained MS/MS spectra of GT hydrazones under low-energy MS/MS conditions. Intense peaks were observed at $[M-59]^+$ and $[M-59-28]^+$ corresponding to the neutral losses of $N(CH_3)_3$ and $N(CH_3)_3CO$ ions, respectively. They have separated nine testosterone ester Girard hydrazones on a micro-bore C_4 HPLC column, using a water-acetonitrile-trifluoracetic acid (TFA) gradient, and analysed by positive-ion ES mode, on a triple quadrupole mass spectrometer. For achieving specificity in plasma analysis, they used the SIM mode for $[M]^+$, $[M-59]^+$, and $[M-59-28]^+$ ions. The on-column detection limit was around 1 ng.

Griffiths's group has started an evaluation of the use of the Girard P hydrazine ([1-(2-hydrazino-2-oxoethyl)pyridinium chloride, $(C_6H_5)_3N^+CH_2CONHNH_2Cl^-$] for analysis of sterols [100,101]. Unlike testosterone most sterols do not posses a 3-oxo-group, and are not suitable for

direct derivatisation with the Girard P reagent. Therefore, the steroids and sterols with a 3β-hydroxy-5-ene group or 3β-hydroxy-5α-hydrogen structure are converted by cholesterol oxidase to 3-oxo-4-ene or 3-oxo analoques, respectively [38,102]. These oxidised steroids/sterols can now be derivatised with Girard P hydrazine. The GP derivatised sterols give very intense signals in both ES and MALDI mass spectra, and most importantly give structurally informative MS/MS spectra [38,57,70,102,103]. Capillary column LC combined to low flow-rate ES is more sensitive for the analysis of sterols from biological samples than nano-ES alone [55]. Griffiths *et al.* in 2006 [38] started the development of a capillary-LC-ES-MS and -MS/MS method for the analysis of sterols from rat brain samples. The sterol fraction obtained after extraction, fractionation, enrichment and oxidation/GP-deivatisation steps was separated on-line using a 150 mm x 180 μm (i.d.), 3 μm particle C_{18} capillary-column, and analysed by positive-ion ES-MS and ES-MS/MS. The improved sensitivity of this method was due to the fact that the sample was subjected to fractionation, enrichment, and derivatisation steps prior low flow-rate ES mass spectrometry analysis, and also due to employing a more sensitive chromatographic technique, i.e capillary LC. The resulting oxidised/GP-derivatised sterols give a 10^2 - 10^3 fold improvement in sensitivity in comparison to underivatised sterols. Kirk *et al.* [104] reported the detection limit of 1 pg/μL for the cationic derivatives of 17α-testosterone hydrazone, 17α-nortestosterone hydrazone, an improvement in sensitivity of only 33 times relative to the underivatised steroids in the absence of low-flow-rate LC-MS.

In summary, the oxidation with cholesterol oxidase and derivatisation with Girard P hydrazine of sterols provides an advantage with respect to both chromatographic and mass spectrometric analysis. The Girard P group enhances the solubility of oxysterols in aqueous solvents, allowing for a greater variety of mobile phase. The presence of a charged group (quaternary nitrogen) improves the mass spectrometric sensitivity by two to three orders of magnitude in comparison to the underivatised analogues [38]. Another advantage of oxidation/GP-derivatisation is a tagging of a specific group to oxysterol molecule. Through oxidation/GP-derivatisation, these tagged oxysterols molecules can be shifted to a new mass

region, in which these oxysterols do not overlap with any other lipid molecular species. Furthermore, all of these tagged oxysterols can be readily distinguished through the facile loss of the derivatised moiety, which can be detected by loss of the tagged moiety during MS^n experiments [105].

1.9 Sterol quantification

In direct-infusion ES-MS, and in the absence of ionisation suppression effects, the mass spectrometric peak intensity is proportional to the concentration of a charged analyte in a mixture. In contrast, in LC-MS, the chromatographic peak area is proportional to the amount of an analyte in a mixture. Therefore, mass spectrometric techniques can identify sterols, as well as measure the abundance of each sterol in a mixture. In general, quantitative analysis is performed to provide absolute quantification or relative quantification. In absolute quantification, the aim is to determine the amount or concentration of the sterol in absolute terms. In contrast, the aim of relative quantification is to determine the amount or concentration of the sterol relative to another sterol, and this approach was adapted in this work.

The internal standard method is the most widely used approach in mass spectrometry quantification. The internal standards are added to the sample prior to extraction, and carried through the extraction process with the endogenous sterols. This method is accurate, because an internal standard can account for deviation in the mass spectrometry response, and sample losses that might occur due to incomplete transfer, oxidation, derivatisation and chromatographic steps. The introduction of internal standard prior to the sample preparation has the benefit of freeing the analyst from having to know the volumes of the extract, including the final volume. Because the calculations are based on ratios between peak areas and mass, no knowledge of extract volume is necessary. The most ideal internal standard is a stable isotope labelled analog of the sterol to be quantified, because its chemical and physical properties are virtually identical to those of the analyte. The use of deuterated internal standards has been reported for the quantification of sterols [21,106-110]. Deuterated analogs are not always available for all sterols, and an alternative deuterated sterol could be used. McDonald *et al.* [41] used

[$^2H_7$]25-hydroxycholesterol as an alternative deuterated analog of 22-hydroxycholesterol, [$^2H_7$]cholesterol as the deuterated standard for 7-dehydrocholesterol, cholestenone, and lathosterol.

As described in section 1.8, sterols are not well suited for analysis in their native state by ES, and individual sterols have varying responses to ES. The more polar oxysterols (e.g. 24,25-epoxycholesterol) are generally more amenable to ES ionisation compared to less polar compounds (e.g. lanosterol) [41]. However, when a pre-charged group is introduced onto the sterol moiety, the charge-tagged sterols give an approximately equal signal in ES spectra [4,55,68,81]. This allows relative quantification of different sterols in a biological sample. This approach was utilised in this work for quantitative analysis. Non-naturally occurring sterols, which have chemical and physical properties similar to those of the analyte, can also be spiked into the sample prior to sample processing. The only requirement is that it should not be isobaric to the analyte or it must elute from a chromatographic column at a different time. There are several problems which need to be resolved for the quantification of sterols by LC-MS. Many sterols are fully resolved by the chromatographic methods [41,111,112]; however, some closely related sterols such as 24R- and 24S-hydroxycholesterol and 25-hydroxycholesterol co-elute. Mass spectrometry can offer an additional level of separation by differentiating co-eluting sterols by *m/z* values. However, the LC-MS technique does not solve the problem for isobaric sterols, if they chromatographically co-elute.

1.10 Where are the oxysterols coming from? Cholesterol biosynthesis and metabolism.

Cholesterol (C^5-3β-ol) is present in all vertebrate cells and it has many important functions in the body. It is a vital constituent of plasma membranes of all cells in the body where it is necessary to maintain the fluidity and the structure of lipid bilayers [113]. Cholesterol also serves as a precursor of bile acids, steroid hormones and vitamin D. Sterols, steroids and bile acids are molecules based on the cyclopentanoperhydrophenanthrene skeleton. Sterols usually contain 27 carbon atoms, while most bile acids contain 24 carbon atoms and steroids hormones 21 carbon atoms or less [82,83].

The cholesterol needs of cells are covered by *de novo* synthesis and uptake from circulating lipoproteins [33]. Most of the mammalian cells are able to biosynthesise cholesterol and express the sophisticated enzymatic machinery required for the *de novo* synthesis. On the whole, the cells in the body are able to liberate and acquire cholesterol to maintain their cholesterol homeostasis because some produce an excess to provide to other cells, some others require exogenous cholesterol because of limited synthetic capacity [43]. To maintain homeostasis excess cholesterol is either exported from the cells or esterified to long-chain fatty acids (cholesteryl esters).

Cholesterol is insoluble in water and is transported in the circulation into the form of lipoproteins. Therefore, the exogenous cell supply of cholesterol is covered via the Low Density Lipoproteins (LDL) cycle and most of the excess of cholesterol is exported by the High Density Lipoproteins (HDL) mechanism (reverse cholesterol transport). Under normal conditions, approximately one half to two thirds of total body cholesterol is biosynthesised, and the remaining is provided by the diet, via the circulating LDL [114,115].

Cholesterol is biosynthesised via the mevalonate pathway which is comprised of 35 enzymes and may be divided into five stages:- 1) synthesis of mevalonate from acetyl-coenzyme (CoA); 2) synthesis of isoprenoid units from mevalonate; 3) condensation of six isoprenoid units to form squalene; 4) cyclisation of squalene to give lanosterol; 5) formation of cholesterol by re-arranging the lanosterol molecule. The rate limiting step is the conversion of 3-hydroxy-3-methylglutaryl-CoA (HMG-CoA) to mevalonate catalysed by the enzyme HMG-CoA reductase (see Figures 1.9 and 1.10) [31,81,114,116,117]. The activity of the enzyme is regulated by a negative feedback mechanism. Defects in cholesterol biosynthesis lead to disease, for example mutations in the enzyme 7-dehydrocholesterol reductase can lead to its malfunction and an accumulation of 7- and 8-dehydrocholesterols. These dehydrocholesterols are characteristic of Smith-Lemli-Opitz syndrome (SLOS) [114,116,118]. This is devastating disorder characterised by severe physical anomaly and mental retardation. Therefore, the measurement of the level of 7-dehydrocholesterol relative to cholesterol allows the diagnosis of SLOS syndrome [119].

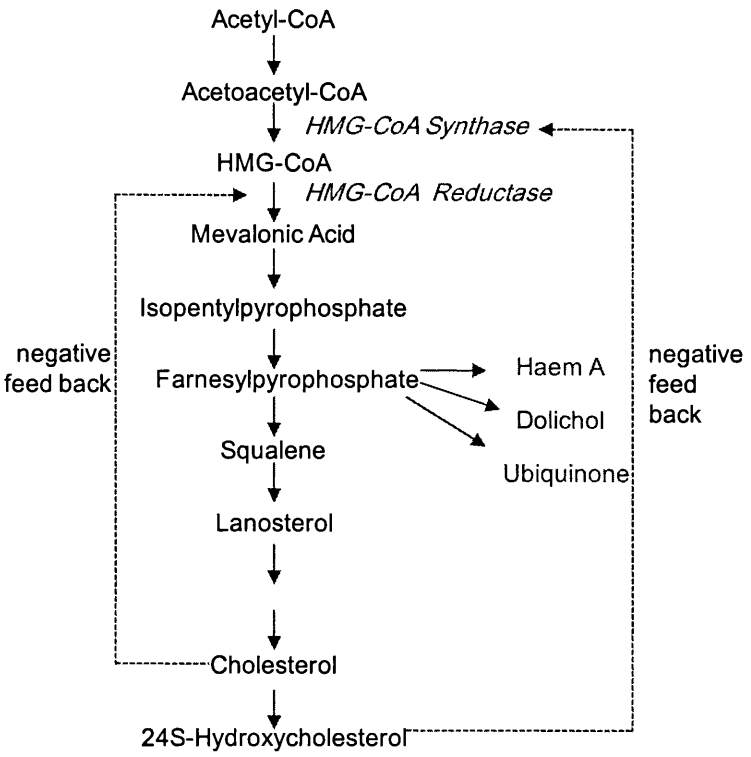

Figure 1.9 The simplified cholesterol biosynthetic pathway. Some of the major intermediates and end-products are indicated. Figure adapted from ref. [116].

An overview of the metabolic and transport pathways that control cholesterol levels in mammalian cells is shown in Figure 1.11. Normal mammalian cells tightly regulate cholesterol synthesis and LDL uptake to maintain cellular cholesterol levels within narrow limits and supply sufficient isoprenoids to satisfy metabolic requirements of the cell [113,114,120]. Cellular cholesterol levels are modulated by a cycle of cholesterol esterification by acyl-CoA:cholesterol acyltransferase (ACAT) and hydrolysis of the cholesteryl esters. In addition cholesterol is removed from the body by oxidation to bile acids, and oxysterols are important intermediates in bile acid synthesis [121,122] (see Figure 1.12). The primary bile acids are synthesised in the liver, amidated with either glycine or taurine, and excreted into the small intestine via the gallbladder. Bile acids play an important role in the absorption of lipids in the intestine and are themselves efficiently reabsorbed (95%) and transported back to the liver as part of the enterohepatic circulation [81]. There are two different pathways in bile acid biosynthesis (Figure 1.12) [81]. The "neutral" pathway begins with the conversion of cholesterol into 7α-hydroxycholesterol (C^5-

3β,7α-diol) through the activity of the enzyme CYP7A1, whereas the "acidic" pathway starts with the hydroxylation of cholesterol at position 27 in the side chain, through the activity of the enzyme CYP27A1 [123]. The "neutral" pathway starts with modification of the steroid nucleous, while the "acidic" pathway is initiated by side-chain oxidation and shortening. The "acidic" pathway may be extrahepatic, as CYP27A1 is present in most cell types, whereas the "neutral" pathway operates in the liver. The enzyme responsible for 7α-hydroxylation of 3β-hydroxycholest-5-en-27-oic acid, and 27-hydroxycholesterol (CYP7B1) is distinct from that responsible for 7α-hydroxylation of cholesterol (CYP7A1) [124].

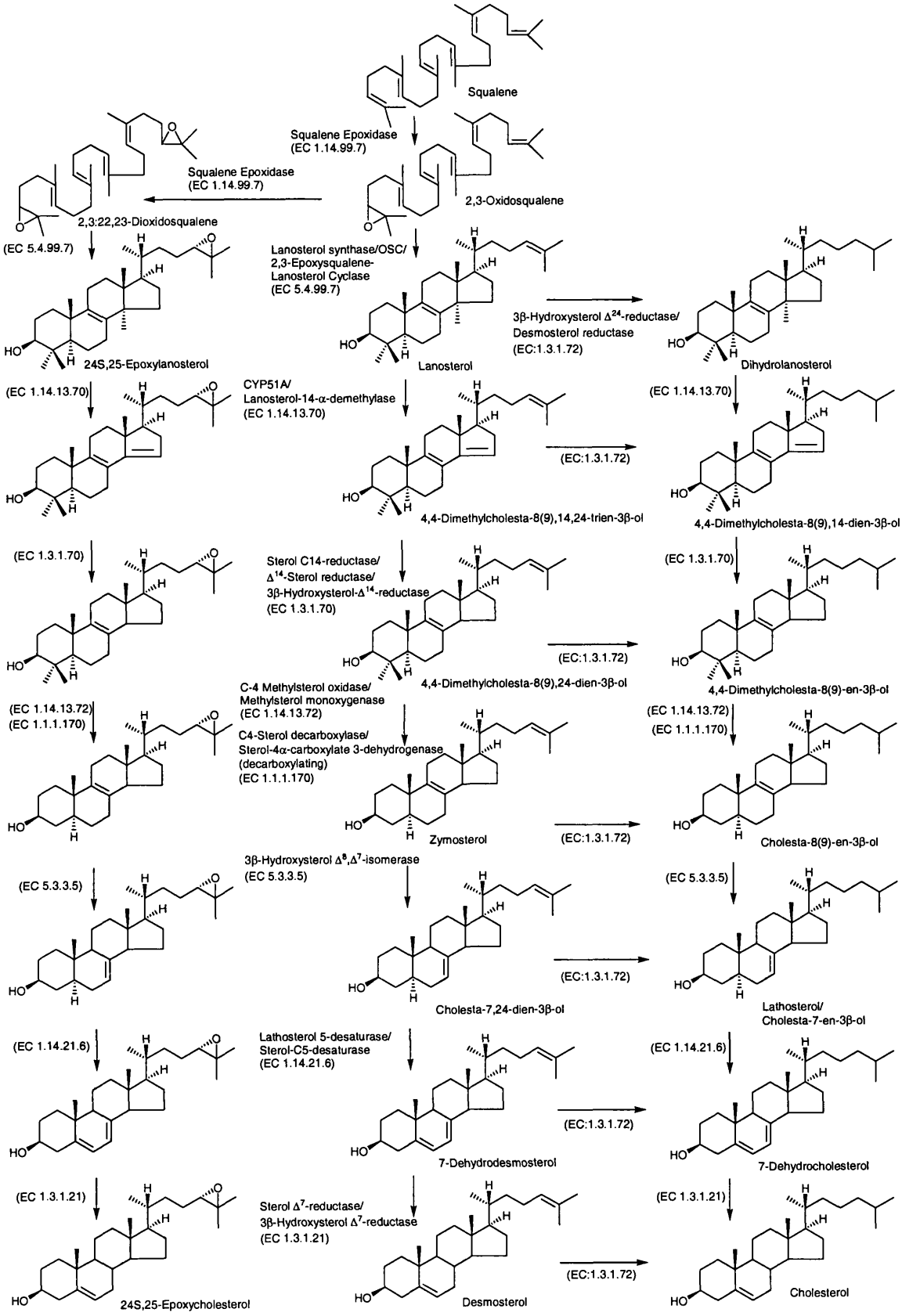

Figure 1.10 Final steps in the cholesterol and 24S,25-epoxycholesterol biosynthetic pathways. Figure adapted from ref. [105].

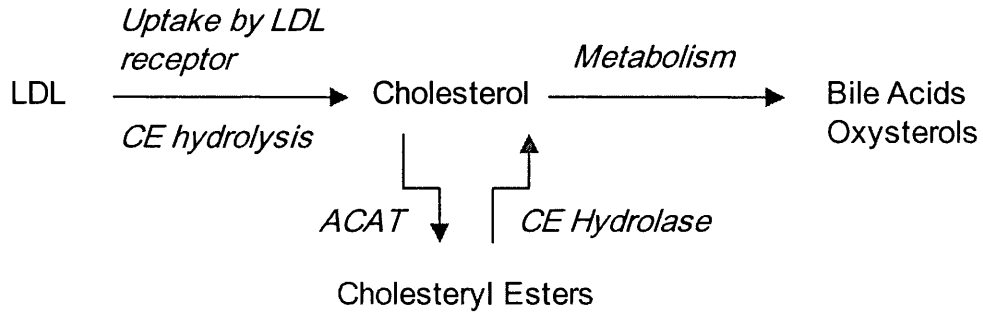

Figure 1.11 Overview of the metabolic and transport pathways that control cholesterol levels in mammalian cells. Apart from *de novo* biosynthesis of cholesterols, cells also obtain cholesterol by uptake and hydrolysis of LDL's cholesteryl esters (CE). End-products derived from cholesterol or intermediates in the pathway include bile acids, oxysterols, cholesteryl esters. ACAT, acyl-CoA:cholesterol acyltransferase. LDL is Low Density Lipoprotein. Modified from ref. [114]

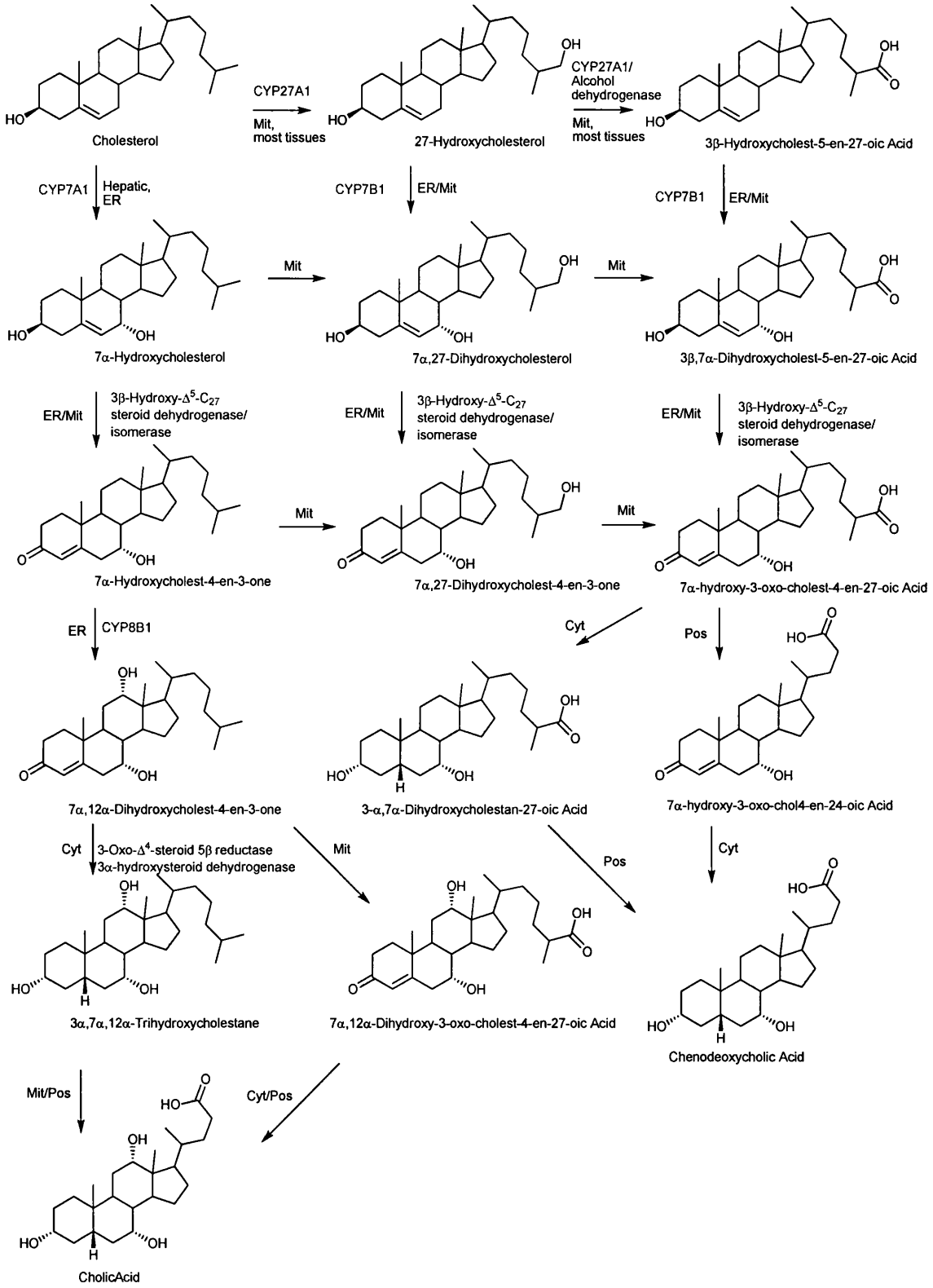

Figure 1.12 Significance of oxysterols in the biosynthesis of bile acids in man. Some enzymes, their distribution and subcellular location are shown. Endopasmic reticulum (ER), Mitochondria (Mit), Peroxisome (Pos), Cytosol (Cyt). Reproduced from ref. [81,125].

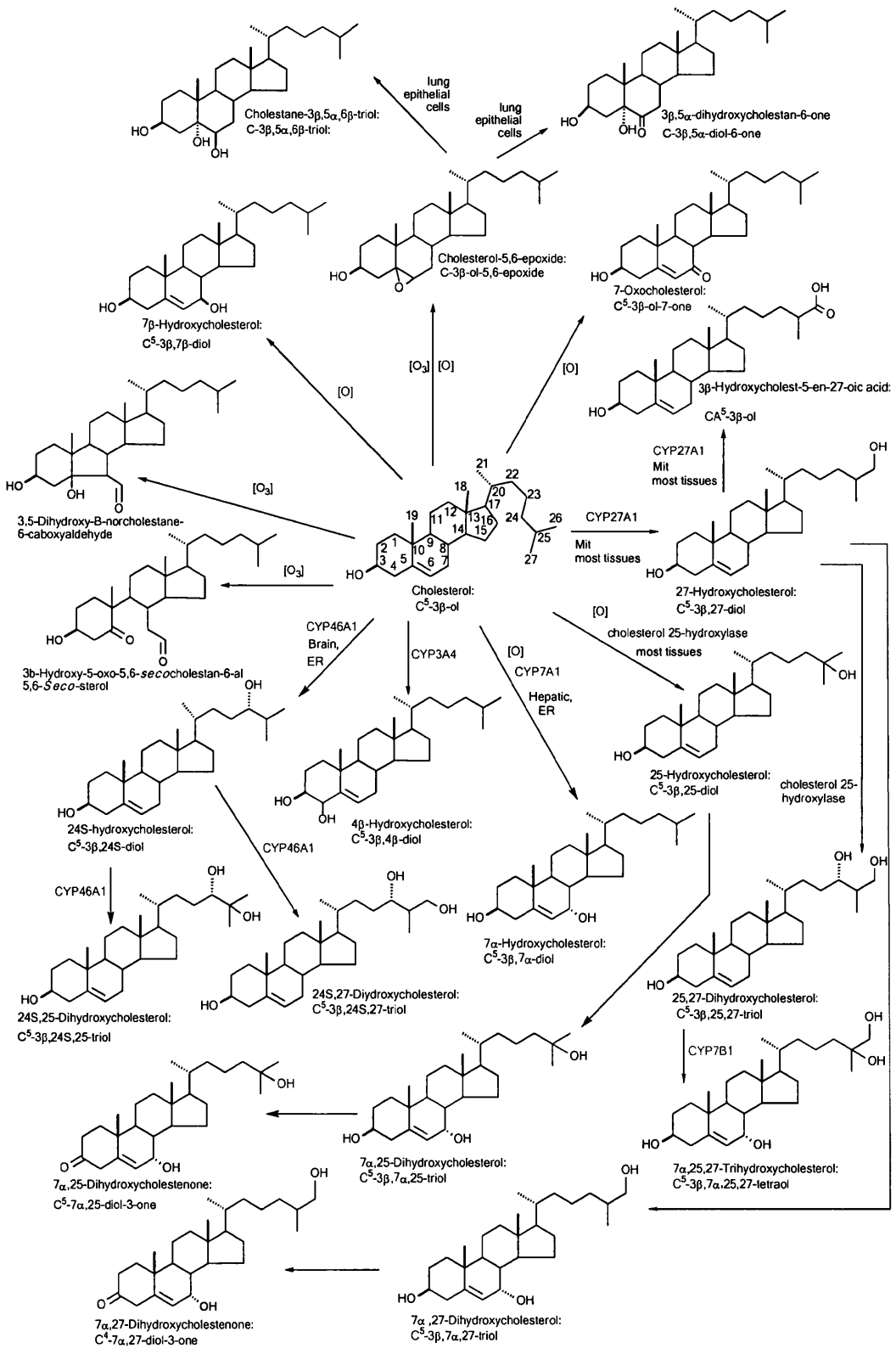

Figure 1.13 Oxysterols found in human and rat. Autoxidation reactions indicated by [O], some enzyme and subcellular locations are shown. The 27-hydroxycholesterol was previously denoted as 26-hydroxycholesterol in older literature. According to rules of priority of numbering the correct description is of 27-hydroxycholesterol is 25R,26-hydroxycholesterol [126]. The medical community uses the name 27-hydroxycholesterol and this name will be used in this report. Modified from ref. [81]

1.11 Oxysterols

Oxysterols are mono-oxygenated derivatives of cholesterol (or precursors to cholesterol) that are important intermediates in the bile acid synthesis and end products of cholesterol excretion pathways [35]. Oxysterols can vary in the type (monohydroxy, dihydroxy, epoxy, keto), number and position of the oxygenated functions introduced, and in the nature of their stereochemistry. Figure 1.13 depicts the structures of some of the more common oxysterols and for some indicates how they are derived. The excretion and rapid degradation of oxysterols is facilitated by their physical properties, which allow them to pass lipophilic membranes and to be redistributed in the body at significantly faster rate than cholesterol itself [23,121,122,127] The introduction of an oxygen function in the cholesterol molecule makes it considerably polar, drastically reduces its half-life and directs it to excretion or to oxidation to water soluble bile acids [36].

Oxysterols are classically found in conjunction with cholesterol in almost all biological locations. However, they are found at significantly lower concentration by 10 to 100 thousand fold less than cholesterol [31,35,92]. Oxysterols may be formed enzymatically, by autoxidation, or by reaction with ozone in biological systems [35]. Since they may be formed by spontaneous or enzyme mediated processes they incline to be distributed across different tissues.

The sites in cholesterol most susceptible to autoxidation are the allylic C-7 carbon and the tertiary C-25 carbon, directing to the formation of a mixture 7α-hydroxycholesterol (C^5-3β,7α-diol), 7β-hydroxycholesterols (C^5-3β,7β-diol), and 7-oxocholesterol (C^5-3β-ol-7-one) or 25-hydroxycholesterol (C^5-3β,25-diol) [31,81,128] (see Figure 1.13). In addition to the autoxidative process some oxysterols are formed by the action of specific enzymes, most of which belong to the cytochrome P450 (CYP) superfamily. The products of such enzymatic reactions represent the majority of oxysterols present in the biological systems. CYP7A1 is a hepatic microsomal enzyme responsible for 7α-hydroxylation of cholesterol; CYP27A1 is mitochondrial, and is expressed in most tissues and hydroxylates C-27 of cholesterol [129]. CYP46A1 is microsomal and is only present in brain and it hydroxylates C-24 carbon of cholesterol, and to a lesser degree C-25 and C-27 [38,81,92,121,122,127,130]. CYP3A4 leads to 4β-hydroxycholesterol production.

Cholesterol 25-hydroxylase is responsible for 25-hydroxylation of cholesterol, but is not a P450 enzyme [122]. 27-Hydroxycholesterol can be converted to 27-carboxylic acids by the action of CYP27A1 or by an alcohol dehydrogenase both in the liver and extrahepatically. Further metabolites are 3β,7α-dihydoxycholest-5-en-27-oic acid (CA^5-3β,7α-diol), and 7α-hydroxy-3-oxocholest-4-en-27-oic acid (CA^4-3β,7α-diol) (see Figure 1.12).

Wentworth and colleagues recently demonstrated that ozone is formed by antibody-catalysed oxidation of water [131] and can react with cholesterol to form oxysterols (*seco*-sterols) [94,95,131-135]. Zhang and colleagues have reported evidence for the production of ozone during inflammation [94]. The reaction between cholesterol and ozone was thoroughly studied by Wang *et al.* in 1993 [136] and the products identified as 3β-hydroxy-5-oxo-5,6-*seco*-cholestan-6-al and 3,5-dihydroxy-B-norcholestane-6-carboxyaldehyde. 3β-Hydroxy-5-oxo-5,6-*seco*-cholestan-6-al (5,6-*seco*-sterol), a ketoaldehyde, and its aldol condensation product, 3,5-dihydroxy-B-norcholestane-6-carboxyaldehyde [131,135], both contain a reactive aldehyde group (Figure 1.13). *Seco*-sterols have been shown to covalently modify amyloid β (Aβ) peptide and initiate amyloidogenesis *in vitro* [94]. Zhang *et al.* [94] identified 3β-hydroxy-5-oxo-5,6-*seco*-cholestan-6-al and 3,5-dihydroxy-B-norcholestane-6-carboxyaldehyde in brain extracts following derivatisation with 2,4-dinitrophenylhydrazine. Identification and quantification of the resulting hydrazones was performed by LC-ES-MS in the negative-ion mode with SIM for the $[M-H]^-$ ion at *m/z* 597, and was made by comparison of mass, retention time and peak intensity with authentic standards. Zhang *et al.* [94] suggested that levels of 5,6-*seco*-sterol and its aldol in Alzheimer's disease (AD) brain are higher than in controls, and it is postulated that the reactive aldehyde groups on 5,6-seco-sterol and its aldol can react with free amino groups of proteins or peptides, e.g. Aβ in AD to initiate amyloidogenesis. This study has come under considerable criticism by the cholesterol community [137]. Smith pointed out that other cholesterol autoxidation products will also give an $[M-H]^-$ at *m/z* 597, and in the absence of further data the identification of 5,6-*seco*-sterol and its aldol, and the hypothesis that they are formed by the reaction of ozone with cholesterol must be treated with considerable scepticism.

Biologically active oxysterols are also formed during ozonolysis of cholesterol in lung surfactant. Pulfer *et al.* in 2004 [132,133] found that 5β,6β-epoxycholesterol and 5,6-*seco*-sterol are major products of cholesterol ozonolysis in lung surfactant. Studies of the metabolism of 5β,6β-epoxycholesterol in lung epithelial cells yielded small amounts of cholestane-3β,5α,6β-triol, and more abundant levels of the unexpected metabolite, 3β,5α-dihydroxycholestane-6-one (Figure 1.13). The mass and elemental composition of 5,6-*seco*-sterol and its aldol (418.3 Da, $C_{27}H_{46}O_3$) is equivalent to that of 3β,5α-dihydroxycholestane-6-one, a metabolite of 5β,6β-epoxycholesterol, and that the 6-oxo group can react with 2,4-dinitrophenylhydrazine to give a derivative with identical mass to the identified hydrazones of 5,6-*seco*-sterol and its aldol, with a $[M-H]^-$ at *m/z* 597 under ES conditions. Further, as pointed out by Leland Smith 3β,5α-dihydroxycholestan-6-one is a common cholesterol autoxidation product [132,133,137]. The formation of unexpected oxysterols and autoxidation products highlights the requirement for unbiased methods for identifying and profiling sterols in biological matrices.

1.12 Biological activity of oxysterols

Kandutch *et al.* in 1978 [138] demonstrated that oxysterols behave as suppressors in the cholesterol synthesis. This has lead to formulation of the "oxysterol hypothesis". The hypothesis suggests that oxysterols mediate feedback regulation of cholesterol biosynthesis rather than cholesterol itself [81,121,122,130]. Thus oxysterols may be of regulatory importance *in vivo* at least in some biological systems. The effect of oxysterols on cholesterol homeostasis may be by three different mechanisms: (i) interaction with the SREBP (sterol-regulatory-element-binding protein) mechanism [139,140]; (ii) effect on the degradation of specific enzymes [36]; (ii) activation of the LXR mechanism [92,141,142].

Brown, Horton and Goldstein [139,140] have demonstrated that cholesterol synthesis in mammals is controlled by a regulated transport of SREBPs from the endoplasmic reticulum (ER) to the Golgi apparatus, where the transcription factors are processed proteolytically to release active fragments. These active fragments activate genes for cholesterol synthesis and uptake. The SREBP-escort binding protein Scap and the anchor protein Insig are key in this

mechanism. SREBPs exit in three forms, SREBP-2 which is primarily involved in cholesterol synthesis, SREBP-1c that stimulates fatty acid synthesis, and SREBP-1a which preferably activates cholesterol synthesis [139]. The abbreviation Insig signifies "insulin-induced gene" [143]. Radhakrishnan *et al.* [144] reported that cholesterol and oxysterols regulate cholesterol synthesis by different mechanisms. Experiments were carried out using purified recombinant versions of Insig and Scap. Cholesterol acts by binding to Scap, causing Scap to bind to the anchor protein Insig. Conversely, oxysterols quite the opposite bind preferentially to Insig with the result that Insig binds to Scap. Therefore, Scap recognises the tetracyclic steroid nucleus and the 3β-hydroxyl group of cholesterol, and Insig binding absolutely requires a polar group on the side-chain located at positions 22R, 24S, 25 or 27.

In principle, cholesterol homeostasis is maintained by the following process, in cholesterol wealthy cells, for example cholesterol binds to the sterol sensing domain of Scap and triggers a conformational change that causes the Scap-SREBP-2 complex to associates with an ER resident protein Insig, and the Scap-SREBP-2 complex is retained in the ER [143]. This prevents transport to the Golgi apparatus and further processing of SREBP-2 to the active forms. Oxysterols interact with Insig to provide the same effect [139,144,145]. However, when cells are depleted of cholesterol, the Scap-SREBP-2 complex dissociates from Insig and transport SREBP-2 to the Golgi apparatus for processing to its active form. HMG-CoA (3-hydroxy-3-methylglutaryl-Coenzyme A) reductase is the first committed enzyme in the mevalonate pathway and its expression is regulated at the transcriptional level by SREBP, and its degradation is also regulated by a sterol-accelerated mechanism [139]. HMG-CoA reductase is subject to feedback inhibition by cholesterol, oxysterols, and methylated sterols such as lanosterol. Oxysterols derived either by the conversion of endogeneous or LDL-derived cholesterol downregulate HMG-CoA reductase through two mechanisms: accelerated degradation of the reductase protein and inhibition of reductase gene transcription by blocking the ER to Golgi apparatus transport of Scap-SREBP [139,146].

The LXRs are members of the nuclear receptor super-family involved in the transcriptional regulation of many of the genes involved in lipid homeostasis [141,147]. Oxysterols behave as ligands for the LXRs, which complexed with its heterodemeric partner, the retinoid-X receptor (RXR), and activate transcription of genes that control cholesterol homeostasis [142]. LXRs target genes include cytochrome P450 7A1 (CYP7A1), the rate-limiting enzyme in the classic pathway of bile acid biosynthesis, and SREBP-1c [35,92,130]. The known physiological oxysterols include 24S-, 27-hydroxycholesterol, and 24,25-epoxycholesterol, although cholesterol precursors, e.g desmosterol, are also active [36]. 24S-hydroxycholesterol and 24S,25-epoxycholesterol are most efficient LXR ligands [36]. They are cell-type specific. For example, 24S-hydroxycholesterol is synthesised exclusively in the brain by the action of the cytochrome P450 enzyme CYP46A1 on preformed cholesterol [19].

1.13 Oxysterols in brain

The brain contains five to ten times more cholesterol than any other organ and this sterol represents 2–3% of the total weight and 20-30% of all lipids in the brain [117,148]. Almost all cholesterol is biosynthesised *de novo* in the brain, since the blood-brain barrier (BBB) efficiently prevents cholesterol uptake from the circulation into this organ, and it is biosynthesised *in situ* from acetyl CoA [33,37,44]. The BBB prevents diffusion of molecules like cholesterol because of tight junction between adjacent capillary endothelial cells. The increased hydrophilicity of oxysterols compared to cholesterol facilitates their ability to cross membranes and move between cells and their intracellular compartments [81].

The significant amount of cholesterol present in the CNS is known to reside in two pools:- (1) in the myelin sheaths (oligodendroglia), and (2) in the plasma membranes of astrocytes and neurons [33,149,150]. About 70% of the brain cholesterol is associated in myelin. The brain is the most cholesterol rich organ in the body due to the fact that about half of the white matter may be composed of myelin [43]. In the brain, the mean sterol concentration is 15-20 mg/g in many species [69]. Although some amounts of desmosterol and cholesteryl esters

have been found in the central nervous system (CNS) of very young animals, in the adult essentially all sterol in the CNS is unesterified cholesterol [33].

The nervous system is capable of cholesterol synthesis and the synthesis rate and cholesterol content increase dramatically during brain development, but declines to a very low level in the adult state. This can be explained by an efficient recycling of the brain cholesterol, and subsequently cholesterol has a extremely long half-life in the adult human brain, estimated to be at least 5 years [19,33,37,44,151]. Cholesterol synthesis has been found in several cultured neuronal cells derived from embryo or newborn animals [81,105,148,151]. According to Pfrieger neurons require glia-derived cholesterol to form synapses [148]. Astrocytes synthesise about 2-3 fold more cholesterol than neuronal cells [33], whereas oligodendrocytes cells responsible for myelinisation, have an even higher capacity for cholesterol synthesis than astrocytes. Pfrieger [148] hypothesised that during postnatal development the neurons may down-regulate their own cholesterol synthesis and rely on delivery of cholesterol from astrocytes. Neurons do not have enough cholesterol to support significant synapses in the absence of glial cells indicates that neuronal cells are dependent upon exogenous cholesterol from other CNS cells. "Outsourcing" of cholesterol synthesis may allow neurons to focus on generation of electrical activity rather than dispense energy on costly cholesterol synthesis.

The reutilisation and recycling of cholesterol between different cells locations in the brain is an important regulatory factor for brain cholesterol homeostasis. In an adult, the rate of synthesis of new cholesterol exceeds requirement. Current data from rodents suggests that about 60% of cholesterol export from brain is achieved *via* 24S-hydroxycholesterol (C^5-3β,24S-diol) which can pass the BBB, and be transported to the liver for further metabolism to bile acids [37]. In addition excess cholesterol from brain is metabolised to neurosteroids and bile acids, which can also pass the BBB. The cytochrome P450 (CYP) enzyme CYP46A1 is responsible for conversion of cholesterol to 24S-hydroxycholesterol (C^5-3β,24-diol), and this enzyme is found to be localised to neurons, and also differentially expressed in different brain

regions [33,44,122,149,152]. 24S-Hydroxycholesterol passes the BBB, and is transported to the liver for further catabolism [35,130,153].

24S-Hydroxycholesterol can be metabolised further by both neurons and astrocytes to additional oxysterols. Brain cells have also been found to metabolise other oxysterols. Zhang *et al.* [24,142,154,155] demonstrated that rat brain microsomes and cultures of cells of the nervous system, 7α-hydroxylate 25- and 27-hydroxycholesterol with their subsequent conversion to 3-oxo-4-ene steroids (see Figure 1.14). A minor fraction of 27-hydroxycholesterol and its 27-hydroxylated metabolites were further converted into 3β-hydroxycholest-5-en-27-oic acid, 3β,7α-dihydroxycholest-5-en-27-oic acid and 7α-hydroxy-3-oxo-cholest-4-en-27-oic acid (Figure 1.14). In contrast 24-hydroxycholesterol (C^5,3β,24-diol) was not found to be 7α-hydroxylated by brain microsomes, or cultures of Schwann cells, astrocytes, or neurons, and it has subsequently been confirmed that CYP7B1 does not 7-hydroxylate 24-hydroxycholesterol. In astrocytes, 27-hydroxycholesterol and 24-hydroxycholesterol become 25-hydroxylated, and endogenous 7α,25-dihydroxycholest-4-en-3-one (C^4-7α,25-diol-3-one), 25-hydroxycholesterol, 7α,25-dihydroxycholesterol (C^5-3β,7α,25-triol) have been reported (Figure 1.14). The 24,25-diol could be possibly cleaved by oxidation into a C_{24} acid, and this could lead to the formation of C_{24} bile acids in brain. Goto and colleagues in 2004 [156] showed that cholic acid, chenodeoxycholic acid (BA-3α,7α-diol) and deoxycholic acid are present in rat brain. Mast *et al.* in 2003 [22] have shown that CYP46A1 has 25- and 27-hydroxylase activity as well as its major 24-hydroxylase activity with the conversion of 24S-hydroxycholesterol to 24,25- dihydroxycholesterol and 24,27-dihydroxycholesterol (C^5-3β,24S,25-triol, C^5-3β,24S,27-triol), in both cultures of HEK293 cell transfected with human CYP46A1 cDNA, and an *in vitro* reconstituted system with recombinant CYP46A1 enzyme.

Other sterols identified in adult brain include 4β-hydroxycholesterol (C^5-3β,4β-diol), 24,25- and 5,6-epoxycholesterols (C^5-3β-ol,24,25-epoxide, C^5-3β-ol-5,6-epoxide) in mouse [41], 20S-hydroxycholesterol (C^5-3β,20S-diol) in rat [157], 22R-hydroxycholesterol (C^5-3β,22R-diol) in human [158], 24-oxocholesterol (C^5-3β-ol,24-one) cholest-4-en-3-one (C^4-3-one), 7-

hydroxycholesterol (C^5-3β,7-diol), and 7-oxocholesterol (C^5-3β-ol-7-one) have been reported by several different laboratories in human and rat brain [41,68,71,81,100,151,159].

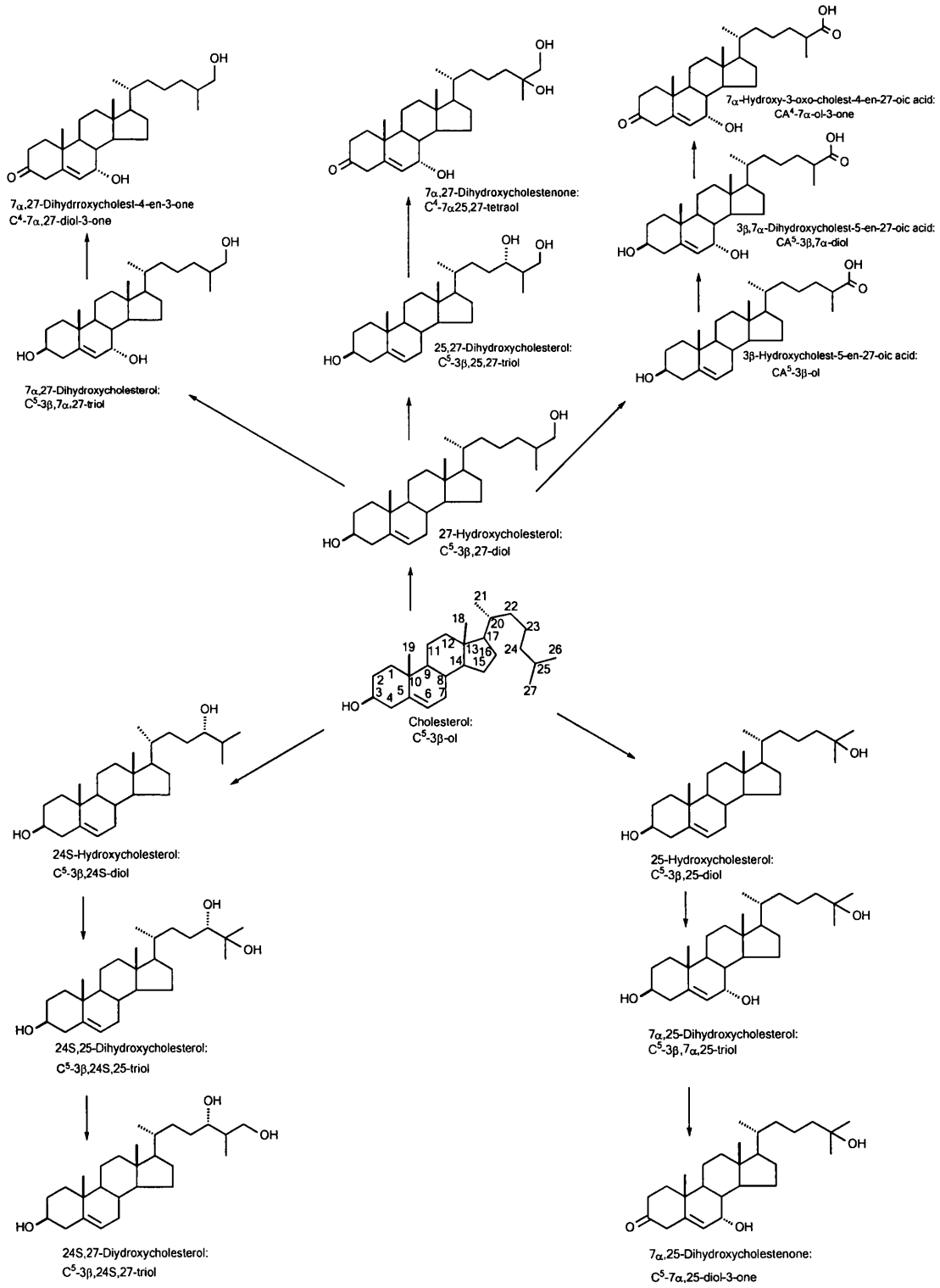

Figure 1.14 Oxysterols found in human and rat brain, and cultured cells from rat brain. The metabolic pathway of cholesterol in astrocytes suggested by Zhang *et al.* [24].

20S- and 22R-Hydroxycholesterols are intermediates in the formation of pregnenolone from cholesterol in a reaction catalysed by CYP11A1 (the cytochrome P450 side chain cleavage enzyme complex, $P450_{scc}$). This step is mandatory in the neurosteroid biosynthetic pathway in brain [157,158]. 22R-Hydroxycholesterol is a potent LXR ligand [142] and also inhibits SREBP-2 cleavage by binding to Insig [144].

24S,25-Epoxycholesterol has a unique origin when compare to other oxysterols. Rather then being derived from cholesterol, 24S,25-epoxycholesterol is produced in a shunt of the mevalonate pathway that also produces cholesterol (Figure 1.10) [160]. Therefore, all cells that can produce cholesterol should be able to biosynthesise 24S,25-epoxycholesterol. Wong *et al.* in 2007 [160] demonstrated that human brain cells can produce 24S,25-epoxycholesterol. 24S,25-Epoxycholesterol is both a ligand to the LXRs and an inhibitor of SREBP-2 processing [142,160]. It is hypothesised that 24S,25-epoxycholesterol provides an early warning system for newly synthesised cholesterol, to protect the cell against accumulated cholesterol, and to control the cellular cholesterol homeostasis [161], 24S,25-epoxycholesterol is synthesised in the endoplasmic reticulum and will cause the retention of Insig-SCAP-SREBP-2 complex.

1.14 Aims of this project

Sterols historically have been analysed by GC-MS [14,53,55]. Sterols are usually analysed following derivatisation of alcohol groups to trimethylsilyl (TMS) ethers [14,53,55]. GC-MS offers the advantages of are producible retention index, structurally informative fragmentation when using electron ionisation (EI), and the existence of extensive spectral libraries [14,53,55]. Oxysterols are also analysed by GC-MS [21,102], but because of the absence of a molecular ion in EI spectra some confusion in compound identification can occur particularly in respect to unknowns. As an alternative to GC-MS, liquid chromatography LC – tandem mass spectrometry (MS^n) is gaining popularity [41,111]. Oxysterols are tend to dehydrate upon atmospheric pressure ionisation (API), leading to the same problem as encountered in GC-MS with respect to molecular weight determination. Also, the lack of a basic or acidic group in most oxysterols leads to a low ionisation by ES. This problem could be overcome by derivatisation of sterols with charge-

tagged groups, so as to enhance ion yields upon ES. In addition, the extraction procedure can be tailored to sample type and information sought.

The objective of this work is the development and implementation of sensitive and specific methods for qualitative and semi-quantitative profiling of oxysterols in biological samples. To reach that objective, following aims were set-up. They are as follows:-

1. To synthesise reference sterol/oxysterol Girard P derivatives.
2. To establish the tandem mass spectra reference library of sterol/oxysterol GP derivatives.
3. To establish capillary LC - tandem mass spectrometry (cap-LC-MS^n) method for the identification of oxysterols/sterols.
4. To identify the cholesterol autoxidation products formed during the sample preparation.
5. To apply the established cap-LC-MS^n method to the analysis of oxysterols in the central nervous system (CNS) from rat and primary cortical neurons. Figure 1.15 shows the adapted analytical work-flow for the analysis of oxysterols in CNS.
6. To investigate the potential of sterol analysis for the prenatal diagnosis of Smith-Lemli-Opitz syndrome by cap-LC-MS^n.

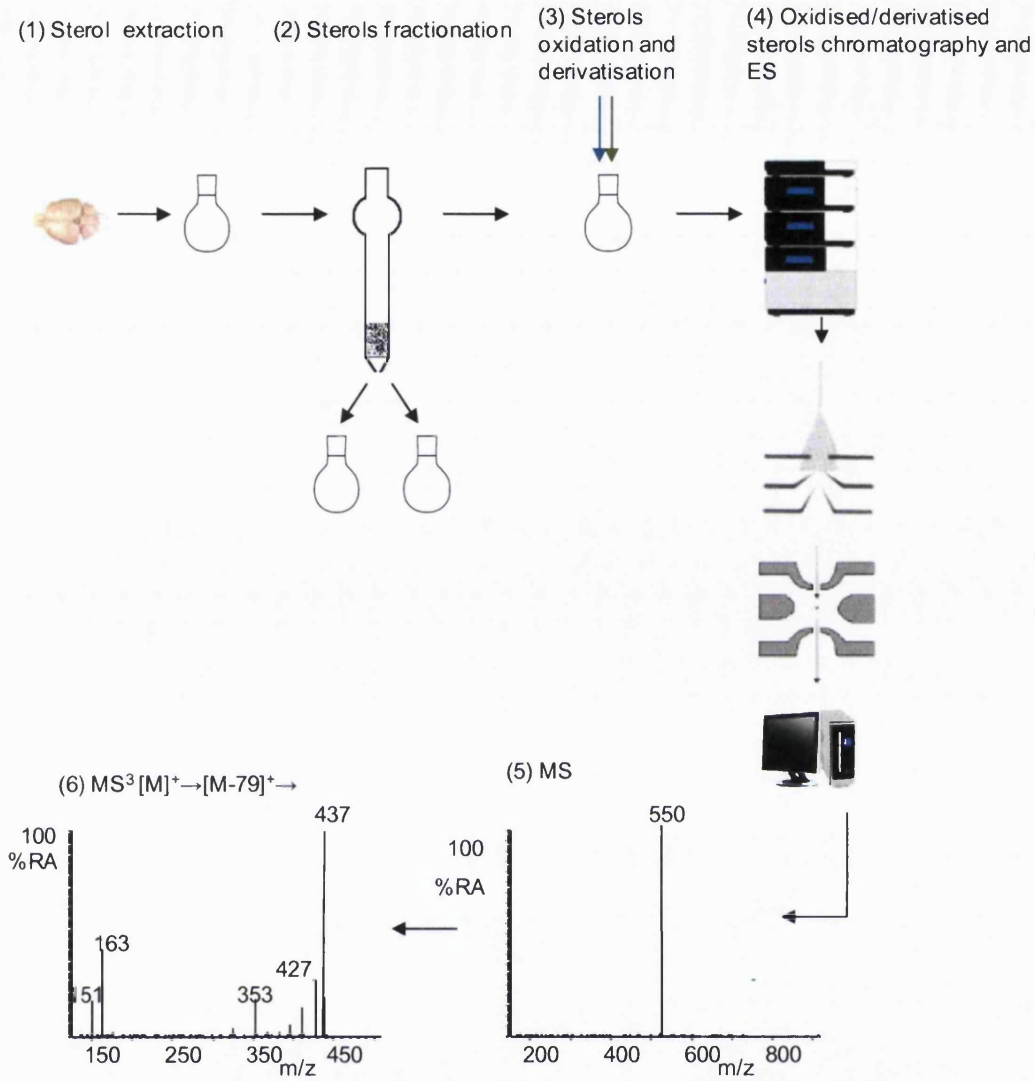

Figure 1.15. Work-flow of mass spectrometry (MS)-based experiment adapted in this work for the analysis oxysterols extracted from central nervous system. This experiment consists of six stages. In stage 1, the sterols to be analysed are extracted from tissues. In stage 2, the sterols are fractionated by chromatographic separation. MS of sterols is less sensitive than of oxidased/GP-derivatised sterols, and the information on mass of the underivatised sterol is lost during ES processes. Therefore, sterols are oxidised and derivatised in stage 3, in this work with cholesterol oxidase to convert 3β-hydroxy-5-ene and 3β-hydroxy-5α-hydrogen sterols to their 3-oxo-4-ene and 3-oxo equivalents. The oxo groups are subsequently derivatised with the Girard P (GP) hydrazine, so as to introduce a quaternary nitrogen to the molecule. In stage 4, such charged molecules of oxidised/GP-derivatised sterols are separated by one step of high-pressure liquid chromatography on a reversed-phase capillary column and eluted into a nano-electrospray ion source where they are nebulised in small, highly charged droplets. After evaporation, charged GP-sterols enter the ion trap analyser of the mass spectrometer and in stage 5, they separated according to the stability of their trajectory in a changing electric field, and a mass spectrum of the GP-sterols eluting at this point is taken (MS). The mass spectrometer is also programmed to select the ions of interest, these ions are subsequently subjected to MS^n experiments (stage 6). The MS and MS^n spectra are typically acquired for 200 ms each, and stored for matching against the reference oxidised/GP-derivatised sterol MS^n database.

Chapter 2

Materials and Methods

2.1 Materials

Reagents and solvents

HPLC grade methanol, isopropanol were obtained from Fischer, UK. HPLC grade hexane, ethyl acetate and chroroform were purchased from Sigma-Aldrich, UK. Ethanol (99.5% purity) was purchased from Fisher-Scientific, UK. Water was from a Milli-Q water system (Milipore, Molsheim, France). The Girard P (GP) hydrazine, [1-(2-hydrazino-2-oxoethyl) pyridinium chloride] ($C_7H_{10}ClN_3O$), acetic acid (99.99% purity), and cholesterol oxidase from *Streptomyces sp.* were purchased from Sigma-Aldrich, UK.

Reference compounds

The oxysterols: 7β-hydroxycholesterol (C^5-3β,7β-diol), 25-hydroxycholesterol (C^5-3β,25-diol), 20α-hydroxycholesterol (C^5-3β,20α-diol), cholesterol (C^5-3β-ol), 22R-hydroxycholesterol (C^5-3β,22R-diol), 22S-hydroxycholesterol (C^5-3β,22S-diol), 6β-hydroxycholestenone (C^4-6β-ol-3-one), 7-oxocholesterol (C^5-3β-ol-7-one) were purchased from Sigma, UK (Table 2.1). Other oxysterols: 6-oxocholestenone (C^4-3,6-dione), 19-hydroxycholesterol (C^5-3β,19-diol), 24S-hydroxycholesterol (C^5-3β,24S-diol), desmosterol ($C^{4,24}$-3β-ol), 7α-hydroxycholesterol (C^5-3β,7α-diol), sitosterol (C^5-24β-ethyl-3β-ol), stigmasterol ($C^{5,22}$-24β-ethyl-3β-ol), lanosterol ($C^{8,24}$-4,4,14-trimethyl-3β-ol), campesterol (C^5-24-methyl-3β-ol), brassicasterol ($C^{5,22}$-24-methyl-3β-ol), lathosterol (5α-C-7-en-3β-ol), 7-dehydrocholesterol ($C^{5,7}$-3β-ol), dihydrocholesterol (5α-C-3β-ol), 4β-hydroxycholesterol (C^5-3β,4β-diol), 3β,5α,6β-trihydroxycholestane (C-3β,5α,6β-triol), 6-oxocholestanol (5α-C-3β-ol-6-one), 3β,7α-dihydroxy-5-cholestenoic acid (CA^5-3β,7α-diol), 3β,7α-dihydroxy-5-cholestenoic acid (CA^5-3β,7β-diol), 5α-epoxy-cholesterol (C-5α,6α-epoxy-3β-ol), 24S,25-epoxycholesterol (C^5-24S,25-epoxy-3β-ol), [25,26,26,26,27,27,27-$^2H_7$] cholesterol ([25,26,26,26,27,27,27-$^2H_7$] C^5-3β-ol) were purchased from Steraloids (Table 2.1). 27-Hydroxycholesterol (C^5-3β,27-diol), 7β,27-dihydroxycholesterol (C^5-3β,7α,27-triol), 7α,25-dihydroxycholesterol (C^5-3β,7α,25-triol), 24-oxocholesterol (C^5-3β-ol-24-one), 3β-hydroxy-5-oxo-5,6-*seco* cholestan-6-al (5,6-*seco*-sterol), 3β-hydroxy-5-hydroxy-B-norcholestan-6-carboxaldehyde (aldol), [2,2,4,4,23-$^2H_5$] 3β-hydroxychol-5-en-24-oic acid ([2,2,4,4,23-$^2H_5$] BA^5-

3β-ol), 3β-hydroxychol-5-en-24-oic acid (BA^5-3β-ol), [16,16,17(or 20),22,22,23,23-$^2H_7$] 3β-hydroxycholest-5-en-27-oic acid ([16,16,17(or 20), 22,22,23,23-$^2H_7$]CA^5-3β-ol) were from previous studies in Karolinska Institutet, Sweden laboratory (supplementary material, Table 1).

Materials for solid phase extraction chromatography

Sep-Pak C_{18} cartridges containing 1 g of sorbent were purchased from Waters, UK. Unisil (silicic acid, 200–325 mesh) was obtained from Clarkson Chromatography Products (Williamsport, PA, USA). Siliconised polyropylene microtubes were purchased from Sigma-Aldrich, UK. Glass columns for solid phase extraction were made by Mr. John Cowley at the Queen Mary & Westfield College, University of London.

2.2 Analysis of reference oxysterols

The analytical scheme for the analysis of reference oxysterols is shown in Figure 2.1. Briefly, sterols with a 3β-hydroxy-5-ene group or 3β-hydroxy-5α-hydrogen structure were oxidised with cholesterol oxidase to 3-oxo-4-ene and 3-oxo analogues. These oxidised sterols were derivatised with GP hydrazine to GP hydrazones. The excess of GP reagent was separated from the GP hydrazones, which were then analysed by direct infusion nano-ES-MS^n and by capillary LC-MS^n with positive-ion electrospray (ES).

2.3 Preparation of reference sterol stock solutions

A series of 1.5 mL siliconised tubes were washed several times with methanol. The tubes were labeled "Name of sterol, concentration and date". Around 1 mg of reference sterol was weighed by difference in each separate tube and dissolved in 1 mL of methanol. All stock solutions were prepared immediately before use.

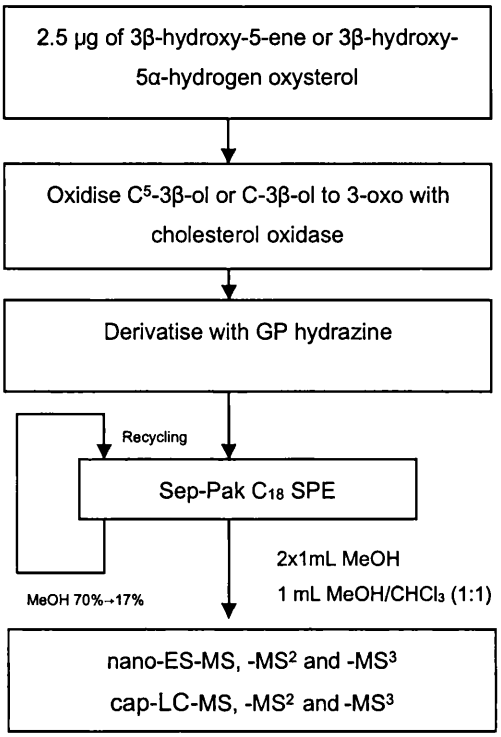

Figure 2.1 Analytical procedure for the analysis of reference oxysterols. The 3β-hydroxy-5-ene or 3β-hydroxy-5α-hydrogen sterols (2.5 µg) were incubated for 60 min at 37°C with 2.5 µL of cholesterol oxidase from *Streptomyces sp.* (2 mg/mL, 44 Units/mg of protein) in 1 mL of buffer (50 mM KH_2PO_4, pH 7). This results in the conversion of 3β-hydroxy-5-ene sterol to 3-oxo-4-ene sterols or 3β-hydroxy-5α-hydrogen sterols to 3-oxo analogues, which were subsequently derivatised with Girard P (GP) hydrazine. The oxysterol GP hydrazone were then separated from excess reagent by extraction on a Sep-Pak C_{18} SPE column. In the first analysis, GP hydrazones were analysed by direct infusion nano-ES-MS,-MS^2 and -MS^3. The next analysis, GP hydrazones were injected on a C_{18} capillary column, and ES-MS, -MS^2 and -MS^3 spectra recorded.

2.4 Oxidation of 3β-hydroxy-5-ene and 3β-hydroxy-5α-hydrogen sterols to 3-oxo-4-ene and 3-oxo sterols

The 3β-hydroxy-5-ene or 3β-hydroxy-5α-hydrogen sterol [both reference sterols (2.5 µg) and those extracted from biological sample (sections 2.14-2.22)] were oxidised with cholesterol oxidase essentially as described by Brooks *et al.* [102] and Griffiths *et.al* [38]. The 3β-hydroxy-5-ene or 3β-hydroxy-5α-hydrogen sterol was dissolved in 50 µL of isopropanol, and 2.5 µL of cholesterol oxidase from *Streptomyces sp.* (2 mg/mL, 44 U/mg protein) in 1 mL of buffer (50 mM KH_2PO_4, pH 7) was added. The mixture was incubated at 37°C for 60 min and subsequently used as the starting solution for reaction with the GP reagent as described below.

2.5 *Derivatisation of 3-oxo-4-ene and 3-oxo sterols with Girard P hydrazine*

The derivatisation of oxosterols to GP hydrazones was carried out essentially as described by Shackleton *et al.* [96] and Griffiths *et al.* [61,162]. The reaction mixture from the oxidation step was used directly after the incubation with enzyme. The oxidation mixture, 1 mL (50 mM phosphate buffer, 5% isopropanol, 4 µg enzyme, and 2.5 µg reference oxosterol) was diluted with 2 mL of methanol to give a 70% methanol solution, and 150 mg of Girard's P (GP) reagent and 150 µL of glacial acetic acid were added. The mixture was mixed well, and was left at room temperature overnight in the dark to allow 3-oxo-4-ene or 3-oxo sterols to be completely derivatised with GP hydrazine.

2.6 *"Recycling" reversed-phase solid phase extraction (C_{18} SPE)*

Even when derivatised with Girard P reagents, sterols may be difficult to solubilise (or retain in solution) when using a highly aqueous mixture of methanol and water. This can make extracton using reversed-phase SPE challenging. A recycling procedure is used in this work in order to solve this problem.

Following overnight incubation, the oxidised/GP-derivatised reaction mixture was then separated from excess GP reagent by extraction on a Sep-Pak C_{18} SPE column utilising a "recycling" method (Figure 2.1). The Sep-Pak C_{18} material was packed to a height of 1 cm in a glass column 0.8 cm (i.d) x 25 cm, with a reservoir for 50 mL. The C_{18} SPE column was conditioned with 10 mL of chloroform-methanol (1:1; v/v), followed by 10 mL of methanol, 10 mL of 10% methanol in water, and finally with 5 mL of 70% methanol in water prior to sample application. All elutions were carried out at room temperature under slight nitrogen pressure, with flow rate about 0.5 mL/min. The GP reaction mixture (~ 3 mL in 70% methanol) after oxidation and GP derivatisation procedures was directly applied on the C_{18} SPE column, followed by 1 mL of 70% methanol (this is a wash of the reaction vessel), and 1 mL of 35% methanol. The effluent was collected into a 50 mL falcon tube (a sample tube). The combined effluent (now 5 mL) was diluted with 4 mL of water. The resulting mixture (now 9 mL in 35% methanol) was again applied to the C_{18} SPE column, followed by a wash with 1 mL of 17%

methanol. The effluent was collected into the sample tube. To the combined effluent, 9 mL of water was added to give 19 mL of about 17.5% methanol. This was again applied to the C_{18} SPE column followed by a wash with 10 mL of 10% methanol in water to remove excess of GP hydrazine. At this point, all the oxidised/GP-derivatised sterols had been extracted on the C_{18} column. The oxidised/GP-derivatised oxysterols were then eluted with two portions of 1 mL of methanol (SPE-Fr1 & -Fr2), followed by 1 mL of chloroform-methanol (1:1, v/v) (SPE-Fr3). The three fractions were analysed separately by direct infusion nano-ES-MS^n. The oxidised/GP-derivatised oxysterols were found predominantly in SPE-Fr1 and SPE-Fr2 fractions. The chloroform-methanol (SPE-Fr3) fraction was dried completely in a SpeedVac, sterols were re-dissolved in 1 mL of SPE-Fr2, and the resulting sample was vortexed for 2 min. Each SPE fraction was analysed twice by cap-LC-MS^n for sterol identification. An aliquot (100 µL) of each SPE-Fr1 and SPE-Fr2 fraction was combined, vortexed and analysed three times by cap-LC-ES-MS^n for sterol quantification. All fractions were stored at -20^{0}C.

2.7 Nano-electrospray mass spectrometry analysis of oxidised/GP-derivatised oxysterols

Nano-electrospray mass spectrometry (nano-ES-MS) analyses were performed on a LCQ^{duo}, ion trap instrument (Thermo Finnigan, now Thermo Fisher Scientific, San Jose, CA, USA) fitted with a nano-electrospray ionisation (nano-ES) source. The LCQ^{duo} mass spectrometer was operated with different scan functions:- single-stage scan, zoom scan, and multi-stage fragmentation scan. All samples were analysed by direct infusion multi-stage fragmentation mass spectrometry (nano-ES-MS^n), and by capillary LC multi-stage fragmentation mass spectrometry (capillary LC-MS^n), in both cases nano-ES-MS, -MS^2 and –MS^3 spectra were recorded.

The data system of the LCQ^{duo} used a Finnigan LCQ^{duo} data processing, and instrument control software called Xcalibur™ (version 1.2). Xcalibur™ Software is flexible windows based data system, which consists of instrument set-up, acquisition, data processing. The data files generated were reviewed with the qualitative browser.

2.8 Direct infusion nano-ES multi-stage fragmentation mass spectrometry (nano-ES-MS^n) analysis of oxidised/GP-derivatised oxysterols

For the analysis of oxidised/GP-derivatised oxysterols, approximately 5 to 10 µL of sample (1.25 ng/µL in methanol) was loaded into a metal-coated PicoTip™ capillary (1.2 mm outer diameter o.d., 0.69 mm inner diameter i.d., New Objective Inc., Woburn, USA) using a Gel-Saver pipette tip (ThermoFisher, UK). The tip of the PicoTip™ capillary was cracked against a metal stopper on the stage of a light microscope to give a spraying orifice of about 5 µm. The PicoTip™ capillary was then installed into the nano-ES source, and the positive nano-electrospray mass spectrum (nano-ES-MS) was acquired. The instrument was operated using the following settings: spray voltage 1.00 to 1.20 kV, capillary temperature 200^{0}C, no sheath or auxiliary gas used. The *m/z* range from *m/z* 50 – 700 was scanned, and centroid data was collected. Other conditions were optimised automatically utilising the autotune function on the oxidised/GP-derivatised 25-hydroxycholesterol.

Data was collected either manually or automatically. Manual acquisition was performed to record MS, MS^2 and MS^3 spectra. MS^2 experiment was performed on a precursor ion, $[M]^+$ or $[M]^{2+}$. MS^2 spectra of oxysterol GP hydrazone, $[M]^+$ ions, are dominated by $[M-79]^+$ and $[M-107]^+$ fragment ions. MS^3 experiments were performed on fragment-ions resulting from a neutral loss of 79 Da or 107 Da in the MS^2 scan. For acquisition of both MS^2 and MS^3 spectra, the collision energy setting was 45%. The MS^2 and MS^3 isolation widths were set at 2.00, so as to allow the selection of precursor ion. MS, MS^2 and MS^3 scans consisted of three averaged "microscans" each with a maximum injection time of 200 ms. An automated program was set-up based on these acquisitions.

2.9 Capillary LC multi-stage fragmentation mass spectrometry (cap-LC-MS^n) analysis of oxidised/GP-derivatised oxysterols

Chromatographic separation was performed utilising a Dionex UltiMate 3000 single capillary LC system (Camberley, Surrey, UK). The LC system consisted of SRD-3600 solvent rack with on-line vacuum degasser, LPG-3600 low pressure dual gradient micro-pumping

system, WPS-3000 well plate auto-sampler, FLM-3100 thermostated flow manager and UVD-3000 UV detector (Figure 3.31).

LC was conducted using a PepMap C_{18} column (180 µm i.d. x 150 mm, 3 µm particles, 100 Å, Dionex, Surrey, UK). The mobile phases were:- mobile phase A, 0.1% formic acid in 50% methanol in water; mobile phase B, 0.1% formic acid in 95% methanol in water; transport solvent (transport delivery solvent) 0.1% formic acid in 63.5% methanol in water. A linear gradient program is shown in Table 2.1 and Figure 2.2. The total run time was 50 min. A sample loop (5 µL, Dionex, Camberley, Surrey, UK) was used. The sample tray was held at 4 ^{0}C. Between sample injections, injector flushing and needle washing were performed using isopropanol-methanol (1:1, v/v) to minimise carry-over of oxidised/GP-derivatised sterols between injections.

Table 2.1 Gradient program used for the separation of GP hydrazones using cap-LC.

Time, min	Flow Rate, µL/min	%A[a]	%B[b]
0.0	0.8	70	30
10.0	0.8	30	70
15.0	0.8	20	80
30.0	0.8	20	80
30.1	0.8	70	30
50.0	0.8	70	30

[a]Mobile-phase A: 50% methanol containing 0.1% formic acid; [b]mobile-phase B: 95% methanol containing 0.1% formic acid.

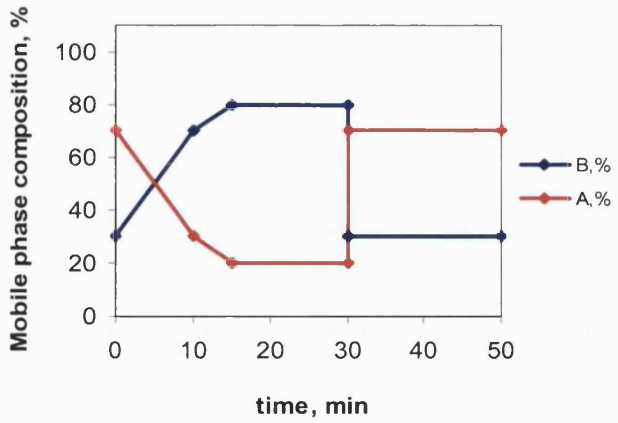

Figure 2.2 Gradient profile used for the separation of oxidised/derivatised oxysterols using cap-LC. Mobile phase A was 50% methanol, 0.1% formic acid, and B was 95% methanol, 0.1% formic acid. Flow rate 0.8 µL/min.

For the analysis of reference compounds, 1 µL of the combined methanol fractions (equivalent to 1.25 ng/µL of the oxidised/derivatised oxysterol) was added to 499 µL of 63.5%

methanol in water containing 0.1% formic acid, and 1-5 µL (equivalent to 2.5-12.5 pg of the oxidised/derivatised oxysterol) was injected onto the analytical column. The sample was loaded via a 5 µL sample loop by means of a six-port valve fitted in the WPS-3000 well plate auto-sampler. The six port valve was switched to allow transfer of sample onto the capillary C_{18} column as descibed in section 3.6.

The capillary C_{18} column eluent was continuously directed into the nano-ES source of the LCQ^{duo} mass spectrometer via a metal coated fused silica PicoTip™ emitter (360 µm o.d., 15 µm tip i.d., New Objective Inc., Woburn, USA).

The LCQ^{duo} mass spectrometer was operated in the positive-ion ES mode using seven scan events over 49 min time period of the capillary LC gradient. The scan events were MS, MS^2 and MS^3. MS^2 was programmed to be performed for expected oxidised/GP-derivatised oxysterols, $[M]^+$→. MS^3 was programmed to be performed on fragment-ions resulting from a neutral loss of 79 Da and 107 Da in the MS^2 scan, $[M]^+ \rightarrow [M-79]^+ \rightarrow$ and $[M]^+ \rightarrow [M-107]^+ \rightarrow$. For acquisition of both MS^2 and MS^3 spectra, the collision energy setting was 45%. The spray voltage was set to 2.00 kV and capillary temperature 200^{0}C. The MS, MS^2 and MS^3 isolation widths were set at 2.00. MS, MS^2 and MS^3 scans consisted of three averaged "microscans" each with a maximum injection time of 200 ms to ensure sufficient data points were obtained across the chromatographic peaks. Scans (typically 50) were averaged for the MS spectra, and approximately 70 scans were averaged for the MS^2 and MS^3 spectra.

One example of seven scan events is shown below for the oxidised/GP-derivatised cholesterol and monohydroxycholesterol:-

Full scan of *m/z* 250-700
MS^2 518 →
MS^3 518 → 439 →
MS^3 518 → 411 →
MS^2 534 →
MS^3 534 → 455 →
MS^3 534 → 427 →

For analysis of the oxidised/GP-derivatised reference oxysterols, a typical analytical sequence consisted of injections of five different oxidised/GP-derivatised reference oxysterols in triplicate. Quality control samples (the oxidised/GP-derivatised cholesterol, 25-

hydroxycholesterol, and 24S-hydroxycholesterol) were injected in the beginning and in the end of the analytical sequence. Three blanks were injected between triplicate injections.

For the determination of relative retention time of each oxidised/GP-derivatised reference oxysterol/sterol, reconstructed ion chromatograms (RICs) were generated for $[M]^+$, and total ion chromatograms (TICs) for $[M]^+ \rightarrow$, $[M]^+ \rightarrow [M-79]^+ \rightarrow$, and $[M]^+ \rightarrow [M-107]^+ \rightarrow$ transitions over the duration of the LC-MS^n run. Relative retention times (RRTs) of oxidised/GP-derivatised oxysterols/sterols were determined in relation to the oxidised/GP-derivatised cholesterol, and are summarised in Supplementary Materials, Table 1.

For analysis of biological samples, a typical analytical sequence consisted of injections of five different biological samples in triplicate, and quality control samples of oxidised/GP-derivatised 25-hydroxycholesterol, and 24S-hydroxycholesterol on three concentration levels in the beginning and in the end of the analytical sequence. Three blanks were injected between triplicate injections.

2.10 Validation of capillary LC-MS method

Working solutions and calibration

Working solutions of the oxidised/GP-derivatised 24S-hydroxycholesterol, 25-hydroxycholesterol, 22R-hydroxycholesterol, and cholesterol were prepared by diluting the primary stock solutions (1.25 ng/μL in methanol) to the final concentration of 50 pg/μL in methanol. A working solution was further diluted with 63.5% methanol in water containing 0.1% formic acid, and solutions were used as calibration standards and as quality control samples in cap-LC-MS^n analysis. Calibration (0.3, 0.5, 1.0, 1.5, 4.0, 8.0, 16.0, 25.0 pg/μL) and quality control (1, 2 and 8 pg/μL) samples were prepared on the day of experiment. A total of 1 μL of each solution was injected onto the capillary reversed phase column. Each calibration point and quality control was analysed in triplicate. The quality control samples were analysed repetitively between biological samples within each analytical sequence. Quantification was performed using the MS^2 $[M]^+ \rightarrow$ transition over the duration of the LC-MS^2 run, and reconstructed ion chromatograms (RICs) generated for the $[M]^+ \rightarrow [M-79]^+$ transitions. The calibration lines were

constructed by plotting the chromatographic peak area versus the amount of analyte injected on-column.

Optimisation of injector washing solvent to prevent carry-over between injections

The oxidised/GP-derivatised cholesterol was analysed by cap-LC-MS using a gradient LC condition described in 2.9, and MS, MS^2 518→ and MS^3 518→439→ spectra were recorded during a single injection. The oxidised/GP-derivatised cholesterol (1 ng) was injected on-column. After this LC-MS run, 5 µL of methanol was injected on-column. Between injections of the oxidised/GP-derivatised cholesterol, different solvents were tested for their ability to flush this sterol from the injector and needle as described in section 3.7.

2.11 Analysis of oxysterols in biological samples

Biological samples

Rat brain

Fresh rat brain from female outbred 15-weeks-old Sprague Dawley, 306 g, (Harlan, UK) was kindly provided by Dr. John Turton and Dr. Sally Brady. The brain was weighed, and excised using a razor blade, and around 100 mg of brain pieces were transferred into siliconised eppendorf tubes. Samples were stored in -80^{0}C.

Embryonic central nervous system

Section of cortex (Ctx), ventral midbrain (VM) and spinal cord (SC) were dissected from 25 – 30 E11 CD1 (Charles River Breeding Laboratories) embryonic mouse brains in Karolinska Institutet, Stockholm, Sweden. Sections of CNS were processed at Karolinska Institutet as described in section 2.19 and the samples (Ctx, VM, and SC) were sent by mail to the School of Pharmacy, University of London, UK.

Primary cortical neurons

Primary cortical neurons were prepared from rat embryonic pups at day 19 (E19), cultured on poly-L-lysine coated plates using 10^8 cells per plate in neurobasal medium (Invitrogen, UK), containing B27 supplement, glutamine, penicilin/sterptomycin and glucose as described by Wang *et al.* [143]. The cultures contained less than 3% glial cells, as verified by

staining with antiglial fibrillary acidic protein (Sigma, UK), performed by Dr. Sabina Muneton from Department of Neuroscience, the School of Pharmacy, University of London.

Amniotic fluids

Amniotic fluid was provided by the Kennedy Krieger Institute, Johns Hopkins University, with Institutional Review Board approval. Subjects gave informed consent. Samples were stored in -80^0 C.

Blood spotted on filter paper (Blood spots)

Six blood spots from Smith-Lemli-Opitz syndrome (SLOS) affected patients were from whole venous blood spotted onto standard newborn screening cards and were provided by the Heritable Disorders Branch, National Institute of Child Health and Human Development, Besthesda with Institutional approval. These were provided to emulate newborn screening from Guthrie card samples, but were actually samples from older infants and children. Samples were stored in -20^0 C.

2.12 Extraction and enrichment of oxysterol from brain tissue

Oxysterols/sterols were extracted from rat brain as follows:- 100 mg of brain was homogenised in 1 mL of ethanol. Ethanol is a good solvent for oxysterols and readily penetrates cell membranes [48,163]. The ethanol extract was vortexed, placed in an ultrasonic bath for 10 min and then centrifuged for 5 min at 4,000 x*g*. The supernatant was retained. The residue was extracted again with 1 mL dichloromethane-methanol, 1:1 (v/v), and centrifuged for 5 min at 4,000 x*g*. The resulting supernatant was added to that retained previously. This solution is called the brain extract. The combined supernatants were dried by a stream of nitrogen. The residue was re-dissolved in 2 mL of hexane-dichloromethane (2:8, v/v).

After extraction of lipids from brain, cholesterol was separated from oxysterols in the earliest possible step to avoid the formation of autoxidation artifacts. The method used for the removal of cholesterol was evaluated as part of the optimisation process; aspects of this optimisation process are described in sections 2.14, 2.15 and 2.16. The original method was

obtained from the Karolinska Institutet, which was evaluated by Professor Jan Sjövall's group. The final method is detailed below.

2.13 Separation of the bulk of cholesterol from oxysterols

The removal of cholesterol was achieved on a straight-phase SPE column, where cholesterol was eluted with hexane-dichloromethane (fraction U1), while oxysterols were eluted in ethyl acetate (fraction U2). A Unisil (200-325 mesh, activated silicic acid) was packed to a height of 8 cm in a glass column 25 cm x 0.8 cm (i.d) with reservoir for 50 mL. The stationary phase was washed with 40 mL of hexane, followed by 40 mL of hexane-dichloromethane (2:8, v/v). After application of the sample prepared in 2 mL of hexane-dichloromethane (2:8, v/v), the column was washed with 80 mL of hexane-dichloromethane (2:8, v/v). The effluent was combined to give fraction U1 ("cholesterol fraction"). An oxysterol fraction was obtained by elution with 10 mL of ethyl acetate giving fraction U2 ("oxysterol fraction").

2.14 Evaluation of the separation of oxysterols from cholesterol

Initially, the performance of chromatographic separation of the bulk of cholesterol from oxysterols was evaluated for a mixture of 22R-hydroxycholesterol; 24S-hydroxycholesterol and cholesterol. 22R-Hydroxycholesterol and 24S-hydroxycholesterol (1 µL of each stock solutions in hexane-dichloromethane 2:8, v/v; 2.5 µg/µL) and cholesterol (1000 µL from a stock solution in hexane-dichloromethane 2:8, v/v; 1.3 µg/µL) were added to 998 µL hexane-dichloromethane (2:8, v/v). The experiment was carried out in triplicate. This solution was then applied to a Unisil SPE column (8 cm x 0.8 cm, 200-325 mesh, activated silicic acid) and chromatographed according to section 2.13. The eluate from both fractions, U1 and U2, was evaporated under a stream of nitrogen, and the residues were re-dissolved in 50 µL of isopropanol. The 3β-hydroxy-5-ene sterols were oxidised with cholesterol oxidase from *Streptomyces sp.* to their corresponding 3-oxo sterols (see section 2.4), which were then derivatised with GP reagent in the same flask (as in section 2.5), and the excess of GP reagent was separated from oxidised/GP-derivatised oxysterols by chromatography on a Sep-Pak C_{18} SPE column (see section 2.6). The samples were analysed by direct infusion nano-ES-MS^n, and capillary LC-MS^n

as described in sections 2.8 and 2.9. For LC-MS^n analyses, 1 µL of the combined methanol eluent (2 x 1 mL) from the SepPak C_{18} bed, was diluted in 99 µL of 63.5% methanol, 0.1% formic acid, and 1 µL of was injected on the LC column. Quantification of 24S- and 22R-hydroxycholesterols was performed by recording only MS^2 $[M]^+ \rightarrow$ spectra, and reconstructed ion chromatogram (RIC) was generated for the $[M]^+ \rightarrow [M-79]^+$ transition over the LC-MS^2 run.

2.15 Investigation of cholesterol autoxidation products formed during the sample preparation (Figure 2.3)

The analytical scheme, which was used for the isolation and analysis of oxysterols from rat brain is shown in Figure 2.3. Rat brain (50 mg) was added to 750 µg of [$^2H_7$] cholesterol (75 µL of a 1 µg/µL stock solution of [$^2H_7$] cholesterol in ethanol). The [$^2H_7$] cholesterol was supplied as 99% pure (according to TLC). The sample was homogenised in 1 mL of ethanol. Sterol and oxysterols were extracted as described in section 2.12. The brain extract in 2 mL of hexane-dichloromethane (1:1, v/v) was then applied to a Unisil SPE column, and chromatographed as described in section 2.13. Fractions U1 and U2 were collected, dried and re-dissolved in 50 µL of isopropanol, and oxidised with cholesterol oxidase (see section 2.4), and derivatised with GP reagent (see section 2.5), and excess of GP reagent was removed as described in section 2.6. The experiment was performed in triplicate.

For brain samples found to contain a significant amount of cholesterol in the ethyl acetate fraction (fraction U2), the eluate was dried, and reconstituted in 2 mL of hexane-dichloromethane (2:8, v/v), re-applied to a fresh Unisil column, and chromatographed as before (see section 2.13). Fraction U1 was discarded. Fraction U2 was dried under reduced pressure using a rotor-evaporator, and re-dissolved in 50 µL of isopropanol and the sample was processed further as described in sections 2.4, 2.5 and 2.6. The extracted GP derivatives from Sep-Pak C_{18} SPE column were then eluted with two portions of 1 mL of methanol (SPE-Fr1, -Fr2), followed by 1 mL of chloroform-methanol (1:1, v/v). The chloroform-methanol fraction was dried completely in a SpeedVac, and dissolved 1 mL of SPE-FR2, and the two fractions were then combined. The experiment was performed in triplicate. The resulting methanol fractions (2 x 1 mL) were analysed by direct infusion nano-ES-MS^n (see section 2.8), afterwards, by

capillary LC-MS^n (cap-LC-MS^n) (see section 2.9). For the analysis of oxidised/GP-derivatised labelled and unlabelled oxysterols, 2 µL of the combined methanol fraction (2 x 1 mL) from the Sep-Pak C_{18} SPE column was diluted with 48 µL of 63.5% methanol in water containing 0.1% formic acid, and 1 - 5 µL was injected onto the capillary LC column.

The elemental composition of labelled and unlabelled oxysterols can be predicted. MS, MS^2, and MS^3 spectra were recorded using programmed transitions for the expected oxidised/GP-derivatised oxysterols/sterols over the chromatographic separation period (as shown in section 2.9). MS^3 was programmed to be performed on ions resulting from a neutral loss of 79 and 107 Da in the MS^2 scan. The oxidised/GP-derivatised labelled and unlabelled oxysterols were identified from their MS, MS^2 and MS^3 spectra on the basis of mass, charge, and retention times.

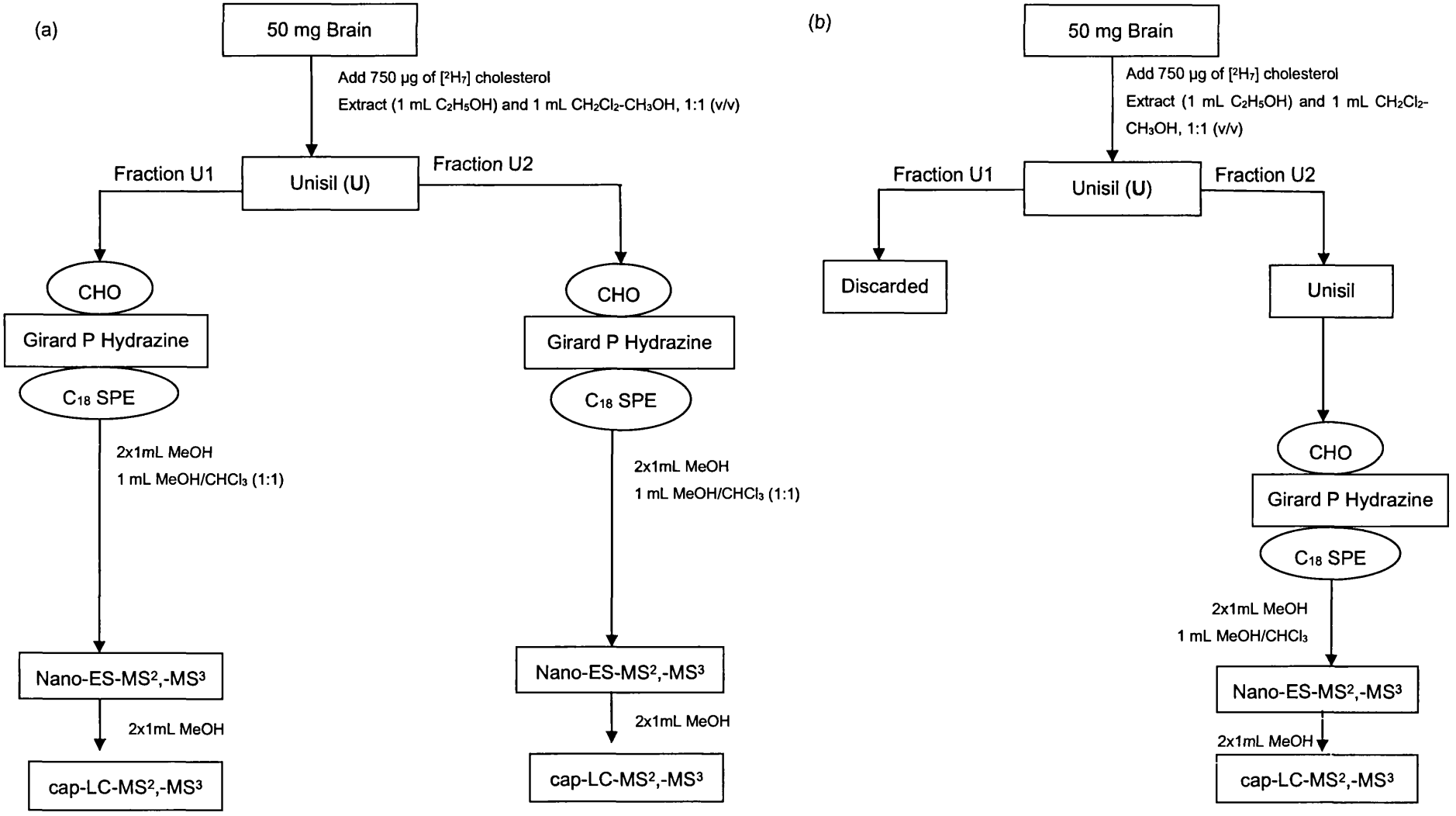

Figure 2.3 Workflow depicting the extraction, spiking with [²H₇] cholesterol, purification and analysis of oxysterols from rat brain
CHO= treatment with cholesterol oxidase from *Streptomyces sp.*; C_{18} SPE = a "recycling" C_{18} solid phase extraction chromatography (SPE);
Unisil = a straight-phase SPE chromatography

2.16 Sample preparation of rat brain

The sample preparation procedure for the profiling of oxysterols from rat brain is outlined in Figure 2.4.

Preparation of U1A fraction (Figure 2.4)

The brain extract in 2 mL hexane-dichloromethane 2:8, v/v, (see section 2.12) was loaded on the Unisil (8 x 0.8 cm, 200–325 mesh, activated silicic acid) SPE column and the "flow through" was collected into a 250 mL round bottom flask, and chromatographed as described in section 2.13. Fraction U1 was collected. This fraction U1 contains non-polar conjugated steroids, steryl esterss and the bulk of cholesterol. The cholesterol fraction was concentrated to around 1 mL in a rotary evaporator and then transferred quantitatively to a pre-washed 1.5 mL siliconised tube, and the remaining solvent was blown out by a gentle stream of nitrogen gas. The dry extract was reconstituted in 50 µL of isopropanol, and the resulting sample was subjected to oxidation with cholesterol oxidase (see section 2.4), followed by derivatisation with the GP hydrazine (see section 2.5), and the excess of GP reagent from GP hydrazones was separated by chromatography on a Sep-Pak C_{18} SPE column (see section 2.6).

Preparation of U1B fraction (Figure 2.4)

Another brain extract from the same rat in 2 mL hexane-dichloromethane, 2:8, v/v, (section 2.12) was loaded on a freshly prepared Unisil (8 x 0.8 cm, 200–325 mesh, activated silicic acid) SPE column, and chromatographed as previously described in section 2.13. The Unisil SPE column was washed with 80 mL hexane-dichloromethane (2:8, v/v). The fraction U1 and "flow through" were combined (U1B fraction). The U1B fraction was subjected to saponification procedure. The solvent from the combined fraction was dried in a rotor evaporator at room temperature. The residue was immediately re-dissolved in 2 mL of 5% (w/v) potassium hydroxide in methanol (0.89 M KOH), and incubated at 50^0C for 2 hours. The reaction mixture was then diluted with 0.5 mL of water, followed by neutralisation with 125 µL

acetic acid. The total volume of the resulting mixture was 2.63 mL. Now free sterols were subjected to extraction on the Sep-Pak C_{18} SPE column.

The Sep-Pak C_{18} material (1 x 0.8 cm) was packed into a glass column. The column was washed with 5 mL methanol, followed by 5 mL of 80% methanol in water. The U1B fraction was passed through the Sep-Pak C_{18} SPE column. The effluent was collected into a 50-mL flask. The column was washed with 1 mL of 40% methanol in water. The "flow through" and "wash" were combined and diluted with water to make a 40% methanol in water solution. The combined effluent (now 6.25 mL) was again recycled through the Sep-Pak C_{18} SPE column, followed by wash with 1 mL of 15% methanol. To the combined effluent (7.25 mL), 10.42 mL of water was added to give 17.67 mL of about 15% methanol. This was again applied to the Sep-Pak C_{18} SPE column, followed by wash with 10 mL of water. The sorbed sterols were then eluted with 3 mL of methanol into a 10-mL flask. The solvent was evaporated to approximately 1.5 mL in the rotor evaporator; the residue was transferred into 1.5 mL siliconised tube, and dried. The residue was re-dissolved in 2 mL hexane-dichloromethane (2:8, v/v) and applied to a fresh Unisil SPE column (8 x 0.8 cm, activated silica, 200-325 mesh) and chromatographed as described in section 2.13. The fraction U1 ("cholesterol fraction") was discarded. The fraction U2 ("oxysterol fraction") was dried, and dissolved in 50 µL of isopropanol. The resulting U1B sample was oxidised with cholesterol oxidase, and derivatised with GP hydrazine to GP hydrazones, followed by the reversed-phase SPE chromatography as described in sections 2.4, 2.5 and 2.6.

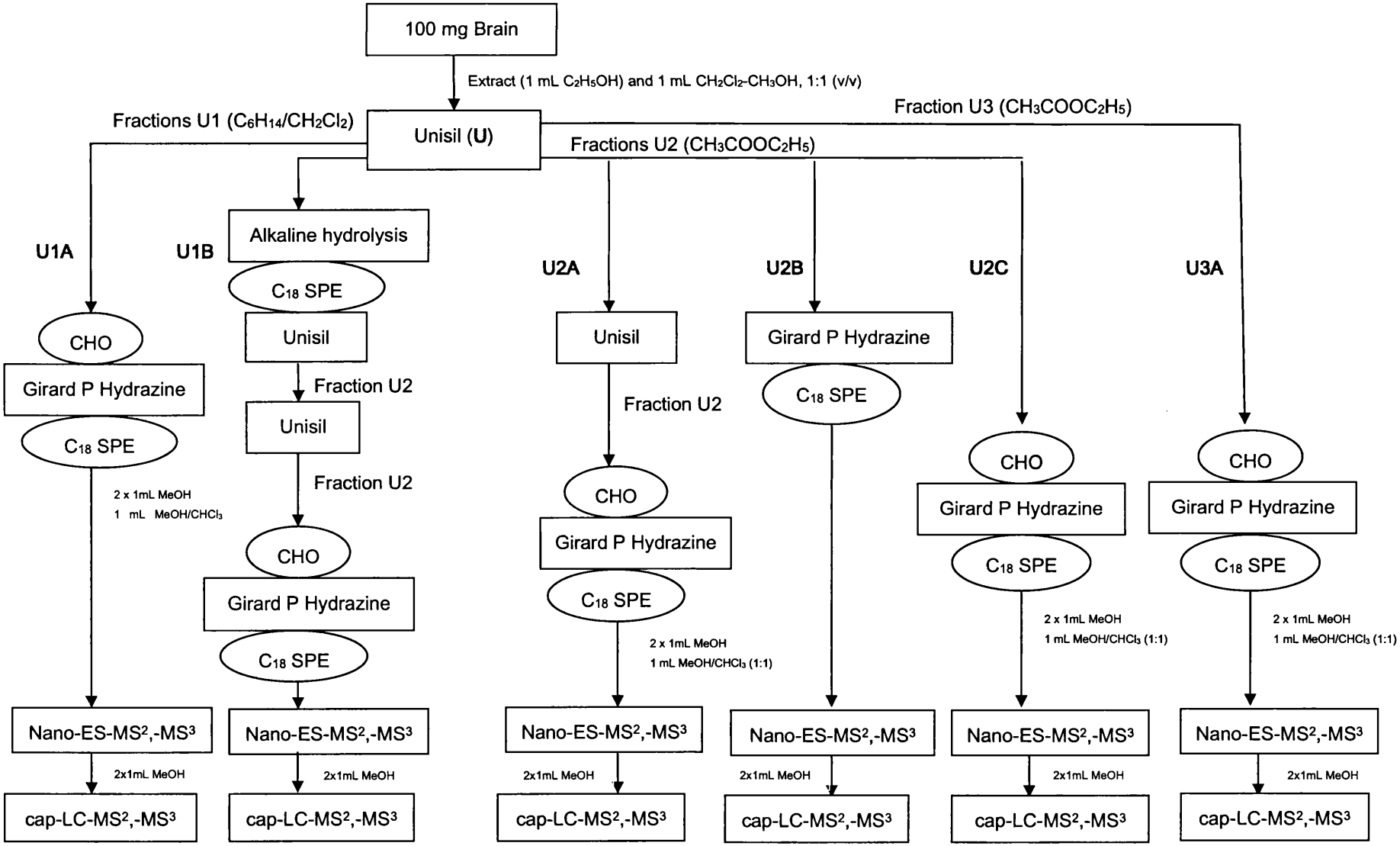

Figure 2.4 Workflow depicting the extraction, purification and analysis of oxysterols from rat brain

CHO= treatment with cholesterol oxidase from *Streptomyces sp.*; C_{18} SPE = a "recycling" C_{18} solid phase extraction (SPE); Unisil = a straight-phase SPE

Preparation of U2A, U2B, U2C and U3A fractions (Figure 2.4)

Following application of the brain extract to the Unisil column and a wash with 80 mL hexane-dichloromethane (2:8, v/v), polar analytes sorbed on the Unisil SPE column were stepwise eluted with two 10 mL portions of ethyl acetate to give fraction U2 and fraction U3, which are "oxysterol fractions" (Figure 2.4).

Three fractions U2 were prepared from 100 mg of the same rat brain, U2A, U2B and U2C. The ethyl acetate from each fraction U2 was evaporated to dryness in the rotor evaporator.

The U2A fraction was re-constituted in 2 mL of hexane-dichloromethane (2:8, v/v) and re-applied to a fresh Unisil SPE column and chromatographed as before (Section 2.13). The eluate from fraction U2 was dried, and the residue was re-dissolved in 50 µL of isopropanol. The U2A sample was then oxidised with cholesterol oxidase (see section 2.4).

The U2B fraction was re-constituted in 2 mL of methanol, followed by addition of 1 mL of water.

The U2C fraction was re-dissolved in 50 µL of isopropanol. The U2C fraction was subjected to oxidation with cholesterol oxidase procedure (see section 2.4).

The derivatisation with GP reagent protocol was applied to U2A, U2B and U2C samples (Section 2.5). The resulting oxidised/GP-derivatised oxysterols were then separated from excess of GP reagent by extraction on a Sep-Pak C_{18} SPE column (see section 2.6).

The fraction U3 was prepared for the evaluation of oxysterols extraction efficiency from the Unisil SPE column. The solvent from the U3A fraction was evaporated. The residue was re-dissolved in 50 µL of isopropanol. 3β-Hydroxy-5-ene groups were converted to 3-oxo-4-enes, and 3β-hydroxy-5α-hydrogen groups were converted to 3-oxo groups by cholesterol oxidase, both oxo-groups were reacted with GP hydrazine (see sections 2.4 and 2.5). The resulting GP hydrazones were then separated from excess GP reagent by extraction on a Sep-Pak C_{18} SPE column (see section 2.6).

2.17 Mass spectrometry analysis of oxysterols/sterols from rat brain (Figure 2.4)

In the first instance, all samples obtained according to Figure 2.4 were analysed by direct infusion nano-ES-MS^n on the LCQ^{duo} ion trap where 5 µL of the methanol fraction was loaded into a metal coated nanospray capillary and electrosprayed into the ion-trap as described in section 2.8, afterwards, by capillary LC-MS^n (cap-LC-MS^n) as described in section 2.9.

For sterol quantification, 5 µL of the combined methanol fraction (2 x 1 mL) from the Sep-Pak C_{18} SPE column (equivalent to 0.25 mg of brain) was diluted with 35 µL of 63.5% methanol in water containing 0.1% formic acid, and 1 - 5 µL was injected onto the capillary LC column (equivalent to 6.25 to 31.25 µg of brain).

The elemental composition of oxysterols can be predicted as oxysterols by definition are cholesterol metabolites with additional oxygen functionalities and/or changed carbon skeleton. Over the chromatographic separation period MS, MS^2, MS^3 spectra were recorded using a programmed transitions for the expected oxidised/GP-derivatised sterols as described in section 2.9. The oxidised/GP-derivatised sterols extracted from biological samples were identified from their MS, MS^2 and MS^3 spectra on the basis of mass, charge, and retention times.

2.18 The relative quantification of 24S-hydroxycholesterol in rat brain by capillary LC-MS analysis

An ethanolic solution of 22R-hydroxycholesterol (20 µg in 10 µL) or ethanol (10 µL, blank sample) was added to the rat brain (54 mg). The experiment was perfomed in triplicate. Lipids were extracted as described in section 2.12. Oxysterols were then enriched using straight-phase chromatography as described in section 2.13. The fraction U1 ("cholesterol fraction"), from the Unisil SPE column, was discarded. The solvent from fraction U2 ("oxysterol fraction") was evaporated under a stream of nitrogen. The residue was re-dissolved in 50 µL of isopropanol. Sterols with 3β-hydroxy-5-ene and 3β-hydroxy-5α-hydrogen structures were converted by cholesterol oxidase to the corresponding sterols with 3-oxo-4-ene and 3-oxo groups; oxo groups were reacted with GP hydrazine as described in sections 2.4 and 2.5. The resultant oxidised/GP-derivatised sterols were then separated from excess of GP reagent by extraction on a Sep-Pak C_{18} SPE column as described in section 2.6. The oxidised/GP-

derivatised oxysterols were then separated by reversed phase capillary LC using a methanol-water gradient as described in section 2.9.

For brain samples found to contain a significant amount of cholesterol in the ethyl acetate fraction (fraction U2), the eluate was dried, and reconstituted in 2 mL of hexane-dichloromethane (2:8, v/v), re-applied to a fresh Unisil column, and chromatographed as before (see section 2.13). Fraction U1 was discarded. Fraction U2 was dried under reduced pressure using a rotor-evaporator, and re-dissolved in 50 µL of isopropanol and the sample was processed further as described in sections 2.4, 2.5 and 2.6.

For the initial identification of monohydroxycholesterols in rat brain, MS, MS^2 (534→), and MS^3 (534→455→) spectra were recorded on the LCQ^{duo} ion trap. For cap-LC-MS^n analysis, 5 µL of the methanol eluent (2 x 1 mL) from the SepPak C_{18} column was diluted with 35 µL of 63.5% methanol, 0.1% formic acid, and 5 µL was injected onto the LC column (equivalent to 15.63 µg of brain).

For the quantification of 24S-hydroxycholesterol, 1 µL of the combined methanol eluent (2 x 1 mL) from the SepPak C_{18} bed was diluted in 99 µL of 63.5% methanol 0.1% formic acid, and 1 µL of was injected on the LC column, and MS^2 534→ spectra were recorded. Reconstructed ion chromatogram (RIC) was generated for the $[M]^+ \rightarrow [M-79]^+$ (534→455) transition over the duration of the LC-MS^2 run. Each sample was analysed in triplicate. The relative amount of 24S-hydroxycholesterol in the sample was directly determined by comparing the area under the chromatographic peak of the oxidised/GP-derivatised 24S-hydroxycholesterol (A_{24}) to the area under the chromatographic peak of the oxidised/GP-derivatised 22R-hydroxycholesterol (A_{22}), (A_{24}/A_{22} ratio).

2.19 Sample preparation and analysis of oxysterols in embryonic E11 mouse central nervous system (CNS) (Figure 2.5)

The sample preparation procedure for the profiling of oxysterols from embryonic E11 mouse CNS is outlined in Figure 2.5. Sections of CNS were processed essentially as described in sections 2.12, 2.13 in Karolinska Institutet, Stockholm, Sweden. In brief, samples of CNS (186 mg cortex, 119 mg spinal cord and 100 mg ventral midbrain) were extracted with ethanol

and dichloromethane-methanol (1:1, v/v), taken to dryness and dissolved in hexane-dichloromethane (2:8, v/v). This solution was passed through previously pre-washed Unisil SPE column, as described in section 2.13. Fractions U1 and U2 were collected, dried and derivatised to trimethylsilyl (TMS) ethers [14]. These samples were then analysed by GC-EI-MS using a dimethyl silicone column in Karolinska Institutet, Sweden.

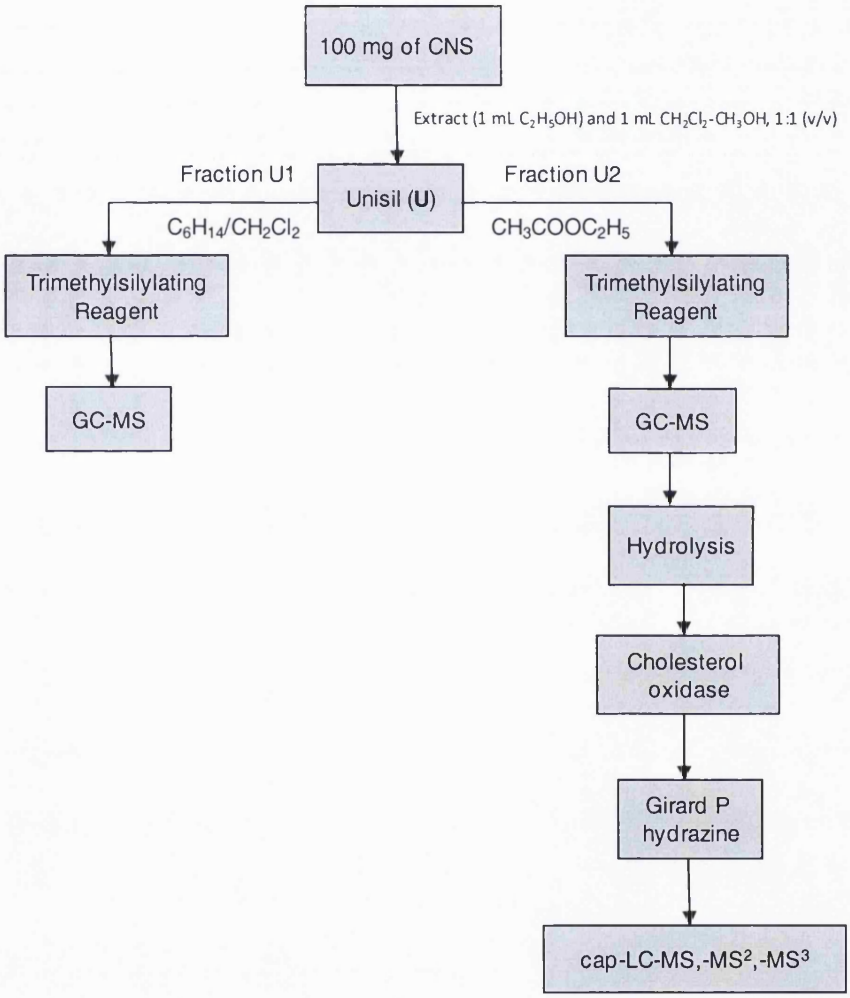

Figure 2.5 Workflow depicting the extraction, purification and analysis of oxysterols from embryonic E11 mouse CNS.

Following GC-MS analysis, the TMS ethers were hydrolysed with dilute hydrochloric acid (HCl), and dried and sent to the School of Pharmacy, University of London, where the samples were prepared for capillary LC-MS^n analysis. The samples were re-constituted in 50 µL of isopropanol, and incubated with cholesterol oxidase from *Streptomyces sp.* (2 mg/mL, 44 U/mg protein) as described in section 2.4. The reaction was stopped with 2 mL of methanol, and the reaction mixture was subjected to derivatisation procedure as described in section 2.5.

Oxidised/GP-derivatised sterols from fraction U1 and oxysterols from fraction U2 were then separated from excess of GP reagent by solid phase extraction (SPE) on a C_{18} column as described in section 2.6. GP derivatives were eluted in 2 mL of methanol, SPE-Fr1 and -Fr2. The most hydrophobic sterols were eluted in a further 1 mL of chloroform-methanol (1:1, v/v). The chloroform-methanol fraction was dried in a Speed Vac, reconstituted in 1 mL of SPE-Fr1 and -Fr2, and the two fractions were combined.

The oxidised/GP-derivatised sterols from embryonic CNS were analysed by direct-infusion nano-ES-MS^n as described in section 2.8, and by capillary LC-MS^n as described in section 2.9. For capillary LC-MS^n analyses, 20 µL of the combined methanol eluate from the C_{18} SPE column was diluted with 11.25 µL of 0.33% formic acid to give a 64% methanol solution containing 0.1% formic acid, and 1 - 5 µL of the resultant solution injected onto a C_{18} capillary column.

2.20 Sample preparation and analysis of oxysterols in cortical neurons (Figure 2.6)

The medium (10 mL) was separated from the cells and diluted with 2 mL of 2 M triethylamine sulphate. The solution was incubated for 5 min at 64°C, and then was passed through a Sep-Pak C_{18} SPE column (2 cm x 0.8 cm) followed by a wash with 10 mL of water. Prior to the sample application the Sep-Pak C_{18} SPE column was washed with 10 mL of methanol, followed by 10 mL of water. Sterols were eluted from the Sep-Pak C_{18} SPE column with 10 mL of methanol. The methanol fraction was dried under reduced pressure using a rotor-evaporator. The residue was dissolved in 2 mL of hexane-dichloromethane (2:8, v/v). Sample was applied to a silicic acid (Unisil) column in hexane-dichloromethane (2:8, v/v), and chromatographed as described in section 2.13. The cholesterol U1 and oxysterol U2 fractions were taken to dryness. The residue from both fractions was dissolved in 50 µL of isopropanol. Sterols with a 3β-hydroxy-5-ene and 3β-hydroxy-5α-hydrogen structure were then converted to their corresponding sterols with 3-oxo-4-ene or 3-oxo groups by oxidation with cholesterol oxidase from *Streptomyces sp.* as described in section 2.4. The resulting mixture was then derivatised with Girard P hydrazine, and the excess of GP hydrazine was separated from

oxidised/GP-derivatised sterols by extraction on a Sep-Pak C_{18} column as described in sections 2.5 and 2.6.

The cells were suspended in 5 mL of ethanol, and vortexed for 3 min. The ethanol extract was placed in an ultrasonic bath for 15 min, and was then incubated for 5 min at 64^{0}C in a water bath. The ethanol extract was diluted with 5 mL of water to give a 50% ethanol solution, and was then centrifuged for 5 min at 12,000 x *g* to allow the formation of a pellet. The supernatant was separated from the pellet. The supernatant (10 mL) was passed through a Sep-Pak C_{18} SPE column (2 cm x 0.8 cm). After a wash with 10 mL of water, the compounds extracted were eluted with 10 mL of methanol (SPE-Fr1, Figure 2.6) and 10 mL of methanol-chloroform (1:1, v/v) (SPE-Fr2, Figure 2.6). The cells of the pellet were further extracted with 5 mL of isopropanol-hexane (1:1, v/v) in an ultrasonic bath for 15 min. Sample was centrifuged at 12,000 x*g* for 5 min. After centrifugation, this extraction was repeated; the two extracts were combined with the eluate from the Sep-Pak C_{18} SPE column. The solvent (30 mL) was taken to dryness in a rotor-evaporator. The residue was dissolved in 2 mL of hexane-dichloromethane (2:8, v/v), and purified by chromatography on a column (8 cm x 0.8 cm) of Unisil packed in hexane and washed with 40 mL of hexane-dichloromethane (2:8, v/v) before use as described in section 2.13. Each fraction (U1 and U2) was dried under reduced pressure using a rotor-evaporator. The residue from both fractions was re-dissolved in 50 µL of isopropanol. The sterols in each fraction were oxidised with cholesterol oxidase as described in section 2.4 and derivatised with the Girard P reagent as described in 2.5. Oxidised/GP-derivatised sterols from fraction U1 and oxysterols from fraction U2 were then separated from excess GP-reagent by solid phase extraction (SPE) on a C_{18} column as described in section 2.6. GP derivatives were eluted in 2 mL of methanol (2 x 1 mL, SPE-Fr1, -Fr2). The most hydrophobic sterols were futher eluted in a further 1 mL of chloroform-methanol (1:1, v/v), SPE-Fr3. The three fractions were analysed separately by direct infusion nano-ES-MS^n (see section 2.8). The GP derivatives were found predominantly in SPE-Fr1 and -Fr2. The chloroform-methanol fraction was dried completely in a Speed Vac, and dissolved 1 mL of SPE-Fr2. For the initial identification of

sterols, SPE-Fr1 and SPE-Fr2 were analysed separately by cap-LC-ES-MS^n analysis. For sterols quantification by cap-LC-ES-MS^n analysis, the two fractions SPE-Fr1 and SPE-Fr2 were combined, and 63 µL of the methanol eluent (2 x 1 mL) from the Sep-Pak C_{18} column was diluted with 37 µL of 0.25% formic acid to give a 63% methanol solution containing 0.1% formic acid, and 2-5 µL injected onto the capillary LC column and analysed as described in section 2.9.

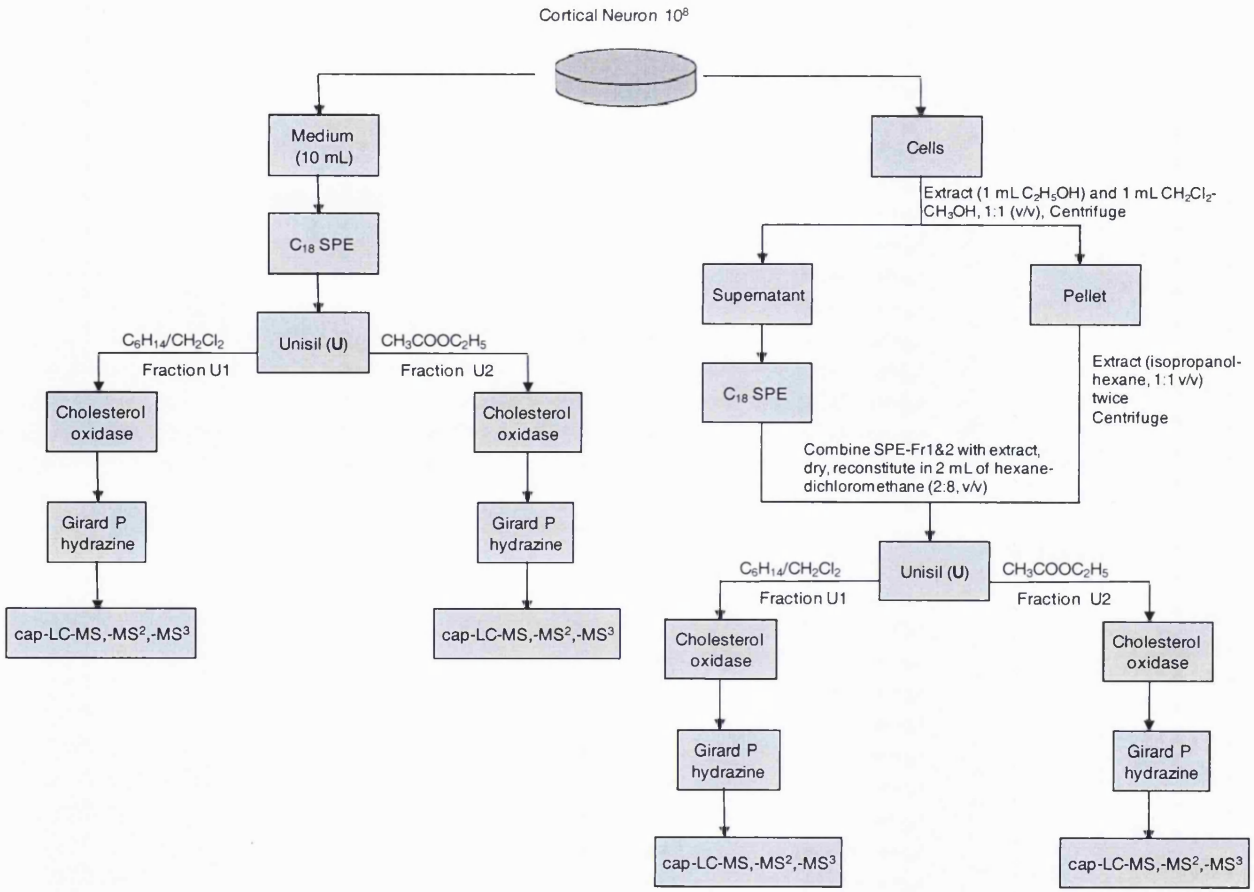

Figure 2.6.Workflow depicting the extraction, purification and analysis of oxysterols from primary cortical neurons. Unisil = a straight-phase SPE, Cholesterol oxidase = treatment with cholesterol oxidase from *Streptomyces sp.*; C_{18} SPE = reversed-phase solid phase extraction (SPE), Girard P = derivatisation with Girard P hydrazine.

2.21 Sample preparation and analysis of sterols in amniotic fluids (Figure 2.7)

Figure 2.7 shows the sample preparation procedure for the analysis of sterols derived from amniotic fluid. In brief, 25 ng of [$^2H_7$]-cholesterol (10 µL of a 2.5 ng/µL stock solution of [$^2H_7$]-cholesterol in ethanol) as the internal standard was added to 10 µL of amniotic fluid, followed by 2.5 µL of cholesterol oxidase from *Streptomyces sp.* (2 mg/mL, 44 U/mg protein) in 1 mL of buffer (50 mM KH_2PO_4 pH 7). The reaction mixture was incubated at 37^{0}C for 60 min in a water bath. The reaction was stopped with 2 mL of methanol, and 150 mg of GP hydrazine and 150 µL of glacial acetic acid were added. The mixture was left at room temperature overnight. The sterol GP hydrazones were then separated from excess reagent by extraction on a Sep-Pak C_{18} SPE column utilising a "recycling" method as described in section 2.6. The extracted GP hydrazones from the reversed-phase SPE column were then eluted with two portions of 1 mL of methanol (SPE-Fr-1, and SPE-Fr-2), followed by 1 mL of chloroform-methanol (1:1, v/v) (SPE-Fr-3). The chloroform-methanol fraction (SPE-Fr-3) was blow down, reconstituted in the methanol fraction (SPE-Fr-2), and the two fractions (SPE-Fr-1 and SPE-Fr-2) then combined.

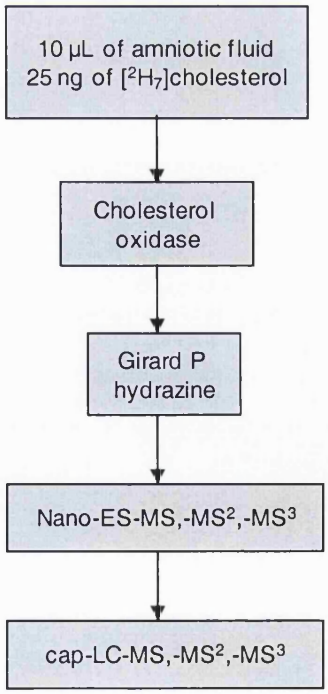

Figure 2.7 Workflow depicting analysis of oxysterols from amniotic fluid.

Capillary-LC-ES-MS^n method was evaluated utilising the same LC-MS system and its configuration, as described in section 2.9. Mass spectra were recorded by the LCQ^{duo} ion trap mass spectrometer. Six µL of the combined methanol fractions (equivalent to 20 nL of amniotic fluid) were diluted with 4 µL of 0.25% formic acid to give a 60% methanol solution containing 0.1% formic acid, and 1 - 3 µL injected (equivalent to 0.003 - 0.01 µL of amniotic fluid) onto a PepMap C_{18} column (180 µm x 150 mm, 3 µm, 100Å, Dionex, Surrey, UK) using a WPS 3000 well plate autosampler, part of a Ultimate 3000 Capillary HPLC system (Dionex). The mobile phases and gradient were the same as described in section 2.9.

For the initial identification of sterols in amniotic fluid, MS, MS^2 $[M]^+\rightarrow$, and MS^3 $[M]^+\rightarrow[M-79]^+\rightarrow$ and $[M]^+\rightarrow[M-107]^+\rightarrow$ spectra were recorded on the LCQ^{duo} ion trap mass spectrometer. LC-MS ion chromatograms were profiled for all potential sterols/oxysterols. For the acquisition of both MS^2 and MS^3 spectra the instrumental parameters were the same as described in section 2.9.

For the quantification of sterols only MS^2 spectra were recorded, and reconstructed ion chromatograms (RICs) generated for the $[M]^+\rightarrow[M-79]^+$ transitions over the duration of the LC-MS^2 run.

2.22 Sample preparation and mass spectrometry analysis of sterols from stored filter paper blood specimens

For blood spot analysis, a 10 mm diameter sample was punched from the filter paper and sliced into small pieces, and 100 µL of isopropanol was added. The sample was vortexed for 5 min, and placed in an ultrasonic bath for 10 min, followed by addition of 1 mL of buffer (50 mM KH_2PO_4 pH 7) containing 2.5 µL of cholesterol oxidase from *Streptomyces sp.* (2 mg/mL, 44 U/mg protein). After 1 hour at 37°C the reaction mixture was used as the starting solution for reaction with the Girard P hydrazine reagent. After dilution with 2 mL of methanol, 150 mg of GP hydrazine and 150 µL of acetic acid were added and the mixture left at room temperature overnight. Oxidised/GP-derivatised sterols/oxysterols were then separated from excess reagent by SPE on a C_{18} column as described in section 2.6. GP derivatives were eluted in 2 mL of methanol (SPE-Fr1, -Fr2). The most

hydrophobic sterols were further eluted in a further 1 mL of chloroform-methanol (1:1, v/v). The chloroform-methanol (SPE-Fr3) fraction was dried completely in a Speed Vac, and sterols were re-dissolved in 1 mL of SPE-Fr2, the sample was vortexed for 2 min.

Sterols in blood spots were analysed by direct infusion nano-ES-MS^n on the LCQ^{duo} ion trap following oxidation/derivatisation, where 5 µL of the combined methanol fractions (5/2000 of the blood spot) was loaded into a metal coated nano-spray capillary and electrosprayed into the ion-source. MS, MS^2 and MS^3 spectra were recorded as described in section 2.8.

Chapter 3

Analysis of reference sterols

3. *Introduction*

Oxysterols are oxygenated derivatives of cholesterol [38,81,164]. The formation of oxysterols constitutes the first step in cholesterol metabolism, they being ultimately converted to bile acids in the liver [31,81,151,162]. Oxysterols are more membrane soluble than cholesterol, can cross the blood-brain barrier, and can be regarded as transport forms of cholesterol. In addition, oxysterols have biological activity, and have been shown *in vitro* to activate the liver X receptors (LXRs) [14,35,37,92]. Oxysterols are present in a matrix of other lipids in biological systems, and are difficult to analyse by atmospheric pressure ionisation mass spectrometry on account of the absence of basic or acidic functional groups in their structures. Hence, it is advisable to apply specific group separation procedures prior to mass spectrometric analysis, followed by derivatisation, to enhance sensitivity, and with LC separation to allow the analysis of individual isomeric compounds. A method for the oxidation/derivatisation of oxysterols prior to LC-MS analysis has been established by Griffiths *et al.* at Karolinska Institutet [38], and this study is a continuation of the method development, and its application for the profiling of oxysterols in biological samples. The method is specific in that only sterols with a 3β-hydroxy-5-ene and 3β-hydroxy-5α-hydrogen structure are oxidised by cholesterol oxidase to their 3-oxo-4-ene and 3-oxo equivalents, which are subsequently derivatised with Girard P (GP) hydrazine, and analysed as their GP-hydrazones (see Figure 3.1). The oxidised/GP-derivatised oxysterols possess a quaternary nitrogen, and are readily analysed by electrospray mass spectrometry. Furthermore, tandem mass spectrometry provides high specificity, and structural information.

This chapter describes the development and validation of direct infusion nano-ES multi-stage mass spectrometry (ES-MS^n), and capillary LC multi-stage tandem mass spectrometry (cap-LC-MS^n) analyses of oxidised/GP-derivatised reference oxysterols/sterols.

Forty reference oxysterols were oxidised and derivatised to GP hydrazones. In the first experiments, GP hydrazones were directly infused into the ion trap mass spectrometer, and secondly after they were passed through a reversed phase capillary column, and in both cases

nano-ES-MS, -MS^2, and -MS^3 spectra were recorded. Mass spectra were recorded from fg to pg amounts of the GP hydrazones injected on the C_{18} capillary column. A library of oxidised/GP-derivatised reference oxysterols was created, consisting of MS, MS^2 $[M]^+ \rightarrow$ and MS^3 $[M]^+ \rightarrow [M-79]^+$ and $[M-107]^+ \rightarrow$ spectra, and their relative retention times to the oxidised/GP-derivatised cholesterol. The identification of oxysterols in biological samples were made by comparison of their relative retention time and MS, MS^2 and MS^3 spectra with authentic standards.

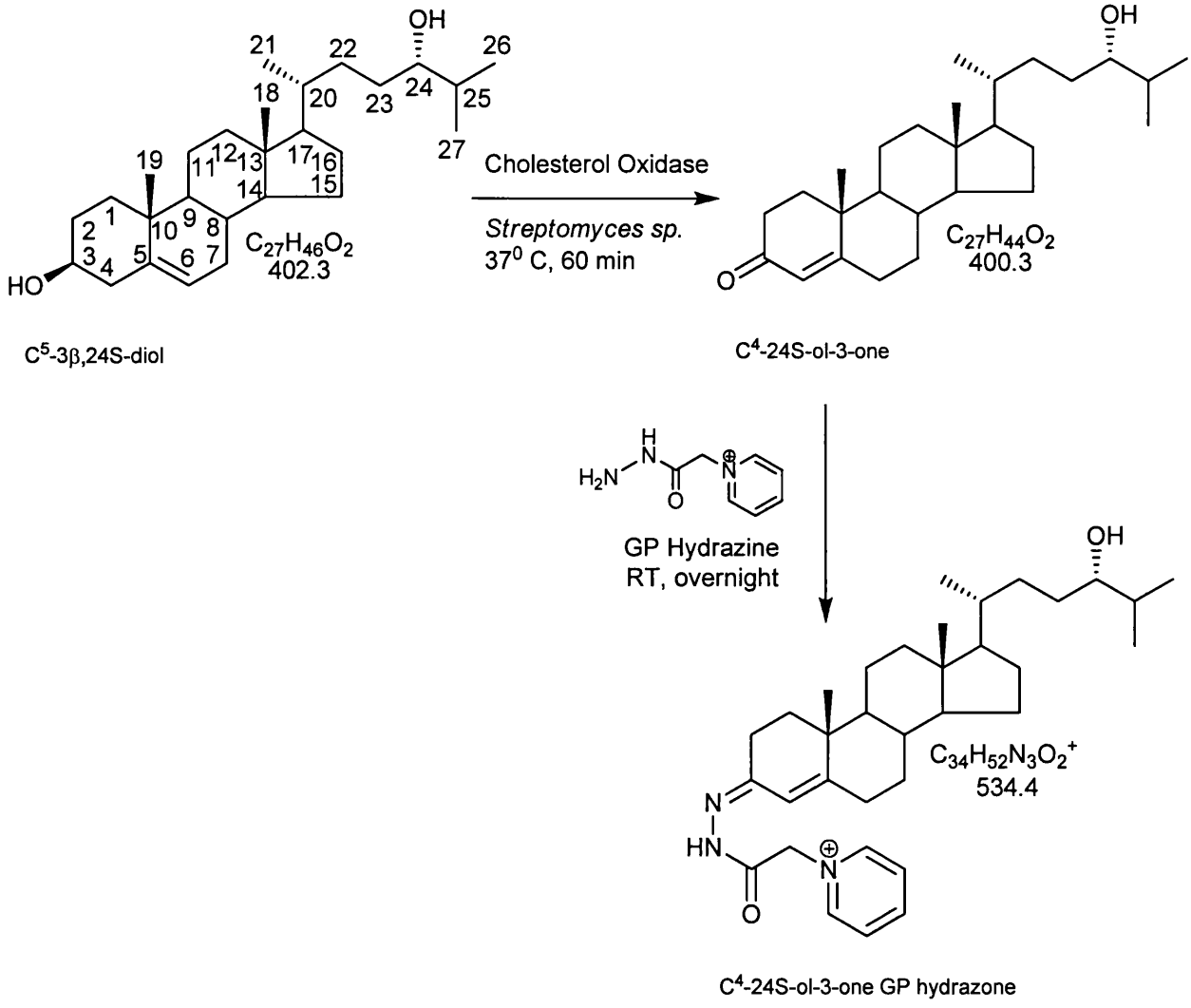

C^4-24S-ol-3-one GP hydrazone

Figure 3.1 Oxidation of oxysterols with cholesterol oxidase, followed by derivatisation with GP hydrazine. 24S-Hydroxycholesterol (C^5-3β,24S-diol) is used as an example. The 3β-hydroxyl group of C^5-3β,24S-diol is converted to the 3-oxo of C^4-24S-ol-3-one by cholesterol oxidase from *Streptomyces sp.* The oxo group of C^4-24S-ol-3-one was then derivatised with Girard P hydrazine to give C^4-24S-ol-3-one GP hydrazone.

3.1 Oxysterols oxidation with cholesterol oxidase and derivatisation with GP hydrazine

Derivatisation chemistry is gaining popularity for analysis of sterols by electrospray (ES) mass spectrometry [14,55], because underivatised oxysterols have low ionisation efficiencies by ES. Griffiths *et al.* [101] has developed derivatisation chemistry for analysis of oxosteroids possessing an oxo group. The oxo group was derivatised with the Girard P reagent ([1-(2-hydrazino-2-oxoethyl)pyridinium chloride]) to give Girard P (GP) hydrazone. The derivatisation method allows the formation a covalent bond to a moiety containing a permanent positively charged nitrogen atom in order to improve the ES sensitivity. The interest of this study is oxysterols, which do not possess an oxo group (e.g. 24S-hydroxycholesterol is the most abundant oxysterol in the human brain, 5-15 ng/mg) [165], and are not derivatised by GP hydrazine. However, sterols and steroids with a 3β-hydroxy-5-ene group or a 3β-hydroxy-5α-hydrogen stereochemistry, when treated with cholesterol oxidase are converted to 3-oxo-4-ene and 3-oxo sterols, respectively as described by Brooks *et al.* [102], MacLachlan *et al.* [166], and Griffiths *et al.* [38]. The previously described procedure by Griffiths *et al.* [38] was optimised for the oxidation of 3β-hydroxy-5-ene or 3β-hydroxy-5α-hydrogen sterols using *Brevibacterium*, to make it compatible with ES-MS analysis. In the current study cholesterol oxidase from *Streptomyces sp.* rather than *Brevibacterium* was selected. This enzyme, also converts 3β-hydroxy-5-ene or 3β-hydroxy-5α-hydrogen sterols to 3-oxo-4-ene or 3-oxo sterols but, unlike the enzyme from *Brevibacterium,* is commercially available. The oxidised sterols now possessing an oxo group are then readily derivatised with the commercially available Girard P reagent [38,57,166,167]. The derivatisation reaction with the Girard P hydrazine was carried out directly on the products of the cholesterol oxidase reaction, without any further purification or extraction (see Figure 3.1).

In summary, the oxidation/GP-derivatisation reactions proceed efficiently for the 3β-hydroxy-5-ene and 3β-hydroxy-5α-hydrogen sterols giving 3-GP hydrazones of the 3-oxo sterols (Figure 3.1). The incorporation of the GP hydrazone group into the 3-oxo sterol structure increases the mass of the sterol ion by 134 Da. Once oxysterols are oxidised and then derivatised, the

resulting GP hydrazones were readily separated from excess GP hydrazine by solid-phase extraction (SPE) on a reversed-phase (C_{18}) SPE column. The reference oxysterols were analysed after oxidation/GP-derivatisation and SPE by direct infusion nano-ES and capillary LC and MS, MS^2 and MS^3 spectra were recorded for both analyses (Supplementary Materials Figures 1-40).

3.2 Optimisation of the LCQ^{duo} mass spectrometer instrument parameters for the analysis of oxidised/GP-derivatised oxysterols

There are several scan types available when deciding on an instrument method for the collection of oxysterol data. The mass spectrometer can be configured for automatic data collection or data can be collected manually. The LCQ^{duo} ion trap mass spectrometer does not have high mass accuracy. However, the instrument has the capability to perform multi-stage fragmentation scans (MS^n), and this method was utilised for the structure elucidation of oxidised/GP-derivatised sterols in this work. However, a full MS scan was used to determine the molecular weight of the compounds.

In MS^n scan, ion selection, activation and the subsequent analysis of the fragment-ions were all carried out in the ion-trap. The ions formed in the nano-ES source were stored in the ion-trap. The precursor ion, $[M]^+$, was then held in the ion-trap, while all others were ejected from the trap. The $[M]^+$ ion corresponds to a singly charged ion of the oxidised/GP-derivatised oxysterol. The $[M]^+$ ion was activated to fragment, and the resulting fragment-ions were stored in the ion-trap, and then were sequentially scanned out of the ion-trap towards the detector to generate a MS^2 spectrum. The precursor ion fragmented with the loss of 79 Da and 107 Da to give a dominant pair of fragment ions $[M-79]^+$ and $[M-107]^+$ in a first fragmentation event (MS^2). The MS^2 experiment is summarised as follows: MS^2 $[M]^+ \rightarrow$. Alternatively, one of the fragment ions ($[M-79]^+$ or $[M-107]^+$) is held in the ion-trap, while the others were ejected, the selected fragment-ion was then activated, and its fragment-ions were scanned out of the ion-trap to generate a MS^3 spectrum. MS^3 experiments are summarised as follows: MS^3 $[M]^+ \rightarrow [M-79]^+ \rightarrow$ or MS^3 $[M]^+ \rightarrow [M-107]^+ \rightarrow$. Zoom scan was performed for the determination of the charge state and molecular weight of an ion.

The MS, MS^n scans, and zoom scans can be combined in various ways for the collection of data. Initially, data was collected manually. The reference oxysterols after oxidation/GP-derivatisation were analysed by direct infusion nano-ES, and manually performing the following scans: MS, MS^2, MS^3, zoom scans. The LCQ^{duo} mass spectrometer was subsequently programmed to automatically selected ions, and to perform the necessary analysis. This was found to be a more effective way of obtaining data. Several approaches to automatic data collection can be designed using different combinations of MS, MS^n, and zoom scans. For example, the data collection experiment used for the oxidised/GP-derivatised 24S-hydroxycholesterol described below involved repeating the programmed scan events for the duration of the analysis time.

Full scan of *m/z* 50-700
Zoom scan on 534
MS^2 534 →
MS^3 534 → 455 →
MS^3 534 → 427 →

3.3. Analysis of reference oxysterols by direct-infusion nano-ES

The oxidised/GP-derivatised oxysterols contain a quaternary nitrogen, and exist as ions in solution. The quaternary nitrogen in the Girard P hydrazone is part of a pyridine ring (Figure 3.1). The oxidised/GP-derivatised oxysterols generate single positively charged, $[M]^+$ ions. Hence, their mass-to-charge ratios are equivalent to their molecular mass. The oxidised/GP-derivatised cholesterol gives a $[M]^+$ ion at *m/z* 518, monohydroxycholesterol at *m/z* 534 (for example the oxidised/derivatised 24S-hydroxycholesterol, Figure 3.2a), dihydroxycholesterol (for example the oxidised/derivatised 7β,25-dihydroxycholesterol, (Figure 3.3b), at *m/z* 550, 3β-hydroxycholestenoic acid at *m/z* 548 and 3β,7-dihydroxycholestenoic acid at *m/z* 564.

Sterols with the 3β-ol-5-ene structure were successfully oxidised and derivatised with the GP reagent. For example, 22R-hydroxycholesterol (C^5-3β,22R-diol), 24S-hydroxycholesterol (C^5-3β,24S-diol), 25-hydroxycholesterol (C^5-3β,25-diol), and desmosterol ($C^{4,24}$-3β-ol) were oxidised

and derivatised to C^4-22R-ol-3-one GP, C^4-24S-ol-3-one GP, and C^4-25-ol-3-one GP, $C^{4,24}$-3-one GP hydrazones, respectively.

Nano-ES mass spectra of the oxidised/GP-derivatised 3β,7β-dihydroxycholest-5-en-27-oic acid and 24S-hydroxycholesterol recorded using the LCQ^{duo} ion trap instrument, are shown in Figures 3.2a,b. The plant sterol, campesterol (C^5-24α-methyl-3β-ol) was oxidised and derivatised to a 3-oxo-4-ene-3-GP hydrazone, and the nano-ES mass spectrum yields intense $[M]^+$ ions at *m/z* 532 (Figure 3.3a).

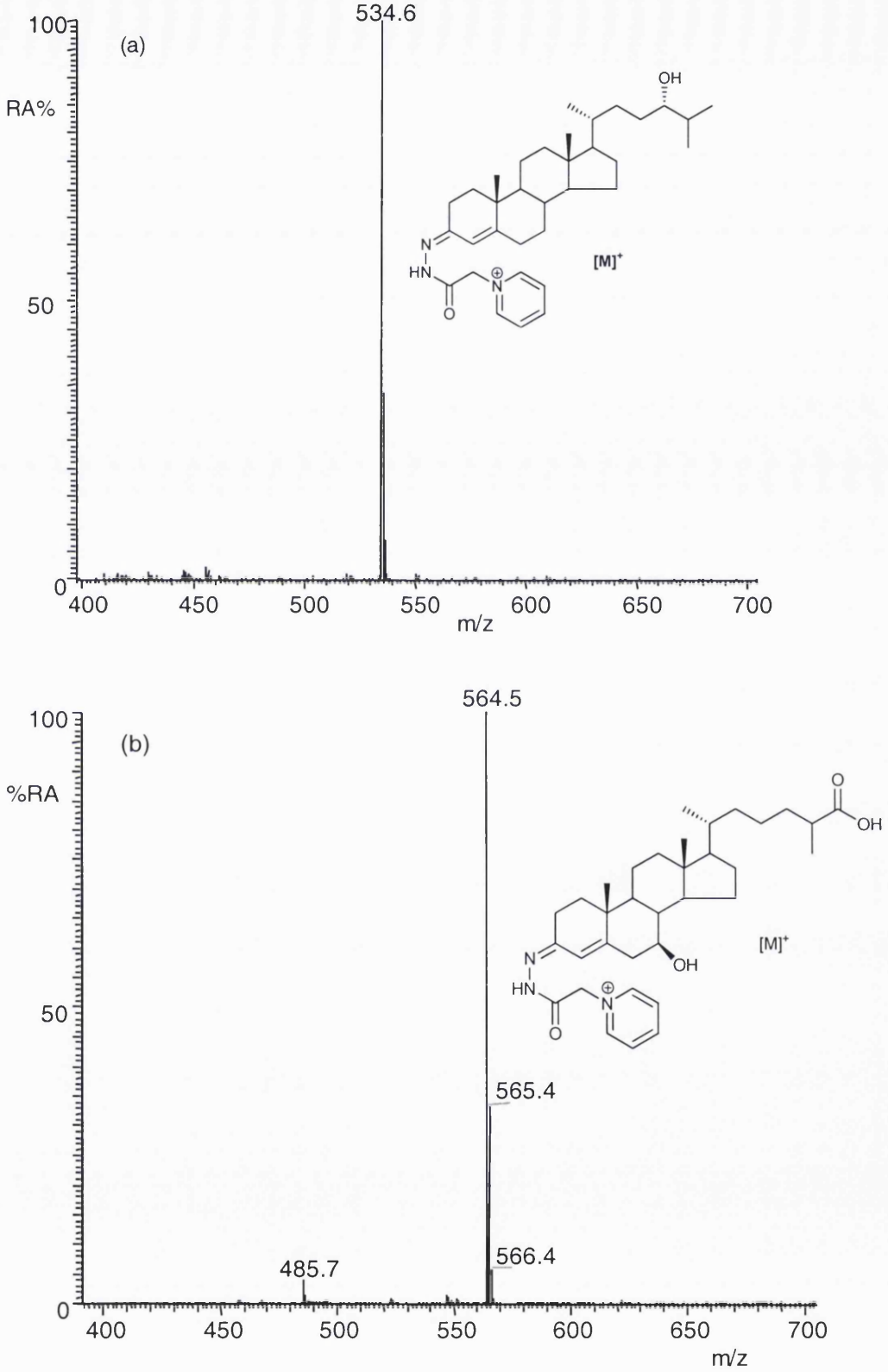

Figure 3.2 (a) Nano-ES spectra of oxidised and GP derivatised 24S-hydroxycholesterol (C^5-3β,24S-diol) *m/z* 534; and of (b) 3β,7β-dihydroxycholest-5-ene-27-oic acid (CA^5-3β,7β-diol) *m/z* 564.

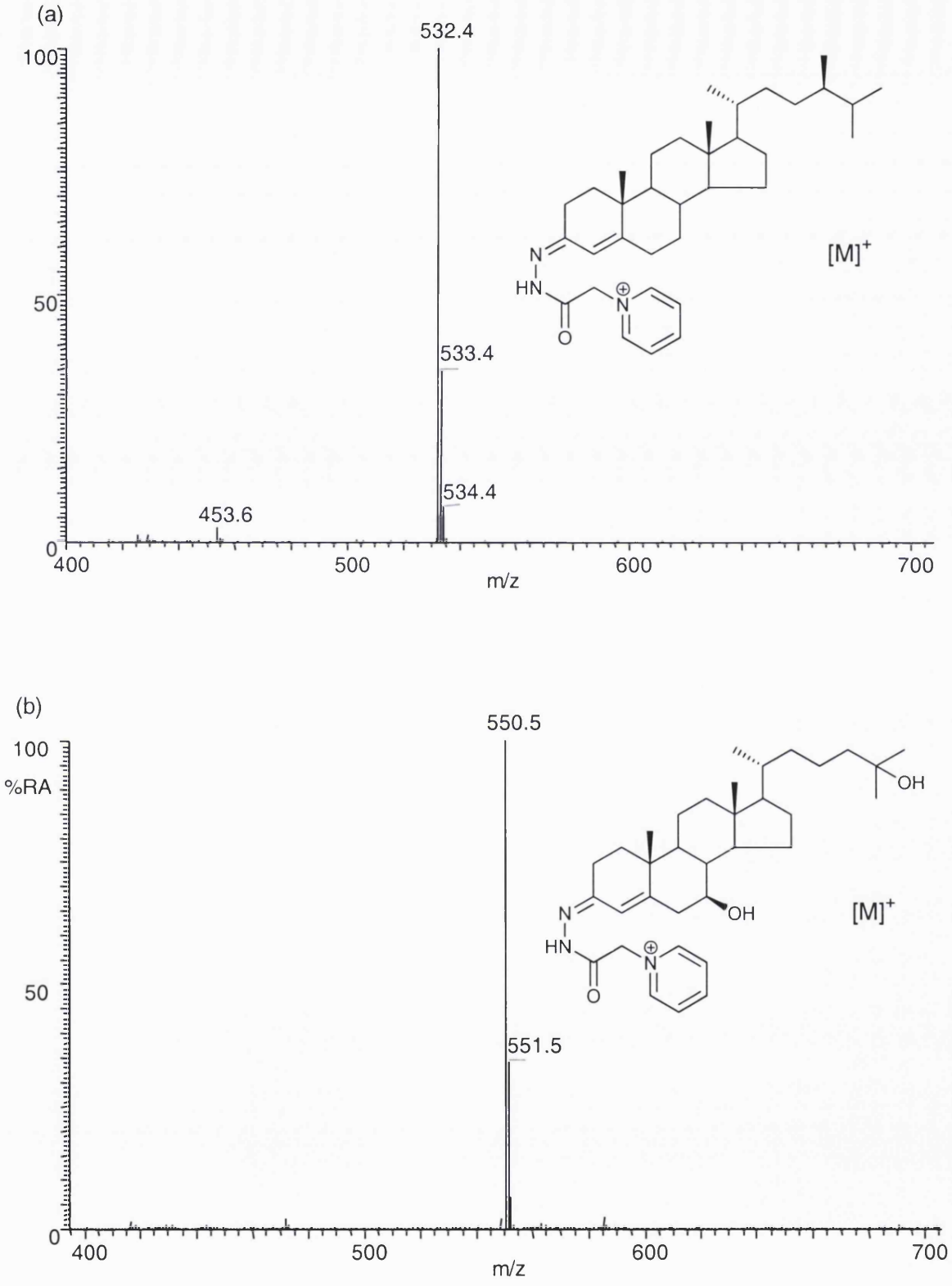

Figure 3.3 (a) Nano-ES-MS spectra of oxidised and GP derivatised campesterol (C^5-24α-methyl-3β-ol) *m/z* 532; and of (b) 7β,25-dihydroxycholesterol (C^5-3β,7β,25-triol) *m/z* 550.

Sterols containing two oxo groups were converted to mono- and to a minor extent to *bis*-GP derivatives. For example, the GP-derivatised 6-oxocholestenone (C^4-3,6-dione) contains two oxo-groups, the major product after derivatisation was the mono-GP corresponding to $[M]^+$ ion at *m/z* 532, and minor *bis*-GP derivative (Supplementary Material, Figure 29a). The *bis*-GP-hydrazone is observed as a doubly charged $[M]^{2+}$ ion at *m/z* 333 in the nano-ES spectra. 7-Oxocholesterol (C^5-3β-ol-7-one), which contains two oxo- groups after treatment with cholesterol oxidase, was converted to the 3-GP hydrazone, as the major product, and the 7-GP hydrazone as a minor product as described in section 3.9. Following oxidation and derivatisation 24-oxocholesterol gave just one product, C^4-3,24-dione GP hydrazone (Supplementary Material, Figure 18a).

The 5α-steroids with a 3β-hydroxy group were oxidised to 3-oxo-5α-steroids. For example, lathosterol (5α-cholest-7-en-3β-ol, 5α-C^7-3β-ol) was oxidised to its 3-oxo equivalent (5α-C^7-3-one), as were a number of other 3β-hydroxy-5α-steroids. The oxidation/GP-derivatisation products of sterols are listed in Tables 3.1 - 3.6.

3.4 Enhancement of ion signal upon oxidation/GP-derivatisation of 24S-hydroxycholesterol

Unoxidised/underivatised and oxidised/GP-derivatised 24S-hydroxycholesterol were analysed by nano-ES in order to compare their ionisation efficiencies. A nano-ES mass spectrum of unoxidised/underivatised 24S-hydroxycholesterol is shown in Figure 3.4. There was slight evidence for the formation of an $[M+H]^+$ ion at *m/z* 403 (relative abundance, RA 3%). However, the dehydrated protonated molecule was found to give a peak at *m/z* 385 $[M+H-H_2O]^+$ (RA 100%), and the doubly dehydrated protonated molecule at *m/z* 367 $[M+H-2xH_2O]^+$ (RA 67%). The limit of detection for the dehydrated protonated 24S-hydroxycholesterol, $[M+H-H_2O]^+$ ion was estimated to be 30 pg/μL (S/N=3, signal/noise 3:1). The nano-ES mass spectrum of oxidised/GP-derivatised 24S-hydroxycholesterol yields intense $[M]^+$ ion signal at *m/z* 534 (Figure 3.2a). The oxidation/GP-derivatisation of 24S-hydroxycholesterol to its GP hydrazone adds 132 Da to its molecular mass.

The intensity of the $[M]^+$ ion signal was linearly proportional to an analyte concentration over the range of 400 fg/μL to 10 pg/μL. The limit of detection was 400 fg/μL (S/N = 3).

This study found that oxidation of 24S-hydroxycholesterol with cholesterol oxidase from *Streptomyces sp.* and derivatisation of the resulting 3-oxo group with GP hydrazine gives an enhancement in sensitivity of about two orders of magnitude relative to the $[M+H-H_2O]^+$ ion, and three orders of magnitude relative to the $[M+H]^+$ ion of the unoxidised/underivatised 24S-hydroxycholesterol. This in agreement with the previous studies using ES-MS, where it was shown that derivatisation of 3-oxo-4-ene sterols to GP hydrazones enhances their ionisation by a factor of at least 1000 [38,57,166,167].

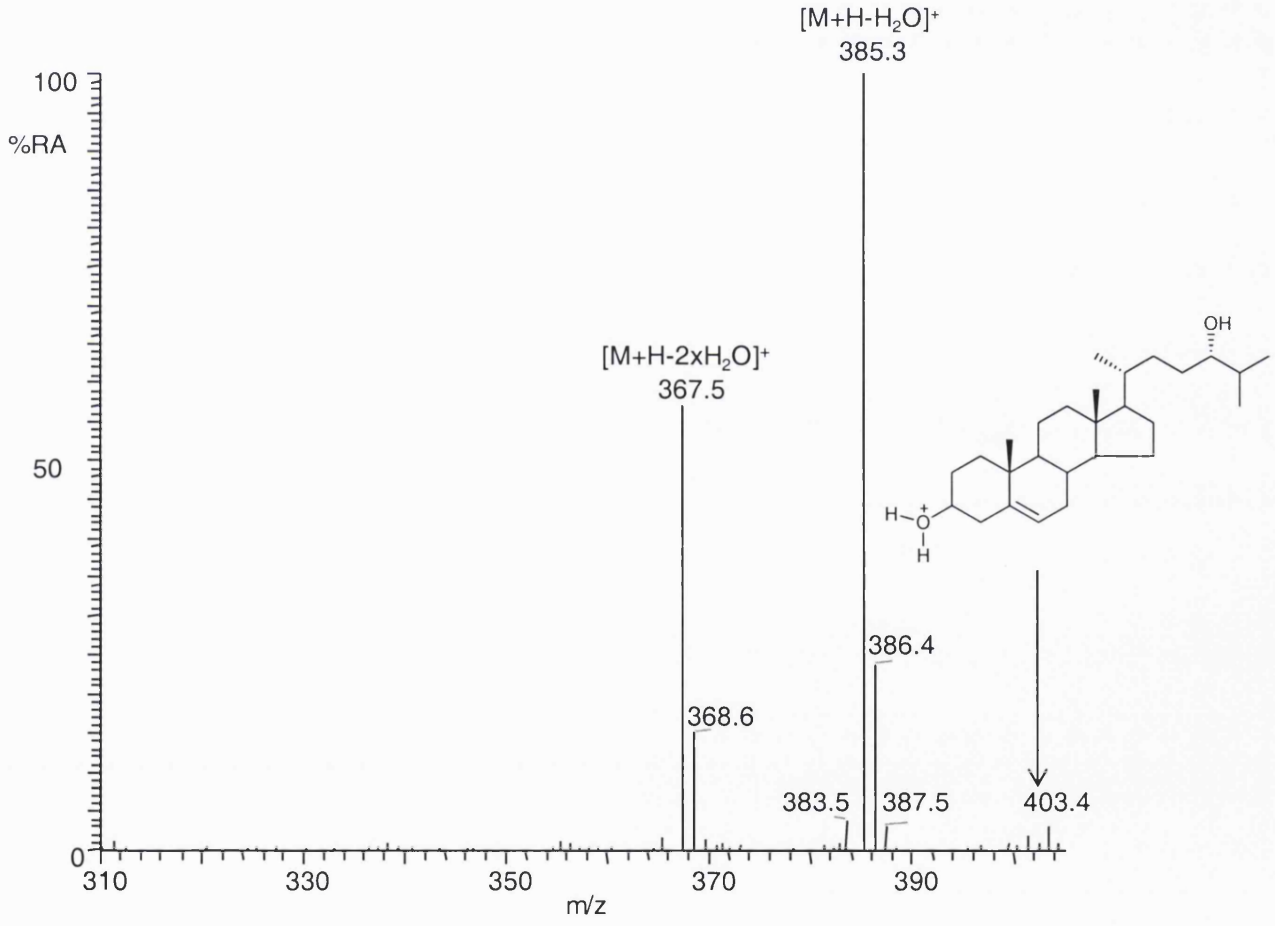

Figure 3.4 Nano-ES-MS spectrum of unoxidised/underivatised 24S-hydroxycholesterol. The spectrum was recorded at an analyte concentration of 200 ng/μL.

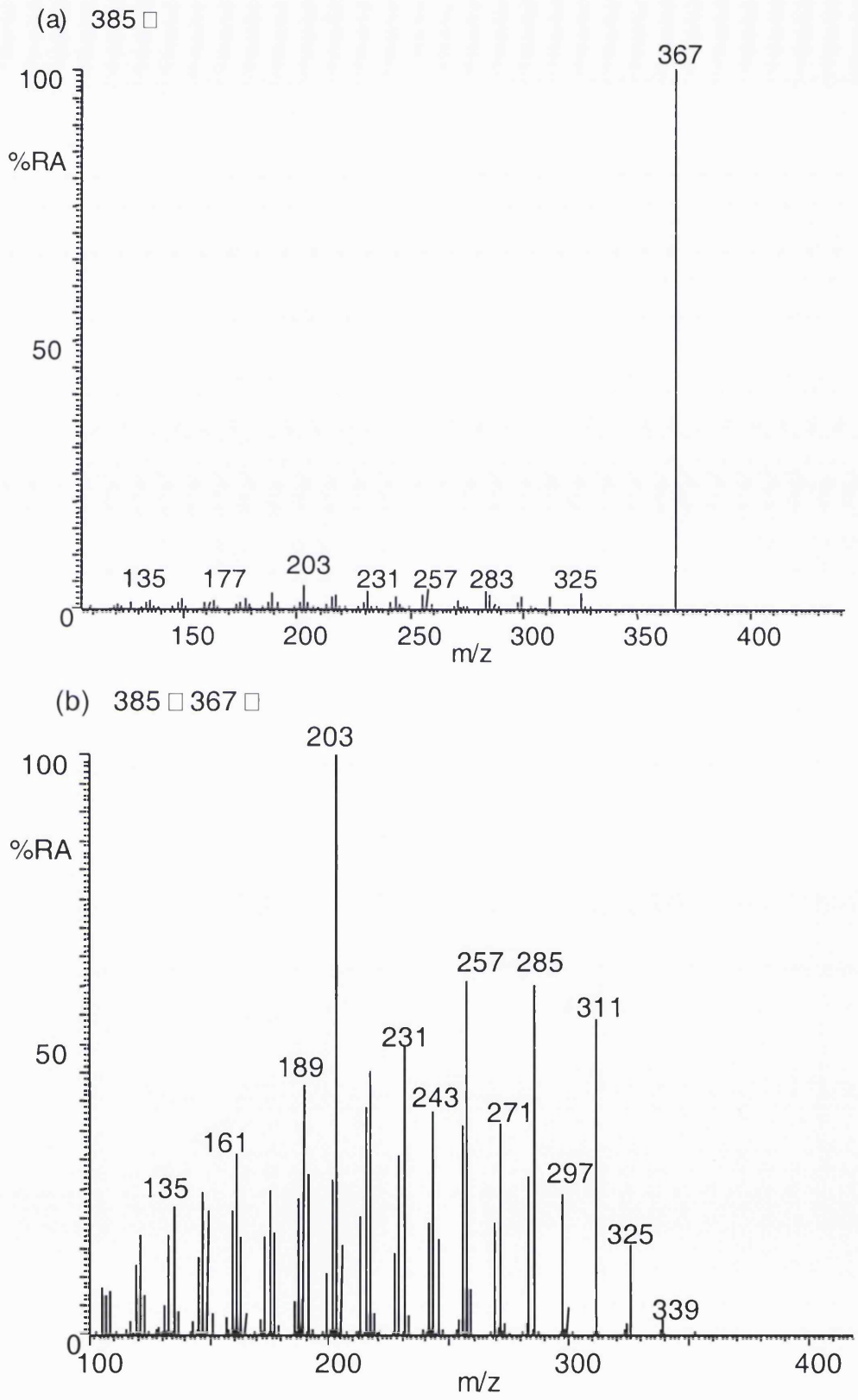

Figure 3.5 (a) MS^2 (385 →) spectrum and (b) MS^3 (385 → 367→) spectrum of the $[M+H-H_2O]^+$ ion of unoxidised and underivatised 24S-hydroxycholesterol.

3.5 *Fragmentation of unoxidised/underivatised 24S-hydroxycholesterol*

Sterols containing alcohol groups tend to become dehydrated in the ES process, and give dehydrated protonated molecules leading to ambiguity in the determination of molecular weight (for example Figure 3.4 of the unoxidised/underivatised 24S-hydroxycholesterol). For 24S-hydroxycholesterol, the $[M+H-H_2O]^+$ (*m/z* 385) ion was the most abundant in full mass spectrum, and was selected as the precursor ion for MS^2 (385→) analysis. The MS^2 (385→) spectrum showed the most abundant fragment at *m/z* 367 corresponding to $[M+H-2xH_2O]^+$ (Figure 3.5a). Further interpretation of the MS^2 spectrum is not straightforward. A MS^3 (385→367→) spectrum was recorded following activation of the most prominent fragment ion at *m/z* 367 in the MS^2 spectrum. The MS^3 385→367→ spectrum was also complex, and its interpretation is not attempted (Figure 3.5b).

3.6 *Multi-stage fragmentation mass spectrometry of reference oxidased/GP-derivatised oxysterols*

The reference oxidised/GP-derivatised sterols were divided into six groups based on their structure and MS^3 spectra. Supplementary Material Table 1 summarises MS, MS^2 and MS^3 data of the oxidised/GP-derivatised reference oxysterols.

MS^2 experiments were performed as follows:- a precursor ion, $[M]^+$, was selected, followed by activation of the $[M]^+$ ion, and recording of its fragmentation pattern, e.g. for oxidised/GP-derivatised cholesterol 518→. MS^2 spectra of most oxysterols are dominated by a $[M-79]^+$ fragment-ion, accompanied by lower abundance $[M-97]^+$ and $[M-107]^+$ ions (Figure 3.6b). Shackleton *et al.* in 1997 [96] and Griffiths *et al.* in 2004 [57] proposed that these fragment ions correspond to the loss of pyridine (C_6H_5N), pyridine plus water (C_5H_7NO), and pyridine plus carbon monoxide (C_6H_5NO), respectively. This was also confirmed by exact mass analysis of these fragments performed at high-resolution (60,000) [57]. Figure 3.8 describes the MS^2 fragmentation of the oxidised/GP-derivatised sterol $[M]^+$ ions to $[M-79]^+$ and $[M-107]^+$ ions. Otherwise, MS^2 spectra are not found to be greatly informative.

MS^3 experiments were performed as follows:- the precursor ion, $[M]^+$, was selected in the ion trap analyser, and then activated, the precursor ion fragments by the loss of 79 Da and 107 Da to give $[M-79]^+$ and $[M-107]^+$ ions in a first fragmentation event (MS^2), this was followed by activation of the $[M-79]^+$ ion and recording its fragmentation pattern, e.g. for oxidised/GP-derivatised cholesterol MS^3 518→439→. Similar MS^3 experiments were performed on the $[M-107]^+$ ions generated from the MS^2 experiment on the precursor ion, $[M]^+$ i.e. 518→411→. The MS^3 spectra are rich in structural information, and allow in some cases the complete structure determination of lipid molecules. GP hydrazones give four main types of fragment ions in their MS^3 ($[M]^+$→$[M-79]^+$→) and ($[M]^+$→$[M-107]^+$→) spectra:-

a) those resulting from sterol ring and C-17 side-chain fragmentation

b) those fragment ions caused by the neutral loss of pyridine, carbon monoxide and water from the precursor ion

c) those fragment ions, which correspond to small hydrocarbon ions.

Table 3.1 Group 1 – Reference sterols and oxysterols analysed in the present study

Sample Name	Abbreviation	Oxidation product	Derivatisation product	$[M]^+$ *m/z*
Desmosterol	$C^{5,24}$-3β-ol	$C^{4,24}$-3-one	$C^{4,24}$-3-one GP	516
Cholesterol[a]	C^5-3β-ol[a]	C^4-3-one	C^4-3-one GP[a]	518
[25,26,26,26,27,27,27,$^2H_7$]-cholesterol	[25,26,26,26,27,27,27,$^2H_7$]-C^5-3β-ol[a]	[25,26,26,26,27,27,27,$^2H_7$]-C^4-3-one	[25,26,26,26,27,27,27,$^2H_7$]-C^4-3-one GP	525
Brassicasterol	$C^{5,22}$-24-methyl-3β-ol	$C^{4,22}$-24-methyl-3-one	$C^{4,22}$-24-methyl-3-one GP	530
Campesterol	C^5-24-methyl-3β-ol	C^4-24-methyl-3-one	C^4-24-methyl-3-one GP	532
Stigmasterol	$C^{5,22}$-24β-ethyl-3β-ol	$C^{4,22}$-24β-ethyl-3-one	$C^{4,22}$-24β-ethyl-3-one GP	544
Sitosterol	C^5-24β-ethyl-3β-ol	C^4-24β-ethyl-3-one	C^4-24β-ethyl-3-one GP	546

[a]Structure are given below.

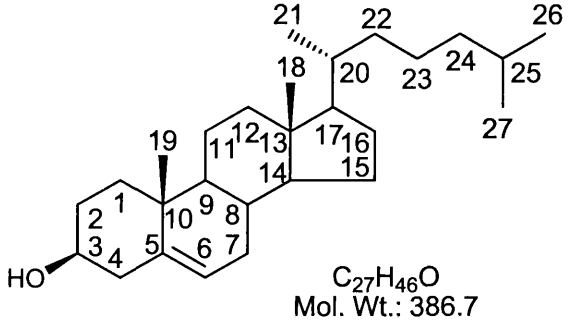

Cholesterol (C^5-3β-ol)

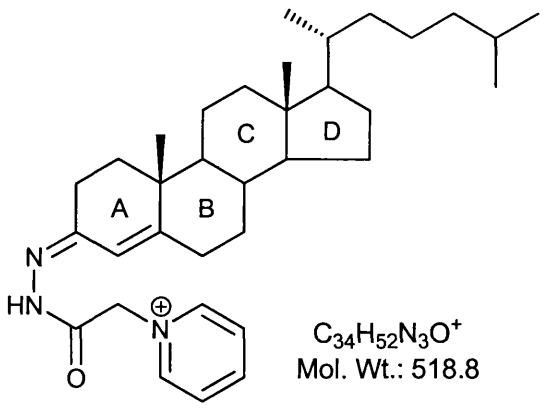

The oxidised/GP derivatised cholesterol (C^4-3-one GP hydrazone)

Group 1 Compounds I to VII (Table 3.1)

Cholesterol, cholestadienes, and side-chain modified cholesterols

During the analysis of oxysterols from biological sources, the oxysterol fractions may be contaminated with cholesterol, its precursors, and possibly the plant sterols present from the diet or introduced inadvertently from laboratory materials. Cholesterol, its precursor desmosterol ($C^{5,24}$-3β-ol), and the plant sterols stigmasterol (24β-ethylcholesta-5,22-dien-3β-ol, $C^{5,22}$-24β-ethyl-3β-ol), sitosterol (24β-ethylcholest-5-en-3β-ol, C^{5}-24β-ethyl-3β-ol), campesterol (24β-methylcholest-5-en-3β-ol, C^{5}-24β-methyl-3β-ol), and brassicasterol (24β-methylcholesta-5,22-dien-3β-ol, $C^{5,22}$-24β-methyl-3β-ol) were oxidised with cholesterol oxidase and derivatised with GP reagent. Cholesterol oxidase converts 3β-hydroxy-5-ene sterols to their 3-oxo-4-ene analogs, and the resulting 3-oxo group derivatised with GP hydrazine giving 3-GP hydrazones. The 3-oxo-4-ene sterols from this group give intense $[M]^+$ ion signal upon nano-ES ionisation.

The simplest sterol to undergo oxidation and GP-derivatisation is cholesterol, which is oxidised to cholest-4-en-3-one. Cholesterol following oxidation/GP-derivatisation gives a $[M]^+$ ion at *m/z* 518. Nano-ES-MS, MS^2 and MS^3 spectra of oxidised/GP-derivatised cholesterol are shown in Figures 3.6a,b and 3.7a,b. The MS^2 (518→) spectrum shows $[M-79]^+$ ions at *m/z* 439 and $[M-107]^+$ at *m/z* 411 (Figure 3.6b). The MS^3 (518→439→) spectrum of oxidised/derivatised cholesterol contains a triad of fragment ions at *m/z* 151, 163, 177 (Figures 3.7a, 3.9). A similar triad of fragment ions is observed in the MS^3 ($[M]^+$→$[M-107]^+$→) spectrum, but with the fragment ions displaced in mass by 28 Da, corresponding to additional loss of CO (Figures 3.7b, 3.10). These fragment ions are characteristic of the derivatised 3-oxo-4-ene structure in the absence of additional groups in the A and B rings. They are formed by cleavage in the B-ring, and are described by two competing series of b-type fragment ions (Figures 3.9 and 3.10).

(i) The *b ion-series corresponds to B-ring fragment ions which have formed via the $[M-79]^+$ intermediate (which corresponds to the precursor ion having lost the pyridine ring). The *b

ion-series of fragment ions are generated in the MS^3 $[M]^+ \rightarrow [M-79]^+ \rightarrow$ spectra. These fragment ions are described as *m/z* 151 ($^*b_1$-12), 163 ($^*b_3$-C_2H_4) and 177 ($^*b_2$) (Figure 3.9).

(ii) Similarly, the MS^3 ($[M]^+ \rightarrow [M-107]^+ \rightarrow$) spectra contain the fragment ions at *m/z* 123 ($^\#b_1$-12), 135 ($^\#b_3$-C_2H_4) and *m/z* 149 ($^\#b_2$), which correspond to B-ring fragment ions that have additionally lost both the pyridine group and CO from GP sterol hydrazone. (Figure 3.7b, 3.10).

The nomenclature used to describe sterol GP hydrazone fragmentation is explained in the caption of Figures 3.9 and 3.10. In summary, the *b and #b ion-series are indicative of the sterols possessing a 3-oxo-4-ene group before GP derivatisation and a 3β-ol-5-ene structure before treatment with cholesterol oxidase and GP reagent, with no additional substituents in the A and B rings. This allows the simple differentiation of e.g. campesterol from 7-oxocholesterol, even though, they have the same molecular weight.

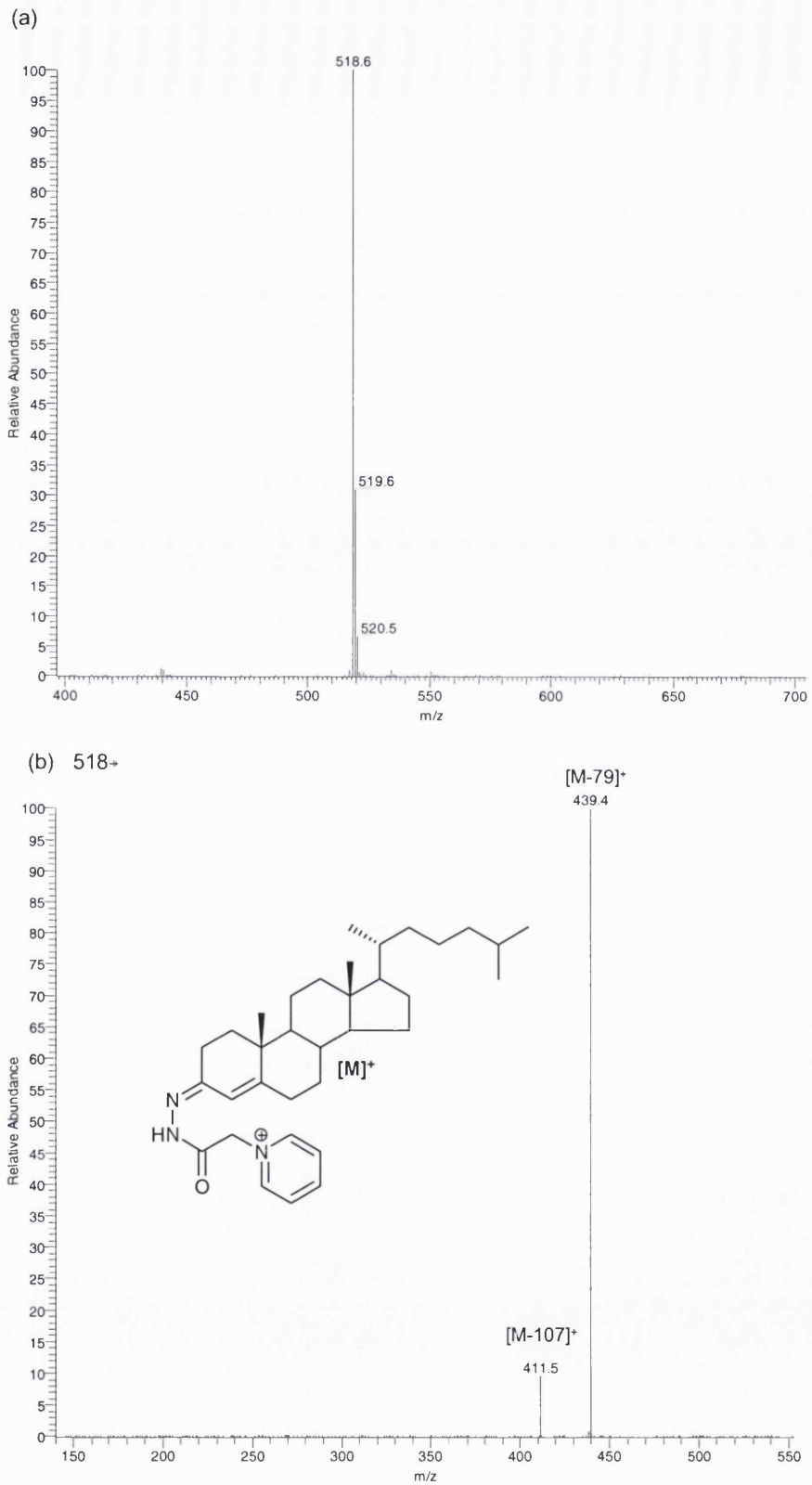

Figure 3.6 (a) Nano-ES mass spectrum of oxidised/derivatised cholesterol *m/z* 518; (b) MS^2 (518→) spectrum of oxidised/derivatised cholesterol.

(a) 518→439→

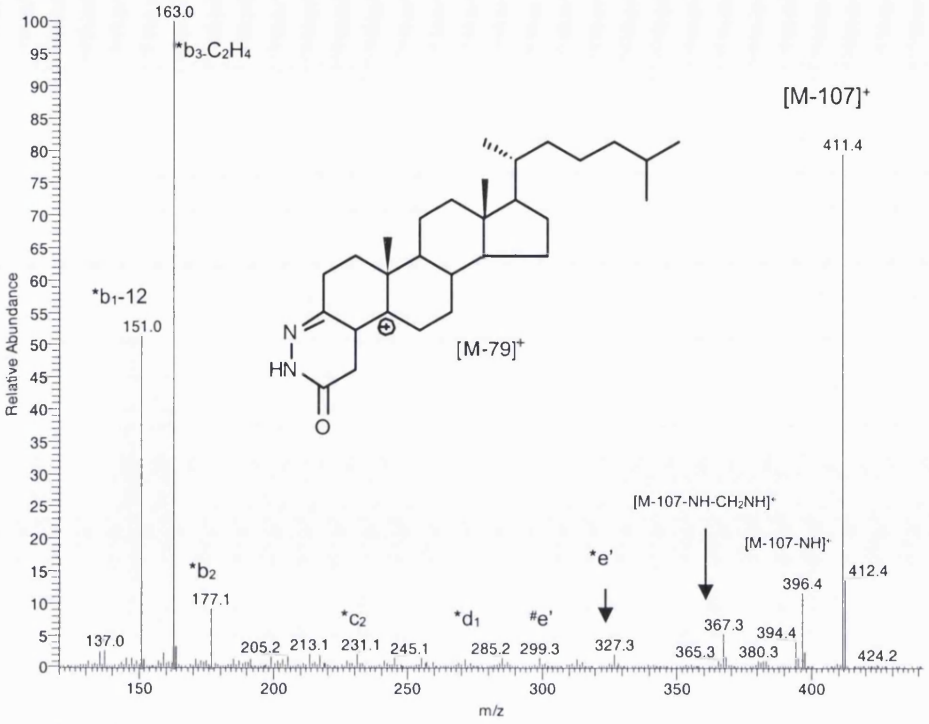

(b) 518→411→

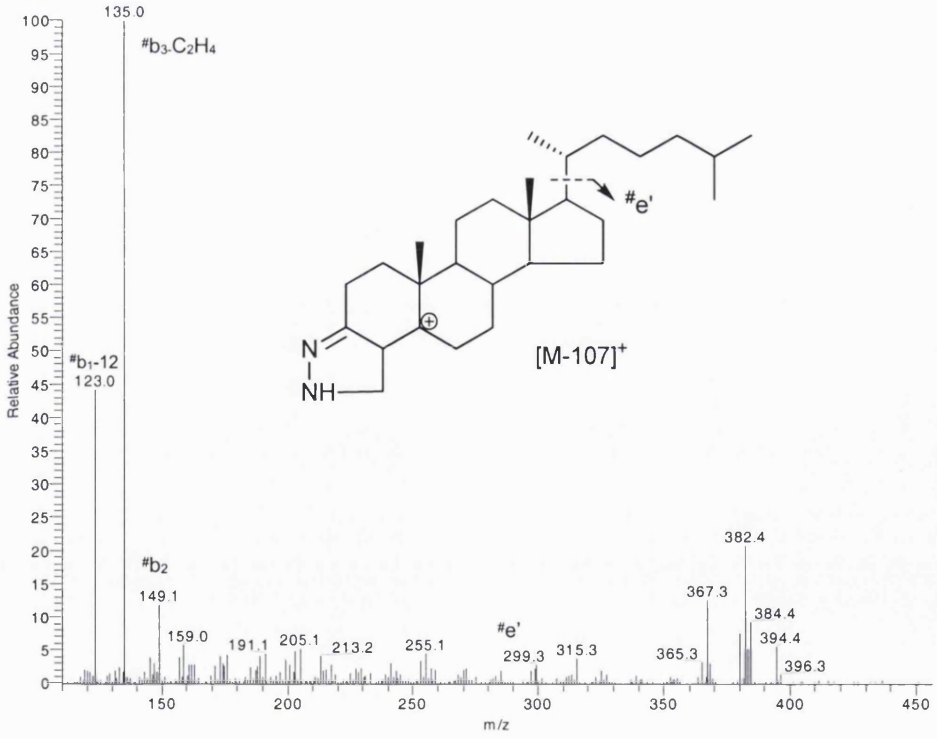

Figure 3.7 (a) Nano-ES-MS^3 (518→439→); and (b) MS3 (518→411→) spectra of oxidised/GP-derivatised cholesterol.

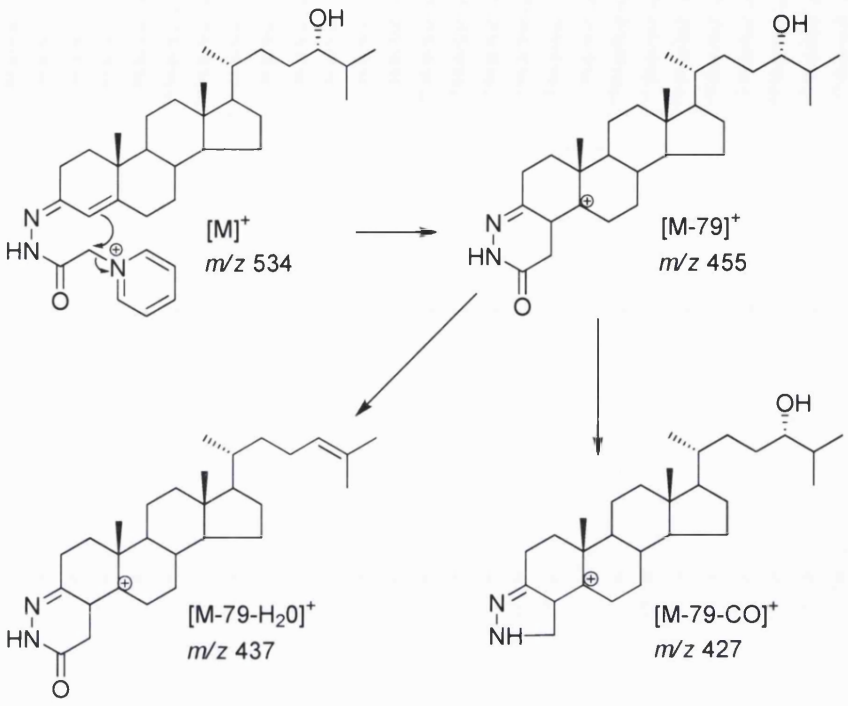

Figure 3.8 MS^2 fragmentation of sterol GP hydrazones. 24S-hydroxycholesterol (C^5-3β,24S-diol) is used as an example.

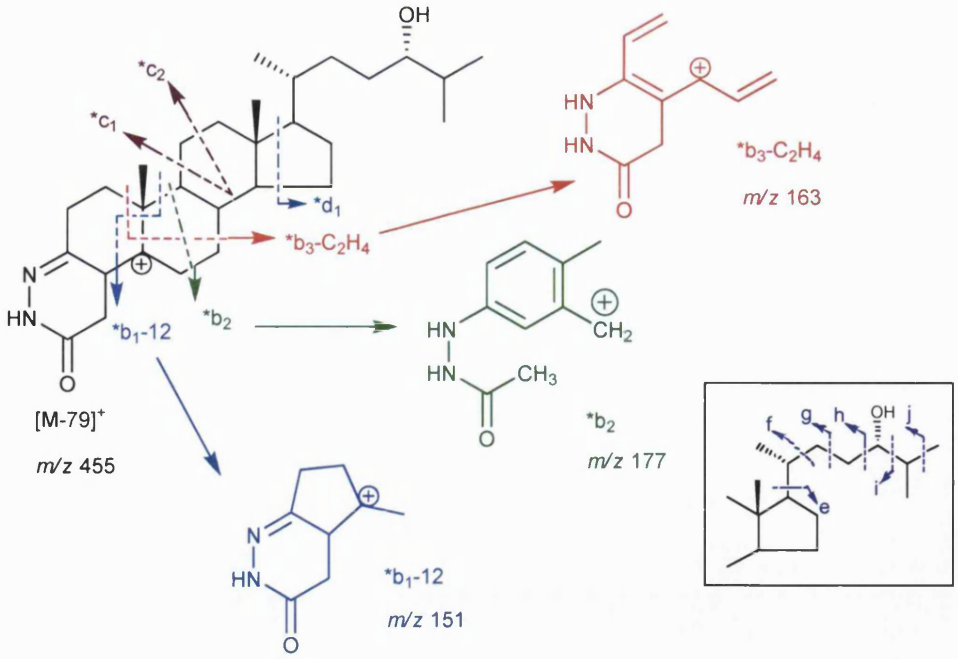

Figure 3.9 MS^3 ($[M]^+ \rightarrow [M\text{-}79]^+ \rightarrow$) fragmentation of 3-oxo-4-ene C_{27} GP hydrazones. 24S-Hydroxycholesterol is used as an example. An asterisk preceding a fragment-ion describing letter e.g. *b_1-12, indicates that the fragment-ion has lost the pyridine moiety from the derivatising group. A prime to the left of a fragment ion describing letter e.g. '*f, indicates that cleavage proceeds with the transfer of a hydrogen atom from the ion to the neutral fragment. A prime to the right of the fragment describing letter indicates that cleavage proceeds with hydrogen atom transfer to the fragment-ion e.g. *e' [101]. The inset indicates fragmentation in the C-17 side chain of the oxidised/GP-derivatised oxysterols.

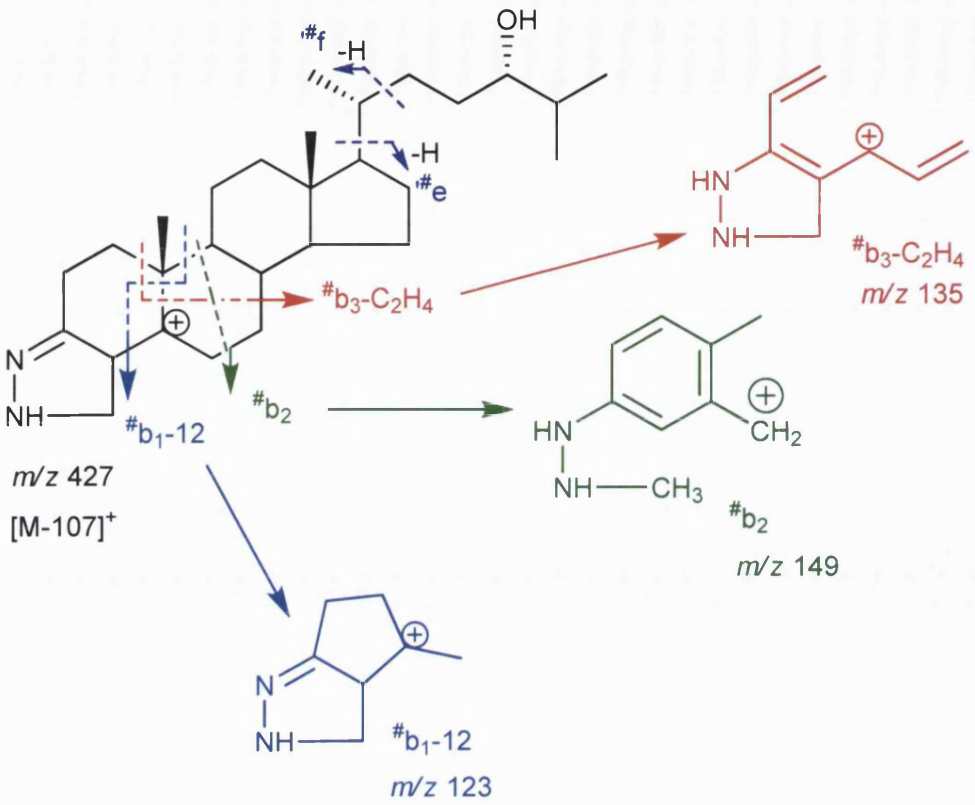

Figure 3.10 MS^3 ($[M]^+ \rightarrow [M\text{-}107]^+ \rightarrow$) fragmentation of 3-oxo-4-ene C_{27} GP hydrazones. 24S-Hydroxycholesterol is used as an example. Fragment ions derived from the $[M\text{-}107]^+$ intermediate ion are designated with a superscript hatch, e.g. $^{\#}b_1$-12 [101].

While the major cleavages in the sterol ring system occur in the B-ring and give abundant fragment ions, minor but important fragment ions are generated by cleavages in the C-and D-rings, and in the C-17 side-chain giving the fragment ions of low abundance in MS^3 spectra. In the MS^3 ($[M]^+ \rightarrow [M\text{-}79]^+ \rightarrow$) spectra of the oxidised/GP-derivatised sterols from Group 1 compounds $^*c_2$, $^*d_1$, $^{\#}$e+H ($^{\#}$e'), and *e+H (*e') fragment ions are consistently observed at *m/z* 231, 285, 299, 327 (e.g. oxidised/GP-derivatised cholesterol (Figure 3.7a), desmosterol, campesterol, see Supplementary Material Figures 1c, 4c and 5c).

Desmosterol is an intermediate in the *de novo* synthesis of cholesterol [31,114]. When oxidised with cholesterol oxidase and derivatised with GP hydrazine, MS^3 ($[M]^+ \rightarrow [M\text{-}79]^+ \rightarrow$) of the resulting $C^{4,24}$-3-one GP hydrazone gives a similar spectrum to those other 3-oxo-4-ene sterols (see Supplementary Material Figure 4c). However, peaks at 353 and 355 corresponding to *f-H ('*f) and

*f+H (*f'); and 325 and 327 corresponding to #f-H ('#f) and #f+H (#f'), are of elevated intensity. These ions are formed by cleavage of the bond between C-20 and C-22.

The MS^3 spectra of the oxidised/GP-derivatised stigmasterol (24β-ethylcholesta-5,22-dien-3β-ol), sitosterol (24β-ethylcholest-5-en-3β-ol), campesterol (24β-methylcholest-5-en-3β-ol), and brassicasterol (24β-methylcholesta-5,22-dien-3β-ol) showed the common features of 3-oxo-4-ene sterol GP hydrazones (Supplementary Material Figures 5c,d; 6c,d; 7c,d; 8c,d). The MS^3 ($[M]^+ \rightarrow [M-79]^+ \rightarrow$) spectrum of oxidised/GP-derivatised sitosterol was very similar to that of cholesterol, however, the peak at 367 in the spectrum of cholesterol (Figure 3.7a), and corresponding to the doubly unsaturated cholestane carbonium ion, was shifted to 395 in the spectrum of the oxidised/GP-derivatised sitosterol, and was shifted to 381 in the spectrum of the oxidised/derivatised campesterol. The MS^3 spectrum of the oxidised/GP-derivatised stigmasterol is characterised by peaks at 381 (*h+H) both formed as a result of cleavage of the C-23-C-24 bond. There is also enhanced abundance of fragment ions at *m/z* 284 (#e'-NH), 299 (#e'), and 327 (*e') each formed as a result of cleavage of the C-17-C-20 bond (Supplementary Material Figures 7c). The presence of methyl group, rather than an ethyl group, attached to C-24 in brassicasterol leads to the same *e' and *h' fragment ions. Similar patterns of fragment ions are observed in the MS^3 ($[M]^+ \rightarrow [M-107]^+ \rightarrow$) spectra, but with the fragment ions displaced in mass by 28 Da, corresponding to additional loss of CO (see Supplementary Material Figure 7d and 8d).

Table 3.2 Group 2 – Reference oxysterols analysed in the present study

Sample Name	Abbreviation	Oxidation product	Derivatisation product	$[M]^+$, *m/z*
24(S)-Hydroxycholesterol	C^5-3β,24S-diol	C^4-24S-ol-3-one	C^4-24S-ol-3-one GP	534
24-Oxocholesterol	C^5-3β-ol-24-one	C^4-3,24-dione	C^4-3,24-dione 3-GP	532
25-Hydroxycholesterol	C^5-3β,25-diol	C^4-25-ol-3-one	C^4-25-ol-3-one GP	534
27-Hydroxycholesterol	C^5-3β,27-diol	C^4-27-ol-3-one	C^4-27-ol-3-one GP	534
20α-Hydroxycholesterol	C^5-3β,20α-diol	C^4-20α-ol-3-one	C^4-20α-ol-3-one GP	534
22(R)-Hydroxycholesterol	C^5-3β,22R-diol	C^4-22R-ol-3-one	C^4-22R-ol-3-one GP	534
22(S)-Hydroxycholesterol	C^5-3β,22S-diol	C^4-22S-ol-3-one	C^4-22S-ol-3-one GP	534
24S,25-Epoxycholesterol	C^5-24S,25-epoxy-3β-ol	C^4-24S,25-epoxy-3-one	C^4-24S,25-epoxy-3-one GP	532
		C^4-24S,25-diol-3-one	C^4-24S,25-diol-3-one GP	550
		C^4-24-ol,25-methoxy-3-one/ C^4-24-methoxy,25-ol-3-one	C^4-24-ol,25-methoxy-3-one GP/ C^4-24-methoxy,25-ol-3-one GP	564

[a]Structure are given below.

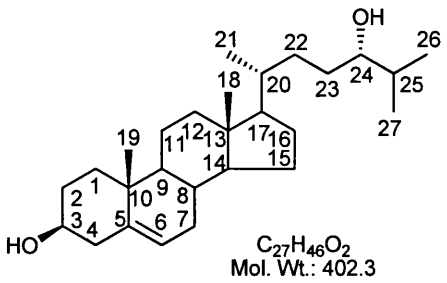

24S-hydroxycholesterol (C^5-3β,24S-diol)

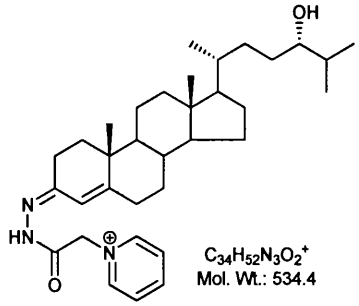

the oxidised/GP derivatised 24S-hydroxycholesterol (C^4-24S-ol-3-one GP hydrazone)

Group 2 - Reference oxysterols (Table 3.2)

Side-chain oxygenated cholesterols

This group contains monohydroxycholesterols and 24S,25-epoxycholesterol with the hydroxyl or epoxy groups on the C-17 side chain. Following treatment with cholesterol oxidase and GP reagent, oxidised/GP-derivatised monohydroxycholesterols give one product corresponding to their $[M]^+$ ion at *m/z* 534 (an example is shown for the oxidised/GP-derivatised 24S-hydroxycholesterol, Figures 3.2a). Their MS^2 spectra are dominated by a pair of fragment ions at *m/z* 455 $[M-79]^+$ and at *m/z* 427 $[M-107]^+$ corresponding to the loss of a pyridine group and the pyridine group plus CO, respectively. The MS^2 spectra do not provide a wealth of structural information, but give information on the lability of the modified cholesterol skeleton. For example, for most oxidised/GP-derivatised monohydroxycholesterols (*m/z* 534), the MS^2 spectra showed $[M-79-H_2O]^+$ ions (*m/z* 437) with relative abundance (RA) of approximately 1%. However, for 25-hydroxycholesterol the lability of the hydroxyl group on tertiary C-25 results in an $[M-79-H_2O]^+$ ion with RA of 15% (examples are shown for the oxidised/GP-derivatised 24S-hydroxycholesterol, 25-hydroxycholesterol, 20α-hydroxycholesterol, 27-hydroxycholesterol, and 22R-hydroxycholesterol; Figures 3.11a, 3.13a, 3.15a, 3.17a, 3.19a).

In contrast to MS^2 spectra, MS^3 spectra of oxidised/GP-derivatised oxysterols provide a wealth of structural information, which contain common patterns of fragment ions, but are sufficiently different to allow their differentiation. The MS^3 spectra are in most cases dominated by a pair of fragment ions at *m/z* 437 $[M-79-H_2O]^+$ and 427 $[M-107]^+$ corresponding to the loss of water and CO from the $[M-79]^+$ ion. The difference in RA between these fragment ions gives information on the lability of the added hydroxy group, and in most cases these ions provide the base peak in the MS^3 spectra. For example, the ratio of RA of *m/z* 437:427 is ~30:1 when the extra hydroxyl group is on a tertiary carbon as in 25-hydroxycholesterol (Figure 3.13b). The ratio is ~3:1 when the extra hydroxyl group is on a secondary carbon as in 24S-hydroxycholesterol (Figure 3.11b), and

~1:3 when the extra hydroxyl group in on a primary carbon as in 27-hydroxycholesterol (Figure 3.17b).

The MS^3 $[M]^+ \rightarrow [M-79]^+ \rightarrow$ spectra contain a triad of fragment ions at *m/z* 151 ($*b_1$-12), 163 ($*b_3$-C_2H_4) and 177 ($*b_2$). These fragment ions are formed by cleavage in the B ring and are characteristic for oxidised and GP-derivatised monohydroxycholesterols, and other 3-oxo-4-ene sterols, which are unmodified by additional substituents in the A and B rings. These ions correspond to B-ring fragment ions, which have lost the pyridine group (examples are shown for the oxidised/derivatised 24S-hydroxycholesterol, 25-hydroxycholesterol, 20α-hydroxycholesterol, 27-hydroxycholesterol, and 22R-hydroxycholesterol; Figures 3.11b, 3.13b, 3.15b, 3.17b, 3.19b). The relative abundances (RAs) of the *m/z* 151 ($*b_1$-12), 163 ($*b_3$-C_2H_4) and 177 ($*b_2$) ions also differ depending on the structure of the reference oxysterols.

In addition each oxidised/GP-derivatised monohydroxycholesterol gives a fragment-ion series specific to its structure. For example, side-chain hydroxylated cholesterols can be differentiated as follows:-

(i) 24S-hydroxycholesterol gives an abundant ion at *m/z* 353('*f) with RA of 25% in the MS^3 ($[M]^+ \rightarrow [M-79]^+ \rightarrow$) spectrum (Figure 3.11b), and a characteristic *m/z* 325 ('#f) with RA of 16% is observed in the MS^3 ($[M]^+ \rightarrow [M-107]^+ \rightarrow$) spectrum (Figure 3.12).

(ii) 20α-hydroxycholesterol gives an abundant fragment at *m/z* 327(*e') with RA of 100% in the MS^3 $[M]^+ \rightarrow [M-79]^+ \rightarrow$ spectrum (Figure 3.15b). An equivalent #e' ion at *m/z* 299 (RA 100%) is observed in the MS^3 ($[M]^+ \rightarrow [M-107]^+ \rightarrow$) spectrum (Figure 3.16).

(iii) 22R-and 22S-hydroxycholesterols give abundant ions at *m/z* 355 in MS^3 ($[M]^+ \rightarrow [M-79]^+ \rightarrow$) spectra with RA of 15% and RA of 22%, respectively (Figure 3.19b). The ion at *m/z* 355 corresponds to *f'. Again the equivalent #f' ion is observed in the MS^3 ($[M]^+ \rightarrow [M-107]^+ \rightarrow$) spectrum (Figure 3.20).

(iv) For 25-hydroxycholesterol, a consequence of ion-current being concentrated in the $[M-79-H_2O]^+$ ion at *m/z* 437, is that all other fragment ions are of low RA (Figure 3.13b).

(v) For 27-hydroxycholesterol, the reverse is true, the lower importance of the $[M-79-H_2O]^+$ ion at *m/z* 437 results in enhanced abundance of other fragments specifically at *m/z* 427 (RA 100%, $[M-107]^+$ and 163 (RA 90%,$^*b_3$-C_2H_4) (Figure 3.17b).

The presence of an oxo group on the side-chain of cholesterol is significant in the MS^3 of oxidised/GP-derivatised 24-oxocholesterol. Following treatment with cholesterol oxidase, 24-oxocholesterol is converted into cholest-4-ene-3,24-dione GP, which could give a mixture of both 3- and 24-mono GP hydrazones (*m/z* 532). The MS^2 and MS^3 spectra are indicative of the GP group being at C-3 of 3-oxo-4-ene sterol. The MS^2 spectrum is dominated by $[M-79]^+$ (*m/z* 453, RA 100%) and $[M-107]^+$ (*m/z* 425, RA 10%), while the MS^3 ($[M]^+ \rightarrow [M-79]^+ \rightarrow$) spectrum shows the triad of fragment ions at *m/z* 151 ($^*b_1$-12), 163 ($^*b_3$-C_2H_4) and 177 ($^*b_2$), and the presence of the oxo group at C-24 results in only minor side-chain fragmentation (Supplementary Material, Figures 18c). The equivalent pattern of #b-series fragment-ions is observed in the MS^3 ($[M]^+ \rightarrow [M-107]^+ \rightarrow$) spectrum (see Supplementary Material, Figure 18d).

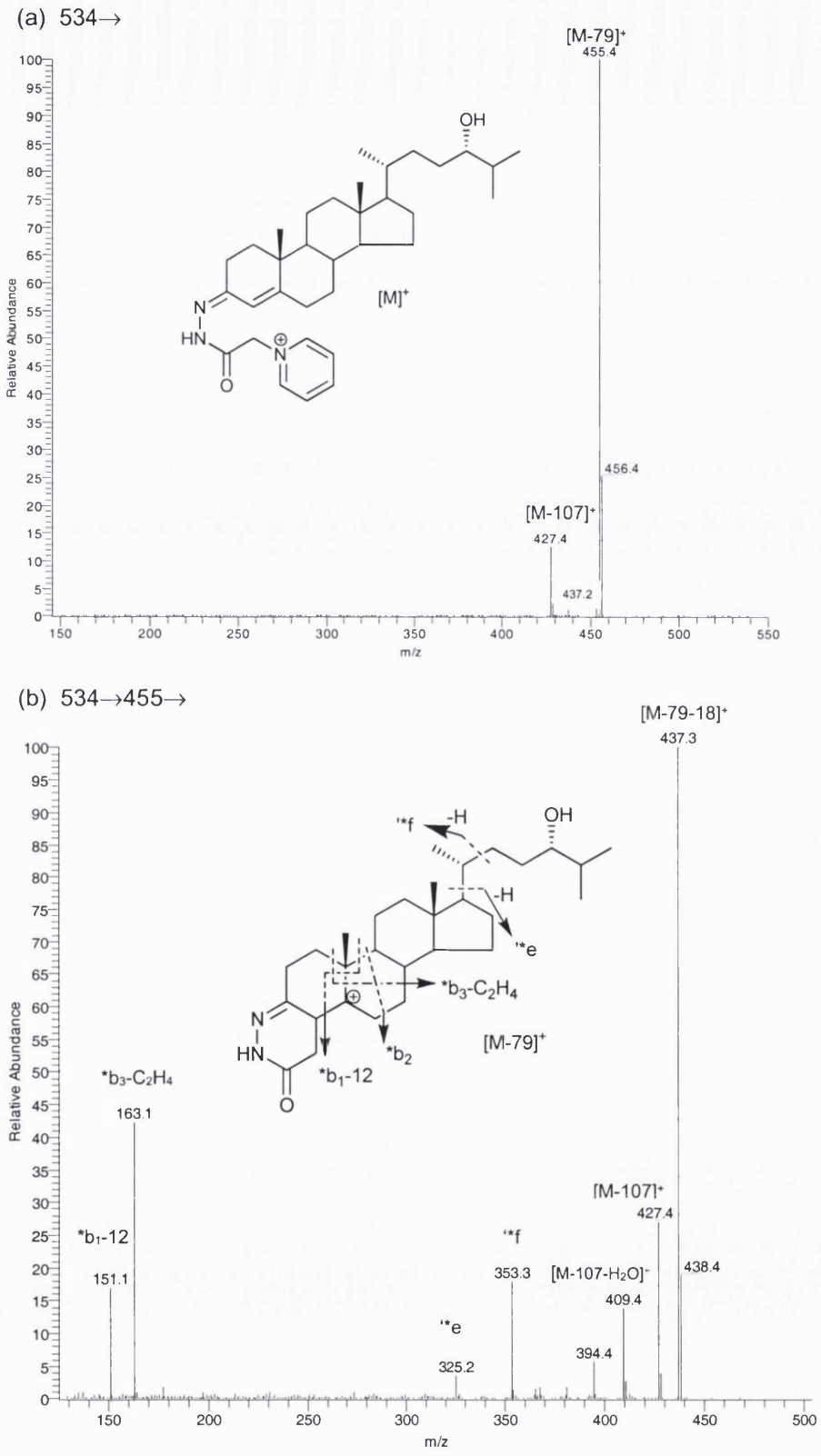

Figure 3.11 (a) MS^2 (534→), and (b) MS^3 (534→455→) spectra of oxidised and derivatised 24S-hydroxycholesterol.

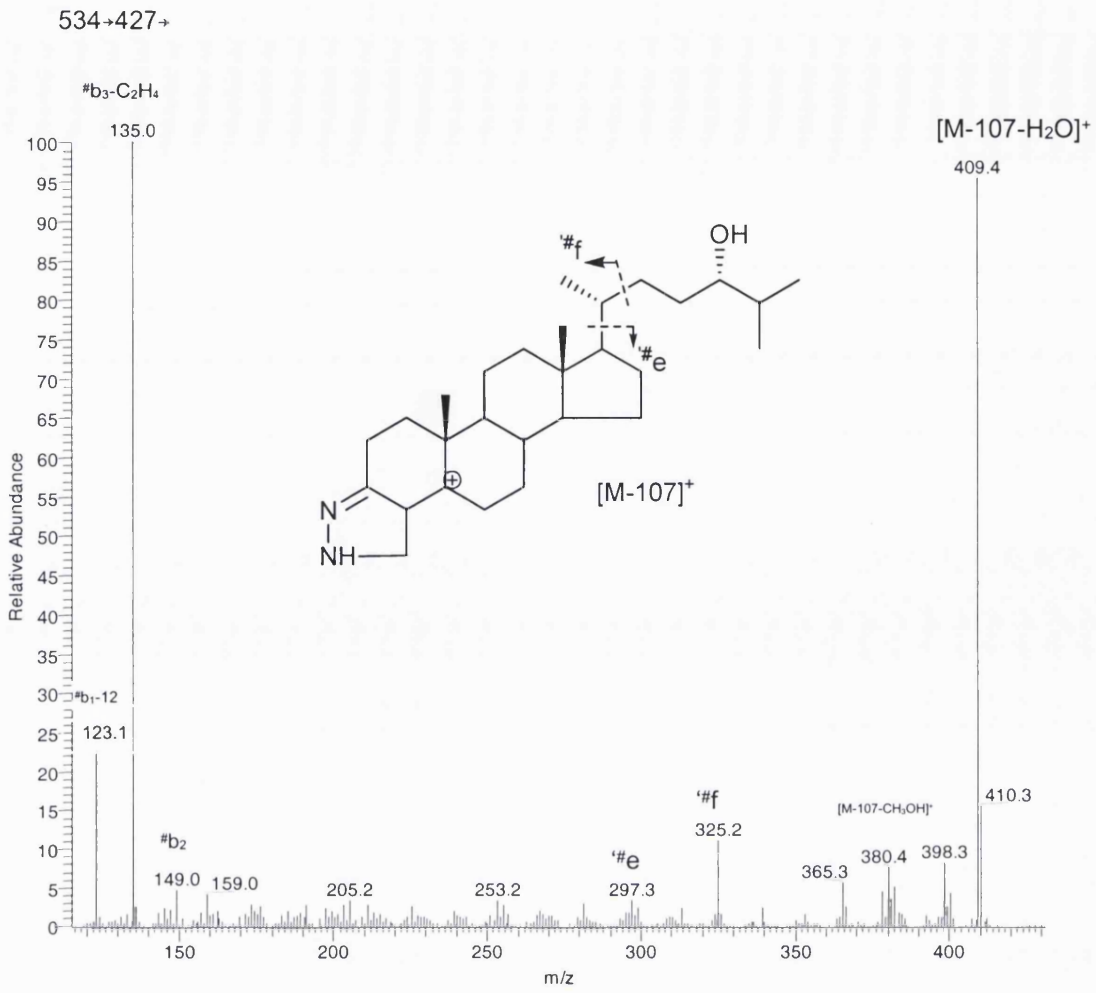

Figure 3.12 Nano-ES- MS^3 (534→427→) spectrum of oxidised and GP derivatised 24S-hydroxycholesterol.

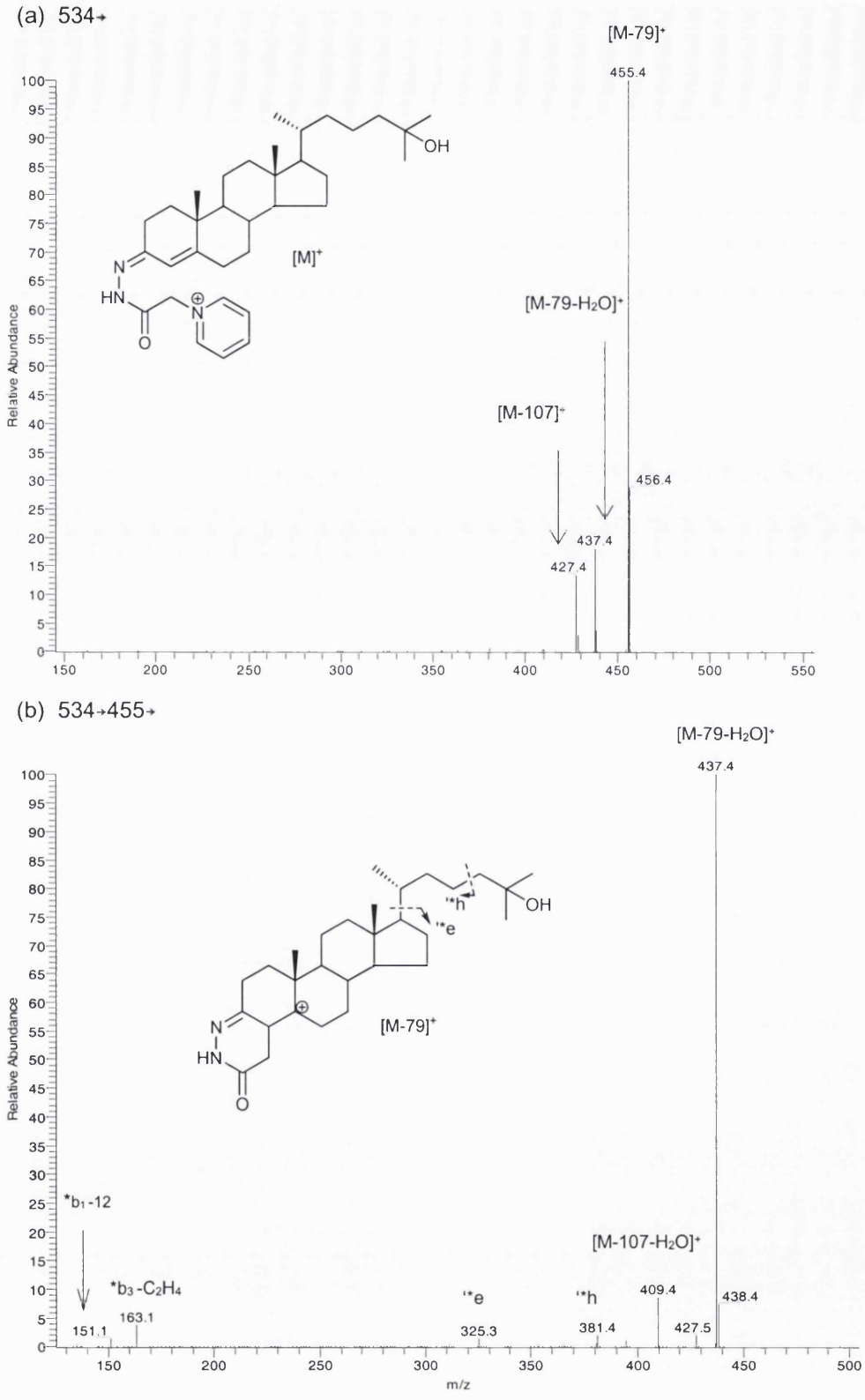

Figure 3.13 (a) Nano-ES-MS^2 (534→), and (b) MS^3 (534→455→) spectra of oxidised and GP derivatised 25-hydroxycholesterol.

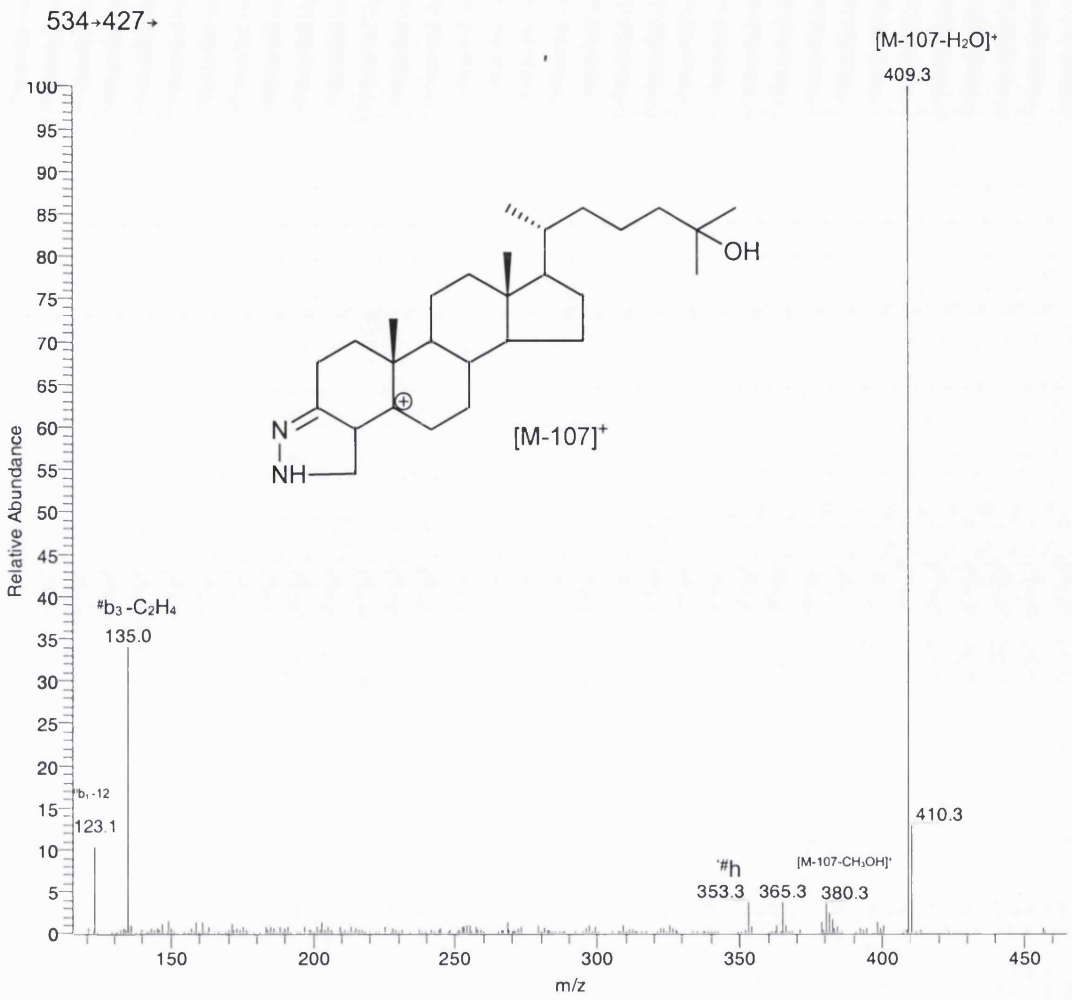

Figure 3.14 Nano-ES-MS^3 (534→427→) spectrum of oxidised and GP derivatised 25-hydroxycholesterol.

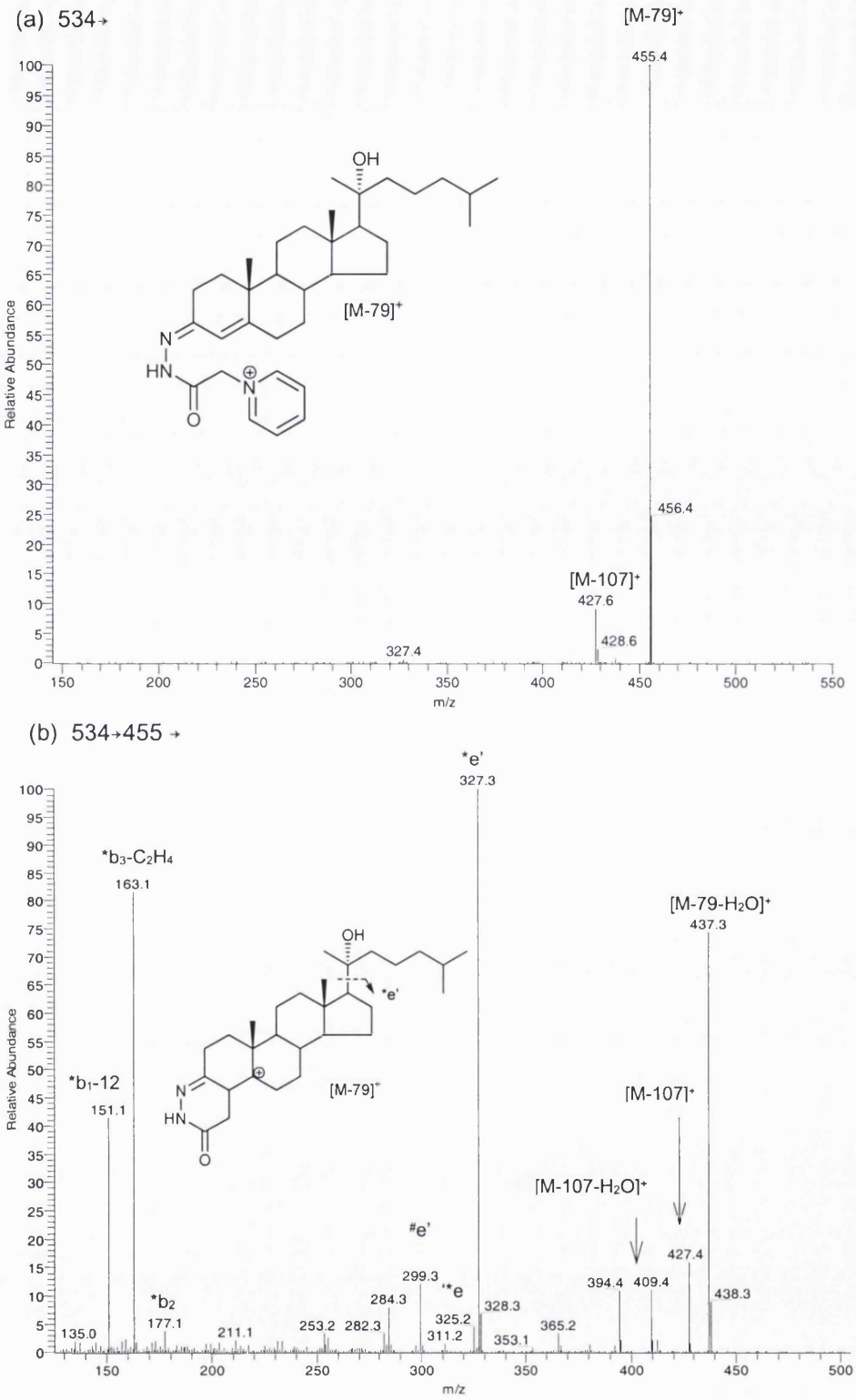

Figure 3.15 (a) Nano-ES-MS^2 (534→), and (b) MS^3 (534→455→) spectra of oxidised/GP-derivatised 20α-hydroxycholesterol.

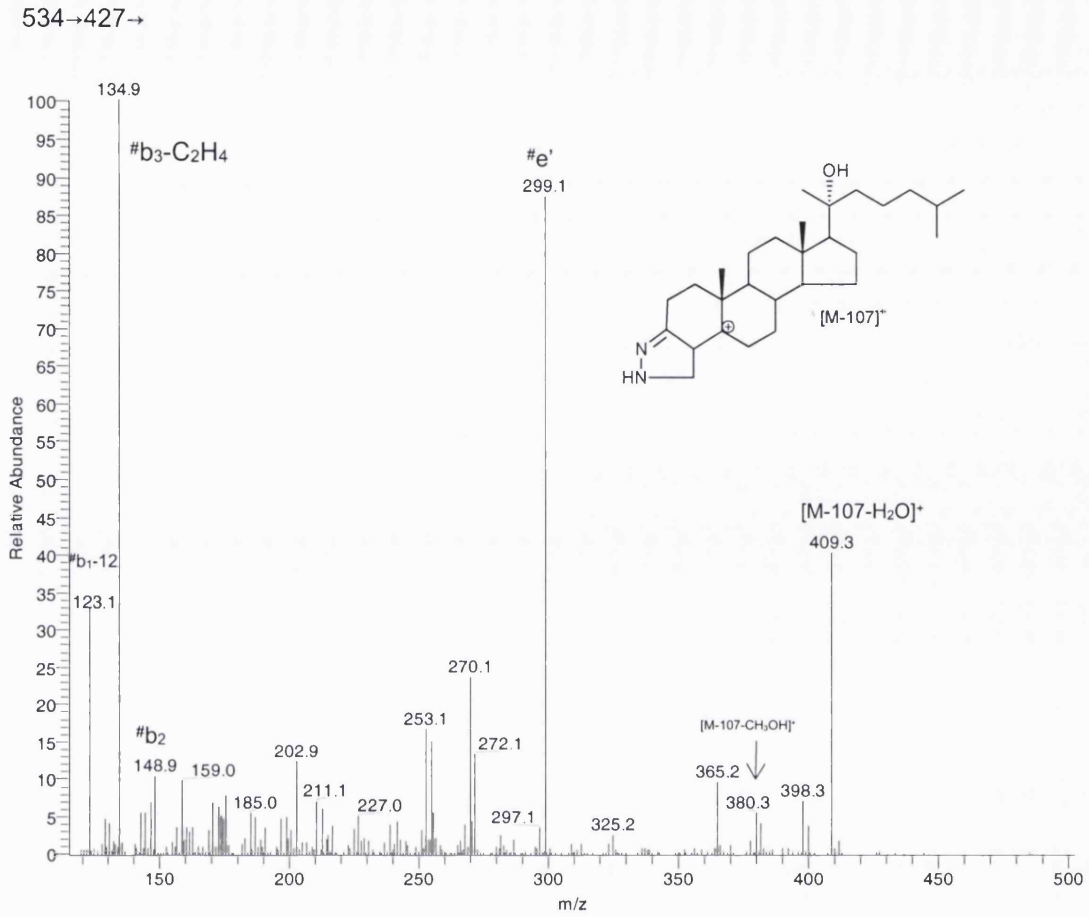

Figure 3.16 Nano-ES-MS^3 (534→427→) spectrum of oxidised and GP derivatised 20α-hydroxycholesterol.

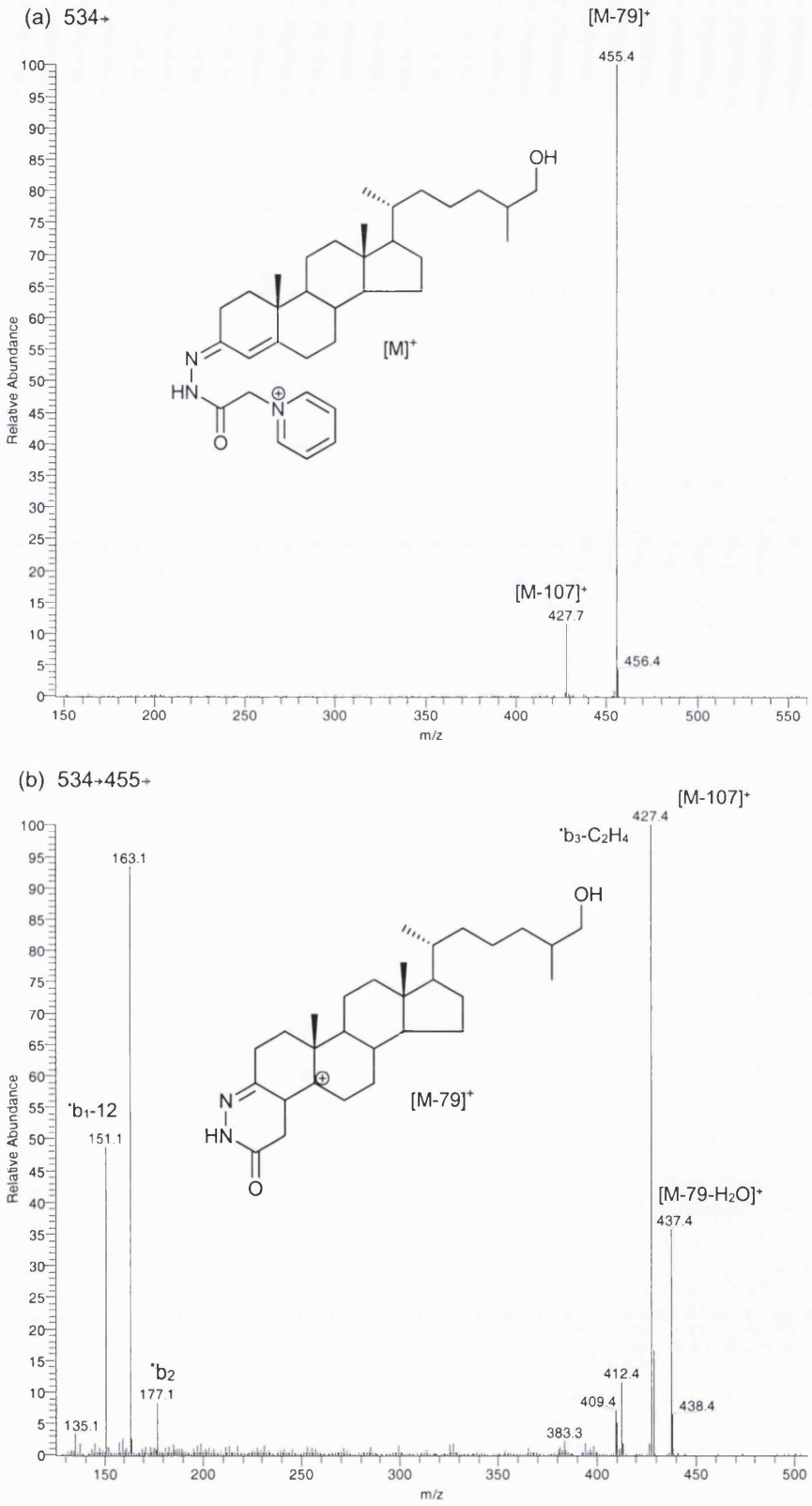

Figure 3.17 (a) Nano-ES-MS^2 (534→), and (b) MS^3 (534→455→) spectra of oxidised and GP derivatised 27-hydroxycholesterol.

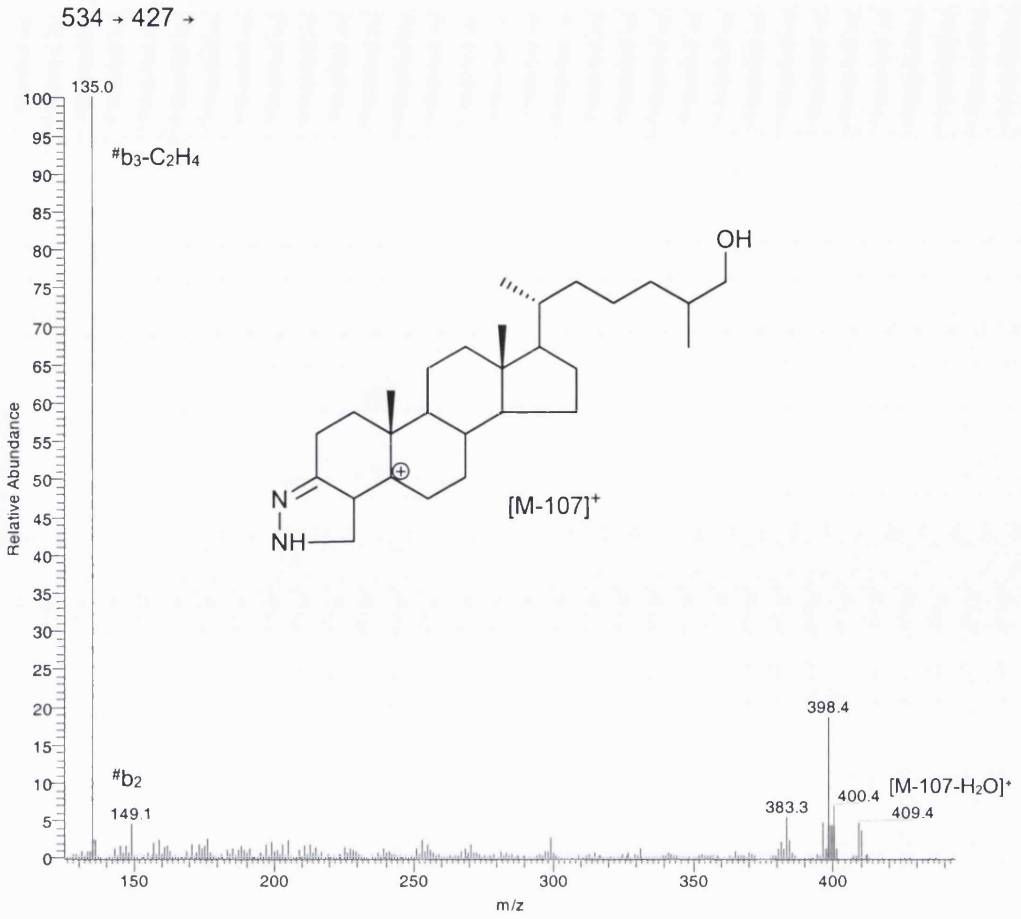

Figure 3.18 Nano-ES-MS^3 (534→ 427→) spectrum of oxidised and GP derivatised 27-hydroxycholesterol.

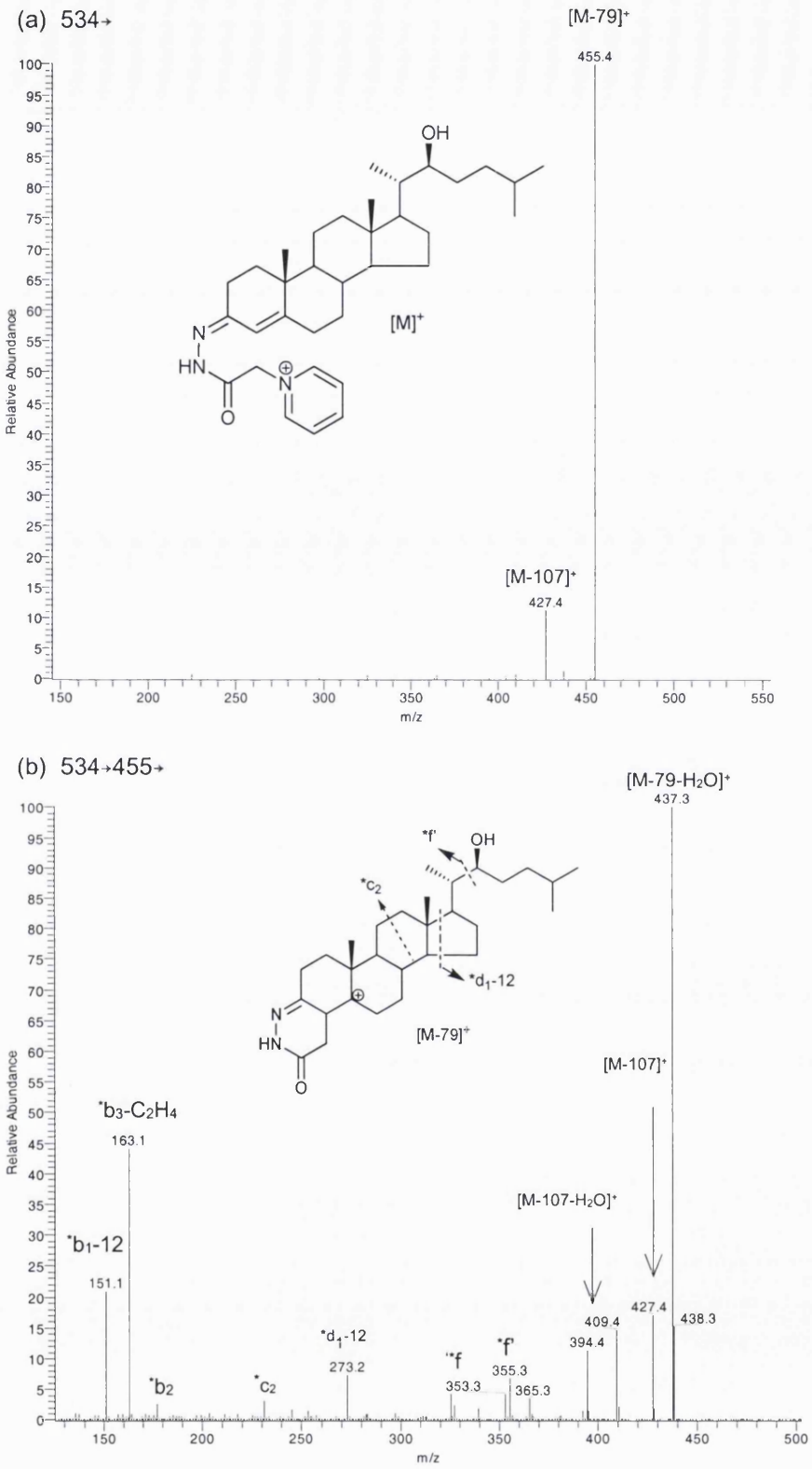

Figure 3.19 (a) Nano-ES-MS^2 (534→), and (b) MS^3 (534→455→) spectra of oxidised/GP-derivatised 22R-hydroxycholesterol.

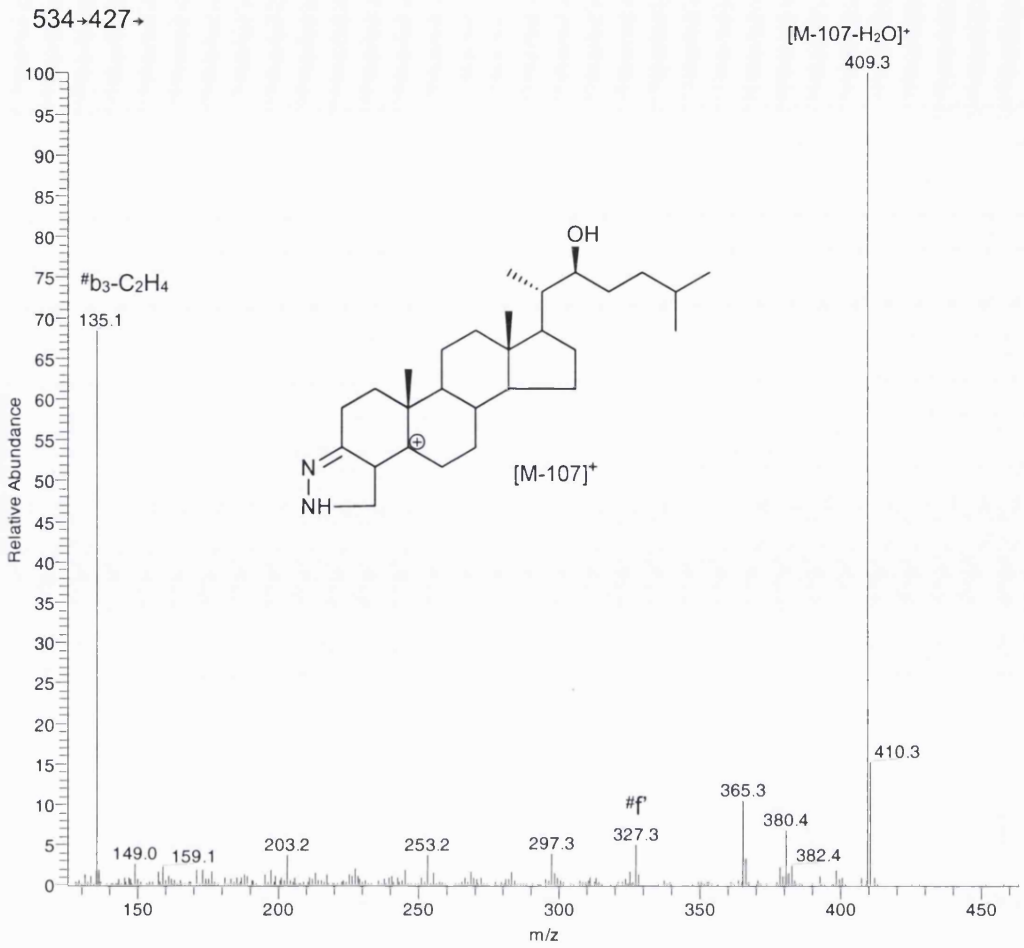

Figure 3.20 Nano-ES-MS^3 (534→427→) spectrum of oxidised and GP derivatised 22R-hydroxycholesterol.

Table 3.3 Group 3 – Reference oxysterols analysed in the present study

Sample Name	Abbreviation	Oxidation product	Derivatisation product	$[M]^+$ *m/z*
7β-Hydroxycholesterol	C^5-3β,7β-diol	C^4-7β-ol-3-one	C^4-7β-ol-3-one GP[a]	534
7α-Hydroxycholesterol	C^5-3β,7α-diol	C^4-7α-ol-3-one	C^4-7α-ol-3-one GP	534
7α,27-Dihydroxycholesterol	C^5-3β,7α,27-triol	C^4-7α,27-diol-3-one	C^4-7α,27-diol-3-one GP	550
7α,25-Dihydroxycholesterol	C^5-3β,7α,25-triol	C^4-7α,25-diol-3-one	C^4-7α,25-diol-3-one GP[a]	550

[a]Structures are given below.

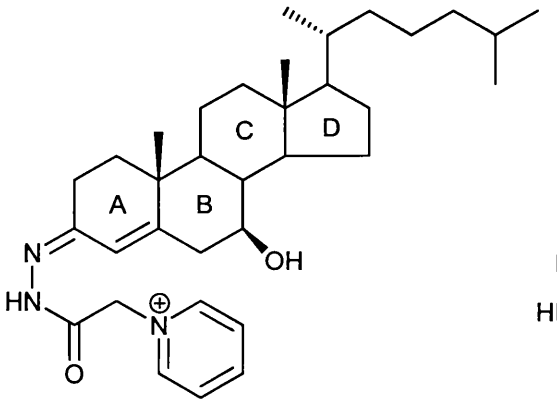

The oxidised/GP-derivatised 7β-hydroxycholesterol
(C^4-7β-ol-3-one GP hydrazone)

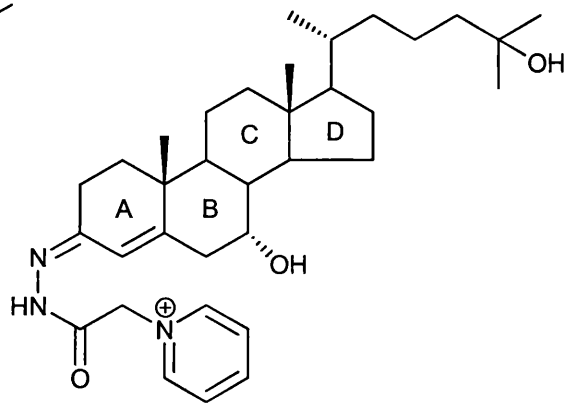

The oxidised/GP-derivatised 7β-hydroxycholesterol
(C^4-7α,25-diol-3-one GP hydrazone)

Group 3 – Reference oxysterols (Table 3.3)

B-ring and side-chain monohydroxycholesterols and dihydroxycholesterols

The MS spectra of the oxidised/GP-derivatised monohydroxy- and dihydroxy-cholesterols give $[M]^+$ ions at *m/z* 534 (Figures 3.21a, 3.23a) and 550 (Figures 3.25a, 3.27a), respectively. The MS^2 spectra of oxidised/GP-derivatised monohydroxycholesterols are dominated by fragment ions corresponding to $[M-79]^+$ (*m/z* 455) and $[M-107]^+$ (*m/z* 427), which are formed by the neutral loss of pyridine, and pyridine plus CO (Figures 3.21b, 3.23b).

Modification of the B-ring by the introduction of a hydroxyl group at C-7 changes the pattern of the B-ring fragment ion in the MS^3 spectra. 7β-Hydroxycholesterol gives an abundant ion at *m/z* 151 ($^*b_1$-12, RA 50%), which dominates the $^*b_1$-12, $^*b_2$, $^*b_3$-C_2H_4 triad in the MS^3 ($[M]^+ \rightarrow [M-79]^+ \rightarrow$) spectrum (Figure 3.22a). The $^*b_3$-C_2H_4 observed at *m/z* 163 in the MS^3 spectrum of oxidised/derivatised 24S-hydroxycholesterol, is shifted by 16 Da to 179 (163+16), and fragment ions at *m/z* 163 (RA 3%) and 177 (RA <1%) are reduced in the MS^3 ($[M]^+ \rightarrow [M-79]^+ \rightarrow$) spectra (Figures 3.22a). Similar patterns of fragment ions are observed in the MS^3 ($[M]^+ \rightarrow [M-107]^+ \rightarrow$) spectra, but with the fragment ions displaced in mass by 28 Da, corresponding to additional loss of CO (Figure 3.22b).

The MS^3 spectra allows the differentiation of closely related isomers, e.g. oxidased/GP-derivatised 7β- and 7α-hydroxycholesterols (Figure 3.22a,b and 3.24a,b). The RA of *m/z* 231 and *m/z* 394 are 2%, 11% for 7β-hydroxycholesterol, and 25%, 55% for 7α-hydroxycholesterol in their MS^3 ($[M]^+ \rightarrow [M-79]^+ \rightarrow$) spectra (Figure 3.22a and 3.24a).

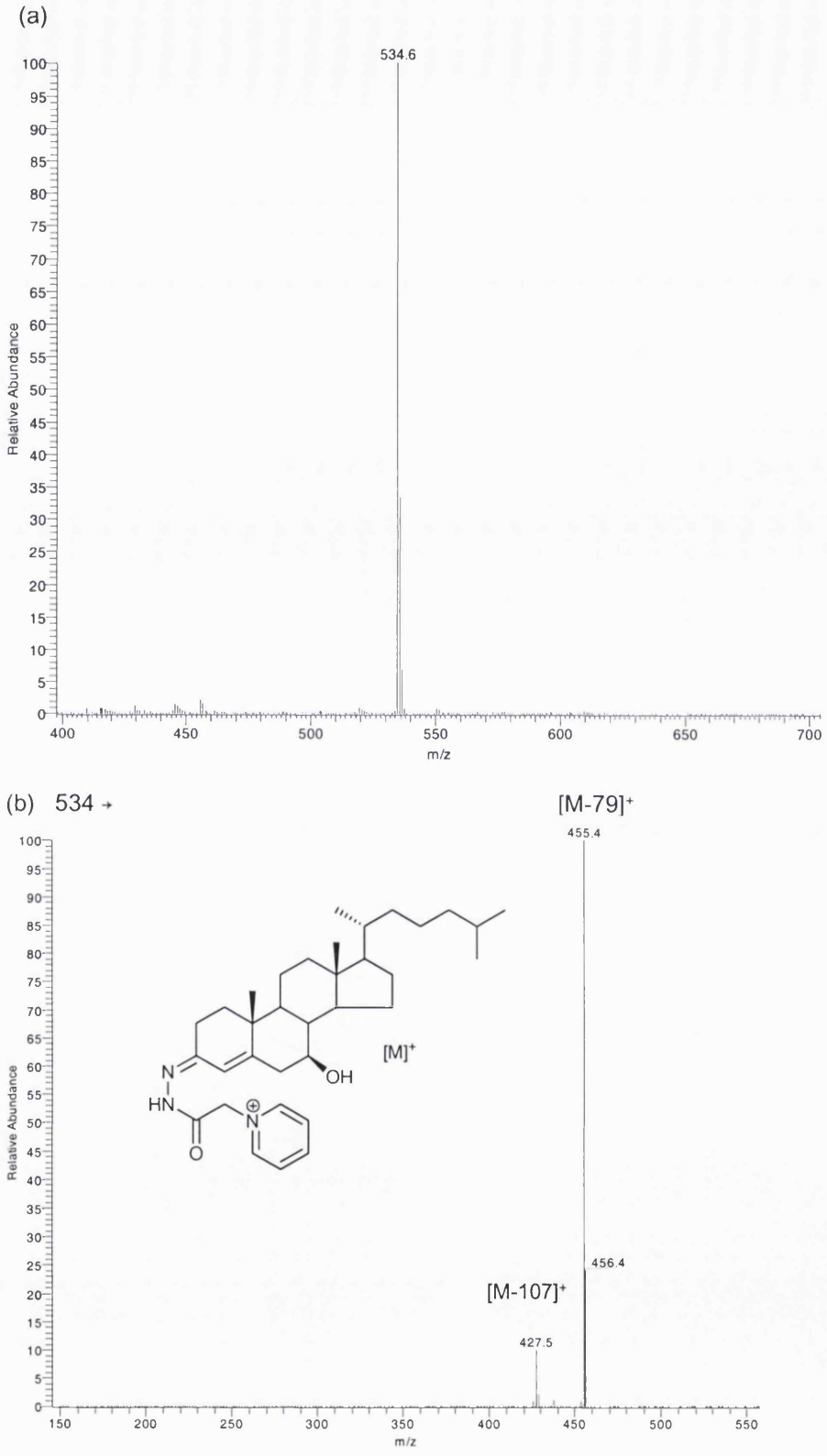

Figure 3.21 (a) Nano-ES-MS, and (b) MS^2 (534→) spectra of oxidised and GP derivatised 7β-hydroxycholesterol.

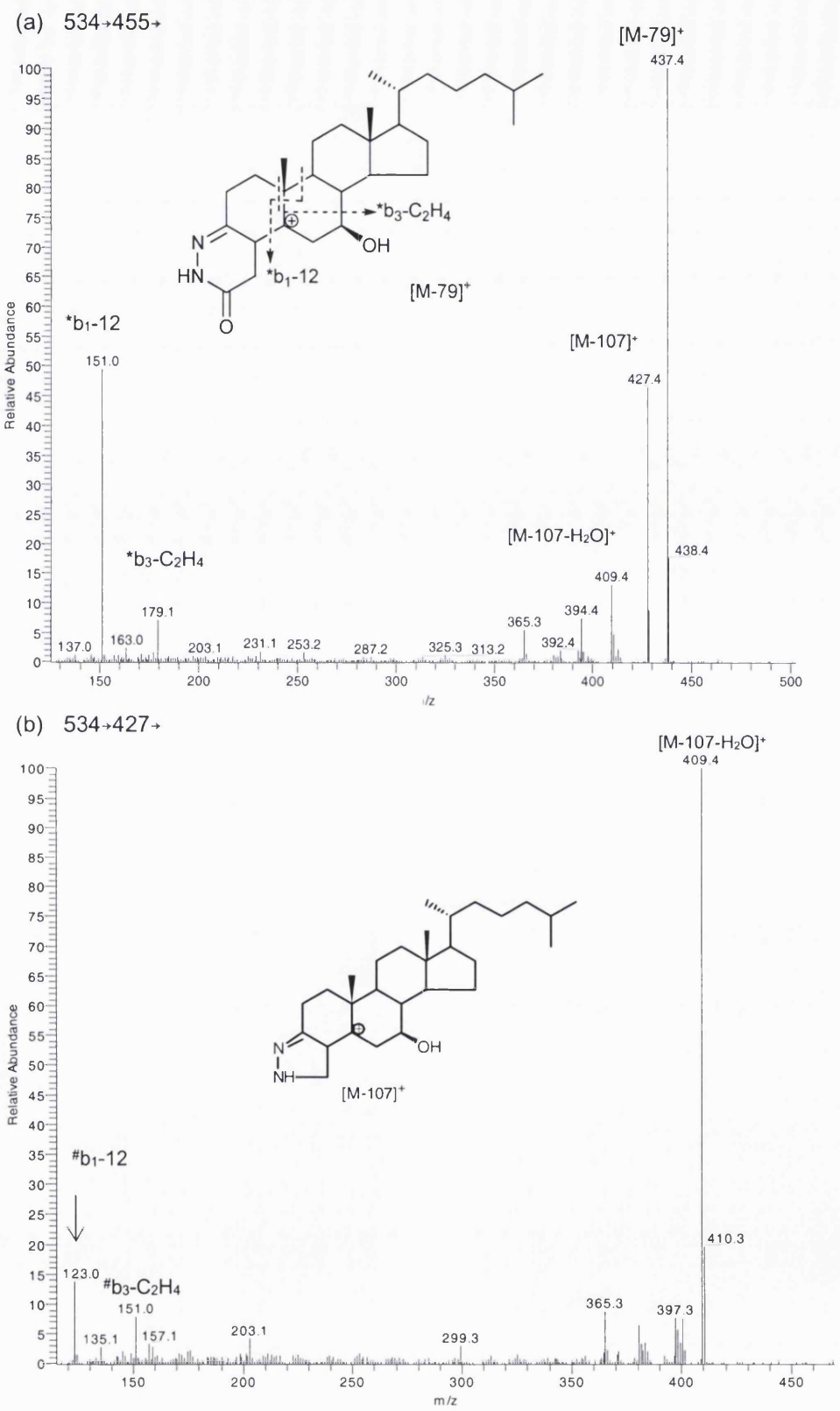

Figure 3.22 (a) Nano-ES- MS^3 (534→455→), and (b) MS^3 (534→427→) spectra of oxidised and GP derivatised 7β-hydroxycholesterol.

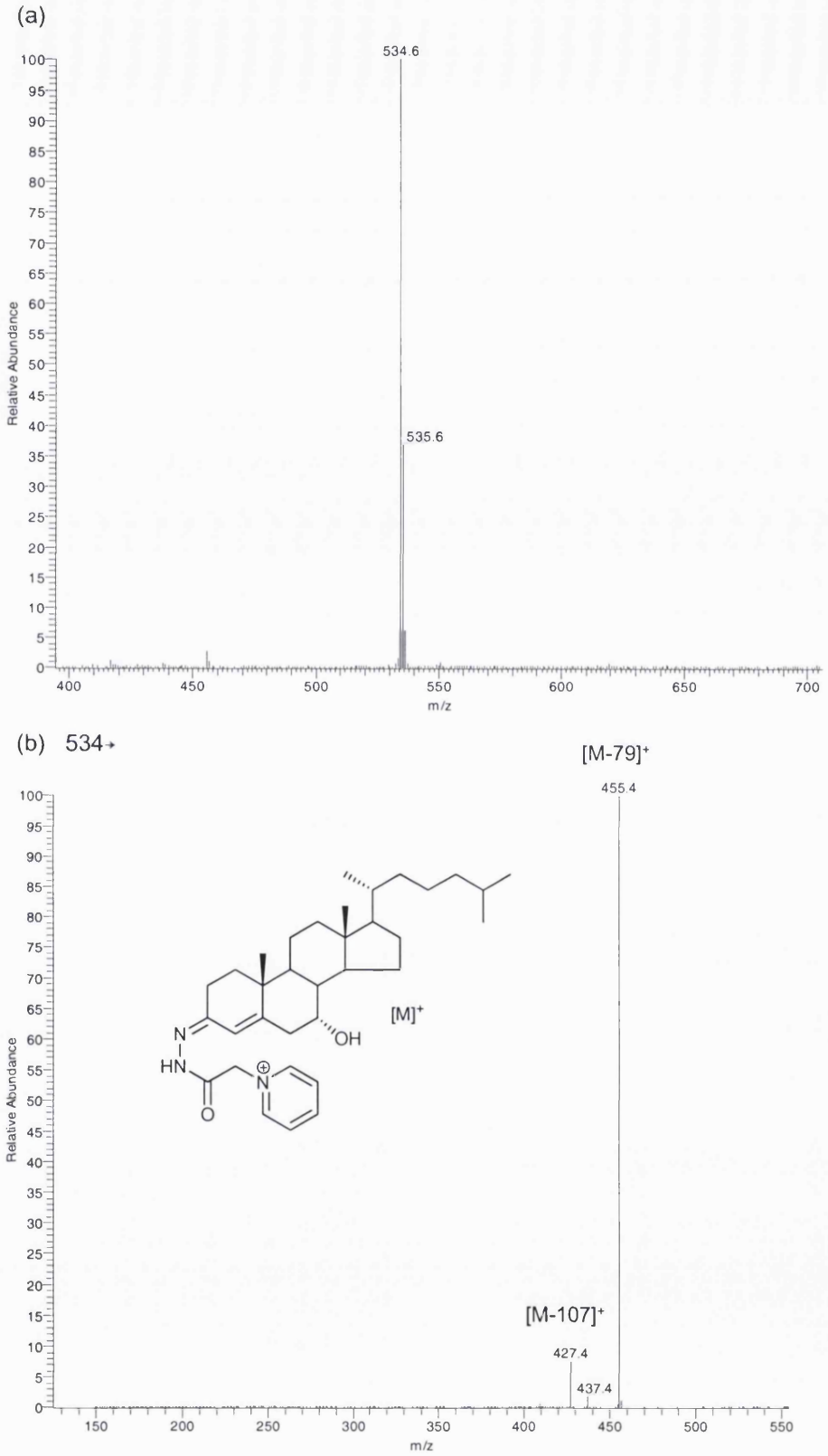

Figure 3.23 (a) Nano-ES-MS, and (b) MS^2 (534→) spectra of oxidised and GP-derivatised 7α-hydroxycholesterol.

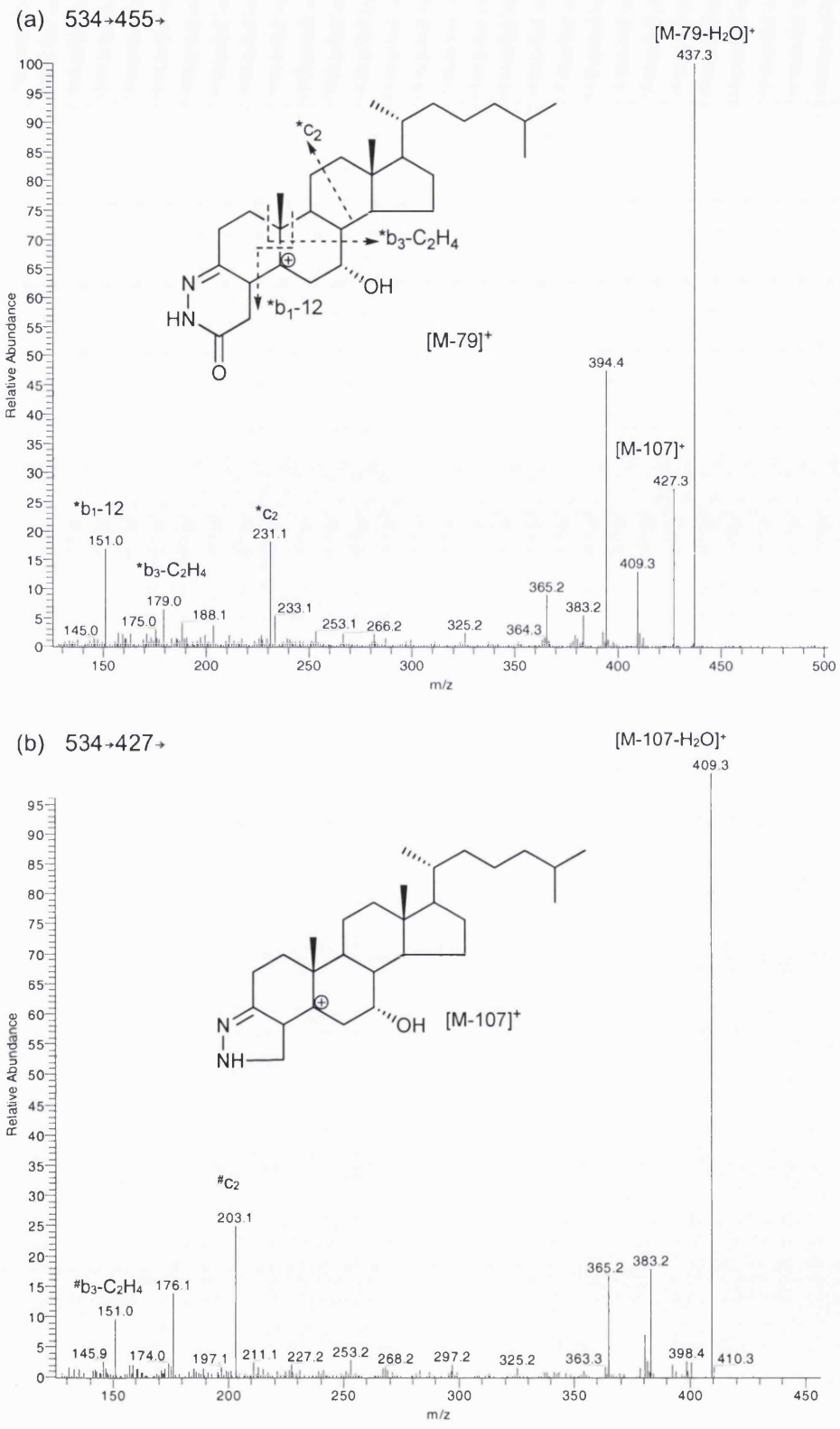

Figure 3.24 (a) Nano-ES-MS^3 (534→455→), and (b) MS^3 (534→427→) spectra of oxidised and GP derivatised 7α-hydroxycholesterol.

The MS^2 spectra of oxidised/GP-derivatised dihydroxycholesterols are dominated by fragment ions corresponding to $[M-79]^+$ and $[M-107]^+$ (*m/z* 471 and 443) as for monohydroxycholesterols. The lability of the added hydroxyl groups is evident by the RA of $[M-79-18]^+$ and $[M-79-(2x18)]^+$ (*m/z* 453 and 435), which correspond to the loss of one and two H_2O molecules from the $[M-79]^+$ ion respectively (Figures 3.25b and 3.27b). For example, the lability of the 25-hydroxyl group relative to the 27-hydroxyl group is evident in the MS^2 spectra of 7,25- and 7,27-dihydroxycholesterols, where the RA of $[M-79-H_2O]^+$ at *m/z* 453 and $[M-79-(2xH_2O)]^+$ at *m/z* 435 are 10%, 5% and 2%, <1% respectively (Figures 3.25b and 3.27b).

The lability of the added hydroxyl groups also greatly affected the RA of ions in the MS^3 spectra. In the MS^3 of the oxidised/GP-derivatised 7,25-hydroxycholesterol, the lability of the 25-hydroxyl group results in an enhancement of ion-current for the $[M-79-H_2O]^+$ at 453, and the low (<10%) RA of all other fragment ions (Figure 3.26a). In contrast, the stability of the 27-hydroxyl group in 7,27-dihydroxycholesterol enhances the abundance of fragment ions containing this alcohol group, e.g. $[M-107]^+$ (*m/z* 443, RA 45%), and $[M-140]^+$ (*m/z* 410, RA 46%) (Figure 3.28a). The ion at *m/z* 410 differs from the $[M-107]^+$ ion in that it has additionally lost H_2O from the B-ring and the NH group from the derivatising group.

The location of the hydroxyl groups also affects ring and side-chain fragmentations. The presence of a hydroxyl group at C-7 results in enhanced abundance of the $*b_1$-12 fragment ion at *m/z* 151 relative to other *b-type ions (Figure 3.28a).

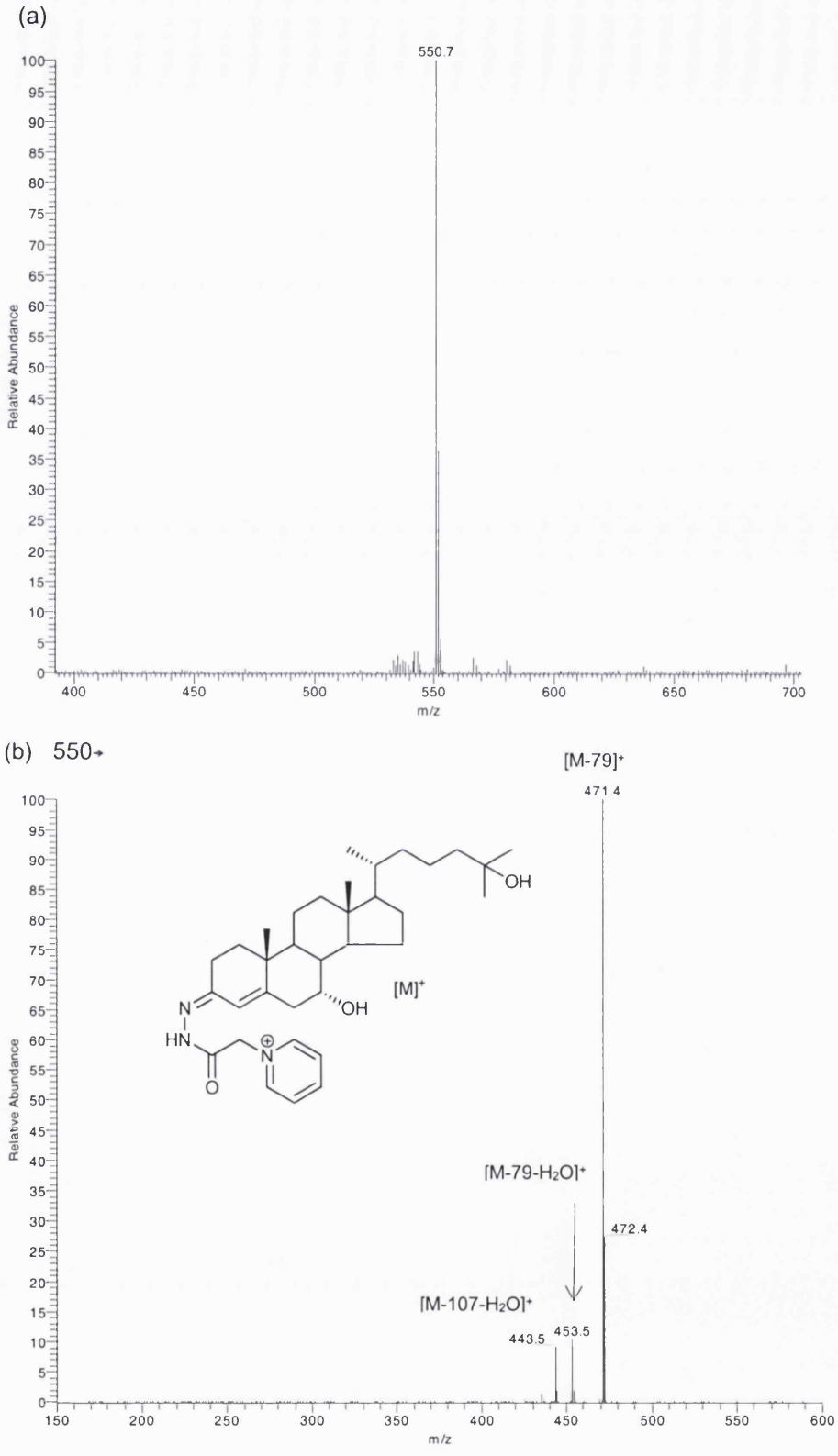

Figure 3.25 (a) Nano-ES-MS, and (b) MS^2 (550→) spectra of oxidised/derivatised 7α,25-dihydroxycholesterol (C^4-7α,25-ol-3-one GP).

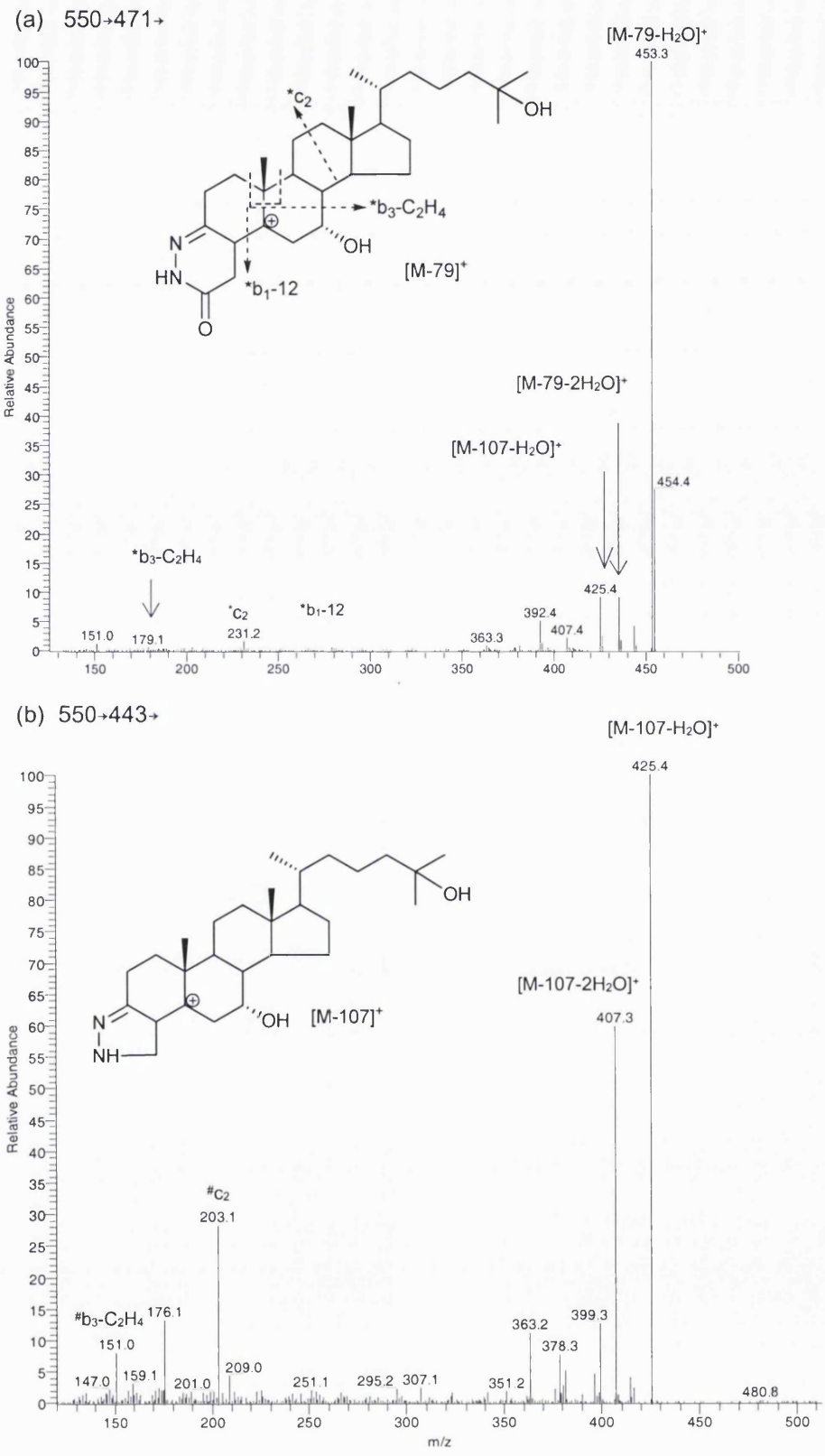

Figure 3.26 (a) Nano-ES-MS^2 (550→ 471→), and (b) MS^3 (550→ 443→) spectra of oxidised/GP-derivatised 7α,25-dihydroxycholesterol (C^4-7α,25-ol-3-one GP).

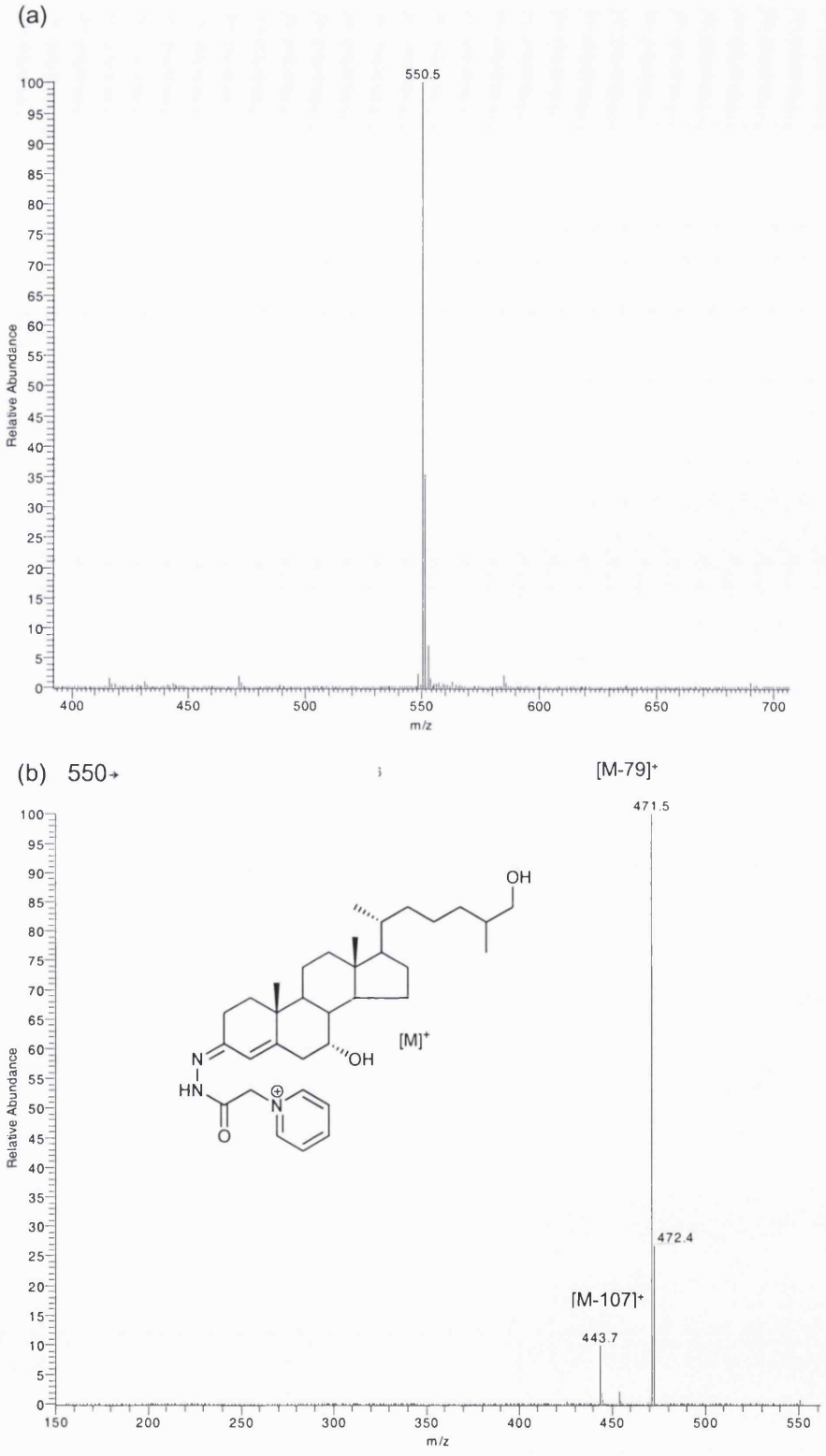

Figure 3.27 (a) Nano-ES-MS, and (b) MS^2 (550→) spectra of oxidised/derivatised 7α,27-dihydroxycholesterol (C^4-7α,27-ol-3-one GP).

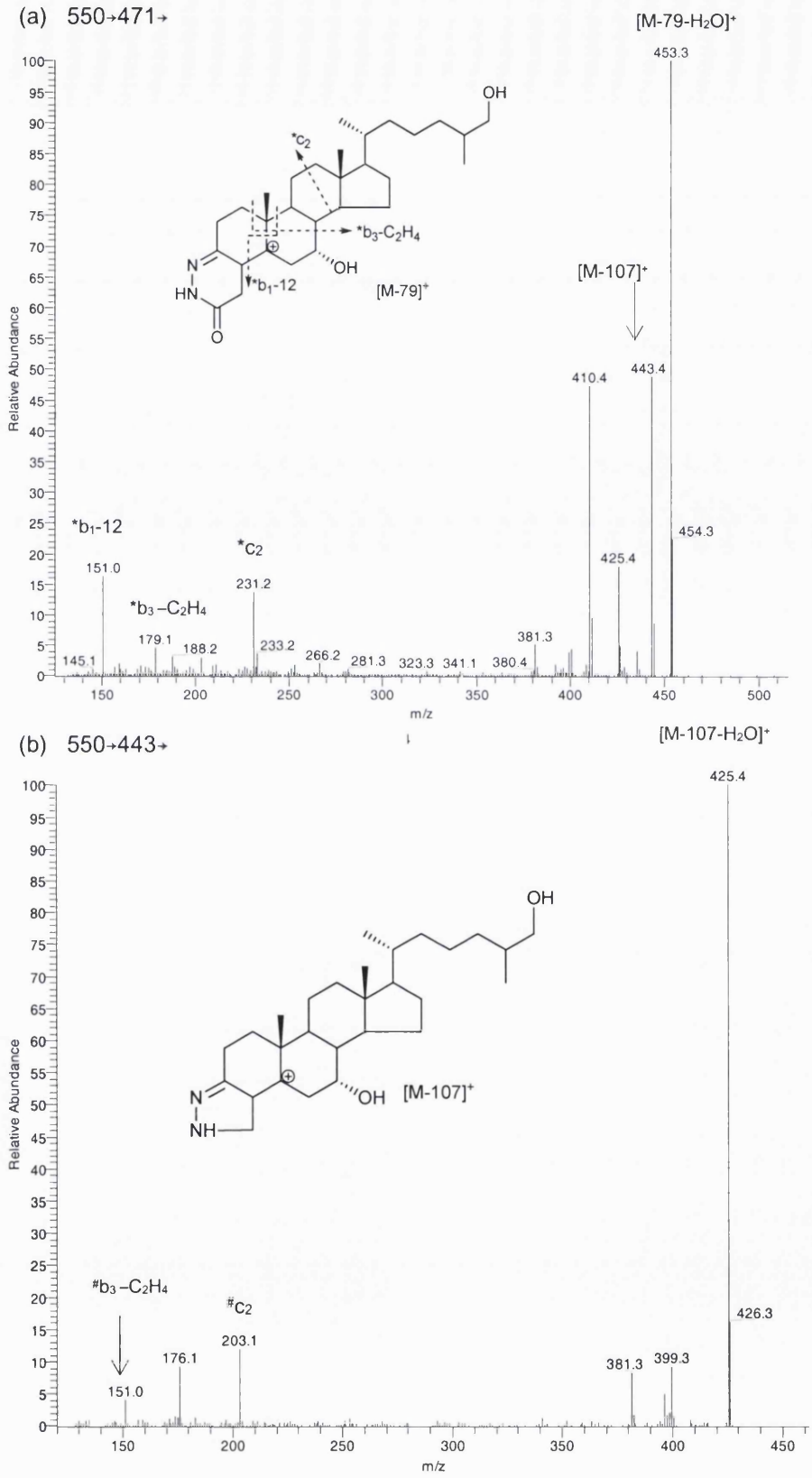

Figure 3.28 (a) Nano-ES-MS^3 (550→471→), and (b) MS^3 (550→443→) spectra of oxidised/GP-derivatised 7α,27-dihydroxycholesterol (C^4-7α,27-ol-3-one GP).

Table 3.4 Group 4 – Reference sterols and oxysterols analysed in the present study

Sample Name	Abbreviation	Oxidation product	Derivatisation product	$[M]^+$, *m/z*
Lathosterol	5α-C-7-en-3β-ol	5α-C-7-en-3-one	5α-C-7-en-3-one GP	518
Lanosterol	$C^{8,24}$-4-4,14-trimethyl-3β-ol	$C^{8,24}$-4-4,14-trimethyl-3-one	$C^{8,24}$-4-4,14-trimethyl-3-one GP	558
Dihydrocholesterol	5α-C-3β-ol	5α-C-3-one	5α-C-3-one GP	520
7-Dehydrocholesterol	$C^{5,7}$-3β-ol	$C^{4,7}$-3-one	$C^{4,7}$-3-one GP	516
19-Hydroxycholesterol	C^{5}-3β,19-diol	C^{4}-19-ol-3-one	C^{4}-19-ol-3-one GP	534
6β-Hydroxycholestenone	C^{4}-6β-ol-3-one[b]	Not Oxidised	C^{4}-6β-ol-3-one GP	534[b]
4β-Hydroxycholesterol	C^{5}-3β,4β-diol	C^{4}-4β-ol-3-one	C^{4}-4β-ol-3-one GP	534
3β,5α,6β-Trihydroxycholestane	C-3β,5α,6β-triol	C^{4}-6-ol-3-one[e]	C^{4}-6-ol-3-one GP[e]	534
16β,27-Dihydroxycholesterol	C^{5}-3β,16β,27-triol	C^{4}-16β,27-diol-3-one	C^{4}-16β,27-diol-3-one GP	550
7-Oxocholesterol	C^{5}-3β-ol-7-one	C^{4}-3,7-dione	C^{4}-3,7-dione GP	532
6-Oxocholestenone[a]	C^{4}-3,6-dione[b]	Not Oxidised	C^{4}-3,6-dione *bis*-GP	333[b,c]
6-Oxocholestenone[a]	C^{4}-3,6-dione[b]	Not Oxidised	C^{4}-3,6-dione GP	532
6-Oxocholestanol	5α-C-3β-ol-6-one	5α-C-3,6-dione	5α-C-3,6-dione GP	534
7-Oxocholestanol	5α-C-3β-ol-7-one	5α-C-3,7-dione	5α-C-3,7-dione GP	534
5α-Epoxycholesterol	C-5α,6α-epoxy-3β-ol	C-5α,6α-epoxy-3β-one	C-5α,6α-epoxy-3-one GP	534

[a]Structure are showed below.

[b]Not Oxidised.

[c]*Bis*-GP derivative formed.

[d]$[M]^{2+}$ of *bis*-GP derivative.

Table 3.4 Group 4 – Reference sterols and oxysterols analysed in the present study

[e]The loss of water.

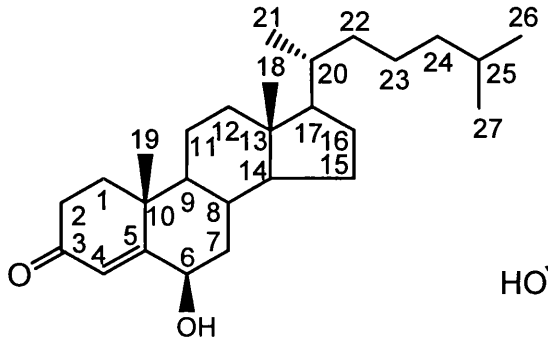

Cholest-4-ene-6β-ol-3-one

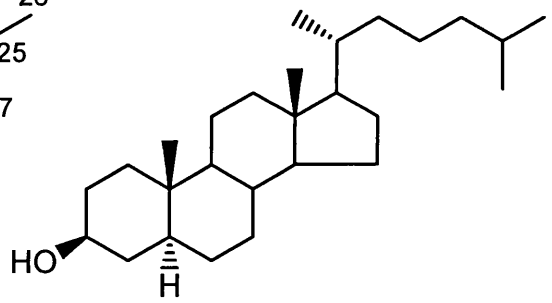

5α-Cholestan-3β-ol
(dihydrocholesterol)

Group 4 – Reference oxysterols (Table 3.4)

Oxocholesterols, oxocholestanols, cholestenediones and other sterols

The reference GP derivatives from this group were oxidased with cholesterol oxidase and derivatised with GP hydrazine, except for 6-hydroxycholestenone and 6-oxocholestenone, which were only subjected to direct derivatisation with Girard P hydrazine. The MS^2 spectra are dominated by fragment ions corresponding to $[M-79]^+$ and $[M-107]^+$ ions. Additional fragment ions at *m/z* 425 $[M-79-30]^+$ (RA 10%) and 504 $[M-30]^+$ (10%) are observed in the MS^2 spectrum of oxidased/GP-derivatised 19-hydroxycholesterol due to the loss of CH_2O (Figure 3.29b).

The MS^3 spectra of oxidised and GP-derivatised A/B ring-substituted sterols do not show the characteristic B-ring fragment-ions (*b- and #b-ion series) of 3-GP sterol hydrazones. Oxidised and derivatised ring-substituted oxysterols give characteristic fragment ions in their MS^3 ($[M]^+ \rightarrow [M-79]^+ \rightarrow$) and ($[M]^+ \rightarrow [M-107]^+ \rightarrow$) spectra that allow their identification as shown below:-

(i) 19-hydroxycholesterol gives abundant fragment ions at *m/z* 427 (RA 100%, $[M-107]^+$), 425 (RA 30%, $[M-109]^+$), and 397 (RA 30%, $[M-137]^+$), where the latter two ions characterise the precursor ion in that they have lost the CH_2O group at C-19 from the $[M-79]^+$ and $[M-107]^+$ ions, respectively (Figure 3.30a). The MS^3 ($[M]^+ \rightarrow [M-107]^+ \rightarrow$) spectrum shows an intense ion at *m/z* 397 (100%) reflecting the loss of CH_2O from C-19 (Figure 3.30b).

(ii) The MS^3 spectrum of the oxidised/GP-derivatised 6-oxocholestanol (5α-cholestan-3β-ol-6-one) is unlike that of isomeric cholest-4-ene-3-ones in that the ion at *m/z* 384 (RA 100%) dominates the spectrum, with the $[M-79-H_2O]^+$ ion at *m/z* 437 (RA <5%) and the $[M-107]^+$ ion at *m/z* 427 (RA 47%) of lower abundance (see Supplementary Material, Figure 27c).

(iii) The introduction of a 6-hydroxyl group, as in 6β-hydroxycholesterol also attenuates fragment ions at *m/z* 151 *m/z* 163, leaving an ion at *m/z* 177. The observation of an ion at *m/z* 177 rather than 193 indicates that the C-6 hydroxyl is no longer present in the $*b_2$ ion (see Supplementary Material, Figure 25c).

(iv) The presence of an oxo group at C-6 eliminates the pattern of B-ring fragment ions.

After treatment with cholesterol oxidase, oxocholesterols can be oxidised to *bis*-oxosterols. Oxocholesterols with an unhindered ketone group are preferentially derivatised with GP reagent [101]. Following derivatisation with GP reagent, oxosterols give singly charged mono-GP derivatives with a $[M]^+$ ion at *m/z* 532, and doubly charged *bis*-derivatives with a $[M]^{2+}$ ion at *m/z* 333. For example, the oxidised/GP-derivatised cholest-4-ene-3,6-dione gives a mono-GP hydrazone (*m/z* 532), and also a *bis*-GP hydrazone (*m/z* 333). The MS^2 spectrum of the $[M]^{2+}$ ion of the *bis*-GP hydrazone (*m/z* 333) is dominated by a singly charged fragment at *m/z* 586 and a doubly charged ion at *m/z* 293. These ions result from the loss of pyridine from the $[M]^{2+}$ ion. In the MS^2 spectrum, the major ions are explained by loss of the complete or parts of the GP-derivatising group from the steroid moiety.

3β,5α,6β-Trihydroxycholestane when oxidised with cholesterol oxidase gives C-5α,6β-diol-3-one which dehydrates to give C^4-6β-ol-3-one under the experimental conditions employed. The ES mass spectrum shows ions at *m/z* 534 (RA of 100%) (Supplementary Material, Figure 26a).

Spectra were also recorded for the other sterols and oxysterols listed in Table 3.4. The spectra are shown in supplementary material Figures 1 to 40.

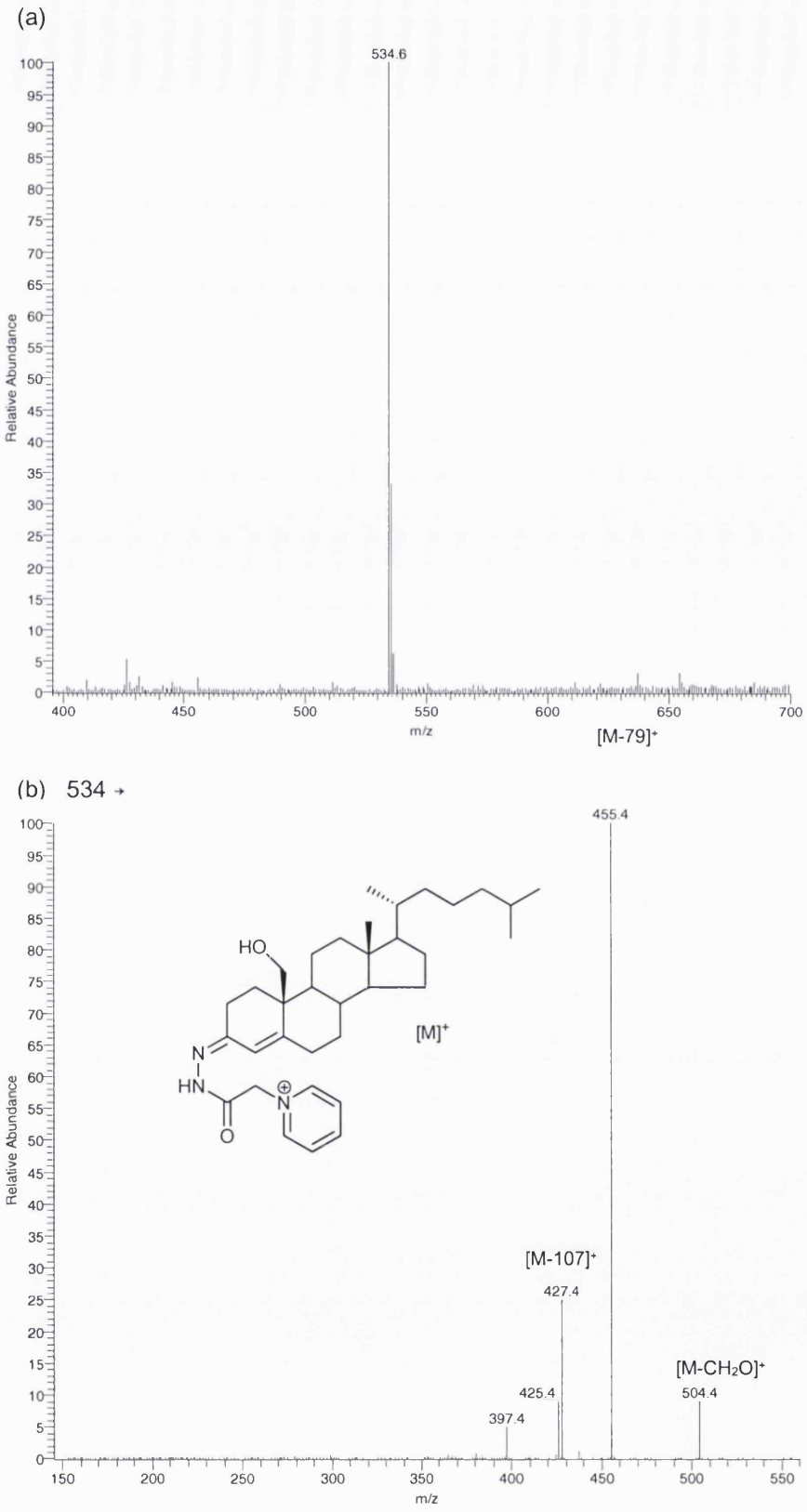

Figure 3.29 (a) Nano-ES-MS, and (b) MS^2 (534→) spectra of oxidised/derivatised 19-hydroxycholesterol (C^4-19-ol-3-one GP).

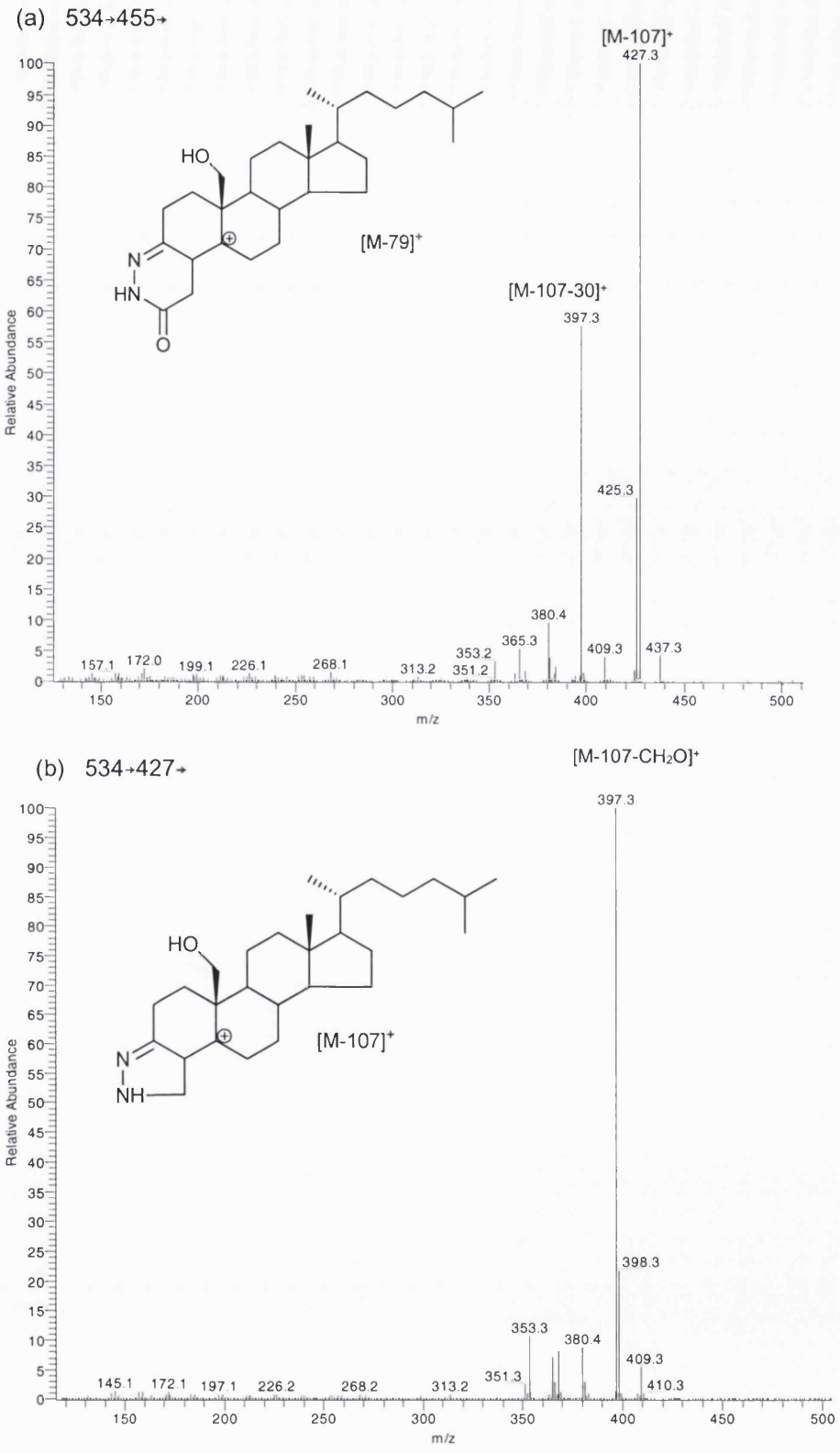

Figure 3.30 (a) Nano-ES-MS^3 (534→455→), and (b) MS^3 (534→427→) spectra of oxidised/derivatised 19-hydroxycholesterol (C^4-19-ol-3-one GP).

Table 3.5 Group 5 – Reference oxysterols analysed in the present study

Sample Name	Abbreviation	$[M]^+$, *m/z*
3β-Hydroxy-5-oxo-5,6-*seco* cholestan-6-al[a]	5,6-Seco-sterol	552
3β-Hydroxy-5-hydroxy-B-norcholestan-6-carboxaldehyde[a]	Aldol	552

[a]Structures are given below.

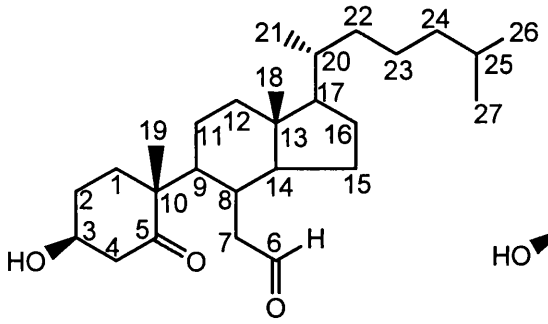

3β-Hydroxy-5-oxo-5,6-*seco* cholestan-6-al

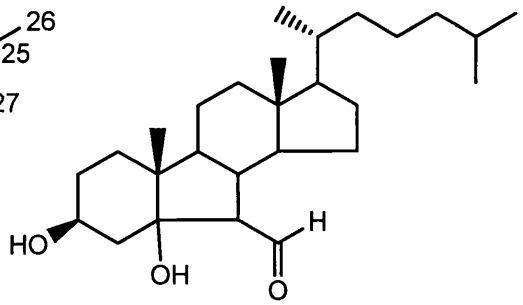

3β-Hydroxy-5-hydroxy-B-norcholestan-6-carboxaldehyde

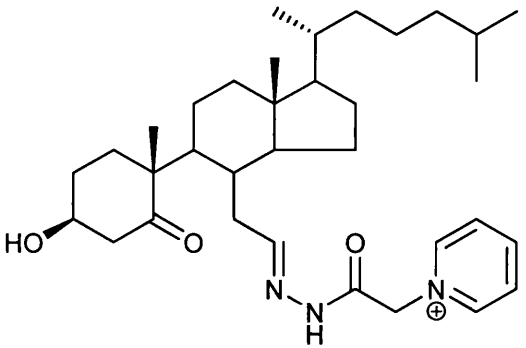

the GP derivatised 3β-Hydroxy-5-oxo-5,6-*seco* cholestan-6-al

Group 5 - Reference oxysterols

Seco-sterols

The presence of 5,6-*seco*-sterol and its aldol condensation product 3,5-dihydroxy-B-norcholestane-6-carboxyaldehyde in human brain was reported by Zhang [94]. The 5,6-*seco*-sterol and its aldol were derivatised with GP reagent, and analysed by direct infusion nano-ES. Nano-ES mass spectra show the peak at *m/z* 552 for both isomers, corresponding to the $[M]^+$ ion (see Supplementary Material Figures 30a and 31a). The MS^2 of the precursor ion spectra allows isomer differentiation. Both spectra dominated by $[M\text{-}79\text{-}H_2O]^+$ ions at *m/z* 455 (RA 100%). However, they differ in the RA of $[M\text{-}107]^+$ ions at *m/z* 445 and $[M\text{-}107\text{-}H_2O]^+$ at 427, where the aldol showed more intense signals (RA 15%, 40%) than the *seco*-sterol (RA 5%, 20%). These and other major fragment ions are formed by cleavage of the derivatising group, and also with the additional loss of water.

Table 3.6 Group 6 – Reference oxysterols analysed in the present study

Sample Name	Abbreviation	Oxidation product	Derivatisation product	$[M]^+$, *m/z*
[2,2,4,4,23-$^2H_5$]3β-Hydroxychol-5-en-24-oic acid	[2,2,4,4,23-$^2H_5$]BA^5-3β-ol	[2,2,4,23-$^2H_4$]BA^4-3-one	[2,2,4,23-$^2H_4$]BA^4-3-one GP	510
3β-Hydroxychol-5-en-24-oic acid	BA^5-3β-ol	BA^4-3-one	BA^4-3-one GP	506
[16,16,17(or20),22,22,23,23-$^2H_7$]3β-Hydroxycholest-5-en-27-oic acid	[16,16,17(or20),22,22,23,23-$^2H_7$] CA^5-3β-ol	[16,16,17(or20),22,22,23,23-$^2H_7$] CA^4-3-one	[16,16,17(or20),22,22,23,23-$^2H_7$] CA^4-3-one GP	555
3β,7α-Dihydroxy-5-cholestenoic acid	CA^5-3β,7α-diol	CA^4-7α-ol-3-one	CA^4-7α-ol-3-one GP	564
3β,7β –Dihydroxy-5-cholestenoic acid	CA^5-3β,7β-diol	CA^4-7β-ol-3-one	CA^4-7β-ol-3-one GP	564

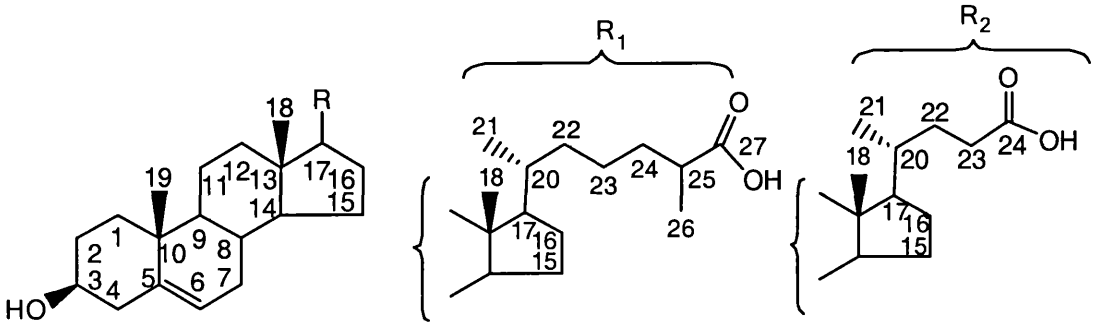

3β-hydroxy-5-ene steroid nucleus

In 3β-hydroxycholest-5-ene-27-oic acid (CA^5-3β-ol) the side chain R_1, and in 3β-hydroxycholest-5-ene-24-oic acid (BA^5-3β-ol) the side-chain R_2 are attached to the 3β-hydroxy-5-ene steroid nucleus.

Group 6 - Reference oxysterols

Bile Acids

Goto and colleagues [156] have identified cholic acid and chenodeoxycholic acid in rat brain. Björkham [36,37] has recently reported on the novel route for elimination of brain sterols across the blood-brain-barrier (BBB) by the conversion into 7α-hydroxy-3-oxo-4-cholestenoic acid. 3β-Hydroxycholest-5-en-27-oic acid and its 7α-hydroxylated analog, and also 3β-hydroxychol-5-en-24-oic acid are known as intermediates in the conversion of cholesterol into primary bile acids [114,168] (see Figure 1.12). The precursors of bile acids with a 3β-hydroxy-5-ene and 3-oxo-4-ene functionalities can be analysed by the current methodology.

After treatment with cholesterol oxidase and GP reagent, 3β-hydroxychol-5-en-24-oic acid and its [2,2,4,4,23-$^2H_5$]-isotopomer give a $[M]^+$ ion at *m/z* 506 and 510 respectively (Supplementary Material, Figures 32a and 33a). Oxidation of these bile acids with cholesterol oxidase results in conversation of the 3β-hydroxy-5-ene function to a 3-oxo-4-ene, during this translocation one of deuterium atoms on C-4 of the deuterated isotopomers is lost to give a mass increase of 4 Da [for example [2,2,4,4,23-$^2H_4$]) compared to the unlabelled isotopomer. The MS^2 spectrum of the oxidised/GP-derivatised 3β-hydroxychol-5-en-24-oic acid is dominated by $[M-79]^+$ and $[M-107]^+$ ions at *m/z* 427 (RA 100%) and 399 (RA 20%), respectively. The MS^3 ($[M]^+ \rightarrow [M-79]^+ \rightarrow$) spectrum shows fragment ions at *m/z* 151 (*b_1-12), 163 (*b_3-C_2H_4) and 177 (*b_2) typical of the 3-oxo-4-ene sterol (see Supplementary Material, Figure 33c). The interpretation of MS^2 and MS^3 spectra was confirmed by acquiring the analogues spectra of the oxidised/GP-derivatised [2,2,4,4,23-$^2H_4$]3β-hydroxychol-5-en-24-oic acid. As predicted, *b and #b-ion series were shifted in mass by 3 Da (Supplementary Material, Figure 32c).

After oxidation of [16,16,17(or20),22,22,23,23-$^2H_7$]3β-hydroxycholest-5-en-27-oic acid with cholesterol oxidase and derivatisation with GP hydrazine, the resulting 3-oxo-4-ene acid was subjected to analysis by direct infusion nano-ES, giving a $[M]^+$ ion at *m/z* 555 (see Supplementary

Material, Figure 34a). The MS^3 spectra shows a characteristic triad of *b and #b-fragment ions confirming the presence of 3-oxo-4-ene functionality in the acid. The presence of $[M-79-H_2O]^+$ ion at *m/z* 458 and $[M-107-H_2O]^+$ ion at *m/z* 430 shows that water can be eliminated from the C-27 acid group (Supplementary Material, Figures 34c and d).

Following oxidation with cholesterol oxidase and derivatisation with GP reagent, 3β,7α- and 3β,7β-dihydroxy-5-cholestenoic acids give a $[M]^+$ ion at *m/z* 564 (see Supplementary Material, Figures 35a and 36a). The presence of a 7-hydroxy group changes the pattern of AB-ring fragment ion to *m/z* 151 ($*b_1$-12), and 179 ($*b_3$-28). The presence of the labile 7α-hydroxy group had the effect of enhancing the intensity of $[M-79-H_2O]^+$ and $[M-107-H_2O]^+$ ions (Supplementary Material, Figures 35c and 36c).

3.6 Configuration of capillary-LC for on-line connection to the LCQ^{duo} ion trap mass spectrometer

A capillary LC system fitted with an analytical column C_{18} (180 μm internal diameter (i.d.), 3 μm particles, 100 Å pore size) interfaced through fused silica to a nano-ES source of a LCQ^{duo} ion trap mass spectrometer was used for the analysis of oxidised/GP-derivatised sterols/oxysterols in this work. Figure 3.31 shows the UltiMate 3000 LC system, and Figure 3.32 shows the LCQ^{duo} ion trap mass spectrometer. During the configuration of the capillary LC system for connection to the mass spectrometer, two significant parameters were taken into consideration:- (i) the volume of sample taken for each injection; (ii) the dead volume in the connecting tube.

Figure 3.33 illustrates the fluid connections for a direct injection analysis with the UltiMate 3000 system. The system allows for gradient-elution operation. The UltiMate 3000 system was configured for the capillary-LC analysis by the use of an integrated FLM-3100 flow splitting system (Figure 3.31c). The FLM-3100 was fitted with a capillary flow splitter. The flow splitter was placed before the six-port valve, and was used to achieve stable flow rates from 0.8–2 μL/min from the micro pump. This micro pump allows rapid changes in solvent composition to be achieved prior to reaching the analytical column. The micro pump is located in the LPG-3600 system (Figure 3.31b).

The WPS-3000 well plate auto-sampler was configured with a five µL sample loop (Figure 3.31e). The "user defined" pick-up injection program was performed, for which only the volume of sample to be injected is taken, preceded, and if required followed by transport liquid. Dead volume causes chromatographic band broadening, and time delays in the LC system.

Figure 3.31 Nano and capillary LC system from Dionex, UK. The UltiMate 3000 system consists of the following modules (a) SRD-3000: Solvent rack with integrated degassing; (b) LPG-3600: Single and dual gradient pump; (c) FLM-3100: Integrated flow manager and column compartment; (d) UVD-3000: UV detector; (e) WPS-3000: Well plate sampler; (f) Capillary PepMap C_{18} column (180 µm i.d. x 150 mm, 3 µm particles, 100 Å) from Dionex, Surrey, UK.

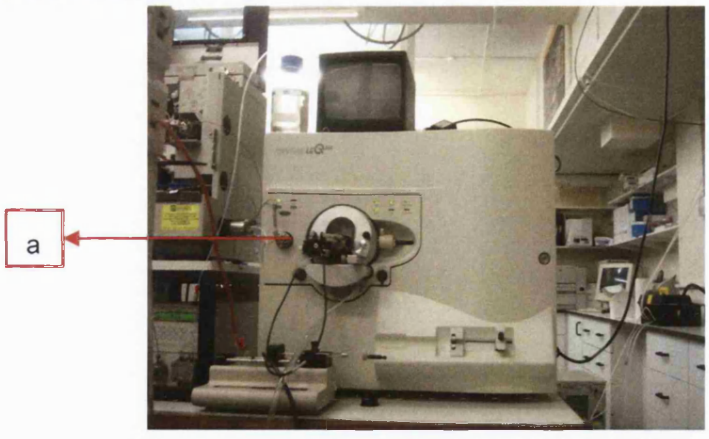

Figure 3.32 LCQ^{duo} ion tap mass spectrometer. (a) the nano-ES probe assembly.

The sample was directly injected onto the analytical column through the six-port valve. Schematic diagram of the six-port valve and its operation is shown Figure 3.34. Before being transferred to the LC column, the sample was loaded into the five µL sample loop (Figure 3.34a). The six-port valve was then switched, and the sample was brought in-line with the LPG-3600 single gradient pump, and was then directed by the mobile phases onto the capillary PepMap C_{18} column

(180 µm i.d. x 150 mm, 3 µm particles, 100 Å) (Figure 3.34b). The LC gradient was started, with the switch of the six-port valve. The five µL loop was chosen in order to inject varying amounts of biological sample onto the analytical column. The UV detector was by-passed in order to avoid band broadening after the sample had left the column. Hence, the distance between the end of the column and the capillary ES probe assembly was minimised. The Ultimate 3000 system was positioned in series to the LCQ^{duo} ion trap mass spectrometer, and the instruments were interfaced to each other through 25 µm i.d. fused silica tubing.

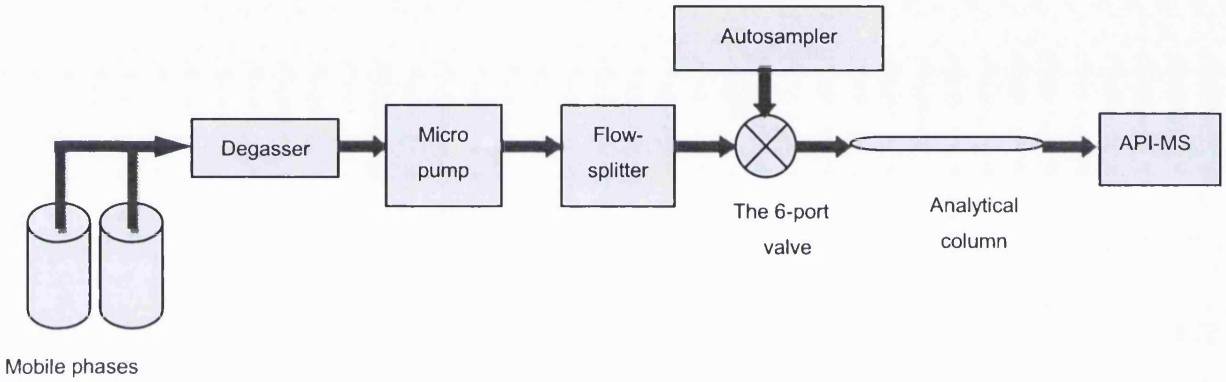

Figure 3.33 Schematic diagram for the fluid connections in the UltiMate 3000 system (direct injection). The UltiMate 3000 system was connected with the atmospheric pressure ionisation mass spectrometer (API-MS).

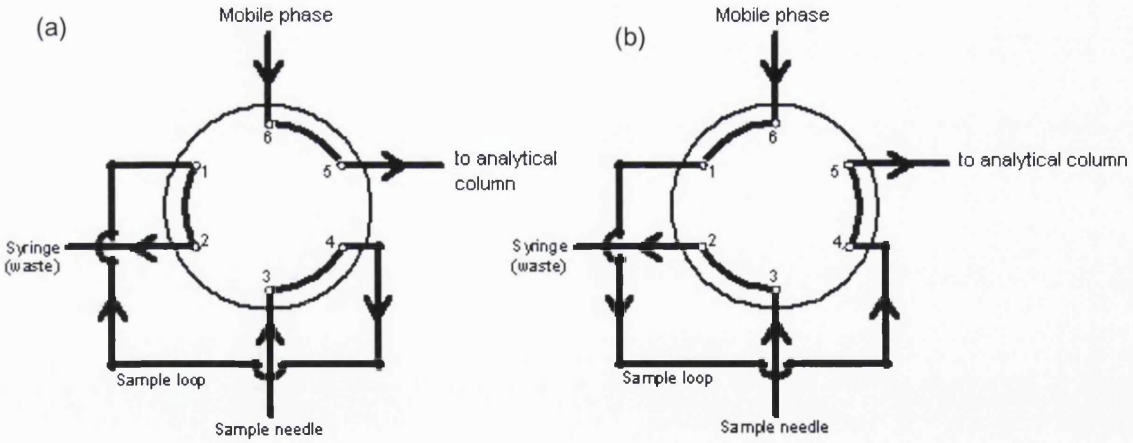

Figure 3.34 Schematic diagram of the six-port valve on the WPS-3000 well plate sampler. (a) six-port valve: sample is loaded onto the sample loop; (b) six-port valve: the 6-port valve is switched and sample is loaded onto the analytical column. Taken from ref. [169].

3.7 Optimisation of capillary-LC for the analysis of oxidised/GP-derivatised oxysterols

Multiple isomeric oxysterols could exist, differing only by the location of the hydroxyl group on the C-17 side-chain, and on the steroid nucleus. Unless separated, the presence of these isomers in a mixture would result in a composite MS^3 spectrum, which is difficult to interpret. Hence, effective chromatographic separation decreases interference caused by isobaric oxidised/GP-derivatised oxysterols in the sample. A combination of reversed phase capillary chromatography and tandem mass spectrometry was adapted in this work for the analysis of oxysterols.

Oxysterols are hydrophobic molecules with limited solubility in aqueous solvents. In a reversed phase chromatographic separation, retention time decreases as the polarity of the oxidised/GP-derivatised oxysterols increases. It is also well known that sterols partition into the reversed phase of the analytical column, and require high organic content of the mobile phase in order to elute them from the column [38,112]. This causes potential problems in the LC-MS analysis, because of the length of the chromatographic runs, and the possibility of carry-over from injection to injection between LC analyses. Oxidised and GP-derivatised oxysterols provide an advantage with respect to both chromatographic and mass spectrometric analysis. The GP group enhances the solubility of oxysterols in aqueous solvents, allowing for a greater variety of mobile phase. While the presence of a charged group improves the mass spectrometric sensitivity by two to three orders of magnitude [38,71].

Gradient elution was used in order to separate a mixture of oxidised/GP-derivatised oxysterols. Derivatised oxysterols were eluted according to their polarity by using a stepwise increase of methanol content in 0.1% formic acid during the chromatographic separation as described in Chapter 2, section 2.9. The optimisation of gradient was carried out with a mixture of the oxidised/GP-derivatised 24S-hydroxycholesterol and cholesterol. The aim was to separate these compounds as much as possible in order to obtain selectivity, and also obtain sharp well-resolved peaks. The oxidised/GP-derivatised monohydroxycholesterol eluted first, followed by cholesterol (Figure 3.35).

The injection solvent was extremely important for oxysterol analysis. The oxysterols were injected in a solution of high methanol content (around 63% of methanol in water). This is desirable to ensure that the oxidised/GP-derivatised oxysterols were dissolved-in, rather dispersed-in, solution.

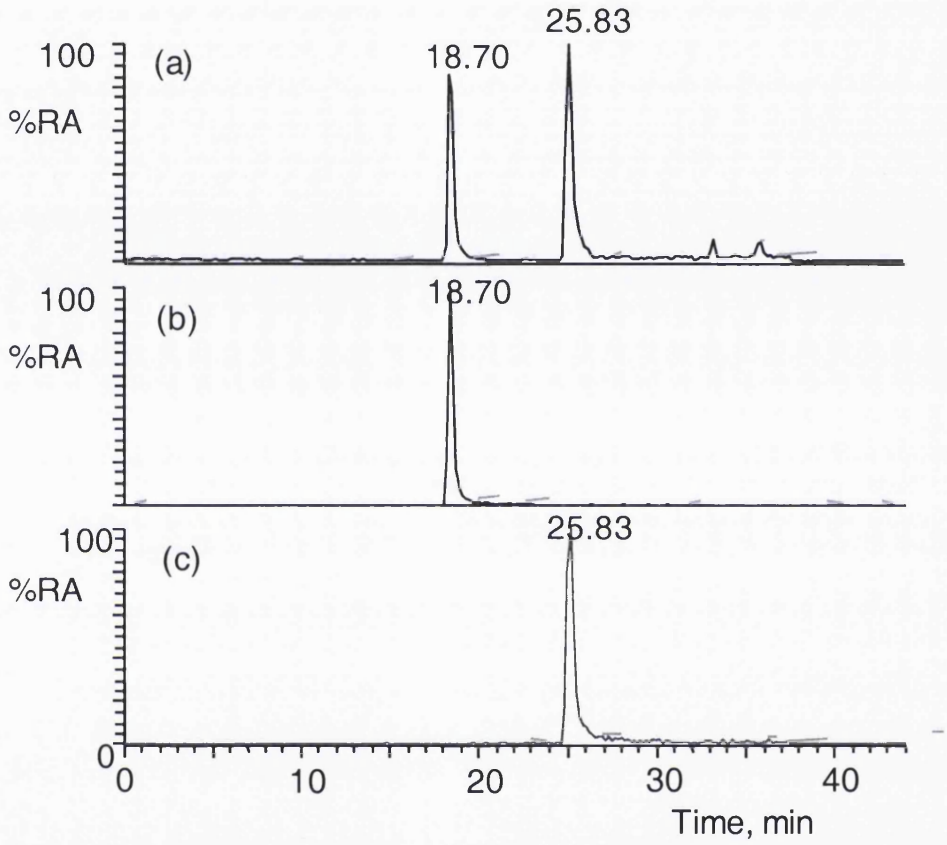

Figure 3.35 (a) Base peak chromatogram of a mixture of oxidised/GP-derivatised 24S-hydroxycholestrol and cholesterol; (b) TIC for the MS^3 (534→455→) transition (24S-hydroxycholesterol), and (c) TIC for the MS^3 (518→439→) transition (cholesterol). The separation was achieved on a PepMap C_{18} column (180 µm i.d. x 150 mm, 3 µm, 100 Å) using a UltiMate 3000 capillary LC system. The mobile phases were:- mobile phase A was 0.1% formic acid in 50% methanol; mobile phase B was 0.1% formic acid in 95% methanol; transport solvent 0.1% formic acid in 63.5% methanol. The gradient program started at 30% B rising to 70% B over ten minutes, then to 80% B over a further five min. The mobile phase composition was maintained at 80% B for a further 15 minutes before returning to 30% in 0.1 min. The column was reconditioned with this mobile phase composition for 20 min. The total run was 50 min and the flow rate 0.8 µL/min.

It was also found that oxidised/GP-derivatised oxysterols required for LC-MS analysis can not be stored in aqueous solvents for extended periods of time. This problem was overcome by diluting the sample into aqueous solvents immediately prior to injection onto the LC column.

In biological systems, oxysterols are normally present only in trace amounts. The excess of cholesterol is almost invariably more than three orders of magnitude higher. Hence, there is the possibility that the presence of a significant excess of cholesterol in an oxysterol fraction could lead to carry-over between LC-MS analyses, and to the formation of autoxidation products due to accumulation of cholesterol, for example in the injection needle. A series of analyses of oxidised/GP-derivatised cholesterol was performed using the gradient as described in section 2.9 but using different washing solvents for the injector (sample loop, and needle) in order to investigate the effect of carry-over. There was a substantial carry-over of the oxidised/GP-derivatised cholesterol from injection to injection when the washing solvent was 70% methanol in water. The first injection of blank solvent after an injection of cholesterol (1 ng) resulted in a signal that was around 1% the intensity of the previous injection for the oxidised/GP-derivatised cholesterol. For the next three injections of blank solvent, the intensity was only reduced to 0.1% of the original signal intensity. This was unacceptable for conducting qualitative or quantitative analyses. After testing several solvent combinations, it was found that washing the sample loop and injection needle five times with 100 µL of methanol-isopropanol (1:1, v/v), resulted in no carry-over from injection to injection.

Column pressure traces were continuously monitored. The amount of oxidised/GP-derivatised oxysterols injected on-column was between 1 pg to 1 ng. When around 100 samples were analysed by capillary-LC-MS^n analysis, the capillary-LC column was thoroughly flushed with a mixture of isopronanol-methanol-water (5:4:1,v/v) at a flow rate of 0.6 µL/min for 4 hours. The column was equilibrated with mobile phase, whereupon analysis of the next 100 samples commenced.

3.8 Strategy used for the analysis of the oxidised/GP-derivatised oxysterols by cap-LC-MS^n

This section describes the evaluation of the use of cap-LC combined with tandem mass spectrometry for the analysis of oxysterols. As discussed in section 3.4, GP hydrazones give abundant $[M]^+$ ions upon positive ion nano-ES ionisation, and fragment in MS^2 experiments to give signals at $[M-79]^+$ and $[M-107]^+$, which correspond to the loss of pyridine and pyridine plus carbon monoxide from the derivatising group, respectively. This allows development of multi-stage fragmentation mass spectrometry (MS^2 and MS^3) experiments providing information about their structure.

Oxidised and GP-derivatised oxysterols were injected onto the capillary PepMap C_{18} column, and MS, -MS^2, and -MS^3 spectra were continuously recorded over the chromatographic separation. When the GP-derivatised oxysterol elutes from the column it is subjected to both MS^2 ($[M]^+\rightarrow$) and MS^3 ($[M]^+\rightarrow[M-79]^+\rightarrow$) analysis. The MS^2 analysis programme was based on knowledge of the oxidised/GP-derivatised oxysterol mass. MS^3 was performed on ions resulting from a neutral loss of 79 Da and 107 Da in the MS^2 scan. For example, the MS^3 experiment was $534\rightarrow455\rightarrow$ for the oxidised/GP-derivatised monohydroxycholesterols. This provides a high degree of specificity to the method as this final product-ion spectrum is only generated from precursor ions of the selected mass giving an $[M-79]^+\rightarrow$ and $[M-107]^+\rightarrow$ intermediate. LC-MS spectra were recorded over the *m/z* range 250-700, which covers the $[M]^+$ and $[M]^{2+}$ ions of all derivatised oxysterols.

Total ion chromatograms (TICs) for reference oxidised/GP-derivatised oxysterols were generated for the $[M]^+\rightarrow$, $[M]^+\rightarrow[M-79]^+\rightarrow$ and $[M]^+\rightarrow[M-107]^+\rightarrow$ transitions over the duration of the LC-MS^n run. For example, Figure 3.35 shows TICs generated for the $[M]^+\rightarrow[M-79]^+\rightarrow$ transitions for oxidised/GP-derivatised 24S-hydroxycholesterol and cholesterol. Reconstructed ion chromatograms (RICs) for reference oxidised/GP-derivatised oxysterols were also generated for the $[M]^+\rightarrow[M-79]^+\rightarrow$ + an unique ion in its MS^3 spectrum over the duration of the LC-MS^n run. For example, Figure 3.40

shows RICs generated for the MS^3 transition 534→455→353 for oxidised/GP-derivatised 24S-hydroxycholesterol.

3.9 Analysis of the oxidised/GP-derivatised reference oxysterols by capillary LC-MS^n

All reference oxysterol GP hydrazones have good LC properties under reversed phase conditions. The peak width at half-height for most reference oxysterol GP hydrazones was around 12 sec (an example is shown for the oxidised/GP-derivatised 25-hydroxycholesterol, Figure 3.36). The *syn-* and *anti-* configurations are formed during the derivatisation reaction, and depending on the analyte were partially separated on the capillary C_{18} column. For example, the *syn-* and *anti-* conformers of the oxidised/GP-derivatised 7α-hydroxycholesterol were partially separated (Figure 3.37).

Over the 50 min duration of the capillary LC gradient, the forty oxidised/GP-derivatised oxysterols analysed in this study eluted in the following order:- bile acids, dihydroxycholesterols, monohydroxycholesterol (with hydroxyl group on the C-17 side-chain), monohydroxycholesterols (with hydroxyl group on the steroid nucleus), cholesterol, and sterols with hydrocarbon substituent on the C-17 side chain (see Figure 3.38). The main factors determining retention of the oxidised/GP-derivatised sterols on the reversed-phase column are the number, type and orientation of polar groups in the molecules, and the number of carbon atoms in the side-chain. The presence of hydroxyl groups in different positions on the steroid nucleus and on the C-17 side chain give rise to very different relative retention times. For example, fifteen GP hydrazones were eluted in the following order: C^4-7α,25-diol-3-one GP, C^4-7α,27-diol-3-one GP, C^4-20α-ol-3-one GP, C^4-22R-ol-3-one GP, C^4-24S-ol-3-one GP, C^4-25-ol-3-one GP, C^4-3,24-dione 3-GP, C^4-27-ol-3-one GP, C^4-22S-ol-3-one GP, C^4-7β-ol-3-one GP, C^4-3,7-dione GP, C^4-3,6-dione GP, C^4-7α-ol-3-one GP, C^4-19-ol-3-one GP, $C^{4,24}$-3-one GP, C^4-3-one GP hydrazones (examples are shown for the oxidised/GP-derivatised 3β-hydroxychol-5-enoic acid, 7α,27-dihydroxycholesterol, 24S-hydroxycholesterol, 22S-

hydroxycholesterol, 7-oxocholesterol, 6β-hydroxycholesterol, 19-hydroxycholesterol, and cholesterol in Figure 3.39).

Relative retention times (RRTs) in relation to the oxidised/GP-derivatised cholesterol are summarised in Figure 3.38. TICs generated for the $[M]^+ \rightarrow [M-79]^+ \rightarrow$ transitions over the duration of the cap-LC-MS^n run were used for the calculation of relative retention times.

Within-day precision values were determined by repetitive measurements of the retention times of quality control samples (the oxidised/GP-derivatised 24S-hydroxycholesterol, 25-hydroxycholestrol and cholesterol) using the cap-LC-MS instrument, and gave coefficients of variance (CV) between 0.06% to 0.15% (n=10, within-day precision).

Repetitive measurements of the retention times of quality control samples (the oxidised/GP-derivatised 24S-hydroxycholesterol, 25-hydroxycholestrol and cholesterol), which were prepared fresh from stock solutions on the day of experiment, during ten consecutive days gave a CV of 7.1% (n=10, between-day precision).

The capillary reversed-phase column was capable of resolving many of the oxidised/GP-derivatised isomers e.g. (i) 22S-hydroxycholesterol and 22R-hydroxycholesterol, (ii) 7α-hydroxycholesterol and 7β-hydroxycholesterol (see Figure 3.37).

Figure 3.36 Reconstructed ion chromatogram (RIC) for *m/z* 534 corresponding to oxidised/GP-derivatised 25-hydroxycholesterol. Separation was achieved on a 180 µm (i.d.) x 150 mm, C_{18} (3 µm, 100 Å) PepMap column at a flow rate set to 0.8 µL/min. The oxidised/GP-derivatised 25-hydroxycholesterol (1 pg) was injected on the column. Mobile phase A was 50% methanol, 0.1% formic acid, and B was 95% methanol, 0.1% formic acid. The gradient program started at 30% B rising to 70% B over ten minutes, then to 80% B over a further five min. The mobile phase composition was maintained at 80% B for a further 15 minutes before returning to 30% in 0.1 min. The column was reconditioned with this mobile phase composition for 20 min. The total run was 50 min and the flow rate 0.8 µL/min.

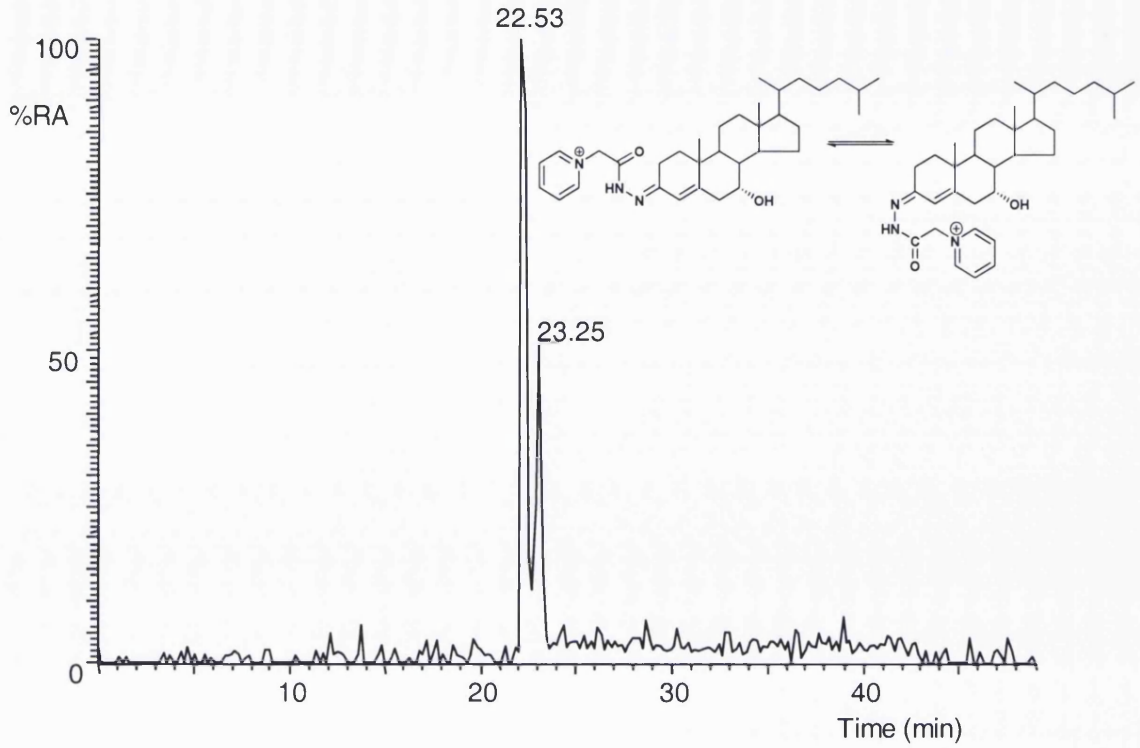

Figure 3.37 RIC for *m/z* 534 of corresponding to oxidised/GP-derivatised 7α-hydroxycholesterol. Separation was achieved on a 180 µm (i.d.) x 150 mm, C_{18} (3 µm, 100 Å) PepMap column at a flow rate set to 0.8 µL/min. The oxidised/GP-derivatised 7α-hydroxycholesterol (1 pg) was injected on the column. Mobile phase A was 50% methanol, 0.1% formic acid, and B was 95% methanol, 0.1% formic acid. The gradient program started at 30% B rising to 70% B over ten minutes, then to 80% B over a further five min. The mobile phase composition was maintained at 80% B for a further 15 minutes before returning to 30% in 0.1 min. The column was reconditioned with this mobile phase composition for 20 min. The total run was 50 min and the flow rate 0.8 µL/min.

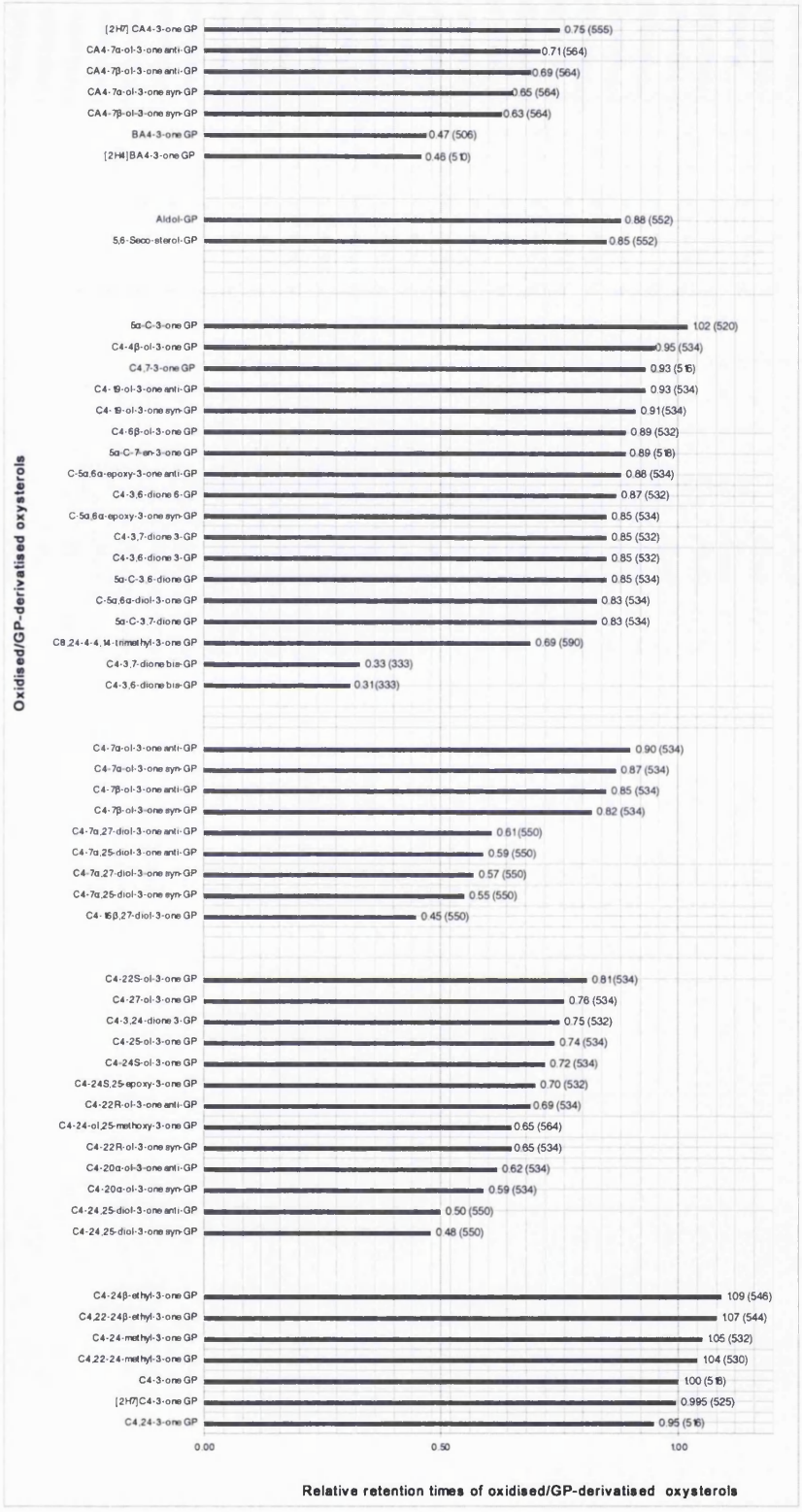

Figure 3.38 Representation of the relative retention times of the oxidised/GP-derivatised oxysterols/sterols to cholesterol (25.83 min) on the C_{18} PepMap column. The LC method and gradient are described in section 2.9.

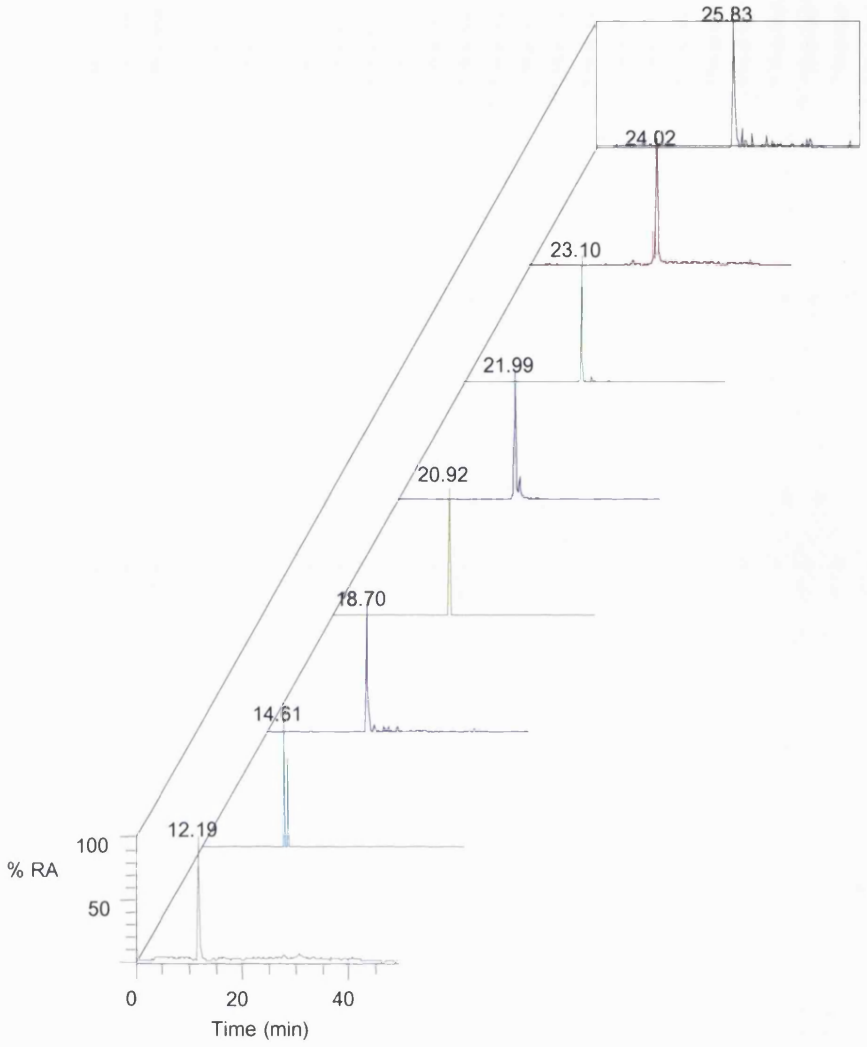

Figure 3.39 Capillary LC-MS^3 separation of the oxidised/GP-derivatised 3β-hydroxychol-5-enoic acid, 7α,27-dihydroxycholesterol, 24S-hydroxycholesterol, 22S-hydroxycholesterol, 7-oxocholesterol, 6β-hydroxycholesterol, 19-hydroxycholesterol, and cholesterol. TIC for MS^3 ($[M]^+ \rightarrow [M-79]^+ \rightarrow$) of BA^4-3-one GP eluted at retention time (RT) 12.19 min, C^4-7α,27-diol-3-one GP eluted at RT 14.61 min, C^4-24S-ol-3-one GP eluted at RT 18.70 min, C^4-22S-ol-3-one GP eluted at RT 20.92 min, C^4-3,7-dione GP eluted at RT 21.99 min, C^4-6β-ol-3-one GP eluted at 23.10 min, C^4-19-one GP eluted at 24.02 min, and C^4-3-one GP eluted at 25.83 min. Separation was achieved on a 180 µm (i.d.) x 150 mm, C_{18} (3 µm, 100 Å) PepMap column at a flow rate set to 0.8 µL/min. Mobile phase A was 50% methanol, 0.1% formic acid, and B was 95% methanol, 0.1% formic acid. The gradient program started at 30% B rising to 70% B over ten minutes, then to 80% B over a further five min. The mobile phase composition was maintained at 80% B for a further 15 minutes before returning to 30% in 0.1 min. The column was reconditioned with this mobile phase composition for 20 min. The total run was 50 min and the flow rate 0.8 µL/min.

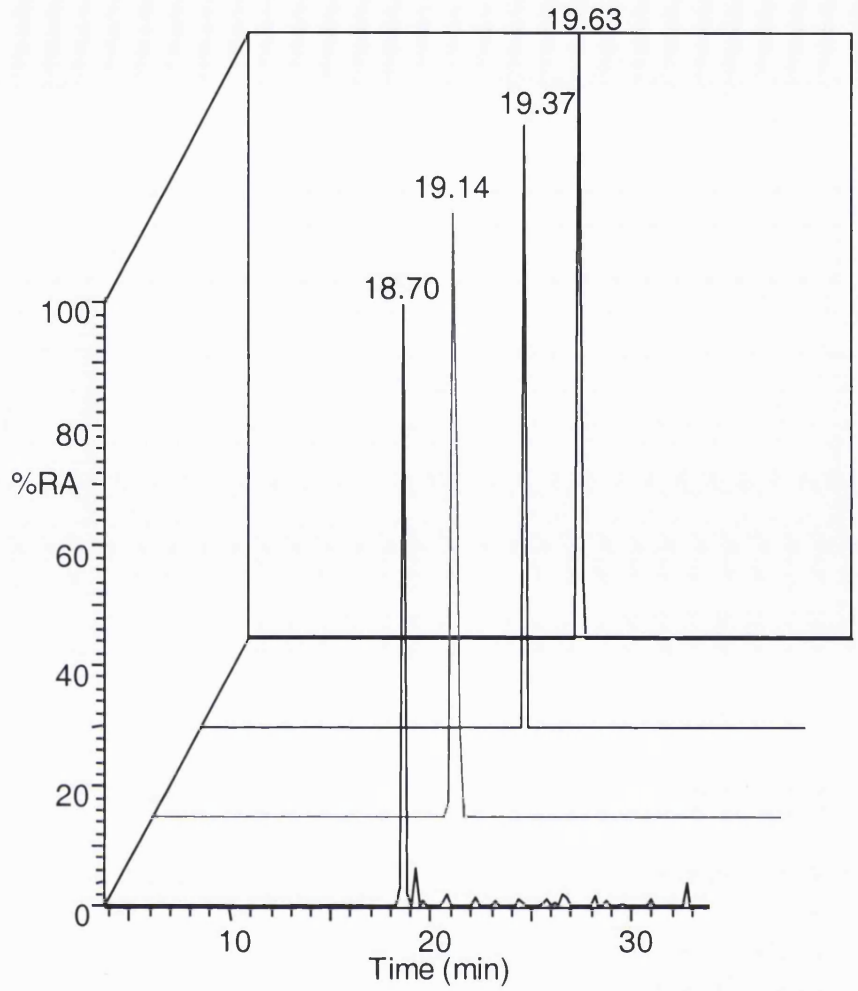

Figure 3.40 Capillary LC-MS^3 separation of the oxidised/GP-derivatised 24S-hydroxycholesterol, 25-hydroxycholesterol, 24-oxocholesterol, 27-hydroxycholesterol. RICs for the MS^3 transition corresponding to 24S-hydroxycholesterol (534→455→353) eluted at RT 18.70 min, 25-hydroxycholesterol (534→455→381) eluted at retention time (RT) 19.14 min, 24-oxocholesterol (532→453→392) eluted at 19.37 min, 27-hydroxycholesterol (534→455→412) at RT 19.63 min. Separation was achieved on a 180 µm (i.d.) x 150 mm, C_{18} (3 µm, 100 Å) PepMap column at a flow rate set to 0.8 µL/min. Mobile phase A was 50% methanol, 0.1% formic acid, and B was 95% methanol, 0.1% formic acid. The gradient program started at 30% B rising to 70% B over ten minutes, then to 80% B over a further five min. The mobile phase composition was maintained at 80% B for a further 15 minutes before returning to 30% in 0.1 min. The column was reconditioned with this mobile phase composition for 20 min. The total run was 50 min and the flow rate 0.8 µL/min.

The most difficult part of the chromatogram to resolve was that comprising RRT from 0.72 to 0.75 and 0.86 to 0.89, which includes four compounds from Group 2 and from Group 4. In particular, 24S-hydroxycholesterol and 25-hydroxycholesterol were partially chromatographically

separated. Oxidised/GP-derivatised monohydroxycholesterols from these groups give an $[M]^+$ ion of *m/z* 534, and different fragment ions in their MS^3 spectra. This allows the MS^3 transition 534→455→ to be monitored over the chromatographic run, and then generating RICs for the combined transition 534→455→ plus a specific fragment-ion (e.g. RIC for the MS^3 transition 534→455→353 corresponding to the oxidised/GP-derivatised 24S-hydroxycholesterol). Figure 3.40 shows that the oxidised/GP-derivatised 24S-hydroxycholesterol (C^4-24S-ol-3-one GP), 25-hydroxycholesterol (C^4-25-ol-3-one GP), 24-oxocholesterol (C^4-3,24-dione 3-GP) and 27-hydroxycholesterol (C^4-27-ol-3-one GP) are chromatographically separated incrementally on the capillary C_{18} column, where 25-hydroxycholesterol and 24S-hydroxycholesterol partially overlap, while 24-oxocholesterol and 27-hydroxycholesterol are resolved.

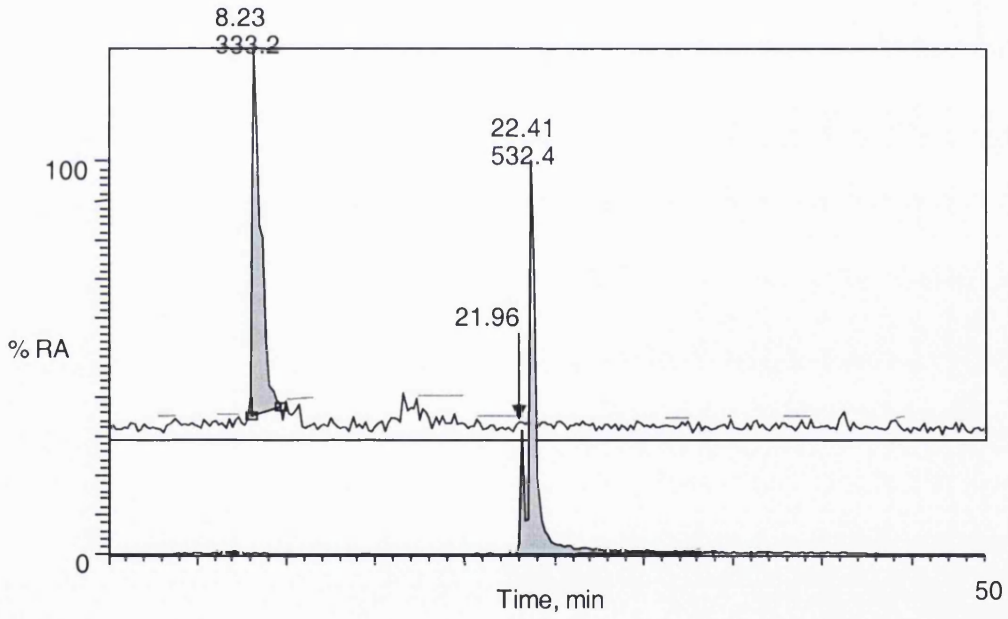

Figure 3.41 Capillary LC-MS separation of C^4-3,6-dione GP hydrazone. RIC for *m/z* 532, corresponding to two mono-GP hydrazones eluted at retention times (RT) 21.96 min (with relative retention time RRT 0.85) and 22.41 min (RRT 0.87); and RIC for *m/z* 333 corresponding to *bis*-GP hydrazone eluted at RT 8.23 min.

Cholest-4-ene-3,6-dione when GP derivatised gives two isomeric mono-GP hydrazones (C^4-3,6-dione 6-GP and C^4-3,6-dione 3-GP, *m/z* 532), and also a doubly charged *bis*-GP hydrazone (C^4-3,6-dione *bis*-GP, *m/z* 333) (Figure 3.41). The mono-GP isomers are separated on the reversed-phase column and give different MS^2 and MS^3 spectra. The MS^2 spectra differ in the

RA of the $[M-107]^+$ ion at *m/z* 425. For the isomer eluting at RT 21.96 min with relative retention time (RRT) of 0.85, this ion has a RA 30%, while for the isomer eluting at RT 22.41 min with RRT of 0.87 its RA 5%, whereas the $[M-79]^+$ ions at *m/z* 453 has a RA of 100% for both isomers.

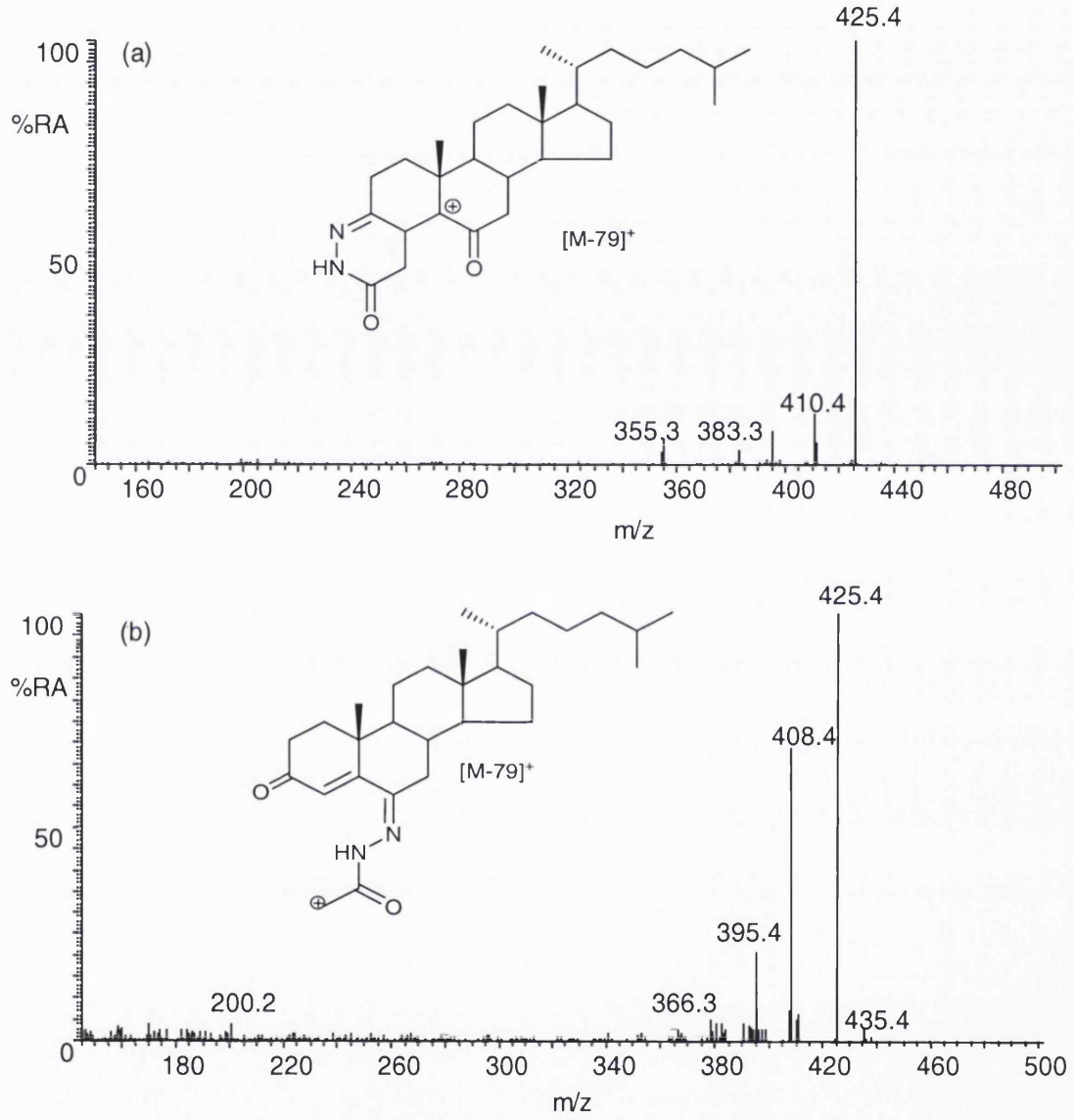

Figure 3.42 MS^3 ($[M]^+ \rightarrow [M-79]^+ \rightarrow$) spectra of chromatographic peaks eluting at (a) 21.96 min; and (b) 22.41 min corresponding to cholest-4-ene-3,6-dione GP hydrazones.

The MS^3 spectra of both isomers were dominated by the $[M-107]^+$ ion at *m/z* 425, for the isomer with RRT 0.85. The second most abundant ion was at *m/z* 410 corresponding to a $[M-107-15]^+$ ion (Figure 3.42a). This fragment is often observed in MS^3 spectra of 3-oxo-4-ene derivatives

(loss of NH from the $[M-107]^+$ ion). In the spectrum of the latter eluting peak the second most abundant fragment is at *m/z* 408 corresponding to $[M-124]^+$ (loss of NH_3 from the $M-107]^+$ ion), a fragment-ion not normally observed in the spectra of 3-oxo-4-ene derivatives, but more in line with the derivative being at the 6-oxo position (Figure 3.42b). The *bis*-GP hydrazone (*m/z* 333) eluted at 8.23 min (Figure 3.41).

3.10 Validation of capillary LC-MS method

The 24S-hydroxycholesterol, 22S-hydroxycholesterol and cholesterol were subjected to oxidation with cholesterol oxidase and derivatisation with GP reagent. The samples were analysed by capillary LC-MS^2. MS signals were recorded by monitoring the MS^2 transition of 534→ (for both oxysterols) over the duration of LC-MS^2 run (see Chapter 2, section 2.10). Reconstructed ion chromatograms (RICs) were generated for the $[M]^+ \rightarrow [M-79]^+$ transitions.

The calibration graphs of the oxidised/GP-derivatised reference 24S-hydroxycholesterol and 22R-hydroxycholesterol are shown in Figure 3.43 (triplicate analyses on the same day). Calibration graphs were plotted of the chromatographic peak area against the amount of standard injected on-column. Linearity was evaluated via the R^2 regression coefficient of determination. The R^2 values for the graphs indicate a high degree of linearity in the response of the detector between 0.4 to 25 pg of 24S-hydroxycholesterol and 22R-hydroxycholesterol loaded onto the column.

(a)

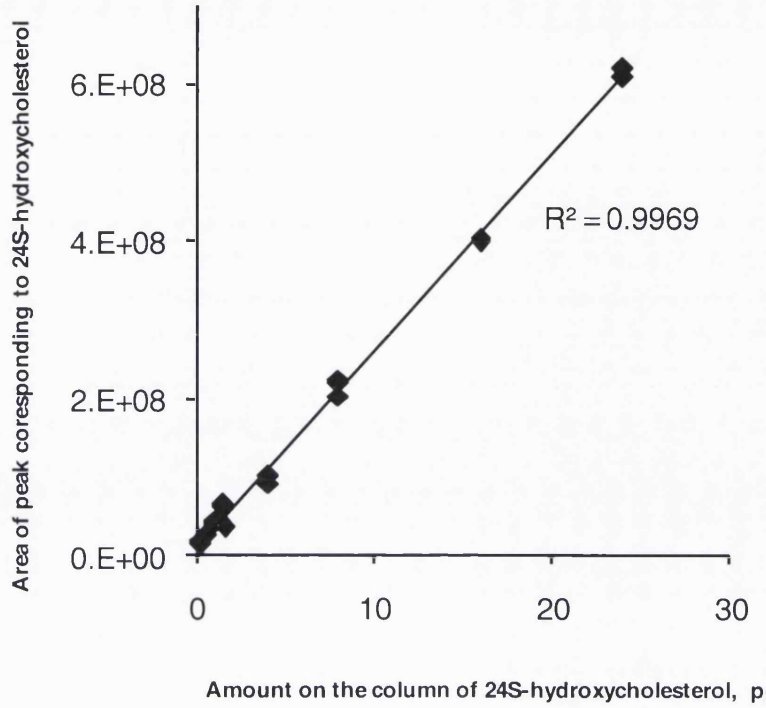

(b)

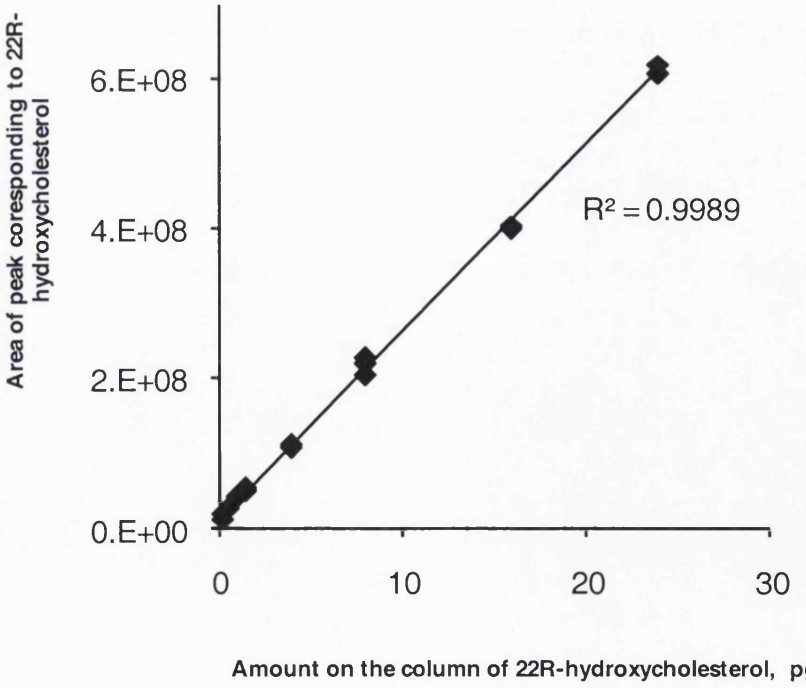

Figure 3.43 Calibration graphs for (a) the oxidised/GP-derivatised 24S-hydroxycholesterol, and (b) 22R-hydroxycholesterol. R^2 values are inset. For details of experiments refer to Chapter 2 sections 2.9 and 2.10. Calibrants were made up at concentrations of 0.3, 0.5, 1.0, 1.5, 4.0, 8.0, 16.0, 25.0 pg/μL as described in section 2.10. Each calibrant was analysed by capillary LC-MS^2 on a LCQ^{duo} ion trap instrument in triplicate.

Limit of detection and limit of characterisation

The limit of detection in RIC for $[M]^+$ ion was determined to be in the range from 400 fg to 600 fg, as injected on the analytical column for most reference GP hydrazones studied, assuming no loss of analyte during sample preparation. Figure 3.44 shows the reconstructed ion chromatogram (RIC) for the injection of 400 fg of the oxidised/GP-derivatised 22R-hydroxycholesterol ($[M]^+$ *m/z* 534) on the C_{18} capillary column. The detection limit is the smallest quantity of analyte that yields a signal that can be distinguished from the background noise (generally a signal equal to three times the background noise). It should be noted that the minimum quantity is not enough to obtain sufficient quality of the characteristic MS^3 spectra. Detailed structural information about the oxysterol/sterol skeleton could be obtained from 800 fg to 1 pg for reference GP hydrazones.

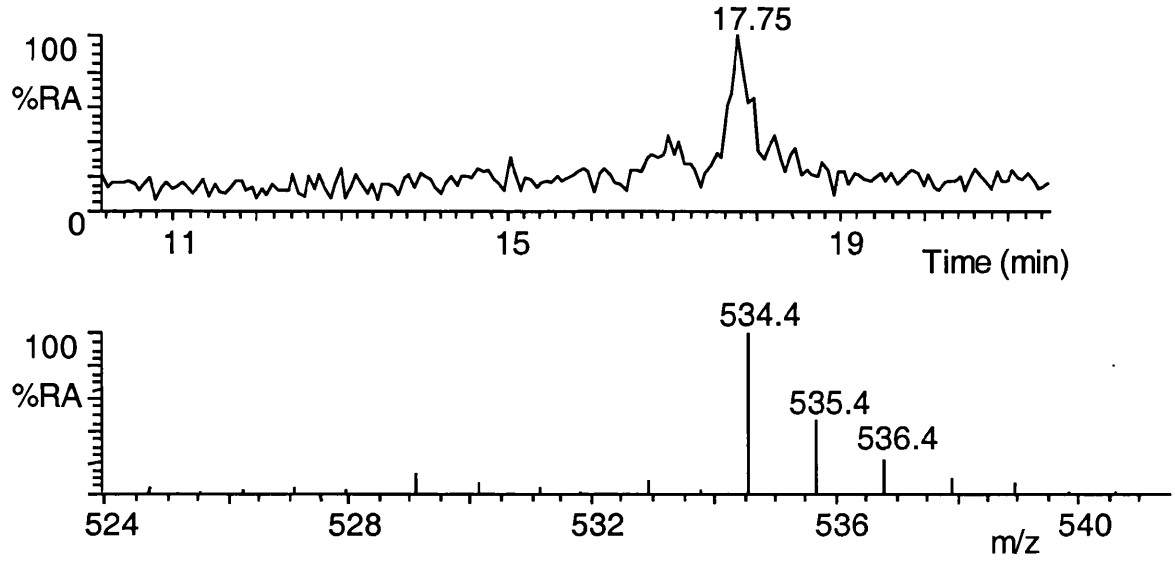

Figure 3.44 RIC for *m/z* 534, $[M]^+$ ion. The oxidised/GP-derivatised 22R-hydroxycholesterol (400 fg) was injected on the capillary C_{18} column. The gradient program, flow rate, capillary C_{18} column and mobile phases as described in section 2.9.

3.11 Discussion

A capillary liquid chromatography multi-stage fragmentation mass spectrometry (cap-LC-MS^n) methodology was developed for the identification of oxysterols with high sensitivity (low pg), selectivity and specificity. The methodology consists of oxidation and derivatisation to add specificity and enhance ES ionisation, and capillary LC-MS^2,-MS^3 to allow selective separation of oxidised/GP-derivatised oxysterols and their structure characterisation.

Neutral sterols are poorly ionised by electrospray, taking 24S-hydroxycholesterol as an example of a 3β-hydroxy-5-ene oxysterol, ES led to the dehydrated protonated $[M+H-H_2O]^+$ ions and an absence of molecular weight information. Tandem mass spectrometry on unoxidised/underivatised 24S-hydroxycholesterol resulted in non-specific fragmentation, namely loss of water and small hydrocarbons fragmentations.

A derivatisation method was employed to introduce a pre-ionised group into the sterols in an effort to improve sensitivity and specificity of the analysis. Oxysterols, generally have a 3β-hydroxy-5-ene or 3β-hydroxy-5α-hydrogen structure (Figure 1.13), and were specifically oxidised with cholesterol oxidase to their 3-oxo-4-ene or 3-oxo analogues, and were then derivatised with Girard P (GP) hydrazine to GP hydrazone (Figure 3.1). GP hydrazones possess a positively charged quaternary nitrogen and give an improvement in ES signal. For example, the improvement in sensitivity for the analysis of 24S-hydroxycholesterol upon oxidation and derivatisation was about two orders of magnitude relative to the $[M+H-H_2O]^+$ ion and three orders of magnitude relative to the $[M+H]^+$ ion of the unoxidised/underivatised 24S-hydroxycholesterol as found in this study. Therefore, this strategy of oxidation/GP-derivatisation adds both specificity and sensitivity to the method in that, only compounds with an oxo-group, or oxidised with cholesterol oxidase to include one, become derivatised with the GP reagent. The GP derivative also improves the solubility of sterols in the mobile phase for reversed-phase chromatography and hence facilitates their analysis by LC-MS.

The reference oxysterols/sterols were analysed after oxidation/GP-derivatisation by direct infusion nano-ES and -MS, -MS^2 and -MS^3 spectra recorded. The data is summarised in supplementary material Table 1 and Figures 1 to 40. MS^2 spectra of most oxysterols are dominated by a $[M-79]^+$ fragment ion, accompanied by lower abundance $[M-79-H_2O]^+$ and $[M-107]^+$ ions. They result from the loss of pyridine (C_6H_5N) ring, pyridine plus water (C_6H_7NO), and pyridine plus carbon monoxide (C_6H_5NO), respectively (Figure 3.8). These losses are characteristic of GP hydrazones. Dihydroxycholesterols additionally give $[M-79-2H_2O]^+$ and $[M-107-H_2O]^+$ ions, which result from the loss of pyridine and two molecules of water ($C_5H_9NO_2$), and pyridine, carbon monoxide, and water ($C_6H_7NO_2$). Although not providing a wealth of structural information, MS^2 spectra complement MS^3 spectra, giving the information on the lability of the modified cholesterol skeleton. In contrast to MS^2, MS^3 spectra of oxidised/derivatised oxysterols provided structural information, in which different functional groups provide different MS^3 fragmentation patterns according to their location [68].

Oxidised/GP-derivatised sterols and oxysterols were then analysed by capillary LC-MS^n. The oxidised/GP-derivatised sterols and oxysterols were separated on a C_{18} column interfaced to an LCQ^{duo} mass spectrometer, and ES-MS, -MS^2 and –MS^3 spectra recorded. In this study LC analysis provides a chromatographic separation of structurally different sterols, many of which have the same molecular weight (isobaric), whereas tandem mass spectrometry provides structural information and molecular characterisation. The relative retention times given in relation to the oxidised/derivatised cholesterol are summarised in Figure 3.38 and in supplementary material Table 1. On-column detection limits were of the order of 800 fg. At this level, MS^2 and MS^3 spectra were sufficiently informative to allow structure determination.

The developed methodology allows targeted analysis of potential oxysterols in biological sample. It is possible to profile LC-MS chromatograms for potential oxysterols, because of their predicted elemental composition. When a "targeted" oxysterol elutes from the capillary C_{18} column it is subjected to MS^2 $[M]^+\rightarrow$, MS^3 $[M]^+\rightarrow[M-79]^+\rightarrow$ and $[M]^+\rightarrow[M-107]^+\rightarrow$ analyses to allow their

characterisation. Reconstructed ion chromatograms (RIC) were generated for potential sterols and oxysteros present in biological sample (see chapters 4, 5 and 6). With the added knowledge of retention time for authentic standards, the identity of many sterols and oxysterols were postulated. Confirmation of identity was achieved by comparison of MS^2 and MS^3 spectra with authentic standards. It was possible to perform multiple repeat LC-MS injections of a biological sample, and in case of brain tissue only 50 µg of brain was required for oxysterol analysis. This level of detection corresponds to 20 ng/g of oxysterols, when 100 g of brain is extracted into 2 mL, and 1 µL injected on-column corresponding to 50 µg of brain tissue.

Chapter 4

The identification of cholesterol autoxidation products formed during the sample preparation

4. *Introduction*

Monooxygenated derivatives of cholesterol, known as oxysterols, are formed as a part of enzymatic cholesterol metabolism or due to autoxidation. The spontaneous oxidation of cholesterol is a well recognised phenomenon generally termed autoxidation [128]. The definition of autoxidation adopted for this work is "the apparently uncatalysed oxidation of a substance exposed to the oxygen of the air" [170]. The common cholesterol autoxidation products formed almost certainly as artifacts of tissue storage and handling are epimeric 7α- and 7β-hydroxycholesterol, 7-oxocholesterol, the isomeric cholesterol-5,6-epoxides, cholestane-3β,5α,6β-triol, cholesta-4,6-dien-3-one, 25-hydroxycholesterol, cholest-4-ene-3β,6β-diol, 3β,5-dihydroxycholestan-6-one, 3β-hydroxy-5α-cholestan-6-one, 5α-cholestane-3,6-dione, 7-methoxycholesterol, and 3β-hydroxy-5α-cholestane-6-one (Figure 4.1) [128,170-172]. Cholesterol autoxidation is an insidious process, encountered erratically in some cases but not in others. The most frequently encountered cholesterol autoxidation products include the epimeric 3β,7-diols of cholesterol, 7-oxocholesterol, 5α-cholestane-3β,5,6β-triol all found in a variety of tissues [34,151,173,174].

All genuine sterol metabolites should have specific enzyme systems associated with their biosynthesis. Of the above autoxidation products only two at present (the 3β,7α-diol and the 3β,25-diol) have also demonstrated enzymic origins. Several cytochrome P450 (CYP) enzymes or a cholesterol 25-hydroxylase participate in the conversion of cholesterol into particular hydroxycholesterols. For example, CYP7A1 produces 7α-hydroxycholesterol as the first committed step in the classical bile acid pathway. Cholesterol 25-hydroxylase is responsible for the 25-hydroxylation of cholesterol (not a cytochrome P450 enzyme). CYP46A1 is a microsomal enzyme present particularly in neurons and produces 24S-hydroxycholesterol, also called cerebrosterol because of its relative abundance in brain. One of most important roles of oxysterols is that they are a precursor to bile acids.

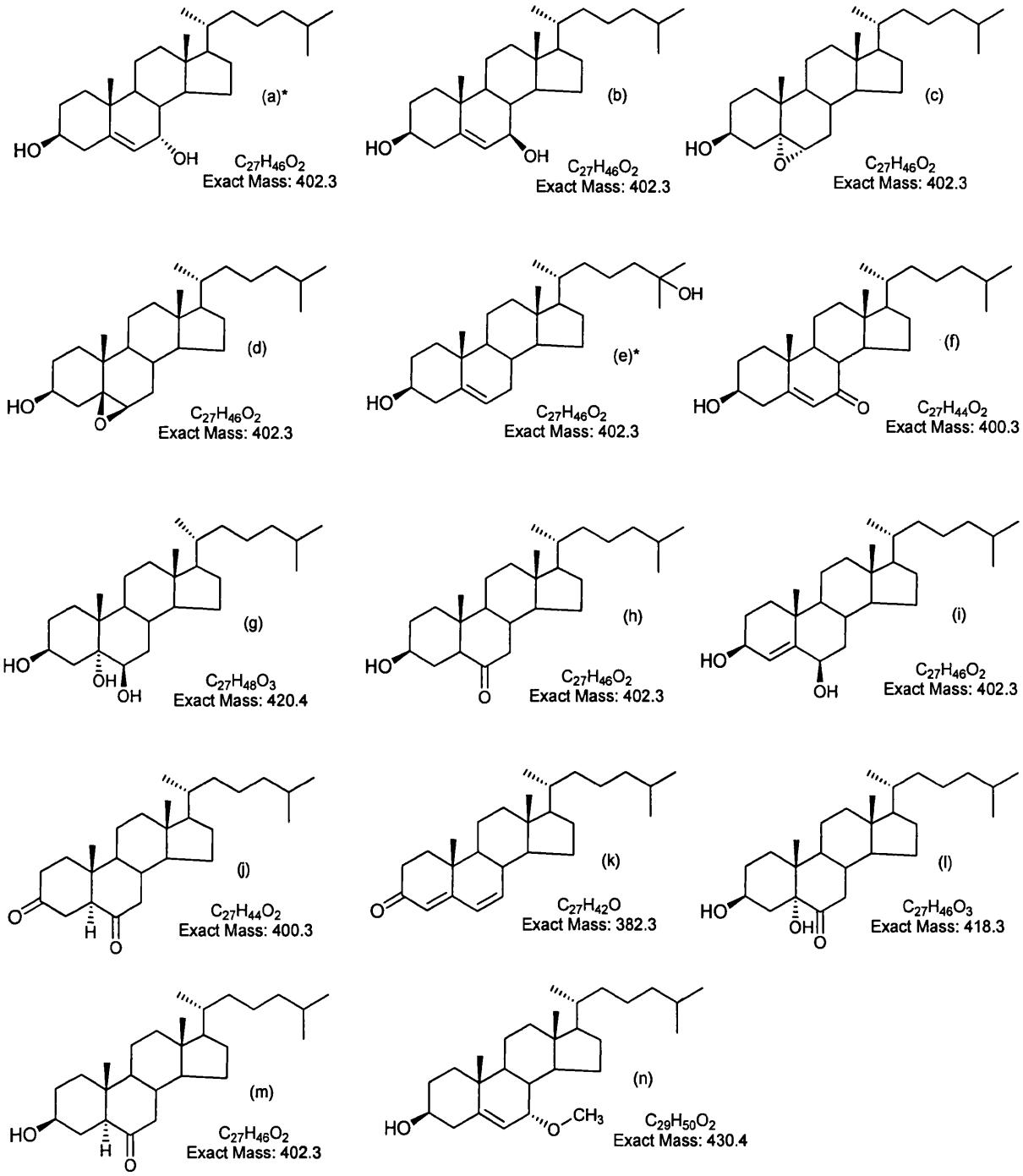

Figure 4.1 Cholesterol oxidation products (a) 7α-Hydroxycholesterol (cholest-5-ene-3β,7β-diol), (b) 7β-Hydroxycholesterol (cholest-5-ene-3β,7α-diol), (c) α-Epoxycholesterol (5α,6α-epoxy-5α-cholestan-3β-ol), (d) β-Epoxycholesterol (5β,6β-epoxy-5β-cholestan-3β-ol), (e) 25-Hydroxycholesterol (cholest-5-ene-3β,25-diol), (f) 7-Oxocholesterol (3β-hydroxy-cholest-5-ene-7-one), (g) Cholestanetriol (5α-cholestane-3β,5α,6β-triol), (h) 6-Oxocholestanol (3β-hydroxy-5α-cholestan-6-one), (i) 3β,6β-Dihydroxy-cholest-4-ene (cholest-4-ene-3β,6β-diol), (j) 5α-Cholestane-3,6-dione, (k) Cholesta-4,6-dien-3-one, (l) 3β,5-Dihydroxy-cholestan-6-one, (m) 3β-Hydroxy-5α-cholestan-6-one, (n) 7α-Methoxycholesterol (cholest-5-ene-3β-ol,7α-methoxy). An asterisk denotes that oxysterol can be formed enzymatically and non-enzymatically in cells or during the sample preparation.

Another well established role is to act as transport forms of cholesterol, since their increased hydrophilicity compared to cholesterol enables them to cross membranes and move between cells and their intracellular compartments, thus acting as transport forms of cholesterol. Oxysterols may also have a role in the regulation of cholesterol homeostasis. This was first demonstrated by Kandutsch, Chen and Heiniger in 1978 [138] and became known as the oxysterol hypothesis of cholesterol homeostasis. This hypothesis contended that oxysterols mediate feedback regulation of cholesterol biosynthesis, rather than cholesterol itself. Cholesterol is synthesised via the mevalonate pathway, which is comprised of 35 enzymes [117]. Enzymes in this pathway are transcriptionally activated by Sterol Regulatory Element Binding Proteins (SREBPs) [121].

This research concentrates on the requirement for the development of sensitive and specific analytical methods for the qualitative and semi-quantitative profiling of oxysterols in biological tissues to further evaluate their biological role, and to learn more about how they are inactivated/metabolised. The work described in Chapter 3 has established the methodology of analysis of reference oxysterols by mass spectrometry, which includes oxidation and derivatisation with GP reagent to enhance ionisation, and cap-LC-MS-,MS^2,-MS^3 to allow their characterisation. This chapter describes further development of the methodology for the analysis of oxysterols in biological tissues and fluids. Oxysterols are present at low levels in tissues (ng/g to µg/g) against a high background of cholesterol (mg/g) [69,71]. Therefore it is important to separate oxysterols from cholesterol early in the sample preparation, and to prevent cholesterol autoxidation during sample preparation and handling. Also, because of the low abundance of oxysterols in a biological sample, removal of cholesterol prevents overloading of the cap-LC-MS system with cholesterol (for example, 15 µg/mg of cholesterol in rat brain) [81], and the resultant degradation of column performance and persistent carry-over. The sample preparation procedure of the separation of cholesterol from oxysterols developed by Sjövall's group at Karolinska Institutet was adopted in this work [38,175]. By using this methodology, cholesterol is separated from oxysterols at the earliest possible step on a

a straight-phase solid phase extraction (SPE) column to avoid the formation of autoxidation products. The enriched oxysterol fraction is then oxidised, derivatised with Girard P reagent and analysed by direct infusion nano-ES-MS and capillary LC-MS^n. The evaluation of the extent to which cholesterol is autoxidised during the sample preparation is carried out by introduction of a known amount of [$^2H_7$] cholesterol prior to any processing of the sample.

4.1 The investigation of artifact formation during the sample procedure and the separation of oxysterols from cholesterol and method validation

In chapter 3 it was demonstrated that the process of oxidising 3β-hydroxyl groups to 3-oxo groups followed by derivatisation to GP hydrazones enhances the oxysterol ion-current by at least two orders of magnitude. However, this method has its drawbacks, one of which is variation in the susceptibility of the 3β-hydroxyl group to oxidation by cholesterol oxidase depending on the overall sterol structure and the enzyme employed. A second consideration is that the reactivity of other oxo groups present on the sterol skeleton to the GP reagent, which varies according to their location (see chapter 3 Figure 3.41 showing an example of the oxidised/GP-derivatised 6-oxocholesterol). Only 2.5 µg of reference sterols were used for optimisation of the oxidation and GP derivatisation reactions, and when incubating these sterols for 60 min at 37°C with ~0.2 U of cholesterol oxidase conversion to 3-oxo-4-ene sterols was maximised, while the formation of oxidation artifacts was avoided [68]. The sterols were supplied as 99% pure (according to TLC), and this level of purity was maintained throughout the oxidation/GP-derivatisation process. It is known that cholesterol is likely to be 10000 more abundant than any oxysterol in the brain [38,52,71], and even as little as 0.1% formation of autoxidation products in the oxidation/GP-derivatisation process would lead to significant artifacts when analysed as part of an oxysterol study. The straight phase chromatography is necessary to remove a matrix of other lipids in the brain, including phospholipids, which can interfere with the oxysterol analysis.

To simulate closely the analytical procedure for the analysis of oxysterols extracted from brain tissue, a mixture of 1 mg of cholesterol and 2.5 µg of both 24S- and 22R-hydroxycholesterols, which approximate to the cholesterol and 24S-hydroxycholesterol content in 100 mg of brain, was subjected to the entire sample preparation procedure [68]. Oxysterols were enriched using straight-phase SPE chromatography, oxidised, derivatised specifically, and separated in their derivatised form by reversed-phase liquid chromatography. In the first experiment, the separation of the bulk of cholesterol from oxysterols was performed by a single passage of the sample mixture through the Unisil SPE column as described in section 2.14, chapter 2. The experiment was performed in triplicate. Fraction U1 ("cholesterol fraction"), which contains the bulk of cholesterol was obtained by elution with 40 mL hexane-dichloromethane (8:2, v/v), and fraction U2 ("oxysterol fraction") was eluted with 10 mL ethyl acetate, and contains oxysterols and some cholesterol. The oxysterol fraction was subjected to the oxidation and derivatisation protocols. The nano-ES mass spectrum of the fraction U2 is shown in Figure 4.2a. A major peak is observed at *m/z* 534, which corresponds to the *m/z* of the $[M]^+$ ion of oxidised/GP-derivatised monohydroxycholesterols. The oxidised/GP-derivatised cholesterol (*m/z* 518) was present at 35% of the oxysterol level; also minor contaminants of *m/z* 532 and 550 were observed (RA ~1.5%). The MS^2 on the *m/z* 550 did not give major $[M-79]^+$ and $[M-107]^+$ fragment-ions, which are characteristic of GP hydrazones (Figure 4.3b).

An aliquot of the fraction U2 was also injected on a capillary reversed phase column and MS, -MS^2, and -MS^3 spectra recorded. Total ion chromatograms (TICs) for the $[M]^+\rightarrow$, $[M]^+\rightarrow[M-79]^+\rightarrow$ and $[M]^+\rightarrow[M-107]^+\rightarrow$ transitions were plotted for all potential contaminants. A minor amount of 6-oxocholestenone (RA 0.3%, *m/z* 532) was identified, as were cholesterol epoxides (RA 0.2%, *m/z* 532) based on their retention times and MS^3 spectra. A minor component with *m/z* 550 was eluted at 23.34 min, and MS^2 spectra gave a non-specific fragmentation pattern (Figures 4.3a and b).

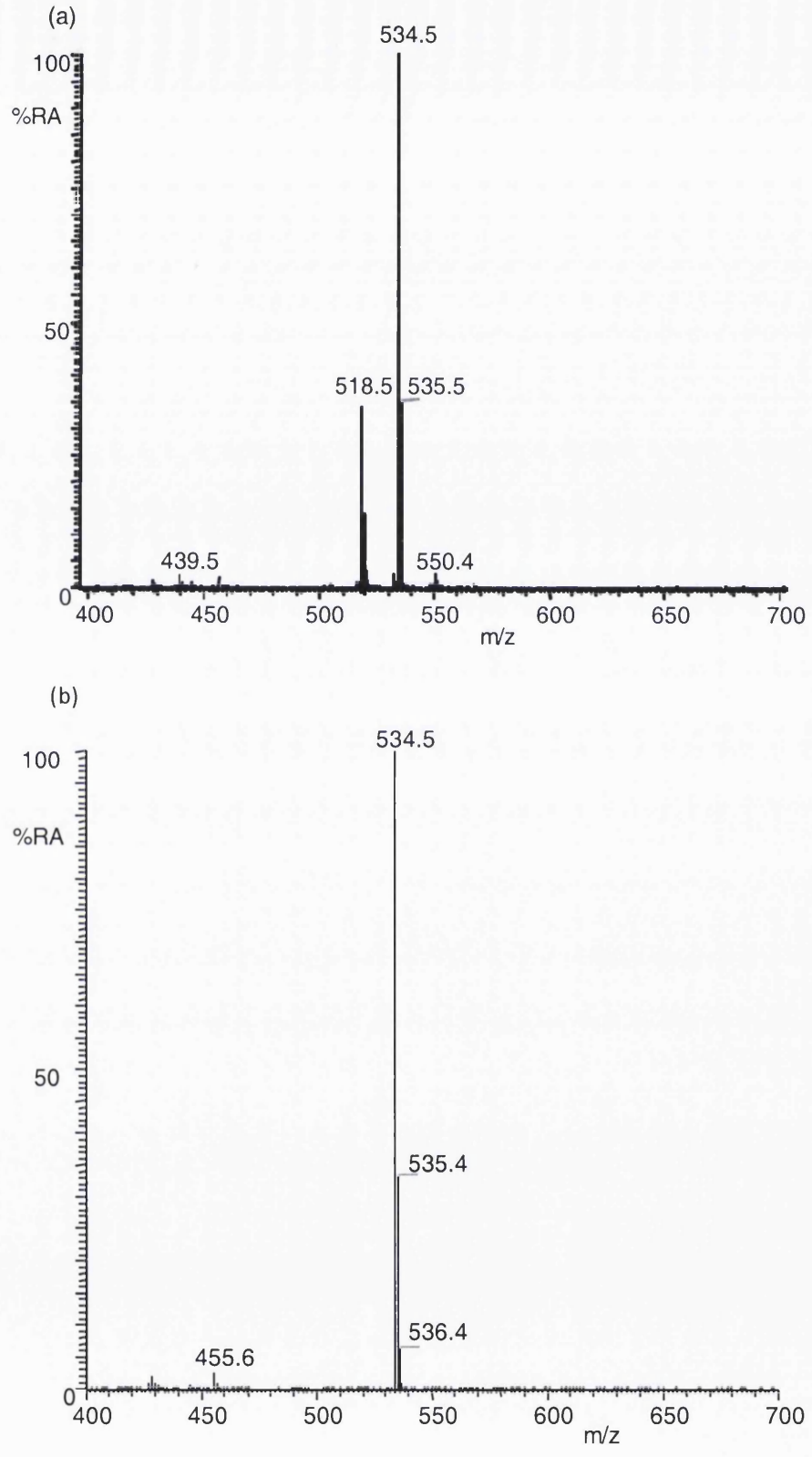

Figure 4.2 (a) Nano-ES mass spectrum of the fraction U2, obtained by a single passage of the mixture 24S-hydroxycholesterol, 22R-hydroxycholesterol and cholesterol through the Unisil SPE column, and (b) by double passage the same sample mixture through a fresh Unisil column.

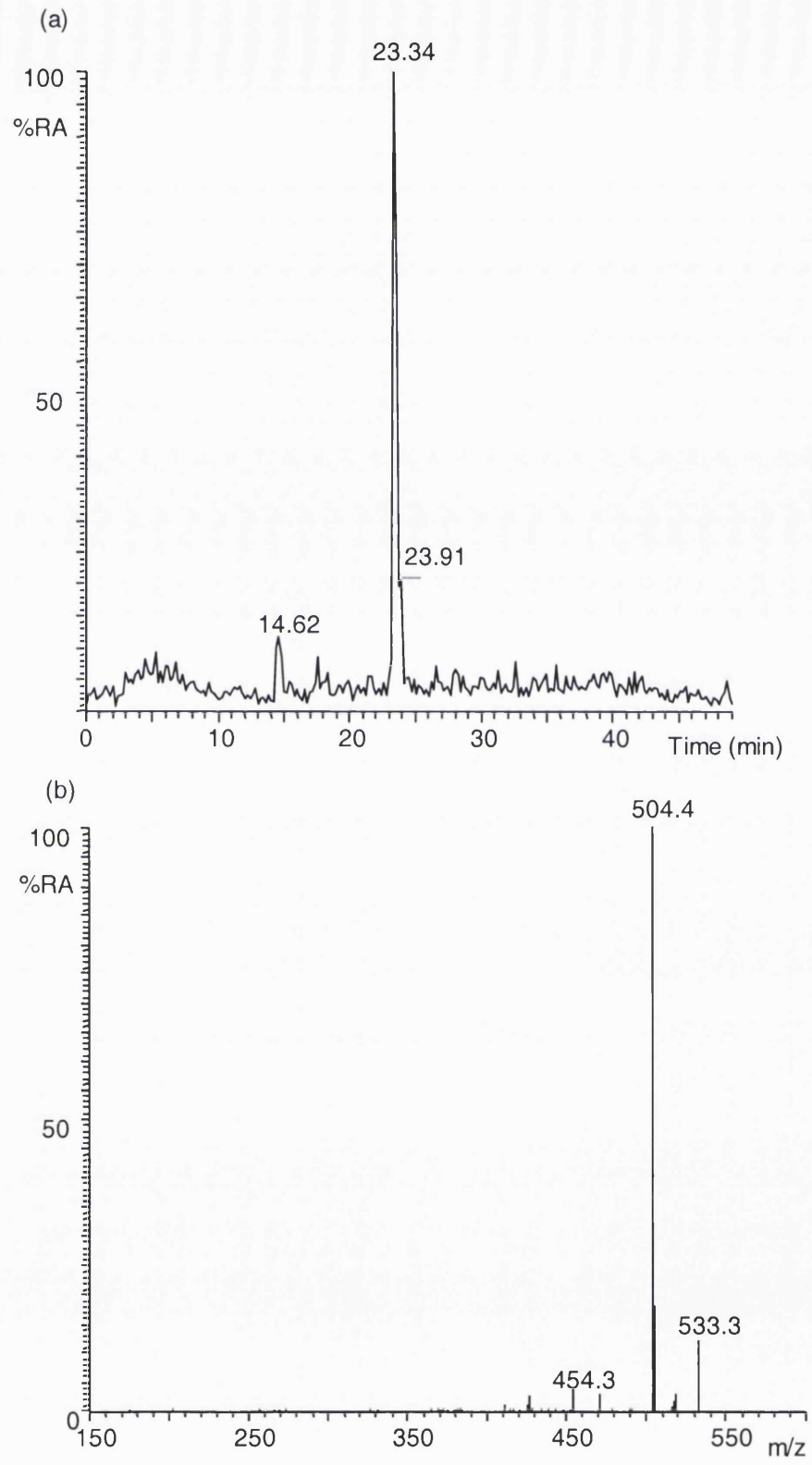

Figure 4.3 (a) TIC for the MS^2 transition 550→ corresponding to the fraction U2, and (b) MS^2 (550→) spectrum for the peak at 23.34 min.

A second passage of the oxysterol fraction (fraction U2) through a fresh Unisil column essentially removed most of cholesterol and its subsequent autoxidation products (Figure 4.2b). This shows that removal of as much of the cholesterol as possible at a very early stage in the sample preparation procedure would markedly reduce the formation of autoxidation products of cholesterol.

Furthermore, the efficiency of the separation of oxysterols from cholesterol was evaluated by calculating the percentage recoveries for 24S-hydroxycholesterol and 22R-hydroxycholesterol after the separation. An experiment was designed to quantify the 22R-hydroxycholesterol and 24S-hydroxycholesterol recovered after separation on the straight-phase chromatography. Capillary-LC-MS^2 with the transition of 534→ was used for quantification. The linear calibration plots were constructed using the reference oxidised/GP-derivatised 24S-hydroxycholesterol and 22R-hydroxycholesterol (as described in section 2.10). The concentration range for the calibrants of 22R- and 24S-hydroxycholesterols, the cap-LC column loading capacity, and the linearity from the MS detector were discussed in section 3.10 (chapter 3).

Evaluation of the percentage recoveries of 24S-hydroxycholesterol and 22R-hydroxycholesterol after the straight-phase chromatography.

Three Unisil SPE columns were loaded with a mixture of 2.5 μg of 24S-, 22R-hydroxycholesterol and 1.3 mg of cholesterol (as described in section 2.13). The oxysterols were separated from cholesterol and the oxysterol fraction was subjected to oxidation/GP-derivatisation procedures and the resulting sterol GP-hydrazones were analysed by cap-LC-MS^n. In an initial run for the identification of analytes, the MS, MS^2 and MS^3 spectra were recorded over the duration of LC-MS run. In a second LC-MS run for the quantification of sterols only MS^2 534→ spectra were recorded, and RIC generated for the $[M]^+ \rightarrow [M-79]^+$ transition. Calibration plots were constructed, the amounts of the 24S- and 22R-hydroxycholesterols extracted from the Unisil SPE were determined, and the percentage recoveries calculated. A typical calibration plot is shown in Figure 3.45 (section 3.10 and the preparation of calibrants is described in section 2.10. All calibration plots had R^2

values of ≥0.99. The percentage recoveries for 24S- and 22R-hydroxycholesterols were 95.1 ± 1.8% and 92.4 ± 2.1%, respectively (mean ± standard deviation, n=3).

A second experiment was performed to determine the recovery of oxysterol from spiked rat brain (section 2.18), a procedure for quantitative extraction of sterols from the brain tissue [38,100,175,176]. A known amount of 22R-hydroxycholesterol (2.0 µg) was added to a sample of rat brain (54 mg), and the sample was homogenised in ethanol. This brain extract was purified using the straight-phase chromatography and the oxysterol fraction was oxidised with cholesterol oxidase, and then treated with a large excess of GP hydrazine. It was previously reported that oxysterols are quantitatively oxidased with cholesterol oxidase and derivatised with GP hydrazine [38,57,101]. It is important to note that 22R-hydroxycholesterol was added to the rat brain prior to extraction and carried through the entire sample preparation procedure with the endogenous compounds.

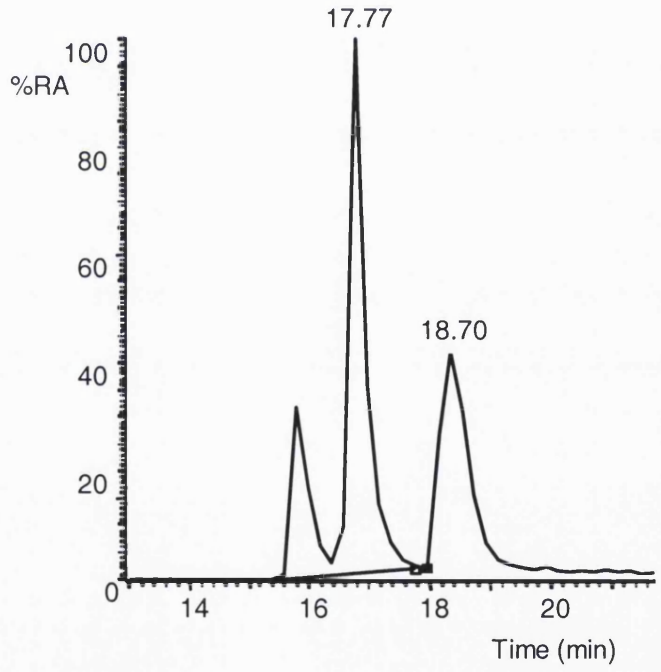

Figure 4.4 RIC for the MS^2 transition 534→455 corresponding to monohydroxycholesterols extracted from a rat brain sample. 22R-Hydroxycholesterol (2.0 µg) was added to rat brain (54 mg), sterols were extracted and purified by straight-phase chromatography. The resulting oxysterol fraction was oxidised with cholesterol oxidase and derivatised with GP reagent and the oxysterols then separated in their derivatised form by capillary reversed-phase chromatography, and MS^2 (534→) spectra recorded. For details of experiments refer to chapter 2 sections 2.9 and 2.18. The experiment was performed in triplicate. Calibrants were made up at concentrations of 0.5, 1.0, 1.5, 4.0, 8.0, 16.0, 25.0 pg/µL, as described in Section 2.10.

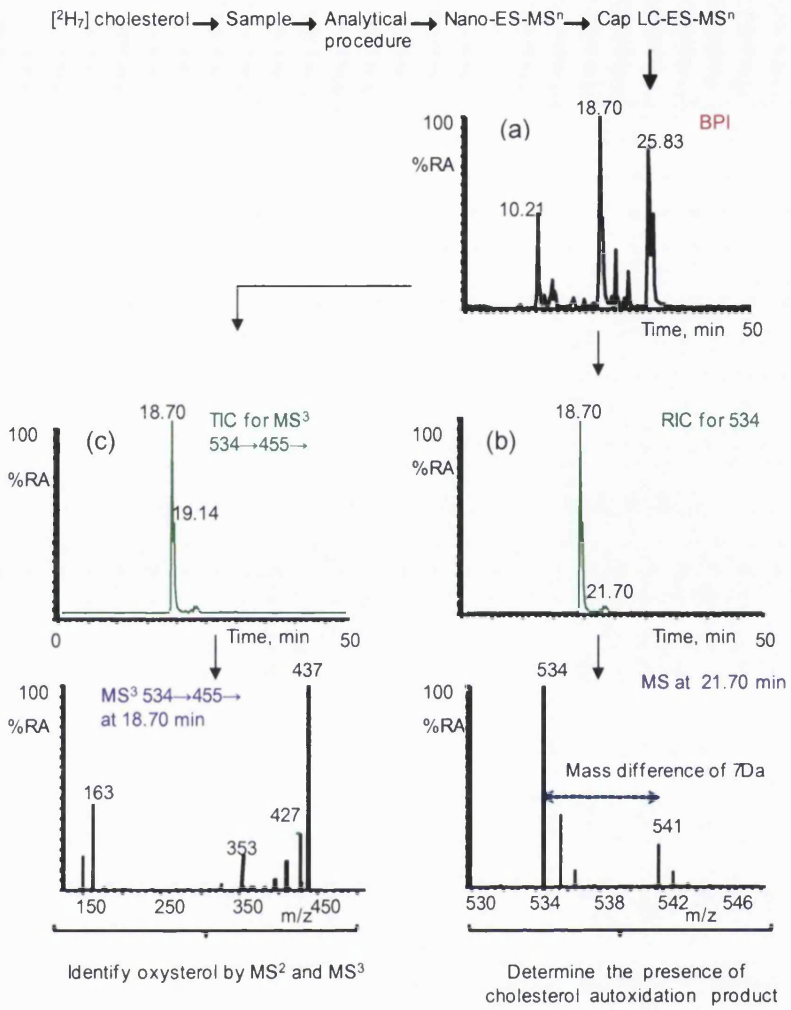

Figure 4.5 General scheme outlining the use of deuterium-labelled cholesterol to detect the formation of oxysterol artifacts produced during the sample preparation.The method involves the addition of [$^2H_7$] cholesterol to 50 mg of rat brain at the initial stage of the analytical procedure as described in Figure 2.3a,b. If an autoxidation of cholesterol occured during the sample preparation, the labelled cholesterol was also oxidised in parallel with the sample's endogenoues cholesterol to generate labelled sterols. These labelled sterols differed in mass by an increment that is directly related to the number of incorporated isotopes. The resulting sample was analysed by cap-LC-MS^n. The data analysis consisted of 3 stages. In stage 1, (a) Base Peak Chromatogram (BPI) was constructed to evaluate the presence of chromatographic peaks and their corresponding *m/z* values. In stage 2, (b) Reconstructed Ion Chromatograms (RICs) were generated for a specific *m/z* value corresponding to a predicted sterol. The labelled and unlabelled sterols give similar chromatographic behaviour and identical signal intensity. The identification of labelled and unlabelled sterols was based on their RRT, MS, MS^2 and MS^3 spectra. Lower panel shows mass spectrum (MS) for a chromatographic peak at 21.70 min corresponding to oxidised/GP-derivatised unlabelled monohydroxycholesterol (*m/z* 534) and its corresponding labelled (*m/z* 541). In stage 3, (c) Total Ion Chromatograms (TICs) for the MS^3 transition $[M]^+ \rightarrow [M\text{-}79]^+ \rightarrow$ were generated for labelled and unlabelled sterols to allow their characterisation. Lower panel shows MS^3 534→455→ spectrum of oxidised/GP-derivatised 24S-hydroxycholesterol (*m/z* 534) of chromatographic peak at 18.70 min.

The resulting oxidised/GP-derivatised sterols were analysed by cap-LC and MS, MS^2, MS^3 spectra recorded. The MS^3 534→455→ and 534→427→ transitions were monitored for the identification purposes, and the MS^2 534→ for the determination of the relative abundance of monohydroxycholesterols. 22R-Hydroxycholesterol was selected, because this sterol elutes just before 24S-hydroxycholesterol from the C_{18} capillary column with RRT of 0.62 and 0.69 (Figure 3.38), and this oxysterol was not identified by the current methodology in rat brain (see Table 5.2 in Chapter 5). Figure 4.4 shows a reconstructed ion chromatogram (RIC) for the MS^2 transition 534→455 for the chromatographic region from 14 min to 23 min. The oxidised/GP-derivatised 22R-hydroxycholesterol eluted at 16.9 and 17.7 min from the capillary C_{18} column due to formation of the *syn*- and *anti*-conformers in the derivatisation of 22R-hydroxycholesterol. Because 22R-hydroxycholesterol gave twin peaks in LC, the combined peaks were used to construct calibration plots. A five point calibration plot was generated for relative quantification of 24S-, and 22R-hydroxycholesterols for the MS^2 transition 534→455 giving an R^2 of 0.99 (as described in Section 2.10). The percentage recovery of 22R-hydroxycholesterol was 92.3 ± 1.7% (mean ± standard deviation, n=3).

4.2 The strategy for the investigation of cholesterol autoxidation products formed during the sample preparation

The results presented in chapter 3 demonstrate that the separation of oxidised/GP-derivatised oxysterols can be achieved by reversed-phase chromatography prior to their characterisation by tandem mass spectrometry (MS^n). The use of LC separation is crucial to the identification of oxysterols in a complex biological sample, as the oxysterols previously identified in brain by others i.e. 24S-hydroxycholesterol, 25-hydroxycholesterol, and 7-hydroxycholesterols, all give a $[M]^+$ ion of *m/z* 534.4 following oxidation/GP-derivatisation. They cannot be distinguished from each other by means of MS detection alone, and if present as a mixture give a composite MS^3 spectrum.

Since the brain contains substantial amounts of cholesterol, measures were required to not only effectively remove cholesterol in the earliest step of the sample preparation, but also to identify oxysterols potentially formed by autoxidation of cholesterol during the sample preparation. Isotopically labelled cholesterol was used to determine whether the autoxidation products of cholesterol are formed during sample preparation. The method involves the addition of [$^2H_7$] cholesterol labelled on the side chain (99% pure by TLC) to the rat brain sample at the initial stage of the analytical procedure. It is worth noting that the [$^2H_7$] cholesterol even at 99% purity may contain an appreciable amount of autoxidation formed oxysterols. The idea of this experiment is that, if autoxidation of cholesterol occurs during the sample preparation, the added labelled cholesterol will also be oxidised in parallel with the sample's endogenous cholesterol to produce labelled oxysterols. If cholesterol is not oxidised during the sample preparation the labelled cholesterol will remain intact. The labelled and unlabelled cholesterol will behave in an identical manner during the sample preparation procedure.

The analytical scheme for the extraction, enrichment and analysis of oxysterols from rat brain is shown in Figures 2.3a and 2.3b (chapter 2, section 2.15), and the data analysis is shown in Figure 4.5. The aim of this experiment was to demonstrate that the formation of autoxidation products of cholesterol during the sample preparation can be readily detected through the use of the deuterium-labelled cholesterol. The method assumes that the addition of an amount of labelled cholesterol is approximately equal to that of the cholesterol present in the rat brain sample. The cholesterol content of the rat brain is around 15 μg/mg [33,81,177,178]. Accordingly, 750 μg of [$^2H_7$]-cholesterol was added to 50 mg of rat brain in order to obtain an approximately 1:1 ratio between the unlabelled and labelled cholesterol in the sample. After homogenation of the spiked rat brain in ethanol, the labelled and unlabelled cholesterol is separated from oxysterols in the first stage of the sample purification by a single or double passage through a Unisil column (the results of two experiments are described below) giving two fractions, i.e. fraction U1 ("cholesterol fraction") and

fraction U2 ("oxysterol fraction"). Oxysterols are then oxidised, derivatised and analysed by capillary LC-MS^n. The first goal was to identify cholesterol autoxidation products in the oxysterol fraction. The second goal was to measure the ratio of labelled to unlabelled sterol in the oxysterol fractions, and to evaluate if this ratio could be used to determine the levels of cholesterol autoxidation products formed during the processing of sample. This type of approach can produce four distinctly different results.

(i) If only [$^2H_0$] unlabelled oxysterols are identified in the final analysis, this would indicate that the identified oxysterols are endogenous oxysterols of the rat brain, and are not formed as autoxidation products during the sample preparation.

(ii) If both [$^2H_7$] labelled and [$^2H_0$] unlabelled oxysterols are present, and their [$^2H_0$]/[$^2H_7$] ratio is ~1:1, this would indicate that the identified unlabelled oxysterol is formed entirely as an autoxidation product during the sample preparation.

(iii) If both [$^2H_7$] labelled and [$^2H_0$] unlabelled oxysterols are present, but the unlabelled to labelled oxysterol [$^2H_0$]/[$^2H_7$] ratio is quite different, this would indicate that a fraction of the unlabelled oxysterol is formed as an autoxidation product during the sample preparation, and that the remaining portion is possibly endogenous to the sample.

(iv) The detection of only labelled [$^2H_7$] sterol would suggest that sterol only comes from [$^2H_7$] cholesterol.

It should theoretically be possible to use the information obtained from the deuterium-labelled cholesterol profile to correct the analytical data for the presence of these autoxidation products formed during the sample preparation.

In general, the deuterium-labelled sterols have essentially the same physico-chemical properties as their unlabelled counterparts, and give similar chromatographic behaviour, and identical signal intensity in mass spectra. However, labelled sterols will differ in mass by an increment that is directly related to the number of incorporated isotopes. This allows a comparison

of their signal intensity, which infers the relative sterol abundance. Cholesterol labelled with deuterium ([25,26,26,26,27,27,27-$^2H_7$] cholesterol, molecular weight 393.4) was used in this work (see Figure 4.6). The site of the labelling on the cholesterol molecule is important since the possibility existed that labelling on the cholesterol ring system may introduce undesirable isotope effects during the oxidation of labelled and unlabelled cholesterol, the chromatographic separation and the mass spectrometry analysis.

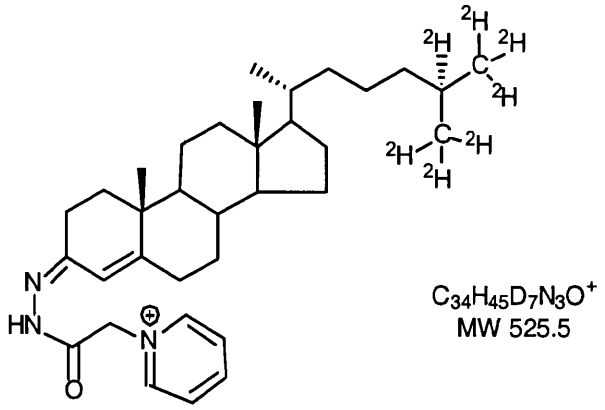

Figure 4.6 The structure of the oxidised/GP-derivatised [$^2H_7$] cholesterol.

The [$^2H_7$]-cholesterol was oxidised with cholesterol oxidase, reacted with GP hydrazine and analysed by direct infusion nano-ES-MS, and capillary LC-MS^n. The deuterium-labelled cholesterol gives a $[M]^+$ ion at *m/z* 525 Da, modified by a mass of 7 Da from the oxidised/GP-derivatised unlabelled cholesterol (see supplementary material Figure 1a and 2a). As discussed in chapter 3, the resulting oxidised/GP-derivatised sterols give characteristic MS^2 (loss of 79 Da) and structurally informative MS^3 spectra. The characteristic fragment-ions corresponding to b-series and $[M-107]^+$ ions are present in the MS^3 spectra of the oxidised/GP-derivatised [$^2H_7$]-cholesterol. The b-series fragment-ions are formed due to fragmentation of the A- and B-rings of the steroid nucleus, and these fragment-ions are the same in the MS^3 spectra of oxidised/GP-derivatised cholesterol and [$^2H_7$]-isotopomer. However, in the spectra for the $[M]^+\rightarrow$, $[M]^+\rightarrow[M-79]^+\rightarrow$, and $[M-107]^+\rightarrow$ transitions of [$^2H_7$]-cholesterol, the fragment-ions $[M-79]^+$, $[M-107]^+$, $[M-122]^+$ and $[M-151]^+$ are 7 Da heavier than

the equivalents ions in the spectra of the monoisotopic isotopomer. This was expected as the deuterium labels are at the C17 side-chain of the sterol molecule. An approximately 1:1 mixture of the oxidised/GP-derivatised labelled and unlabelled cholesterol was analysed by capillary-LC-MS^n, and the relative retention time of [$^2H_7$]-cholesterol was determined to be 0.995 in relation to [$^2H_0$] cholesterol (see Figure 3.38). Even though labelled and unlabelled sterols are not well chromatographically resolved, the mass difference between these two compounds is 7 Da, and this will allow their differentiation.

It is important to note that the current methodology generates data, which is quantitative once the sample is derivatised to the GP hydrazone, equivalent sterols give an equal response upon ES process. The separation of oxidised/GP-derivatised [$^2H_0$]- and [$^2H_7$]-sterols is not significant in the current capillary LC-MS^n analysis. Therefore, it is possible to determine the relative abundance of different labelled and unlabelled sterol found in rat brain after the sample preparation. The unlabelled to labelled ratio is then calculated for each identified sterol by dividing the intensity of an unlabelled $[M]^+$ ion with the intensity of its corresponding deuterium-labelled $[M]^+$ ion.

In addition to the LC-MS considerations, side-chain labelling of cholesterol as in [25,26,26,26,27,27,27-$^2H_7$] cholesterol should minimise isotope effect during autoxidation of cholesterol since most of the autoxidation products of cholesterol are derived from reactions on the A and B rings of the steroid skeleton. One possible exception is 25-hydroxycholesterol, in which the 25-position is the site of oxidative attack. This particular topic will be discussed in detail later.

4.3 The identification of oxysterols formed due to autoxidation of cholesterol during the sample preparation of rat brain

The experimental design used for the analysis of oxysterols in rat brain is outlined in Figures 2.3a and 2.3b (chapter 2, section 2.15). Following the addition of the deuterium-labelled cholesterol to the rat brain, extraction, and a single passage of the brain extract through Unisil SPE column was carried out. The obtained oxysterol fraction (fraction U2) was oxidised/GP-derivatised with GP hydrazine, and sterol GP hydrazones were separated by reversed-phase chromatography,

and analysed on the LCQ^{duo} ion trap mass spectrometer. The presence of oxysterols in human, rat, and mouse brains has been previously reported [4,24,38,41,52,68,121,154,155]. These include 24S-hydroxycholesterol, 27-hydroxycholesterol, 25-hydroxycholesterol, 7α-hydroxycholesterol, 4β-hydroxycholesterol, 24,25-epoxycholesterol, 5,6-epoxycholesterol, 7-oxocholesterol, 20-hydroxycholesterol, cholesterol 5,6-*seco*-sterol and its aldol [24,41,155,156]. The studies by Mast and Zhang show that brain cells also metabolise oxysterols [24,154,155] to 7,25- and 7,27-dihydroxycholesterol with their subsequent conversion to 3-oxo-4-ene sterols. They also showed that a minor fraction of 27-hydroxycholesterol and its 27-hydroxylated metabolites were further converted into 3β-hydroxycholest-5-en-27-oic acid, 3β,7α-dihydroxycholest-5-en-27-oic acid and 7α-hydroxy-3-oxo-cholest-4-en-27-oic acid. Therefore, sterols involved in the metabolism of cholesterol would possibly be found in the current rat brain, and were considered for analysis by cap-LC-MS^n.

Figure 4.5 shows the work-flow utilised for the acquisition and analysis of data. In an initial run, the instrument was programmed to record the full mass spectra (meaning that MS scans were only recorded). After collecting scan data, the recorded raw data was analysed for the presence of all potential labelled and unlabelled oxysterols based on their predicted elemental composition. For example, the *m/z* of the ions monitored for labelled and unlabelled monohydroxycholesterols were 541 and 534; for labelled and unlabelled dihydroxycholesterols were 557 and 550; and for labelled and unlabelled oxocholesterols were 539 and 532, respectively. RICs for the *m/z* values of these and other oxysterols were generated. In a second LC-MS run, MS^2 and MS^3 spectra were recorded for $[M]^+ \rightarrow$, $[M]^+ \rightarrow [M-79]^+ \rightarrow$ and $[M]^+ \rightarrow [M-107]^+ \rightarrow$ transitions for all potential labelled and unlabelled sterols suggested to be present from the initial LC-MS run. MS^2 were preferentially performed on the *m/z* values of the $[M]^+$ ions, and MS^3 was programmed to be performed on ions resulting from a neutral loss of 79 or 107 Da in the MS^2 scan. Then, total ion chromatograms (TICs) for specified $[M]^+ \rightarrow$, $[M]^+ \rightarrow [M-79]^+ \rightarrow$ and $[M]^+ \rightarrow [M-107]^+ \rightarrow$ transitions were displayed individually.

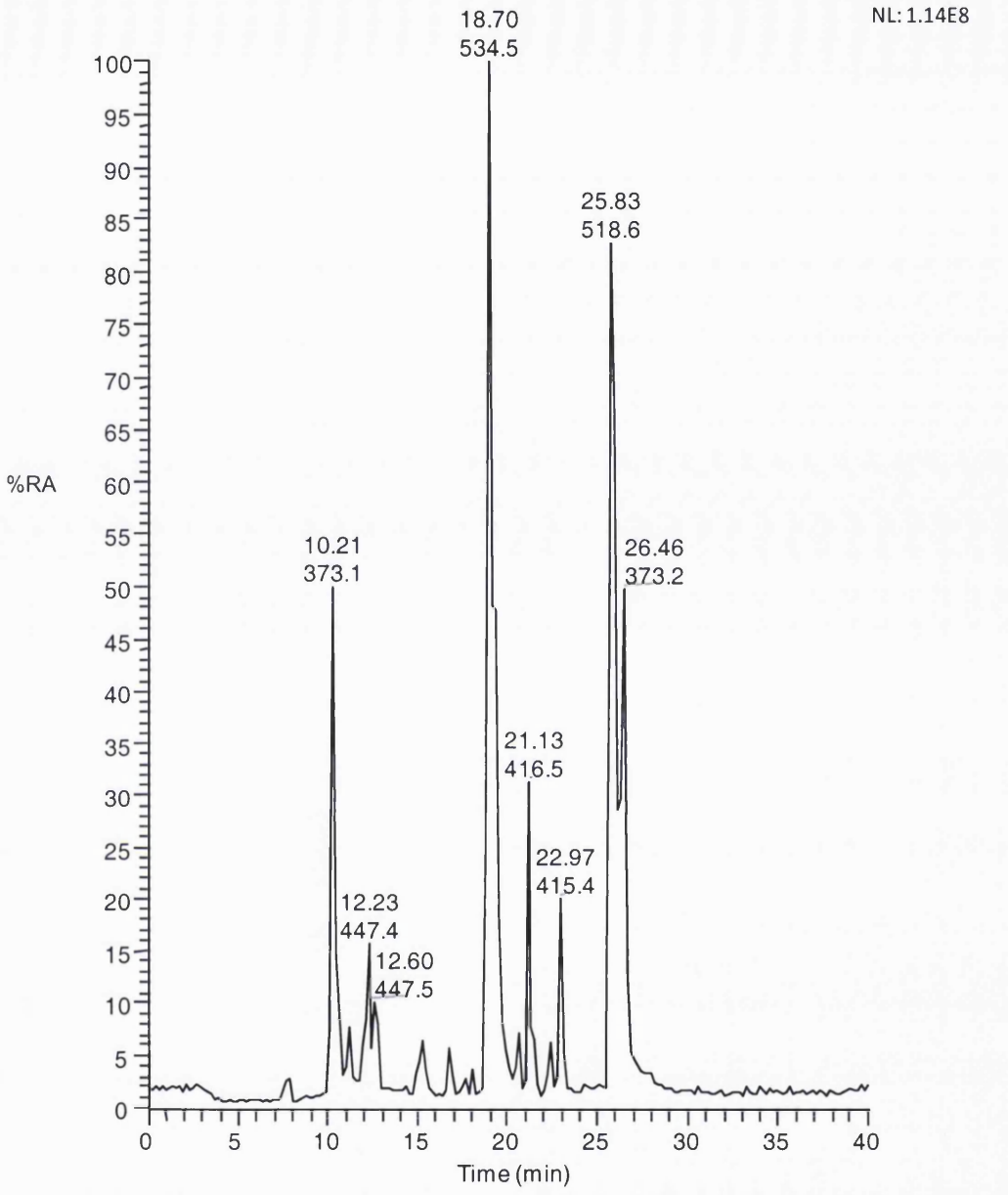

Figure 4.7 Base peak ion chromatogram of the oxidised/GP-derivatised oxysterols obtained from rat brain. [$^2H_7$]-Cholesterol (750 µg) was added to rat brain (50 mg). The sample was homogenised in ethanol. Cholesterol was separated from oxysterols, by a single passage of the rat brain extract through a Unisil SPE column (as shown in Figure 2.3a). The obtained oxysterol fraction was subjected to oxidation with cholesterol oxidase, and derivatisation with GP hydrazine. The oxidised/GP-derivatised oxysterols were separated on a C_{18} capillary column (PepMap C_{18} column, 180 µm x 150 mm, 3 µm, 100 Å) at a flow rate set to 0.8 µL/min. Mobile phase A was 50% methanol, 0.1% formic acid, and B was 95% methanol, 0.1% formic acid. Gradient elution was performed starting at 30% B, rising to 70% B over ten minutes, then to 80% B over a further five min. The mobile phase composition was maintained at 80% B for a further 15 minutes before returning to 30% in 0.1 min. The total run time was 50 min. The equivalent of 20 µg of rat brain was injected on-column.

It is important to note that the MS^3 scan adds specificity to the current methodology, in which fragmentation pathways can be recorded for precursor ions specifically giving an $[M-79]^+$ "intermediate". Other ions that coincidentally have the same nominal mass as derivatised oxysterols and are co-selected in the MS^2 event do not give an $[M-79]^+$ intermediate, and hence their fragment ions do not contaminate the final fragment ion MS^3 spectrum.

Using this methodology, seventeen different sterols were identified in rat brain based on their MS, MS^2, MS^3 spectra, and their relative retention times (Table 4.1). The identification of novel oxysterols in rat brain is described in chapter 5. This chapter is only concerned with the identification of autoxidation products of cholesterol during the sample preparation.

Figure 4.7 shows a base peak chromatogram of an aliquot of the oxysterol fraction, U2 (obtained by passing the brain extract once through the Unisil SPE column) injected on the capillary reversed-phase column. A single passage of the brain extract through the Unisil SPE column removes a significant amount of labelled and unlabelled cholesterol from the final oxysterol fraction, U2. The relative abundance (RA) of cholesterol in these samples amounts to 84% of the major oxysterol in the U2 fraction. The major sterol in the oxysterol fraction has an *m/z* 534.4 (RA 100%) and elutes from the capillary C_{18} column with retention time 18.70 min (relative retention time RRT 0.72) corresponding to RRT of the oxidised/GP-derivatised reference 24S-hydroxycholesterol (see Figure 4.8). TICs were constructed for the MS^2 534→, MS^3 534→455→ and 534→427→ transitions (see example of TIC for the MS^3 transition 534→455→ in Figure 4.9c). Both the MS^2 and MS^3 spectra are identical to those from the authentic compound, the oxidised/GP-derivatised 24S-hydroxycholesterol (see example of MS^3 (534→455→) spectra, Figures 4.10a and 4.10b). The oxidised/GP-derivatised 24S-hydroxycholesterol is the product of cholesterol oxidase mediated oxidation of 24S-hydroxycholesterol and derivatisation reaction with GP reagent. The identification of 24S-hydroxycholesterol in rat brain is in agreement with the work by Björkhem [19,37,44,165,179] has shown that 24S-hydroxycholesterol is the major oxysterol in brain. Lund *et al.* [164,180] have shown

that CYP46A1, is the enzyme responsible for 24S-hydroxylation of cholesterol, is expressed exclusively in the brain, and normally in neurons.

It is also possible to determine the approximate relative abundance of different oxysterols in the brain. For example, 24S-hydroxycholesterol is a major oxysterol in the fraction U2. Therefore, RAs of all oxysterols could be measured relative to 24S-hydroxycholesterol. Normalised display mode values are also displayed in the chromatogram or the MS spectrum; for examples see Figures 4.7 and 4.8. In the normalised display mode, all peaks are reported with peak heights relative to the highest peak in the chromatogram or the MS spectrum. Therefore, the NL value gives the intensity of the signal of a mass of interest.

TICs were constructed for the transitions MS^2 541→, MS^3 541→462→ and MS^3 541→434→, which correspond to deuterium-labelled monohydroxycholesterols, which could possibly be formed due to the autoxidation process of labelled cholesterol during the sample preparation (see Figure 4.9a corresponding to TIC for the MS^3 transition 541→462→). A peak at 18.70 min was not detected, at which the authentic oxidised/GP-derivatised 24S-hydroxycholesterol normally elutes. It was previously determined in chapter 3 that labelled and unlabelled sterols are not chromatographically well resolved (Figure 3.38). There is also the possibility that the high abundance of 24S-hydroxycholesterol could obscure the presence of low abundant sterols. To overcome this problem MS scans between 18.60 min to 19.25 min were combined. In this way, low abundance sterols with different *m/z* values, which elute very close together in time with the oxidised/GP-derivatised 24S-hydroxycholesterol, are visualised (see Figure 4.8). The combined MS spectra will give information on possible co-eluting or partially chromatographically resolved compounds of low abundance.

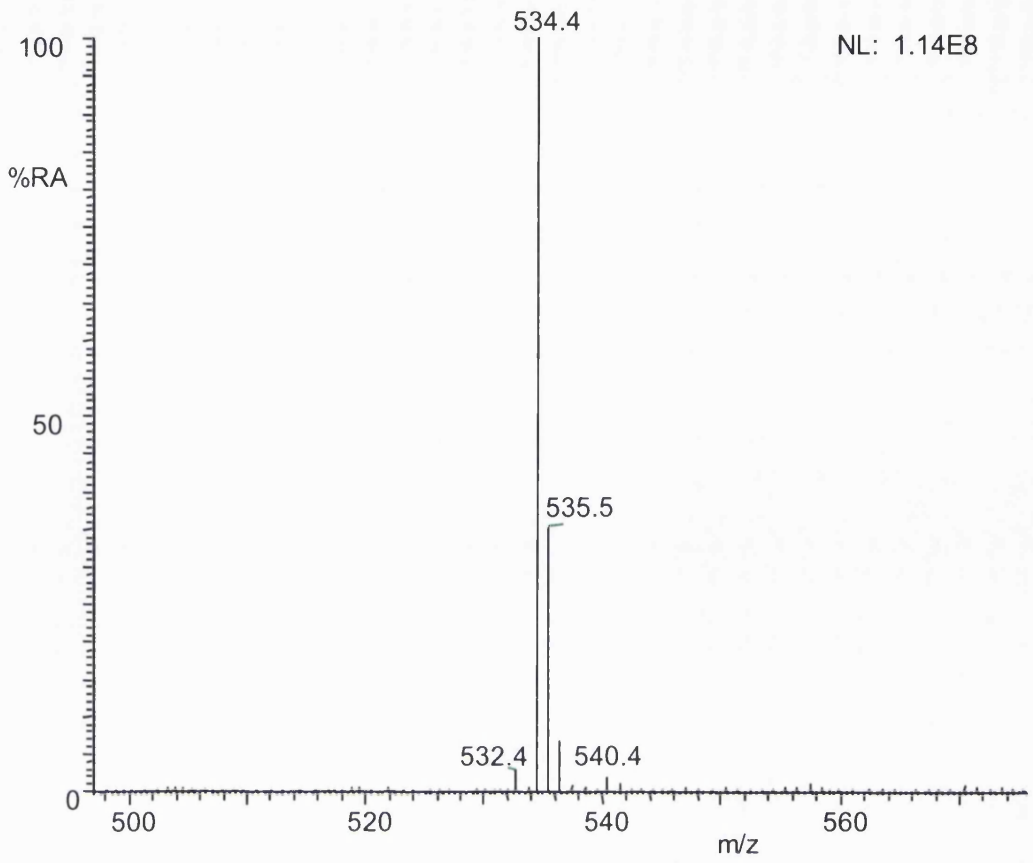

Figure 4.8 MS spectrum of the chromatographic region from 18.60 min to 19.20 min for base peak ion chromatogram refer to Figure 4.7.

Figure 4.8 shows the absence of labelled 24-hydroxycholesterol in our processed oxysterol fraction U2, which would have been detected at retention time 18.70 min as a *m/z* 541 peak. This indicates that the 24S-hydroxycholesterol found in rat brain is not generated by autoxidation of cholesterol during extraction, enrichment or oxidation and GP derivatisation. This concurred therefore with the view of Björkhem *et al.* [19,35,37,44,92,164,180] that 24S-hydroxycholesterol present *in vivo* is of enzymatic origin, and that our sensitive and specific capillary LC-MS^n method establishes its presence in rat brain.

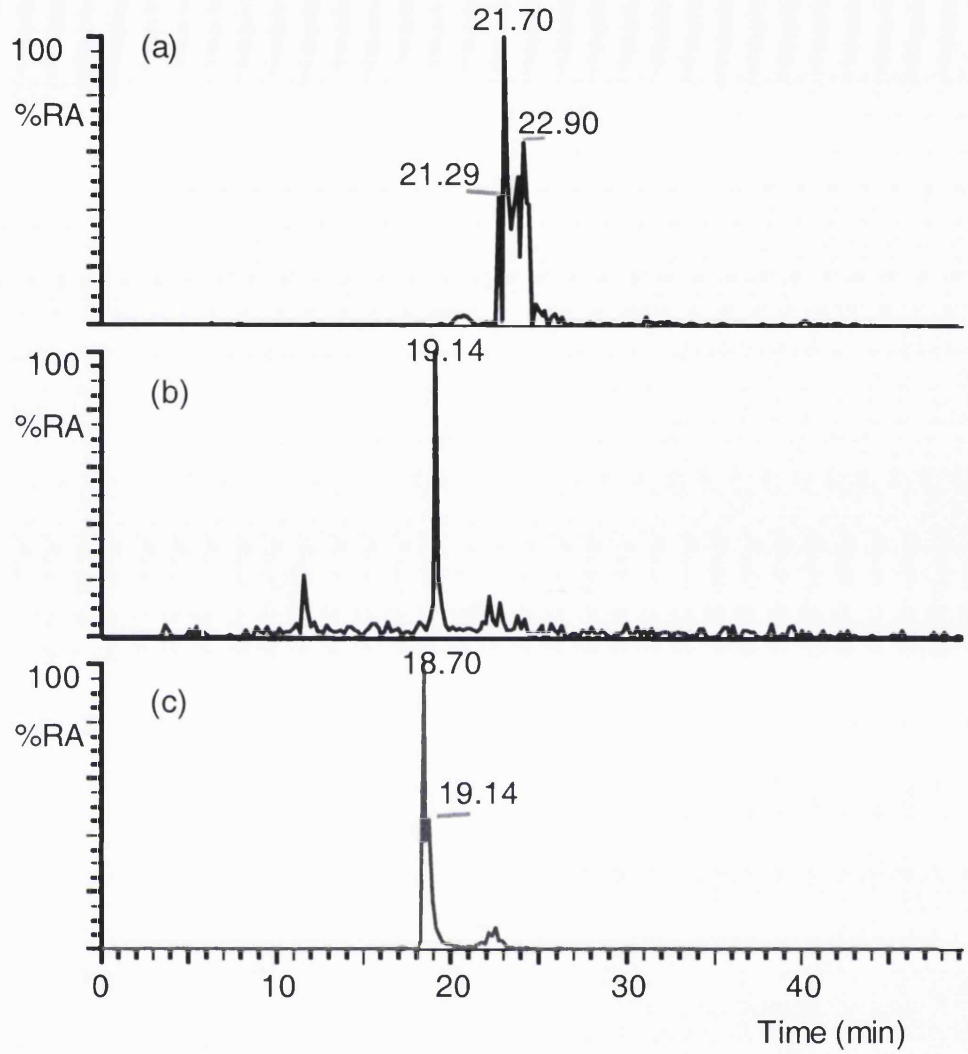

Figure 4.9 Identification of monohydroxycholesterols and monohydroxy[$^2H_7$]-cholesterols in rat brain. Oxysterols were isolated from rat brain (50 mg) spiked with [$^2H_7$]-cholesterol (750 µg) as illustrated in Figure 2.3a. Oxysterols were oxidised and derivatised with GP reagent and analysed by capillary LC-MS^n. Chromatographic and mass spectrometry conditions are described in section 2.9. (a) TIC for the MS^3 transition 541→462→ corresponding to oxidised/GP-derivatised labelled monohydroxycholesterols, (b) TIC for the MS^3 transition 540→461→ corresponding to oxidised/GP-derivatised labelled monohydroxycholesterols, (c) TIC for the MS^3 transition 534→455→corresponding to oxidised/GP-derivatised monohydroxycholesterols.

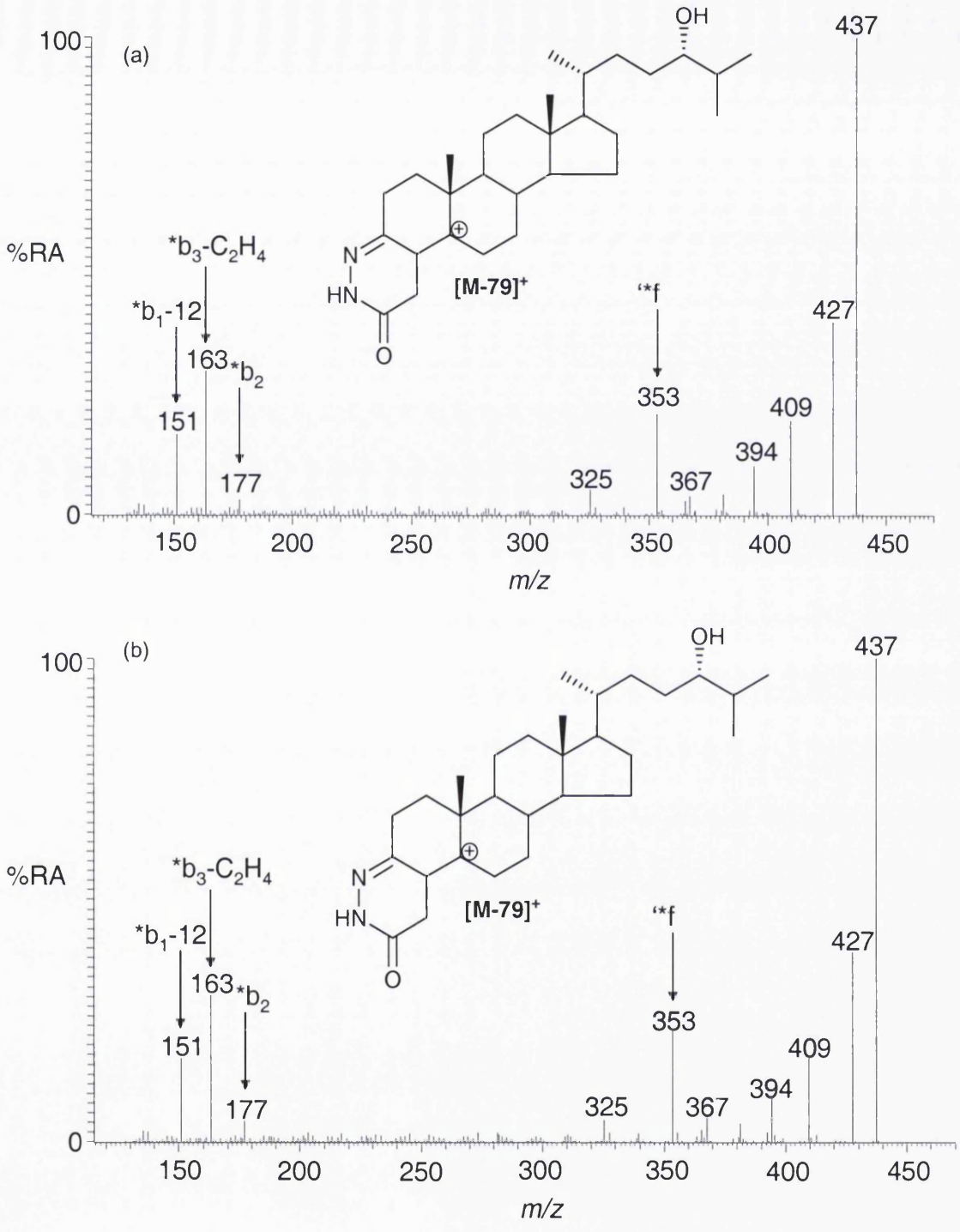

Figure 4.10 (a) MS^3 (534→455→) spectrum of the chromatographic peak eluting at 18.70 min corresponding to oxidised/GP-derivatised monohydroxycholesterol from rat brain (refer to Figure 4.9c), and (b) authentic oxidised/GP-derivatised 24S-hydroxycholesterol with a similar retention time. Therefore, the component eluting at 18.70 min was identified as the oxidised/GP-derivatised 24S-hydroxycholesterol.

The formation of labelled 25-hydroxycholesterol involves oxidative attack at the 25-position of [$^2H_7$]-cholesterol. Because of the presence of a deuterium atom in the C-25 of the deuterated cholesterol, one of the deuterium atoms on C-25 is lost to give an overall mass increase of 6 Da, compared to the unlabelled cholesterol.

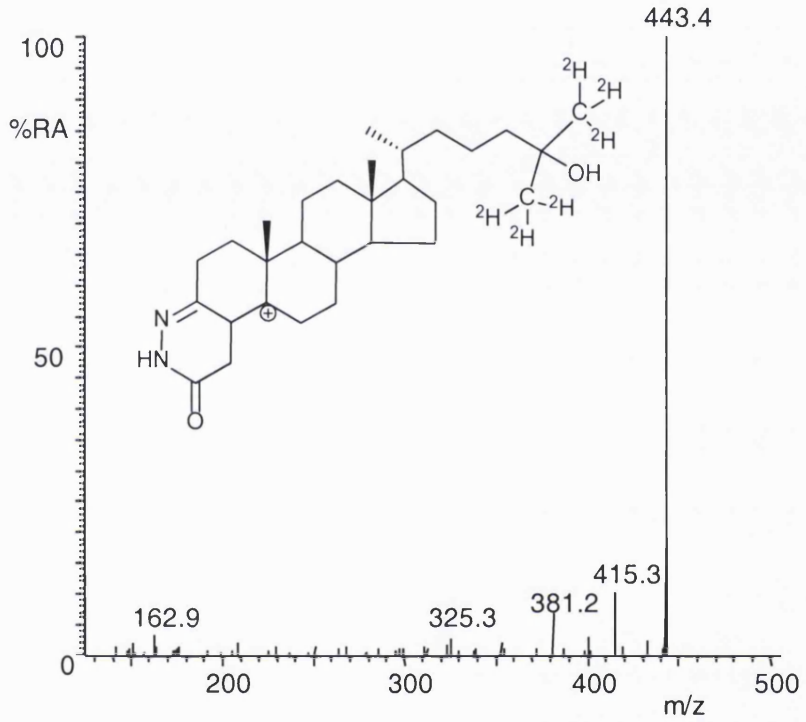

Figure 4.11 MS^3 (540→461→) spectrum of the chromatographic peak eluting at 19.14 min, refer to Figure 4.9b,c.

The oxidised/GP-derivatised hexadeuterium-labelled 25-hydroxycholesterol gives an $[M]^+$ ion of *m/z* 540.4, which was found at 1% of the level of 24S-hydroxycholesterol in the fraction U2 (see Figure 4.8). The oxidised/GP-derivatised 25-hydroxycholesterol was not well resolved from 24S-hydroxycholesterol on the capillary column, and was identified based on MS^2, MS^3 and its retention time. A low chromatographic resolution for the 24S-hydroxycholesterol and 25-hydroxy-[$^2H_7$]-cholesterol can be overcame by constructing TIC for MS^3 transitions 534→455→ and 540→461→ (Figures 4.9b and 4.9c). In addition, MS^2 (540→) and MS^3 (540→461→) spectra allow their differentiation. The MS^3 spectrum for the chromatographic peak at 19.14 min shows that the

$[M-79-18]^+$ ion dominates the MS^3 (540→461→) spectrum at the expense of all other fragment ions. This is a characteristic feature of the hydroxyl group at C-25 position of the oxysterol (Figure 4.11, see supplementary material for spectra of authentic samples). The 25-hydroxycholesterol found in various rat tissues is shown to be a product of cholesterol autoxidation, but enzymatic origins for 25-hydroxycholesterol has also been suggested [108,159,171,172,181].

The presence of the component with *m/z* 532 with RA 3% that of 24S-hydroxycholesterol (see Figure 4.8), encourage to plot TIC for the MS^3 transition 532→453→, which revealed a chromatographic peak at 19.28 min and gave MS^2 (532→) and MS^3 (532→453→) spectra identical to that of authentic oxidised/GP-derivatised 24-oxocholesterol. Deuterium-labelled 24-oxocholesterol was not detected in this sample, indicating an endogenous origin of the 24-oxocholesterol.

By utilising capillary-LC-MS^n, 7α- and 7β-hydroxycholesterols were chromatographically separated from monohydroxycholesterols with the hydroxyl group on C-17 side chain (see Table 3.38 of their RRTs). The authentic standard of 7β-hydroxycholesterol is chromatographically resolved from the 7α-isomer by about 65 sec in the LC system (Table 3.38). As discussed in chapter 1, brain cells synthesise cholesterol *de novo*, and neurons metabolise cholesterol to 24S-hydroxycholesterol. Alternatively, cholesterol may potentially be metabolised further by both neurons and astrocytes to additional oxysterols, for example 7α,25- and 7α,27-dihydroxycholesterol. 7α-Hydroxycholesterol is formed by the action of cholesterol 7α-hydroxylase in the liver, which is the rate-limiting enzyme in the major pathway from cholesterol to bile acids. Small amounts of 7α-hydroxycholesterol may also be formed as a side product of cholesterol autoxidation [19,41,81,159,168,170,181]. 7β-Hydroxycholesterol is a known product of the autoxidation of cholesterol [108,110,121,122,127,159,181]. If present in brain the probable origin of 7α-hydroxycholesterol is the circulation.

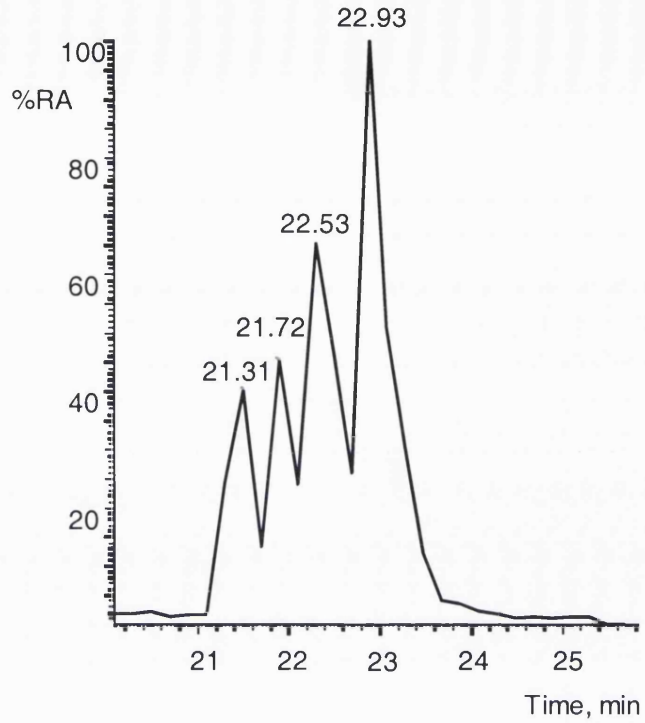

Figure 4.12 RIC for *m/z* 534.4 corresponding to the $[M]^+$ ion of oxidised/GP-derivatised monohydroxycholesterols in rat brain. Oxysterols were isolated from rat brain (50 mg) spiked with $[^2H_7]$ cholesterol (750 µg) as illustrated in Figure 2.3a. Oxysterols were oxidised and derivatised with GP reagent and analysed by capillary LC-MS^n. Chromatographic and mass spectrometry conditions are described in Chapter 2, section 2.9.

The RIC for *m/z* 534.4 corresponding to the $[M]^+$ ions of oxidised/GP-derivatised monohydroxycholesterol revealed at least four peaks at 21.31, 21.72, 22.53 and 22.93 min in the chromatographic region from 20.0 to 25.8 min (see Figure 4.12), and compared with that of 24S-hydroxycholesterol, all are of low abundance (RA <4%) in the oxysterol fraction U2 obtained by a single passage through the Unisil SPE column. The peak at 21.31 min revealed MS^2 and MS^3 spectra compatible with that expected for GP-derivatised 7β-hydroxycholesterol (see Figure 4.13b, see also supplementary material for spectra of authentic sample). The second peak (21.72 min) gave MS^2 (534→), MS^3 (534→455→) spectra corresponding to oxocholestanol or cholestan-dione (Figure 4.14a, see figure comments). The chromatographic peak at 22.53 min was identified as 7α-hydroxycholesterol based on MS^2, MS^3 and retention time, and tandem mass spectra were identical to the authentic standard (see Figure 4.15b and supplementary material for a comparison with

spectra of authentic sample). The chromatographic peak eluting at 22.93 min gave MS^2 (534→), MS^3 (534→455→) compatible with the GP-derivatised 6-hydroxy-cholest-4-ene-3-one (see Figure 4.17a, and supplementary material for a comparison with spectra of authentic sample). As discussed in chapter 3, MS^3 spectra allow isomer differentiation based on their characteristic fragment-ions and relative abundances. 6-Hydroxycholest-4-ene-3-one GP gives a significant fragment ion at *m/z* 383 (RA 50%), which is minor in the MS^3 (534→455→) spectra of 7α-and 7β-hydroxycholesterols (see Figures 4.13b, 4.15a and 4.17a). This fragment ion was also observed in the MS^3 (541→462→) spectrum corresponding to GP-derivatised deuterium-labelled 6-hydroxy-[$^2H_7$]-cholest-4-ene-3-one, but a shift to upper mass by 7 Da (Figure 4.17b). To improve visualisation of RICs the combined transitions 534→455→383 and 541→462→390 were constructed corresponding to the transitions of oxidised/GP-derivatised 6-hydroxycholest-4-ene-3-one and its deuterated-labelled analogue respectively (see Figure 4.16).

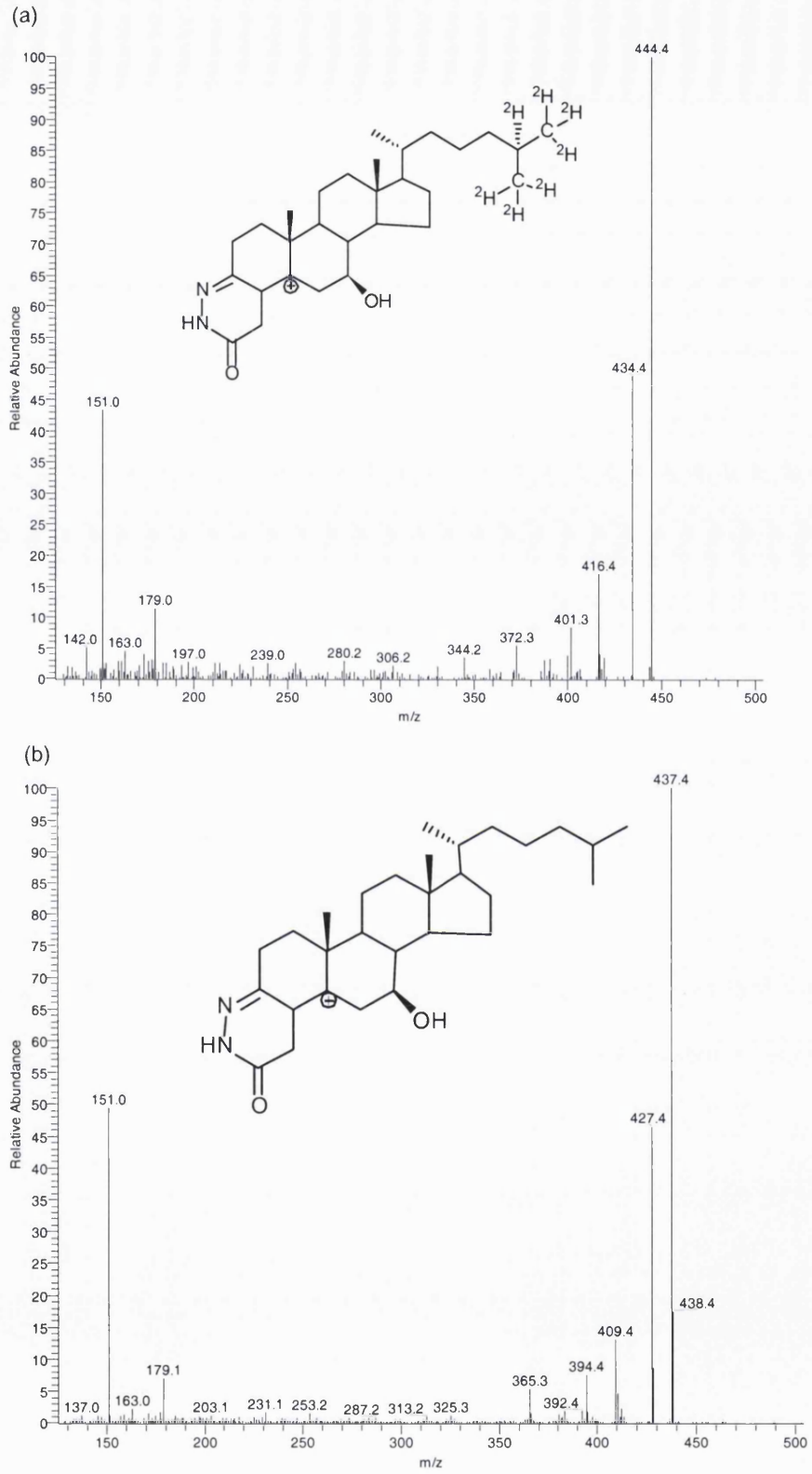

Figure 4.13 (a) MS^3 (541→462→) spectrum of the peak eluting at 21.29 min identified as the oxidised/GP-derivatised 7β-hydroxy-[$^2H_7$]-cholesterol, and (b) MS^3 (534→455→) spectrum of the peak eluting at 21.31 min, identified as the oxidised/GP-derivatised labelled 7β-hydroxycholesterol found in rat brain.

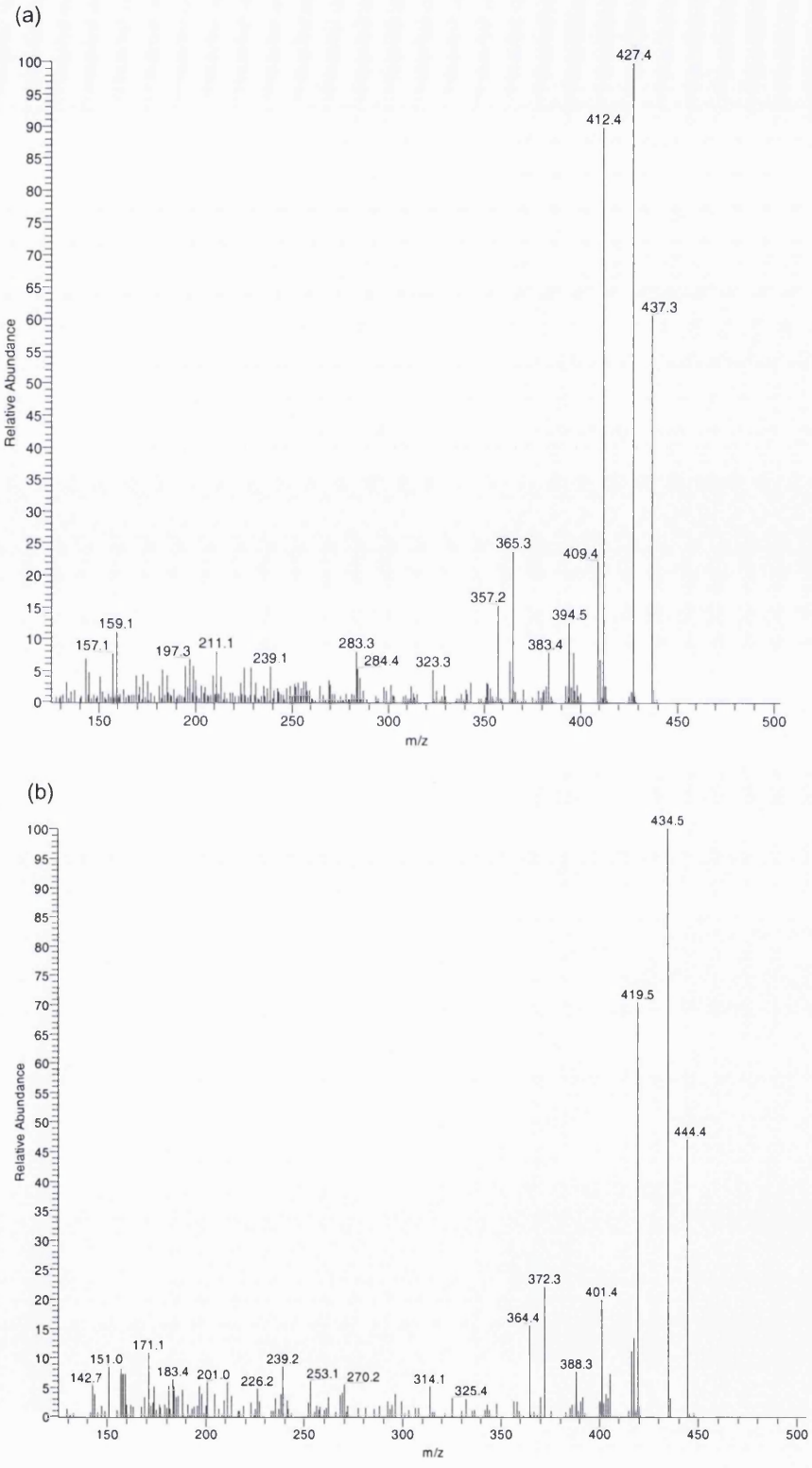

Figure 4.14 (a) MS^3 (534→455→) spectrum of the peak eluting at 21.72 min possibly derived from oxidised/GP-derivatised 3β,5α,6-trihydroxycholestane found in rat brain, (b) MS^3 (541→462→) spectrum of the peak eluting at 21.70 min possibly derived from oxidised/GP-derivatised 3β,5α,6-trihydroxy-[$^2H_7$]cholestane from the rat brain spiked with [$^2H_7$]cholesterol for the experimental description see section 2.15.

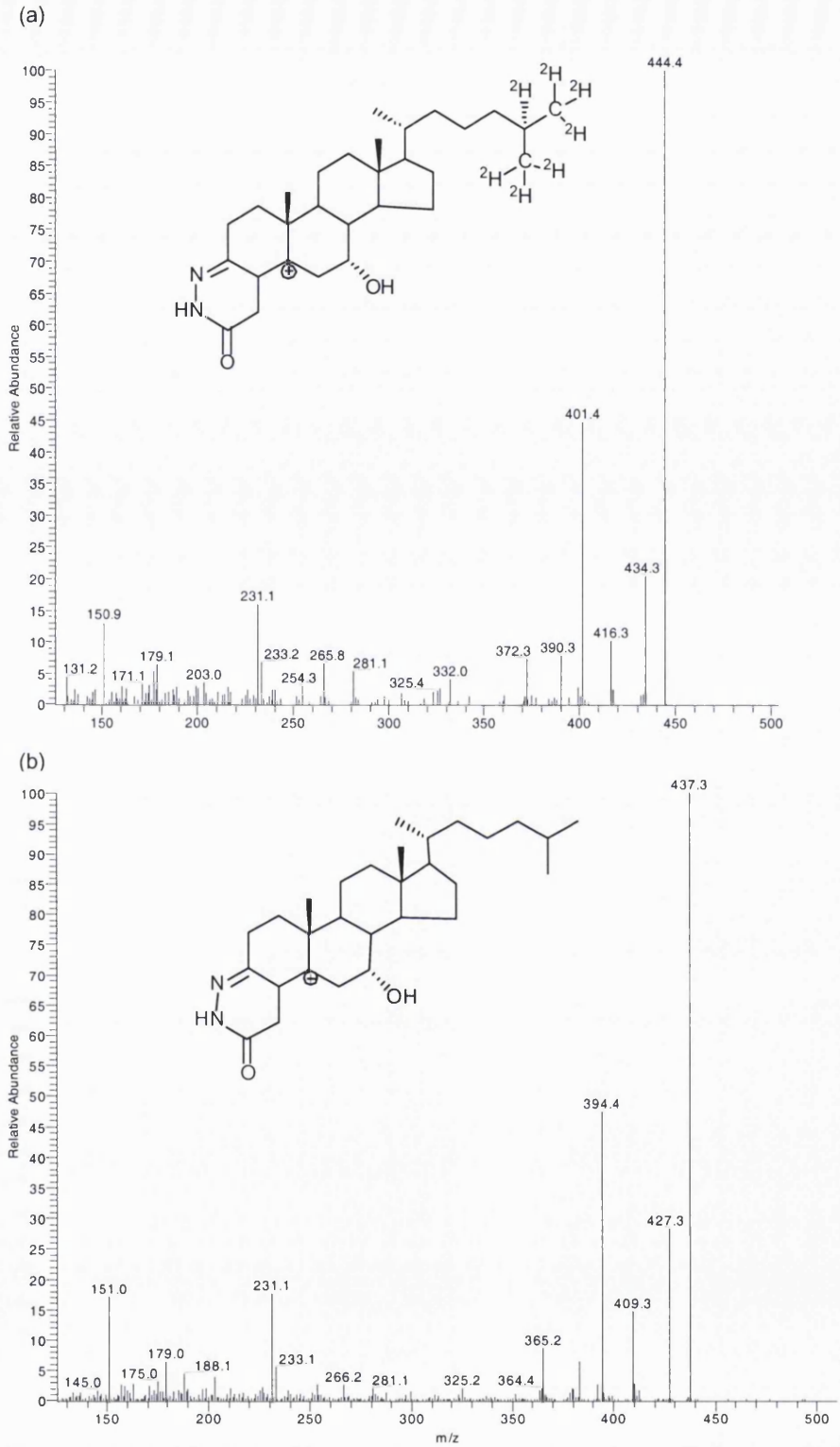

Figure 4.15 (a) MS^3 (541→462→) spectrum of the peak eluting at 22.41 min identified as the oxidised/GP-derivatised 7α-hydroxy-[$^2H_7$]cholesterol and (b) MS^3 (534→455→) spectrum of the peak eluting at 22.53 min, identified as the oxidised/GP-derivatised deuterium-labelled 7α-hydroxycholesterol found in rat brain.

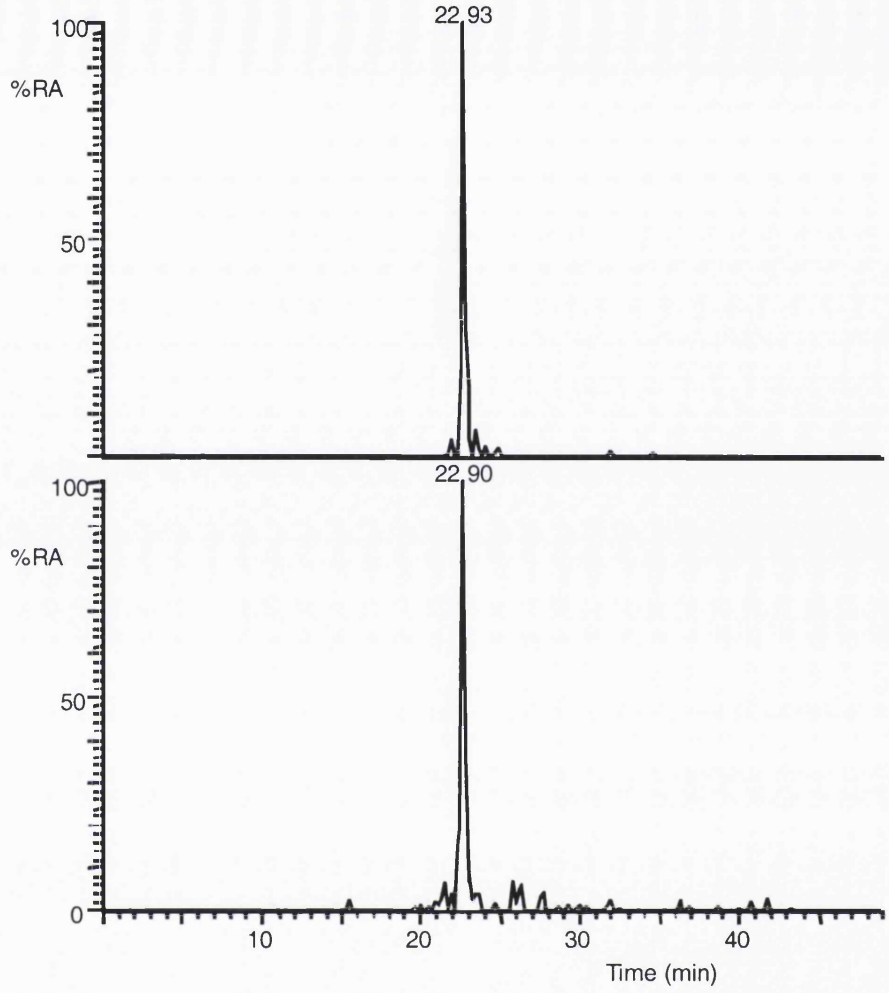

Figure 4.16 RICs for the combined MS^3 transition 534→455→383 (upper trace), and the combined MS^3 transition 541→462→390 (lower trace) corresponding to the GP-derivatised 6-hydroxycholest-4-ene-3-one from rat brain extract spiked with [$^2H_7$]-cholesterol for the experimental description see section 2.15, Figure 2.3a.

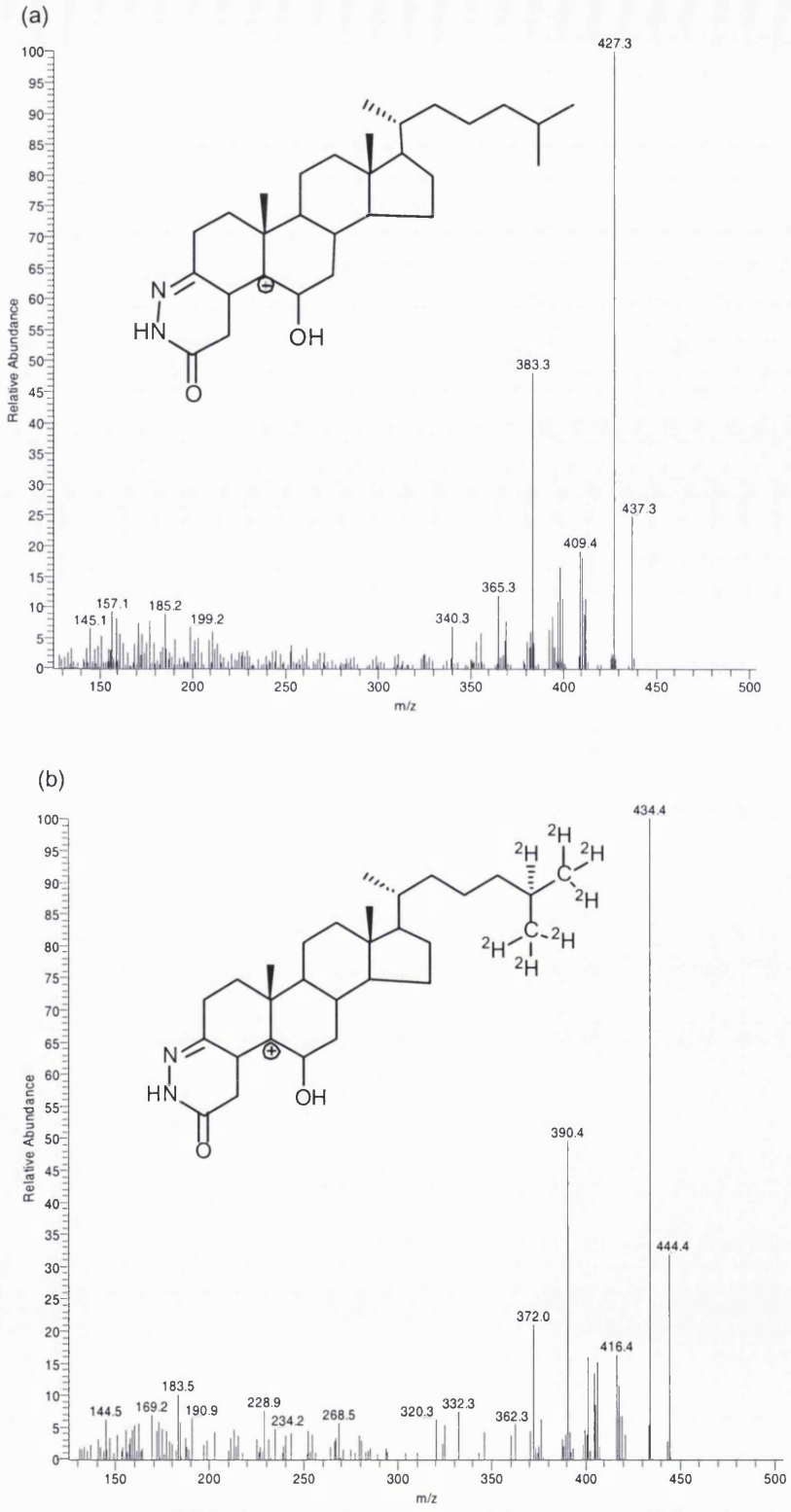

Figure 4.17 (a) MS^3 (534→455→) spectrum of the peak at 22.93 min identified as the GP-derivatised 6-hydroxycholest-4-ene-3-one, (b) MS^3 (541→462→) spectrum of the peak eluting at 22.90 min identified as the GP-derivatised 6-hydroxy-[$^2H_7$]cholest-4-ene-3-one found in rat brain.

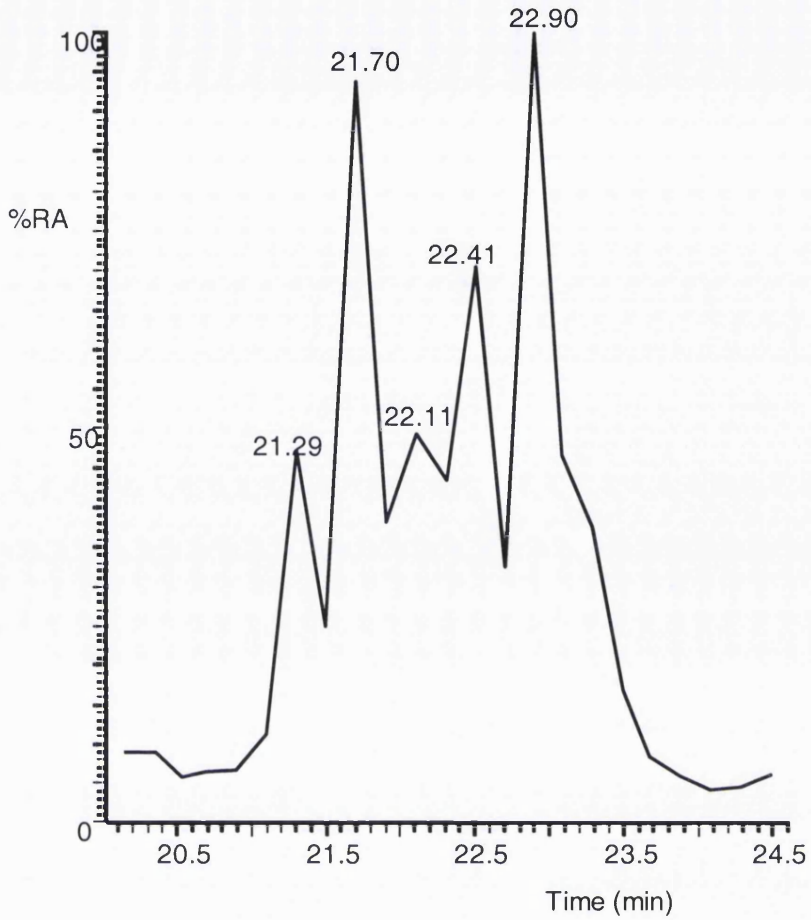

Figure 4.18 RIC for *m/z* 541.4 corresponding to the $[M]^+$ ion of oxidised/GP-derivatised $[^2H_7]$monohydroxycholesterols in rat brain (50 mg) spiked with $[^2H_7]$-cholesterol (750 µg) for the experimental procedure see section 2.15, Figure 2.3a. The RIC shown here differs from that shown in Figure 4.9a due to the faster scan time afforded by MS acquisition compared to MS^3 acquisition. This allows greater chromatographic resolution in RIC from TIC.

The RIC for *m/z* 541 corresponding to the $[M]^+$ ion of GP-derivatised deuterium-labelled monohydroxycholesterol revealed five peaks (see Figure 4.18). The abundance of these peaks was less than 4% of the 24S-hydroxycholesterol. As expected, the chromatographic peak eluting at 21.29 min gave a $[M-79]^+$ fragment-ion in its MS^2 ($[M]^+\rightarrow$) spectrum, and an MS^3 ($[M]^+\rightarrow[M-79]^+\rightarrow$) spectrum compatible with that corresponding to the 7β-hydroxy-$[^2H_7]$cholesterol (see Figure 4.13a and 4.13b for a comparison of MS^3 spectra of the deuterium-labelled 7β-hydroxycholesterol eluted at 21.29 min and unlabelled oxidised/GP-derivatised 7β-hydroxycholesterol eluted at 21.31 min). Predictably, the MS^3 spectrum of the 7β-hydroxy-$[^2H_7]$cholesterol shows $[M-97]^+$ at *m/z* 444; [M-

107]$^+$ at *m/z* 434; [M-107-H_2O]$^+$ at *m/z* 416; [M-C_5H_5N-CO-H_2O-NH]$^+$ at *m/z* 401; and [M-C_5H_5N-CO-H_2O-NH-$NHCH_2$]$^+$ at *m/z* 372, which were shifted up by 7 Da in comparison to the MS^3 for the same transition of the oxidised/GP-derivatised 7β-hydroxycholesterol. 7β-Hydroxycholesterol is a well-known autoxidation product of cholesterol [108,110,121,122,159,181]. It was found in the rat brain of both the labelled and unlabelled forms in the ratio 0.81 ± 0.05% (mean ± standard deviation, n=3), which suggests 7β-hydroxycholesterol was not biosynthesised enzymatically (Table 4.1). This is in agreement with other laboratories, where 7β-hydroxycholesterol was found in human blood samples formed during the sample preparation [159].

The peak at 21.70 min elutes at a similar time to reference oxidised/GP-derivatised 3β,5α,6β-trihydroxycholastane, and MS^2 and MS^3 spectra were very similar to those of the GP derivative of the authentic standard (Figures 4.18 and 4.14b). Following oxidation/GP-derivatisation of authentic cholestane-3β,5α,6β-triol, a [M]$^+$ ion at *m/z* 534 is found, and once separated on the reversed-phase column gives two chromatographic peaks. The late eluting peak at 22.90 min was identified as 6-hydroxycholest-4-ene-3-one, which is formed during the oxidation/GP-derivatisation procedures, and is also the dehydration product of cholestane-3β,5α,6β-triol. The chromatogram of the authentic oxidised/GP-derivatised 3β,5α,6β-trihydroxycholestane is shown in supplementary material S4.1a-c. The cholestanetriol detected on the basis of its unlabelled to labelled ratio could be attributed to a cholesterol autoxidation product formed during the processing of the sample (Table 4.1).

The MS^3 (541→462→) spectrum for the chromatographic peak at 22.11 min showed similar fragment-ions at *m/z* 412 (40%), *m/z* 392 (10%), *m/z* 383 (12%) as in the MS^3 spectrum for the reference 5α,6α-epoxy-cholesterol, but the peaks were shifted up by 7 Da (Figure 4.19a,b). The formation of 5,6-epoxy-cholesterol is a non-enzymatic process. This is in agreement with studies by Breuer *et al.* [108,110].

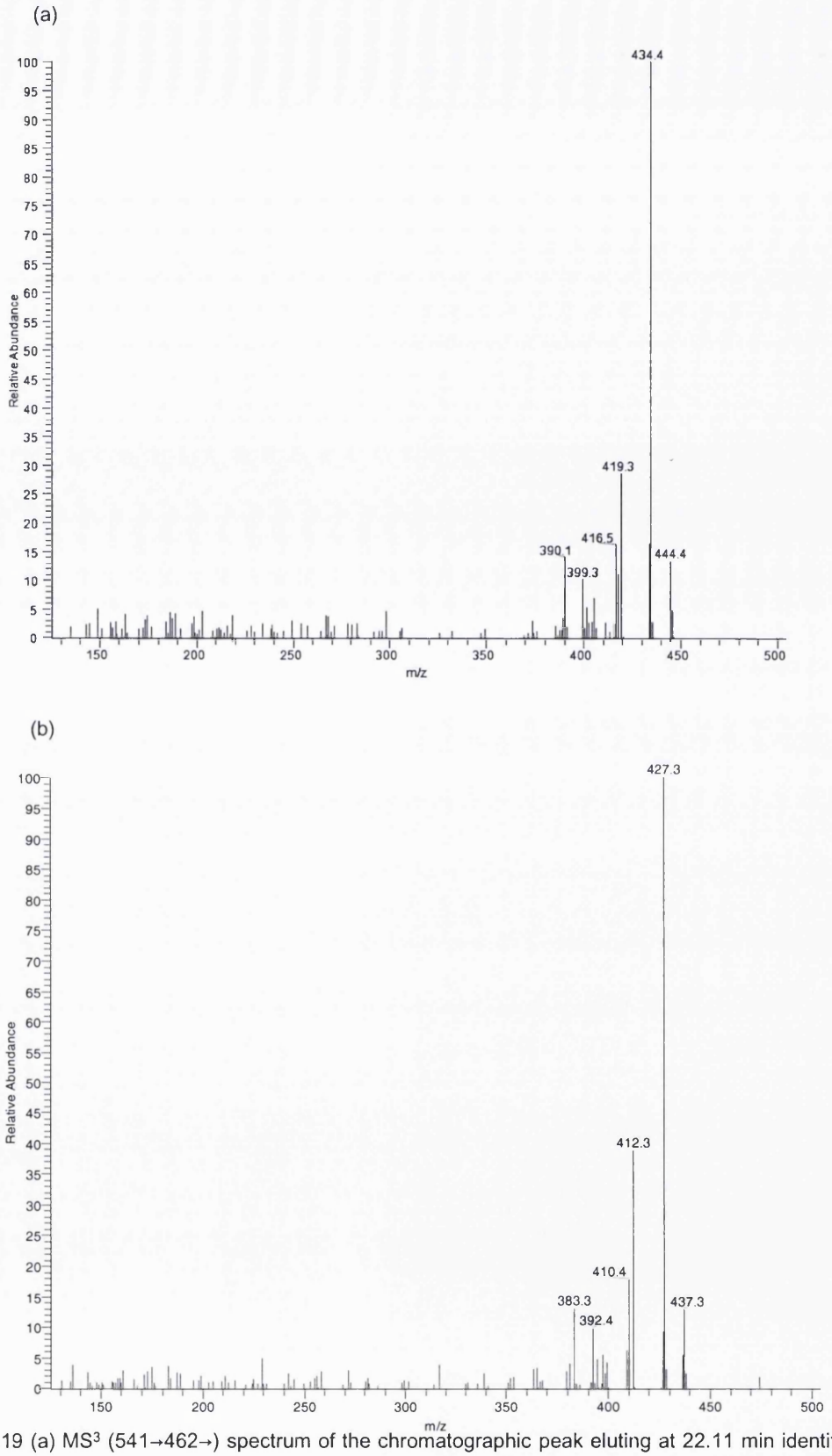

Figure 4.19 (a) MS^3 (541→462→) spectrum of the chromatographic peak eluting at 22.11 min identified as the oxidised/GP-derivatised 5,6-epoxy-[$^2H_7$]cholesterol, (b) MS^3 (534→455→) spectrum of the peak at 22.13 min identified as the GP-derivatised 5,6-epoxy-cholesterol found in rat brain.

The chromatographic peak at 22.41 min gave MS^2 and MS^3 spectra compatible with the identity of deuterium-labelled 7α-hydroxycholesterol (see Figures 4.15a and 4.15b for a comparison of MS^3 (534→455→ and 541→462→) spectra corresponding to the deuterium-labelled and unlabelled 7α-hydroxycholesterol in rat brain). A cytochrome P450-mediated conversion of cholesterol into 7α-hydroxycholesterol would result in a product identical to that of a non-enzymatic reaction, and by using [$^2H_7$]-cholesterol it is possible to discriminate between these different types of reactions by estimating the ratio of [$^2H_0$]/[$^2H_7$], which was 1.62 ± 0.06% (mean ± standard deviation, n=3) (see Table 4.1). This ratio suggests that at least some of the 7α-hydroxycholesterol is formed endogenously.

Cholesta-4,6-dien-3-one derivatives gives a $[M]^+$ ion at *m/z* 516, and elutes just after desmosterol, but before cholesterol with RRT 0.97 (the retention time is 25.01 min) from the capillary C_{18} column. The corresponding deuterium-labelled cholesta-4,6-dien-3-one has a $[M]^+$ ion at *m/z* 523, and was identified based on MS^3 spectra and its retention time (see supplementary material, Figures S4.2a-c). Cholesta-4,6-dien-3-one is present in air-aged cholesterol as described by Smith [128,137,170] and Ansari [173,174].

Monohydroxycholesterols can be converted by hepatic and extrahepatic cytochrome P450 enzymes to dihydroxycholesterols, the oxidised/GP-derivatised versions of which give a $[M]^+$ ion which appears at *m/z* 550 [81]. In Figure 4.20 several distinct peaks are observed corresponding to dihydroxycholesterol isomers. The characterisation of novel dihydroxycholesterols in rat brain is described in chapter 5. The TICs were constructed for the MS^3 transitions 557→478→, 555→476→, and 556→477→ which correspond to deuterium-labelled dihydroxycholesterol. The chromatograms showed no peaks above the noise level, if they are present in the oxysterol fraction U2, and they are below the on-column limit of quantification of 0.8 pg (section 3.10, chapter 3). It should be noted that it was decided not to discriminate between 3-oxo-and 3β-ol-sterols in this experiment.

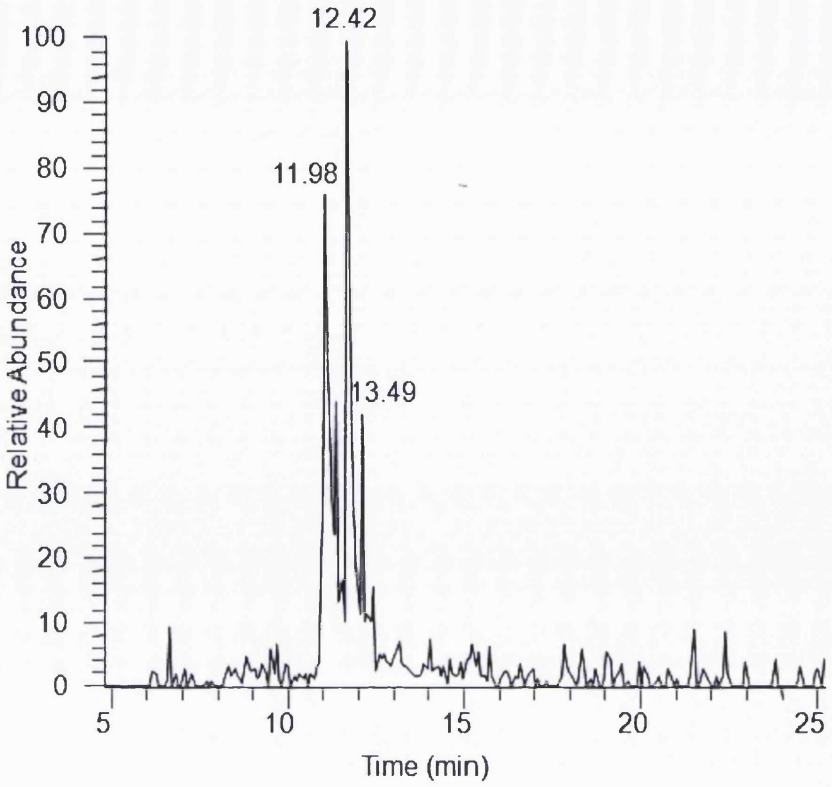

Figure 4.20 RIC for *m/z* 550.4 corresponding to the $[M]^+$ ion of oxidised/GP-derivatised dihydroxycholesterols in rat brain.

By using this approach, deuterium-labelled and unlabelled oxysterols in rat brain were identified and summarised in Table 4.1. A total of ten out of fourteen cholesterol oxidation products were identified in the oxysterol fraction U2 to contain deuterium by passing the spiked brain extract with $[^2H_7]$ cholesterol once through a Unisil SPE column, oxidation with cholesterol oxidase and derivatisation with GP reagent.

Table 4.1 Ratio of unlabelled oxysterol/sterol to its corresponding labelled analogue in the oxysterol fraction U2 obtained from rat brain (50 mg) sample spiked with [25,26,26,26,27,27,27-$^2H_7$] cholesterol (750 µg). The analytical scheme for oxysterols isolation and analysis is shown in Figure 2.3a.

Identified oxysterol	Mass of oxidised/GP-derivatised identified unlabelled sterol	Mass of its oxidised/GP-derivatised labelled sterol	[$^2H_0$] / [$^2H_7$] peak area ratios (±standard deviation, n=3)[b]
Cholesterol	518	525	1.45 ±0.07
7α-Hydroxycholesterol	534	541	1.62±0.06
7β-Hydroxycholesterol	534	541	0.81±0.05
7-Oxocholesterol	532	539	1.12±0.07
6-Hydroxycholest-4-ene-3-one	534	541	0.76±0.02
5,6-Epoxycholesterol	534	541	1.30±0.01
4β-Hydroxycholesterol	534	n/d	-
6-Oxocholestenone	532	539	0.97±0.01
Cholesta-4,6-dien-3-one	516	523	0.98±0.02
3β,5α,6β-Trihydroxylcholestane	534	541	0.67±0.01
24-Oxocholesterol	532	n/d	-
25-Hydroxycholesterol	534	540[a]	1.59 ±0.10
24S-Hydroxycholesterol	534	n/d	-
24S,25-Epoxycholesterol	550	n/d	-
24S,25-Epoxycholesterol	564	n/d	-
7α-Methoxycholesterol	566	573	0.81±0.03
3β-Hydroxy-5-oxo-5,6-*seco* cholestan-6-al	552	n/d	-
3β-Hydroxy-5-hydroxy-B-norcholestan-6-carboxaldehyde[a]	552	n/d	-

[a] Loss of one deuterium from C-25 is occurred during the air-oxidation of [$^2H_7$] cholesterol

[b] Mean ± standard deviation of triplicate assays (n=3)

n/d not detectable

Figure 2.3b (chapter 2) shows the analytical scheme for the isolation of oxysterols from rat brain and their analyses. After the addition of [$^2H_7$]-cholesterol to the brain sample, homogenisation, cholesterol was separated from oxysterols by a double passage of the brain extract through successive Unisil SPE columns. A second separation of cholesterol from oxysterols was performed on a fresh Unisil SPE column. Oxysterols were then oxidised, derivatised and analysed by cap-LC-MS. Nano-ES mass spectrum and a base peak chromatogram of an aliquot of the oxysterol fraction is shown in Figures 4.21a and 4.21b.

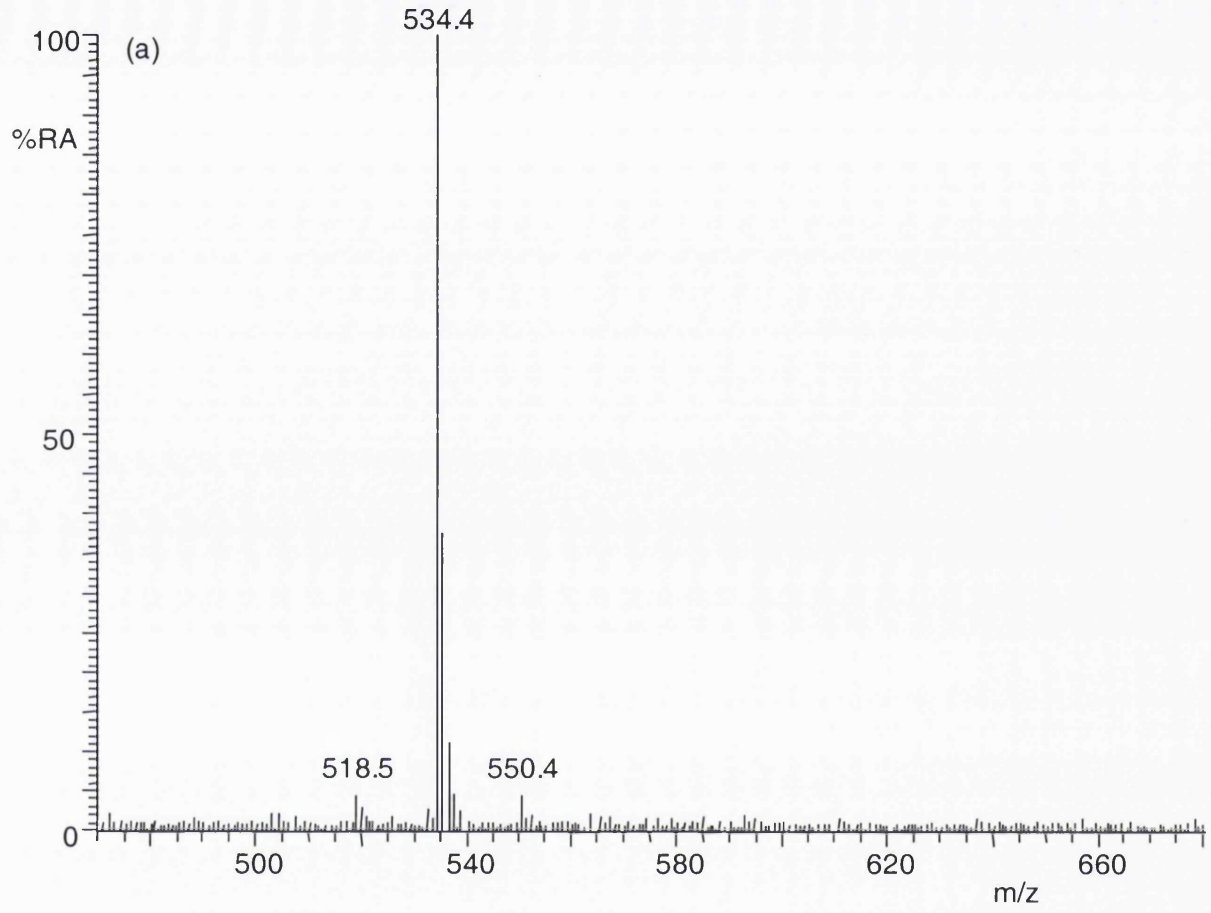

Figure 4.21 (a) Nano-ES mass spectrum of the oxysterol fraction U2. [$^2H_7$]-Cholesterol (750 µg) was added to rat brain (50 mg), and the sample was homogenised in ethanol. The brain extract was passed twice through Unisil SPE columns (for the analytical workflow see Figure 2.3b). The oxysterol fraction was then subjected to oxidation with cholesterol oxidase and derivatisation with GP hydrazine. The oxysterol fraction was directly infused into the LCQ^{duo} ion-trap mass spectrometer, as described in section 2.8.

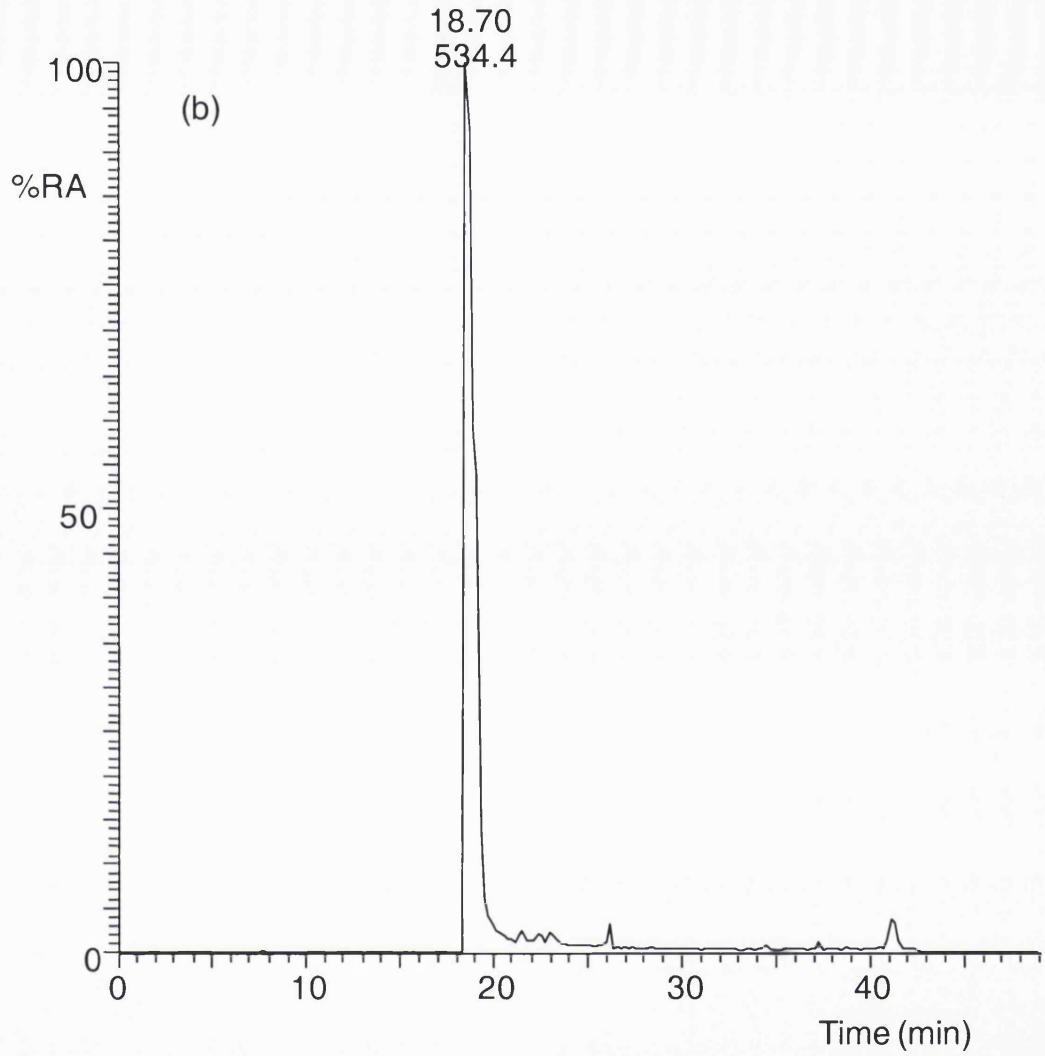

Figure 4.21 continued. (b) Base peak ion chromatogram of the oxidised/GP-derivatised oxysterol fraction. The oxysterol fraction was injected on the cap-LC-MS system, and the GP-derivatives were separated on a C_{18} capillary column (PepMap C_{18} column, 180 µm x 150 mm, 3 µm, 100 Å) and analysed by the LCQ^{duo} ion-trap mass spectrometer as described in section 2.9.

The major peak at retention time of 18.70 min was identified as 24S-hydroxycholesterol, and all others were of low abundance (RA<5%). RICs and TICs were constructed for cholesterol autoxidation products previously identified. Out of ten identified cholesterol autoxidation products in this study (Table 4.1), only four were identified (Table 4.2). Therefore, with the second passage of the spiked brain extract through the Unisil SPE column very little of the identified autoxidation products were observed. The difference is most probably due to the rapid and nearly complete separation of cholesterol from oxysterols.

Table 4.2 Ratio of unlabelled oxysterol to its corresponding labelled analogue in the oxysterol fraction U2 obtained from rat brain (50 mg) sample spiked with [25,26,26,26,27,27,27-$^2H_7$]-cholesterol (750 µg). The analytical scheme for oxysterols isolation and analysis is shown in Figure 2.3b.

Identified oxysterol	Mass of oxidised/GP-derivatised identified unlabelled oxysterol	Mass of its oxidised/GP-derivatised labelled oxysterol	[$^2H_0$] / [$^2H_7$] peak area ratios (± standard deviation, n=3)[b]
7α-Hydroxycholesterol	534	541	1.76±0.05
7β-Hydroxycholesterol	534	541	0.89±0.02
5,6-Epoxycholesterol	534	541	1.41±0.01
24-Oxocholesterol	532	n/d	-
25-Hydroxycholesterol	534	540[a]	1.69±0.11
24S-Hydroxycholesterol	534	n/d	-
24S,25-epoxycholesterol	550	n/d	-
24S,25-epoxycholesterol	564	n/d	-
3β-Hydroxy-5-oxo-5,6-*seco* cholestan-6-al	552	n/d	-
3β-Hydroxy-5-hydroxy-B-norcholestan-6-carboxaldehyde[a]	552	n/d	-

[a] Loss of one deuterium from C-25 is occurred during the air-oxidation of [$^2H_7$] cholesterol

[b] Mean ± standard deviation of triplicate assays (n=3)

n/d not detectable

4.4 Discussion

Oxysterols are found in cholesterol-rich tissues, and many of these compounds are present at very low levels (pg/g, ng/g and µg/g), against a high background of cholesterol (mg/g). Oxysterols are biologically active molecules. They act as ligands for the liver X receptor [122,142], the β form of which is expressed in the brain, and have also been proposed to interact (indirectly) with steroid regulatory element binding proteins (SREBP), transcription factors which regulate the expression of enzymes involved in cholesterol synthesis [121,139,140,161]. The present study focuses on enzymatically derived oxysterols, which have greater credibility as potential physiological regulators. Because of their biological role it is important to eliminate any oxysterols, which are formed due to cholesterol autoxidation during the sample preparation. However, one should also consider a possibility of oxysterols formation by non-enzymatic cholesterol oxidation *in vivo,* which still remains controversial, due to high cholesterol level in biological samples.

To prevent cholesterol autoxidation during the sample preparation, cholesterol was rapidly separated from oxysterols using Unisil SPE columns before derivatisation and detection. Addition of

deuterium-labelled cholesterol at the very beginning of the work-up procedure was performed to ensure the detection of cholesterol autoxidation products during the sample preparation. It was found that much of the autoxidation can be prevented by protecting samples from light, and by completing the extraction and oxidation/GP-derivatisation rapidly.

Ten cholesterol autoxidation products were unambiguously identified by passing the spiked rat brain extract once through the straight-phase Unisil SPE column (see Table 4.1). The identified cholesterol autoxidation products were formed in negligible amounts in comparison to 24S-hydroxycholesterol in rat brain (less than 4%). The most readily formed autoxidation products were 6-hydroxycholest-4-ene-3-one, cholestanetriol and cholesterol-5,6-epoxide, which have been shown to be physiologically irrelevant. It was also found that a double passage of the spiked brain extract through a Unisil SPE column results in nearly complete removal of cholesterol, and minimal cholesterol air-oxidation. Only four deuterium-labelled autoxidation products were identified (Table 4.2) and, of the four, two have previously been reported as the products of an enzymatic action, and cholesterol autoxidation, namely 7α- and 25-hydroxycholesterols. 7α-Hydroxycholesterol is a known product of the key enzyme in bile acid synthesis, cholesterol 7α-hydroxylase (CYP7A1) [36,124,129,151,159]. The side-chain oxysterol, 25-hydroxycholesterol, is a product of enzymatic reaction, and is formed by cholesterol 25-hydroxylase [35]. It is generally believed that 7β-hydroxycholesterol is predominantly of non-enzymatic origin [35,108-110,159,181].

It is interesting to compare the results obtained with those of other laboratories. To correct for cholesterol autoxidation during sample handling Kudo *et al.* [159] added highly purified [^{13}C] cholesterol to plasma before analysis to be able to quantify sterols formed by cholesterol autoxidation. When correcting for artifactually formed sterols, they concluded that cholesterol-5α,6α-epoxide, cholesterol-5β,6β-epoxide and cholestanetriol were formed during sample handling. Breuer and Björkhem [110] developed an ^{18}O inhalation technique, wherein rats were exposed to an $^{18}O_2$ atmosphere. Incorporation of ^{18}O into sterols in tissues indicated *in vivo* formation. With this

technique, enrichment of ^{18}O was found in 7α- and 7β-hydroxycholesterol, 7-ketocholesterol, 24-hydroxycholesterol, and 27-hydroxycholesterol. No labeling of 5α,6α-epoxy-cholesterol and cholestanetriol was demonstrated, and it is possible that these compounds are mainly of dietary origin or artifacts produced *in vitro.*

In conclusion, the methodology developed allows sensitive and specific analysis for the qualitative and quantitative profiling of oxysterols in rat brain. This involves an enrichment of oxysterols using straight-phase chromatography, specific oxidation and derivatisation, and separation of their derivatised form by reversed-phase liquid chromatography prior to mass spectrometry analysis, which allows structure characterisation.

Chapter 5

Oxysterols in the central nervous system: a targeted lipidomic study

5. *Introduction*

Oxysterols are found in the brain at low levels (ng/g to µg/g) against a high background of cholesterol (mg/g) [4]. As such their analysis can be challenging. To overcome these challenges it is advisable to perform specific group separation procedures prior to mass spectrometric analysis. Traditionally, these molecules have been analysed by gas chromatography (GC)-mass spectrometry (MS), however, the absence of molecular ions in GC-MS spectra, even from derivatised molecules, can make the discovery and identification of novel oxysterols difficult.

Our analytical methodology includes separation by straight-phase chromatography on a Unisil SPE column, where more hydrophobic sterols like cholesterol are separated from oxysterols. The next step of our analytical methodology is the incorporation of a Girard P-tag on the oxysterol analytes by oxidation/GP-derivatisation (Figure 3.1). The benefits of the oxidation/GP-derivatisation procedure are as follows:- (i) it is specific to compounds possessing a carbonyl group, or in oxysterols those oxidised to possess one, (ii) it directs the fragmentation of the resulting $[M]^+$ ion in the MS^2 event, predominantly giving $[M-79]^+$ and $[M-107]^+$ ions (loss of pyridine and pyridine plus CO, respectively), (iii) MS^3 can be performed on ions specifically formed from the GP-containing $[M]^+$ ion, and (iv) MS^3 spectra contain specific information on the structure of analyte. The last step of the analytical methodology is performed to allow the analysis of individual Girard-P tagged sterol analytes by separation of a mixture of GP-tagged sterols on reversed-phase capillary LC column and MS^n analysis. Low-flow-rate liquid chromatography (LC) combined with nano-electrospray ionisation was employed to provide maximum sensitivity of GP-tagged oxysterol analyte in the eluting peak.

The objective of this study was to apply the analytical methodology described earlier to profile the oxysterol content of rat brain, three regions of embryonic (E11) mouse central nervous system, and primary cortical neurons derived from embryonic rat brain.

5.1 Oxysterols in rat brain

Cholesterol in brain is biosynthesised *de novo* throughout life [33,182]. A significant amount of the cholesterol in brain goes to make up the myelin sheaths coating axons, and as such is turned over at a very slow rate (half life of brain cholesterol in adult rats 2 – 4 months) [19,183]. Cholesterol cannot cross the blood-brain-barrier, and in order to maintain cholesterol balance in the brain, cholesterol can be converted to 24S-hydroxycholesterol. Therefore, 24S-hydroxycholesterol is regarded as a transport form of cholesterol, that can diffuse the BBB [19,37,179,180]. In mouse, rat, and probably in human, metabolism of cholesterol to 24S-hydroxycholesterol accounts for about 60% of cholesterol turnover [19,150]. It is not clear whether this is the only mechanism by which cholesterol is turned over in the brain. In the brain, 24S-hydroxycholesterol is biosynthesised by the action of CYP46A1, normally expressed only in neurons, on preformed cholesterol [180]. In addition to being transport forms of cholesterol, oxysterols have biological activity [35,151]. They have been identified *in vitro* as ligands for the LXRs [142,184] and they are involved in the posttranslational control of sterol regulatory element-binding proteins (SREBPs) which are themselves transcription factors for genes involved in cholesterol and fatty acid synthesis [139,144].

The aim of this section of the work was to profile oxysterol content in rat brain and to evaluate the analytical method described in chapters 3 and 4. The analytical scheme used for oxysterol isolation from rat brain and analysis is shown in Figure 2.4 (Section 2.16). The experimental method involves homogenisation, and extraction of oxysterols from brain tissue with ethanol. Ethanol is a good solvent for oxysterols and readily penetrates cell membrane. Cholesterol was separated from oxysterols immediately after extraction by straight-phase chromatography on a Unisil SPE column, where cholesterol and more hydrophobic sterols elute with hexane-dichloromethane (Fraction U1, or "cholesterol fraction", U1A), while oxysterols elute in ethyl acetate (Fraction U2, or "oxysterol fraction", U2A,B,C).

The oxidised/GP-derivatised oxysterol fractions U2C and U2A of rat brain (Figure 2.4)

The resulting oxysterol fractions were then oxidised with cholesterol oxidase, and derivatised with Girard P reagent. The oxidation reaction is only applicable to substrates with a 3β-hydroxy-5-ene or 3β-hydroxy-5α-hydrogen function, and this reaction gives quantitative conversion of 3β-hydroxy-5-ene oxysterols to their 3-oxo-4-ene analoques. Similarly, derivatisation reaction conditions have been used so as to give quantitative conversion of 3-oxo-4-ene oxysterols/sterols to their GP derivatives. Finally, the products of the derivatisation reaction were separated from unreacted starting material by SPE on a reversed phase column. Derivatised sterols/oxysterols were eluted from the SPE C_{18} column with methanol (2 x 1 mL, SPE-Fr1, Fr2), and with methanol-chloroform (1 x 1 mL, SPE-Fr3) as described in section 2.6.

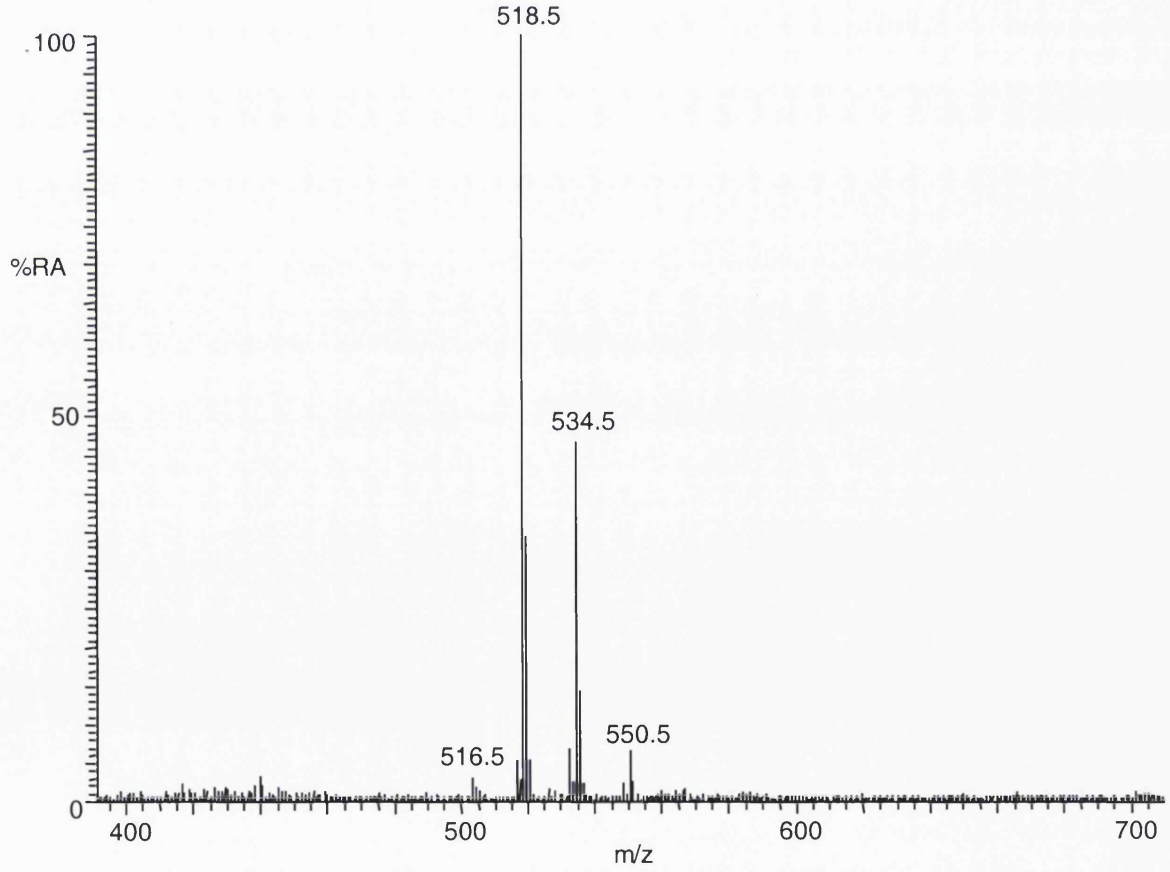

Figure 5.1 Nano-ES mass spectrum of the oxidised/GP-derivatised oxysterol fraction U2C of rat brain.

Sterol analysis was performed by nano-ES-MS^n and capillary-LC-ES-MS^n utilising an LCQ^{duo} ion-trap mass spectrometer fitted with a nano-ES source. An initial investigation was performed by nano-ES-MS^n using the LCQ^{duo} ion-trap mass spectrometer to evaluate the oxysterol content of fractions (section 2.8). Upon nano-ES conditions GP-tagged oxysterols give maximum signal out of all other possibly present lipids. Figure 5.1 shows the nano-ES mass spectrum of the oxidised/GP-derivatised U2C fraction. The nano-ES mass spectrum was recorded from the equivalent of ~40 μg of brain loaded on the glass capillary tip. Peaks at *m/z* 534 (RA 45 %), 550 (RA 7%) and 518 (RA 100%) were observed in the ES spectrum, which correspond to the *m/z* of the $[M]^+$ ion of the oxidised/GP-derivatised monohydroxycholesterol (*m/z* 534), dihydroxycholesterol (*m/z* 550), and cholesterol (*m/z* 518). The peak at *m/z* 534 is 45% of the abundance of that at *m/z* 518, indicating that by a single passage of the brain extract through a Unisil SPE column (U2C fraction), a significant amount of cholesterol was removed, but not all.

Table 5.1 Oxysterols present in the oxidised/GP-derivatised oxysterol fraction U2C of rat brain

Sterol before oxidation/derivatisation	Precursor-ion mass	RA, %	Neutral loss of 79 and 107 Da in MS^2 spectrum	Characteristic sterol MS^3 spectrum
Cholesterol	518.4	100	√	√
Dihydroxycholesterol	550.4	8	√	√
Oxohydroxycholesterol	548.4	3	√	√
Monohydroxycholesterol	534.4	45	√	√
Oxocholesterol	532.4	5	√	√
Cholestadienes	516.4	5	√	√

Table 5.1 summarises the peaks and their relative abundances. MS^2 of these ions generate the neutral losses of 79 Da and 107 Da from $[M]^+$ ion, corresponding to $[M-79]^+$ and $[M-107]^+$ ions, which are indicative of a GP hydrazone. However, maximum structural information is obtained by fragmenting the $[M-79]^+$ or $[M-107]^+$ in MS^3 experiments (chapter 3). In MS^3 (534→455→) spectra fragment ions at *m/z* 151 ($*b_1$-12), 163 ($*b_2$) and 177 ($*b_3$-C_2H_4) are present, which are characteristic of derivatised 3-oxo-4-ene sterols. For example, the MS^2 ($[M]^+$→) and MS^3 ($[M]^+$→$[M-79]^+$→) spectra on the ion at *m/z* 534 were similar but not identical to that from the oxidised/GP-derivatised

authentic 24S-hydroxycholesterol (Figure 5.2a and 5.2b). By recording MS^2 ($[M]^+\rightarrow$) and MS^3 ($[M]^+\rightarrow[M-79]^+\rightarrow$ or $[M-107]^+\rightarrow$) spectra on the ion of *m/z* 550, it was confirmed that some components at this *m/z* are oxidised/GP-derivatised dihydroxycholesterols (Figure 5.2c and 5.2d). It is however possible those isobaric ions are being subjected to MS^n experiments. The final identification of the oxidised/GP-derivatised hydroxycholesterols is carried out by comparison of their chromatographic relative retention time (RRT) with that of authentic standards. In summary, although direct infusion ES-MS can, in principle, be used for sterol profiling analysis, it cannot be used when oxidised/GP-derivatised sterols need to be definitively identified, due to its inability to distinguish mixtures of structural isomers.

The oxidised/GP-derivatised U2C fraction was subsequently analysed by cap-LC-MS^n. In an initial cap-LC-MS run, the instrument was used to record mass spectra (MS). RICs were plotted for all potential oxysterols/sterols. In a second cap-LC-MS run, the MS^2 transition ($[M]^+\rightarrow$) and MS^3 transition ($[M]^+\rightarrow[M-79]^+\rightarrow$ and $[M-107]^+\rightarrow$) for all potential oxidised/GP-derivatised sterols/oxysterols were programmed for cap-LC-MS^n analysis, suggested to be present from the initial cap-LC-MS run, and direct infusion nano-ES analysis. Figure 5.3a shows base peak chromatogram of the oxysterol U2C fraction, and RICs of oxidised/GP-derivatised sterols and oxysterols. For example shown in Figure 5.3b-f shows the RIC for *m/z* 518, 516, 532, 534 and 550 corresponding to oxidised/GP-derivatised cholesterol, cholestadienes, oxocholesterols, monohydroxycholesterols and dihydroxycholesterols present in rat brain.

The RIC for *m/z* 518 corresponding to the $[M]^+$ ion of oxidised/GP-derivatised cholesterol revealed a chromatographic peak at 25.83 min (Figure 5.3b). This ion gave a $[M-79]^+$ fragment-ion in its MS^2 ($[M]^+\rightarrow$) spectrum, and an MS^3 ($[M]^+\rightarrow[M-79]^+\rightarrow$) spectrum compatible with that expected for the oxidised/GP-derivatised cholesterol.

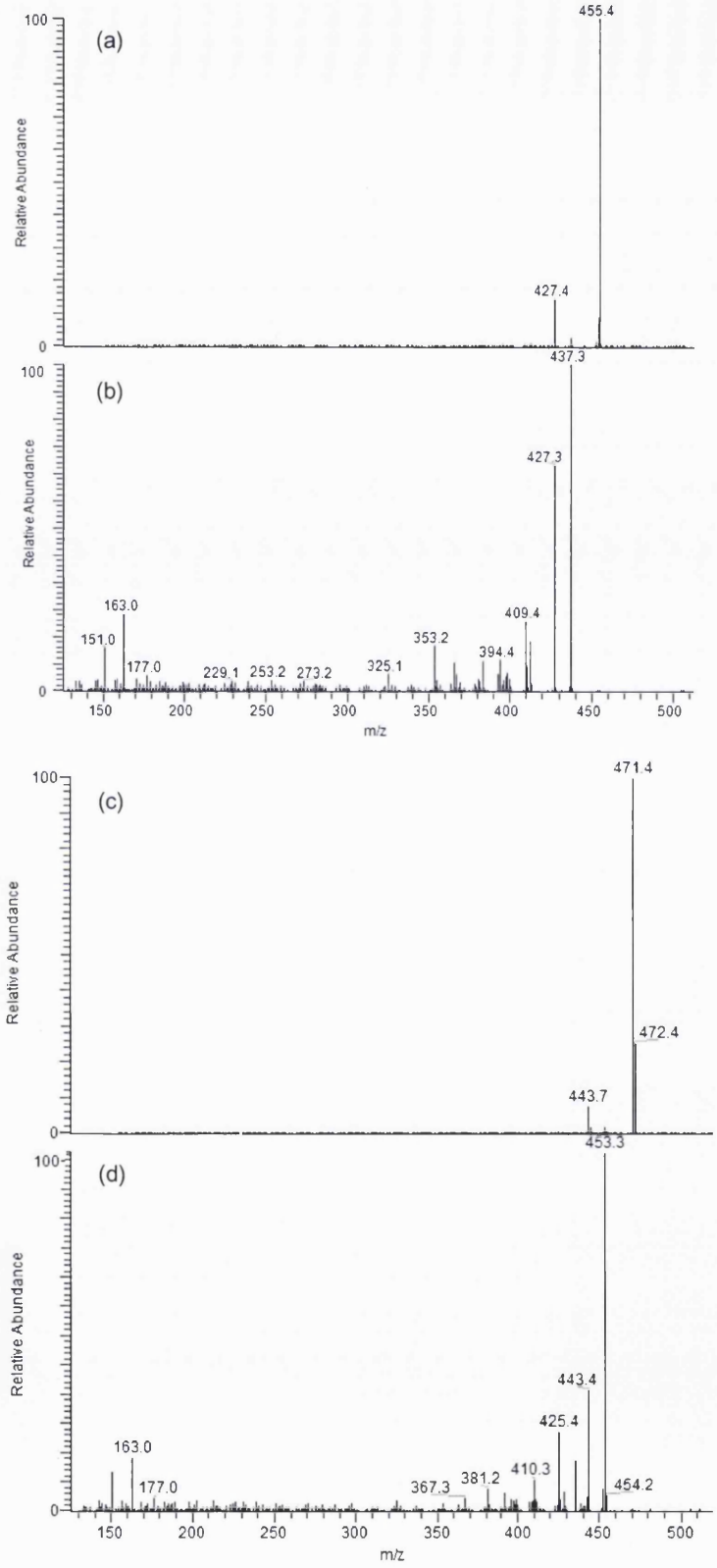

Figure 5.2 MS^2 ($[M]^+ \rightarrow$) and MS^3 ($[M]^+ \rightarrow [M-79]^+ \rightarrow$) spectra of oxidised/GP-derivatised oxysterols in the oxysterol fraction U2C of rat brain. (a) 534→ and (b) 534→455→ corresponding to monohydroxycholesterols; (c) 550→ and (d) 550→471→ corresponding to dihydroxycholesterols.

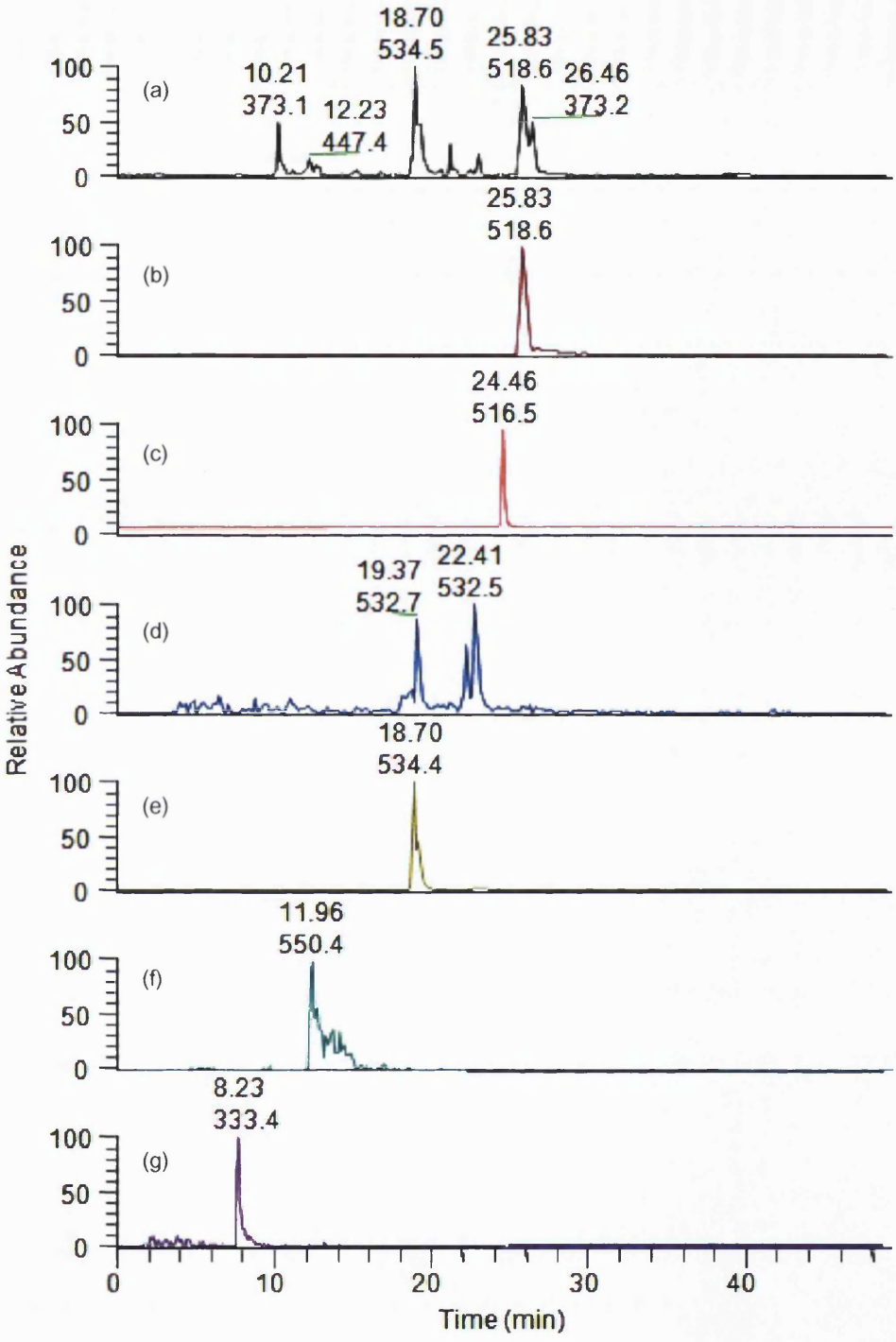

Figure 5.3 (a) Base peak chromatogram of the oxysterol U2C fraction from rat brain. RICs for oxidised/GP-derivatised sterols/oxysterols from the oxysterol U2C fraction of rat brain for *m/z* (b) 518, (c) 516, (d) 532, (e) 534, (f) 550, and (g) 333. Chromatographic conditions are described in the experimental section 2.19. The rat brain (40 µg) was injected on a C_{18} capillary column. Shown in Figure 5.4 are MS and MS^3 spectra of desmosterol identified in rat brain and MS^3 spectrum of the corresponding authentic sample. For the identification of chromatographic peaks see also Table 5.3.

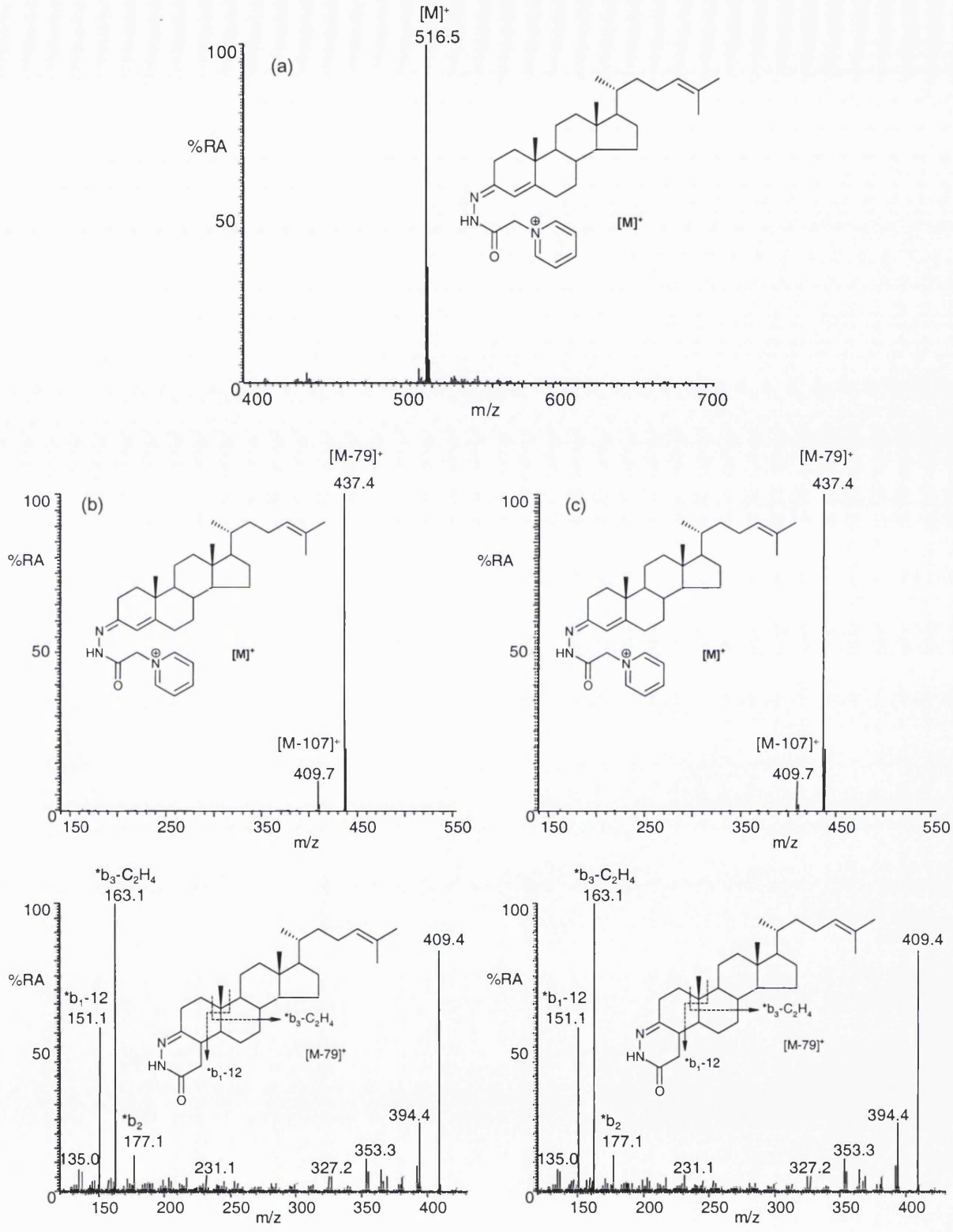

Figure 5.4 (a) MS spectrum of the chromatographic peak eluting at 24.46 min. (b) MS^2 (516→, upper panel) and MS^3 (516→437→, lower panel) spectra of the oxidised/GP-derivatised cholestadiene eluting at 24.46 min, and (c) the MS^2 (516→, upper panel) and MS^3 (516→437→, lower panel) spectra of the oxidised/GP-derivatised authentic desmosterol.

The RIC for the $[M]^+$ ion of *m/z* 516 revealed one chromatographic peak at 24.46 min (Figure 5.3c) with a RRT of 0.94, which was identical to the oxidised/GP-derivatised desmosterol. Figure 5.4a shows a MS spectrum for the retention time of 24.46 min with a base peak at *m/z* 516 corresponding to the $[M]^+$ ion of the oxidised/GP derivatised desmosterol. Its MS^2 (516→) and MS^3 (516→437→) spectra were identical to that of oxidised/GP-derivatised desmosterol (Figure 5.4b,c).

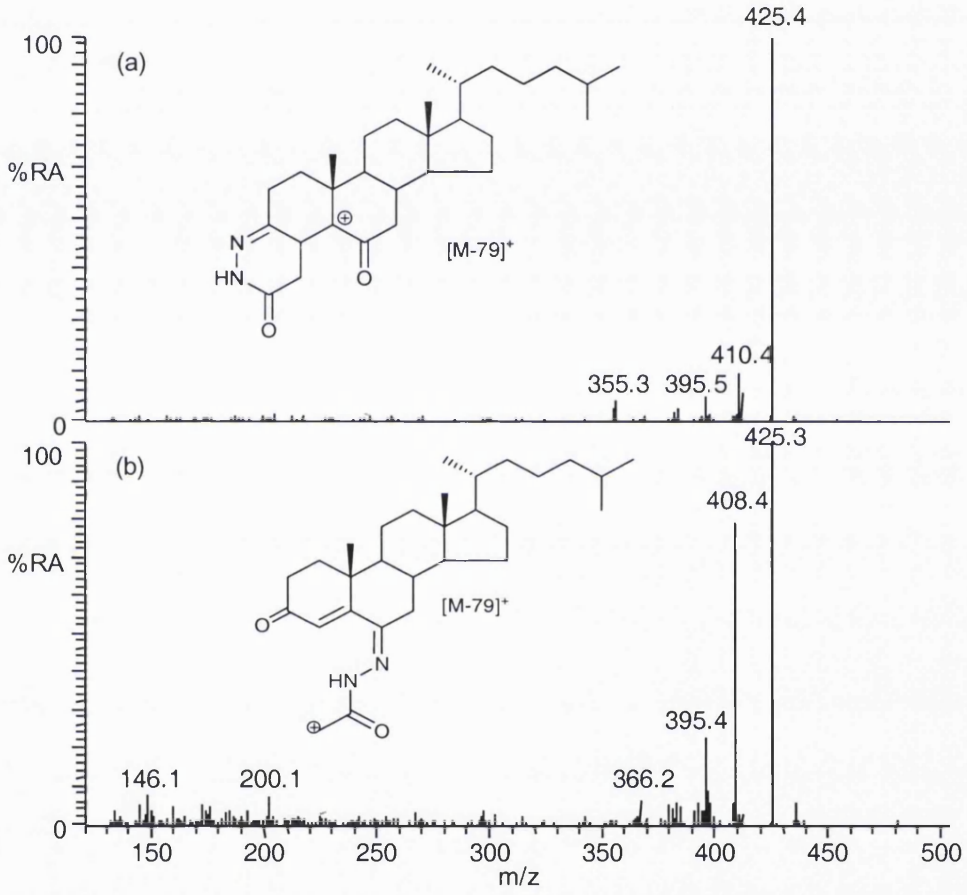

Figure 5.5 MS^3 (532→453→) spectra of the GP-derivatised cholest-4-ene-3,6-dione eluting at (a) 21.96 min, and (b) 22.41 min. These spectra are consistent with those of GP-derivatised authentic cholest-4-ene-3,6-dione.

24-Oxocholesterol with an extra hydroxyl group in the steroid nucleus, which is presumably formed via 24-oxocholesterol, has been previously identified [22], the oxidised/GP-derivatised version of which gives a $[M]^+$ ion which appears at *m/z* 548, while oxidised/GP-derivatised 24-oxocholesterol gives an $[M]^+$ ion at 532. In the RIC of this *m/z* three chromatographic peaks were observed at 19.37, 21.96 and 22.41 min (Figure 5.3d). The chromatographic peak at 19.37 min

gave MS^2 and MS^3 spectra identical to those of authentic oxidised/GP-derivatised 24-oxocholesterol. Comparison of retention time with the authentic standards revealed that the two peaks in Figure 5.3d correspond to the RRTs of GP-derivatised cholest-4-ene-3,6-dione. As discussed in section 3.9, cholest-4-ene-3,6-dione when GP derivatised and separated on the capillary C_{18} column gives two isomeric mono-GP hydrazones ($[M]^+$ ion, *m/z* 532, RRTs 0.85 and 0.87), and also a doubly charged *bis*-GP hydrazone ($[M]^{2+}$, *m/z* 333, RRT 0.31) (see Figure 3.41). Figure 5.5a,b shows MS^3 (532→453→) spectra corresponding to the chromatographic peaks of 21.96 and 22.41 min and these spectra are identical to the GP-derivatised cholest-4-ene-3,6-dione (Figure 3.42). The RIC of *m/z* 333 revealed one chromatographic peak at 8.23 min (Figure 5.3g), and its RRT of 0.31 and MS^2 spectrum was identical to the GP-derivatised authentic cholest-4-ene-3,6-dione.

The RIC for the $[M]^+$ ion of *m/z* 534 revealed two unresolved chromatographic peaks at 18.70 min and 19.14 min in the region between 17-21 min (Figure 5.6a). A MS spectrum for the chromatographic peak at 18.70 min is shown in Figure 5.6b. MS^2 (534→) spectra for the two peaks showed similar fragment ions at *m/z* 427 ($[M-107]^+$), 437 ($[M-79-H_2O]^+$) and *m/z* 455 ($[M-79]^+$), but in different abundance ratios (see Figure 5.6c,d). The MS^2 534→ for the chromatographic peak at 19.14 min shows a fragment ion at *m/z* 437 ($[M-79-H_2O]^+$, RA 15%), and RA of this fragment ion indicates that the hydroxyl-group is located on tertiary C-25 (see Figure 5.6d). The chromatographic peak eluting at 18.70 min corresponds to 24S-hydroxycholesterol, and the MS^3 (534→455→ and 534→427→) spectra indicate a monohydroxy derivative of a 3-oxo-4-ene sterol. In the MS^3 spectrum (Figure 5.6e) the pattern of fragment ions at *m/z* 151, 163, and 177 confirms the 3-oxo-4-ene sterol. The location of the hydroxyl group on C-24 is indicated by the MS^3 (534→455→) fragment ion at *m/z* 353 (side chain fragment '*f, RA 25%), and the MS^3 (534→427→) fragment ion at *m/z* 325 (side chain fragment '#f, RA 16%).

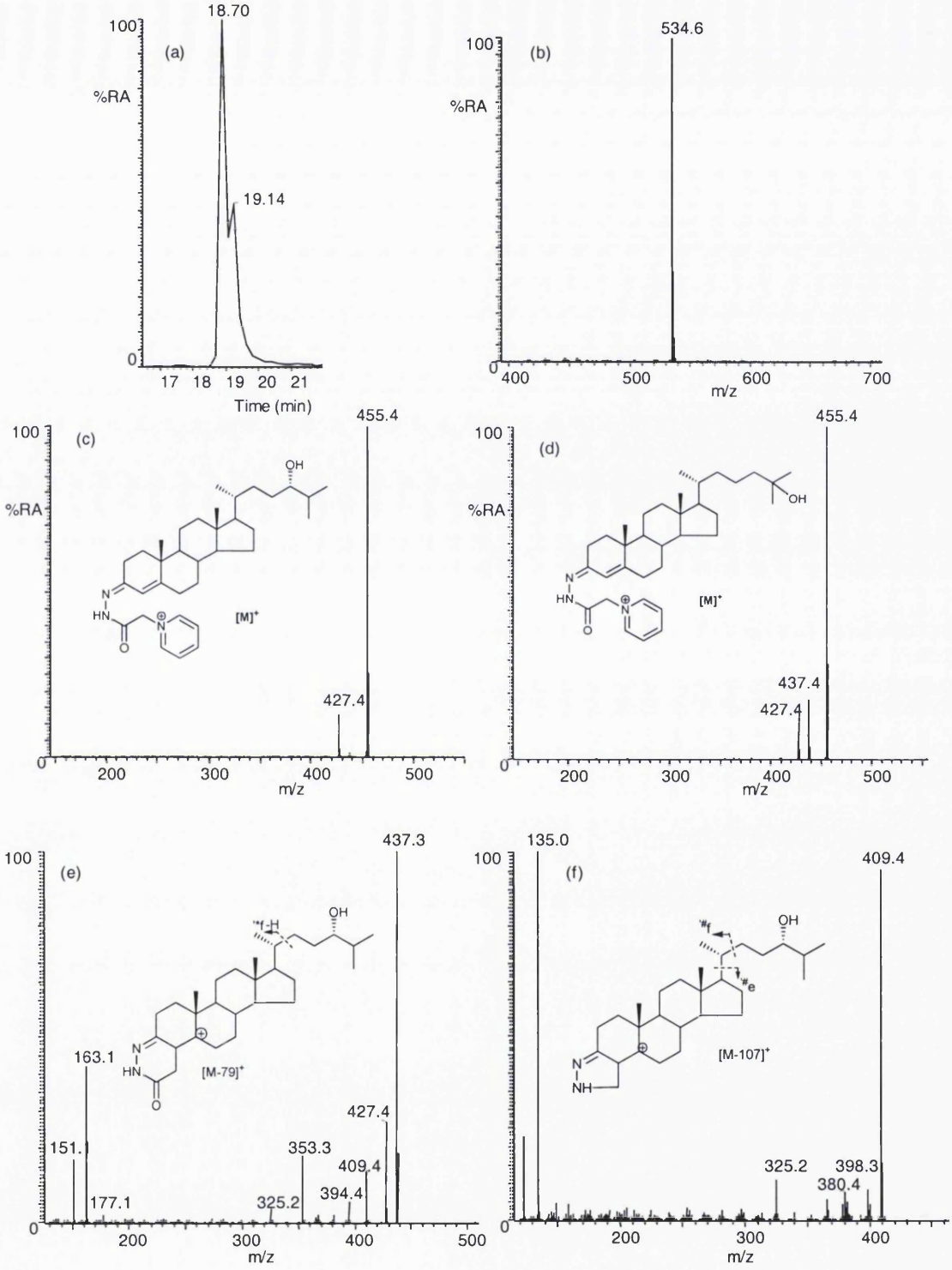

Figure 5.6 (a) RIC for *m/z* 534 in rat brain for the chromatographic region from 17–21 min. (b) MS spectrum of the chromatographic peak at 18.70 min. MS^2 (534→) spectra of the oxidised/GP-derivatised monohydroxycholesterols eluting at (c) 18.70 min, and (d) 19.14 min, (e) MS^3 (534→455→), and (f) MS^3 (534→427→) spectra of the oxidised/GP-derivatised monohydroxycholesterols eluting at 18.70 min. These spectra are consistent with those of oxidised/GP-derivatised (d) 25-hydroxycholesterol, (c,e,f) 24S-hydroxycholesterol, respectively.

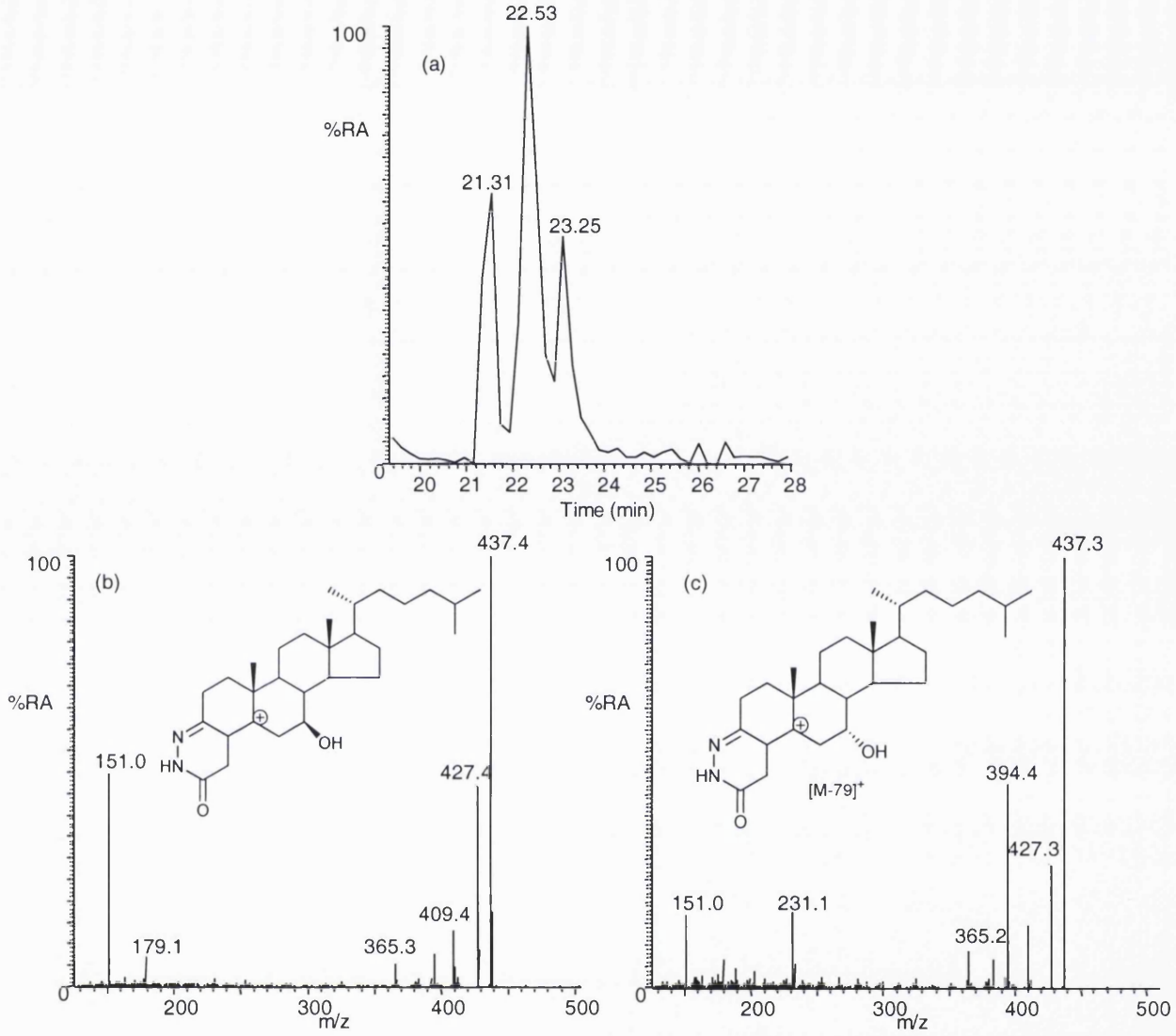

Figure 5.7 (a) RIC for *m/z* 534 in rat brain for the chromatographic region from 20-28 min. MS^3 (534→455→) spectra of the oxidised/GP-derivatised monohydroxycholesterols eluting at (b) 21.31 min, and (c) 22.53 min. These spectra are consistent with those of oxidised/GP-derivatised (b) 7β-hydroxycholesterol, and (c) 7α-hydroxycholesterol, respectively.

Figure 5.7 shows the RICs for *m/z* 534 for the chromatographic region between 21-28 min, and reveals three resolved chromatographic peaks. The chromatographic peaks at 21.31, 22.53 min eluted at a similar retention time to that of the 7β- and 7α-hydroxycholesterols authentic standards, and gave a characteristic pattern of 7-hydroxycholesterols in its MS^3 (534→455→ and 534→427→) spectra. The MS^3 (534→455→) spectrum shows an abundant ion at *m/z* 151 (RA 50% for 7β-hydroxycholesterol, Figure 5.7b; and RA 15% for 7α-hydroxycholesterol, Figure 5.7c; $*b_1$-12)

which dominates the *b_1-12, *b_2, *b_3-C_2H_4 triad. The chromatographic peak eluting at 23.25 min gave MS^2 and MS^3 spectra similar to that eluting at 22.53 min, and it is concluded that these are *syn* and *anti* isomers of the GP derivative of 7α-hydroxycholesterol.

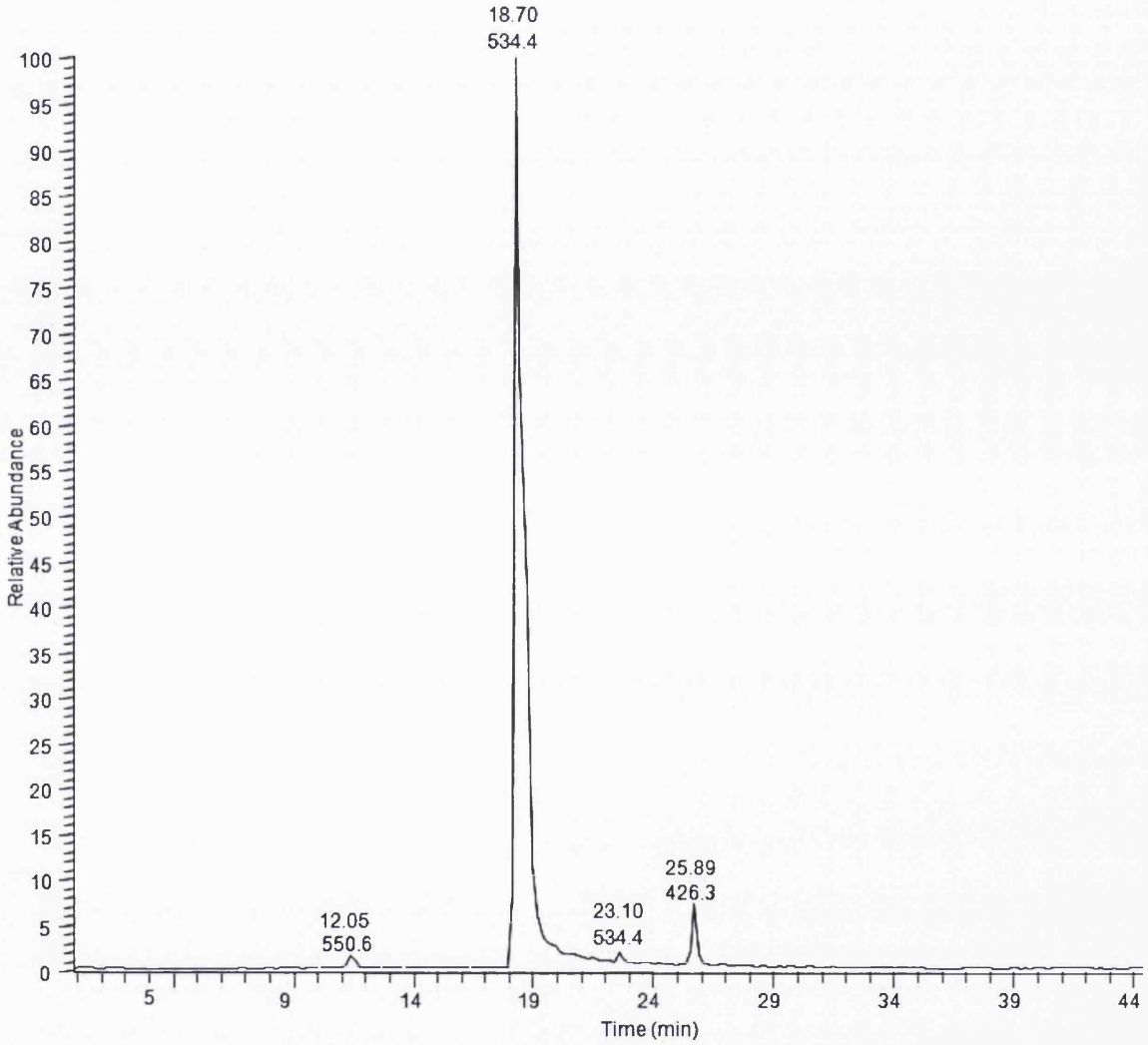

Figure 5.8 Base peak chromatogram of the oxysterol fraction U2A obtained as described in Figure 2.4. Chromatographic conditions are described in the experimental section.

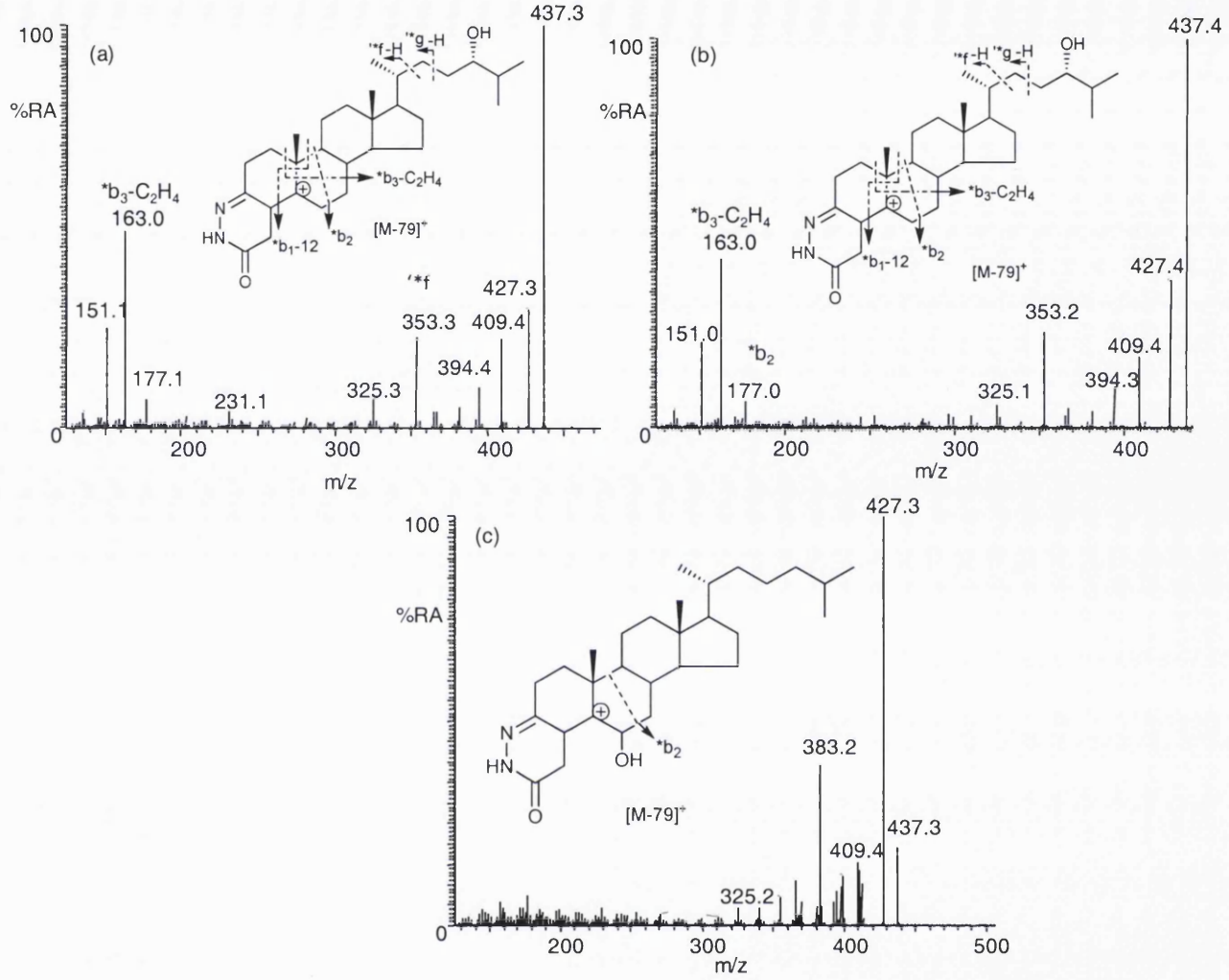

Figure 5.9 MS^3 (534→455→) spectra of (a) the oxidised/GP-derivatised monohydroxycholeterol eluting at 18.70 min (refer to Figure 5.8), (b) the authentic standard of oxidised/GP-derivatised 24S-hydroxycholesterol, (c) the oxidised/GP-derivatised monohydroxycholeterol eluting at 23.10 min identified as the oxidised/GP-derivatised 6-hydroxycholest-4-ene-3-one.

Passing the brain extract twice through successive Unisil SPE columns effectively removes all the cholesterol and desmosterol from the final oxysterol U2A fraction. The RA of cholesterol and desmosterol in these samples amount to <2% and <0.1% of the major oxysterol in the fraction (Figure 5.8). The sterol in the oxysterol fraction U2A eluting at 18.70 min with RRT of 0.72 has an *m/z* 534 (RA 100%), which is identical to that of oxidised/GP-derivatised 24S-hydroxycholesterol (see Figure 3.38 for a comparison of RRT with the authentic 24S-hydroxycholesterol). Both MS^2

and MS^3 spectra are identical to those from the authentic compound (see Figures 5.9a and 5.9b for a comparison with the authentic standard), thereby confirming identity of 24S-hydroxycholesterol.

This project was not only concerned with the profiling of oxysterols in brain tissue, but also with the determination of their semi-quantitative levels. The level of 24S-hydroxycholesterol was determined with the use of an internal standard. 22R-Hydroxycholesterol was selected as the internal standard because it was not identified by the current methodology in rat brain. Rat brain (54 mg) was added to 22R-hydroxycholesterol (2.0 μg), sterols were extracted, and enriched using straight-phase chromatography, oxidised and derivatised specifically, and separated in their derivatised form by reversed-phase liquid chromatography prior to mass spectrometry analysis (section 2.19). The oxidised/GP-derivatised sterols were eluted from the analytical column, and ES-MS, -MS^2 and -MS^3 spectra recorded. With the use of the internal standard for quantification losses are accounted for and corrected automatically. A control experiment was performed in parallel, where only 50 mg of rat brain was subjected to the entire sample preparation procedure and analysis by capillary LC-MS^n. The MS^3 transitions 534→455→ and 534→427→ were monitored for the identification of monohydroxycholesterols, 24S-hydroxycholesterol was the most abundant oxysterol present in the fraction U2A, and 22R-hydroxycholesterol was not detected in the control. The MS^2 534→ transition was monitored for the quantification of 24S-hydroxycholesterol. Therefore, the MS^2 transition 534→455 could be generated for the determination of relative abundance of monohydroxycholesterols in rat brain; also other MS^2 transitions for identified oxysterols were used in this work. Figure 5.10 shows a RIC generated for the MS^2 transition 534→455 for the chromatographic region from 14 to 23 min of fraction U2A derived from the rat brain sample with added internal standard (see section 2.15, Figure 2.3a). As discussed in section 4.1, the oxidised/GP-derivatised 22R-hydroxycholesterol elutes from the capillary C_{18} column as twin peaks, which arise on account of the formation of *syn* and *anti* derivatives. With the use of the internal

standard the level of 24S-hydroxycholesterol was found to be 20.3 ± 3.4 µg/g of brain (mean ± standard deviation, n=3), in good agreement with values for other mammals [23,185].

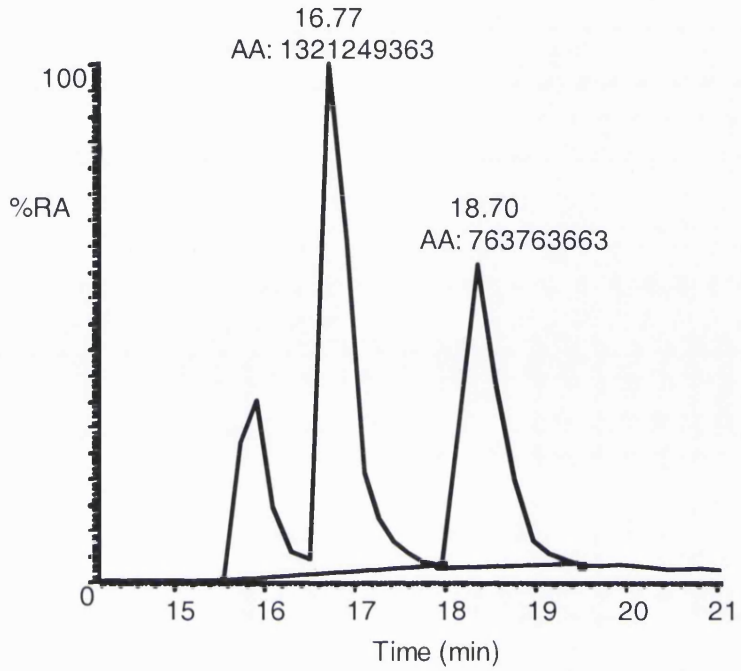

Figure 5.10 RIC for the MS^2 transition 534→455 corresponding to the oxidised/GP-derivatised monohydroxycholesterol from rat brain. Rat brain (54 mg) was spiked with 22R-hydroxycholesterol (2.0 µg), and the sample was homogenised in ethanol. Cholesterol was separated from oxysterols by a double passage of the brain extract through Unisil SPE columns. The experiment was performed in triplicate. Oxysterols were oxidised with cholesterol oxidase, derivatised with GP reagent, then separated in their derivatised form by reversed-phase liquid chromatography, and eluent was directed to the nano-ES source of a LCQ^{duo} mass spectrometer, and MS spectra was acquired. For details of experiments refer to sections 2.9 and 2.18.

Because the data are semi-quantitative in that once derivatised to the GP hydrazone, sterols give an approximately equal response upon ES. Therefore, it is possible to determine the approximate relative abundance of other identified oxysterols in rat brain. Quantitative estimates of the identified sterols/oxysterols in fractions U2C and U2A were made by estimation of their relative abundances in comparison to the relative abundance of the oxidised/GP-derivatised 24S-hydroxycholesterol, and assuming 100% recovery of oxysterols in these fractions.

The hydroxylated version of oxocholesterol has an *m/z* of 548, and gave a peak (RA <0.5%) that eluted from the capillary column with a retention time of 15.92 min and gave MS^2 and MS^3 spectra compatible with those of an oxidised/GP-derivatised oxohydroxycholesterol (Figure 5.11).

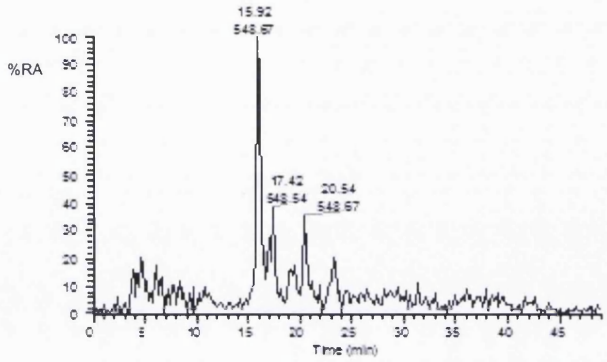

Figure 5.11 RIC for *m/z* 548 corresponding to the $[M]^+$ ion of the oxidised/GP-derivatised oxysterol from the oxysterol U2A fraction of rat brain. Chromatographic conditions are described in the experimental section 2.9.

Evidence from experiments with recombinant CYP46A1 and HEC293 cells transfected with CYP46A1, suggest that this enzyme can further metabolise 24S-hydroxycholesterol to 24,25- and 24,27-dihydroxycholesterols [22,68]. Additional products of the incubation of 24S-hydroxycholesterol with CYP46A1-transfected HEC 293 cells were partially characterised as 24,X-dihydroxycholesterol, 24,25,X-trihydroxycholesterol, and 24,27,X-trihydroxycholesterol, where the hydroxyl group as signified by X is in the steroid nucleus [22,68].

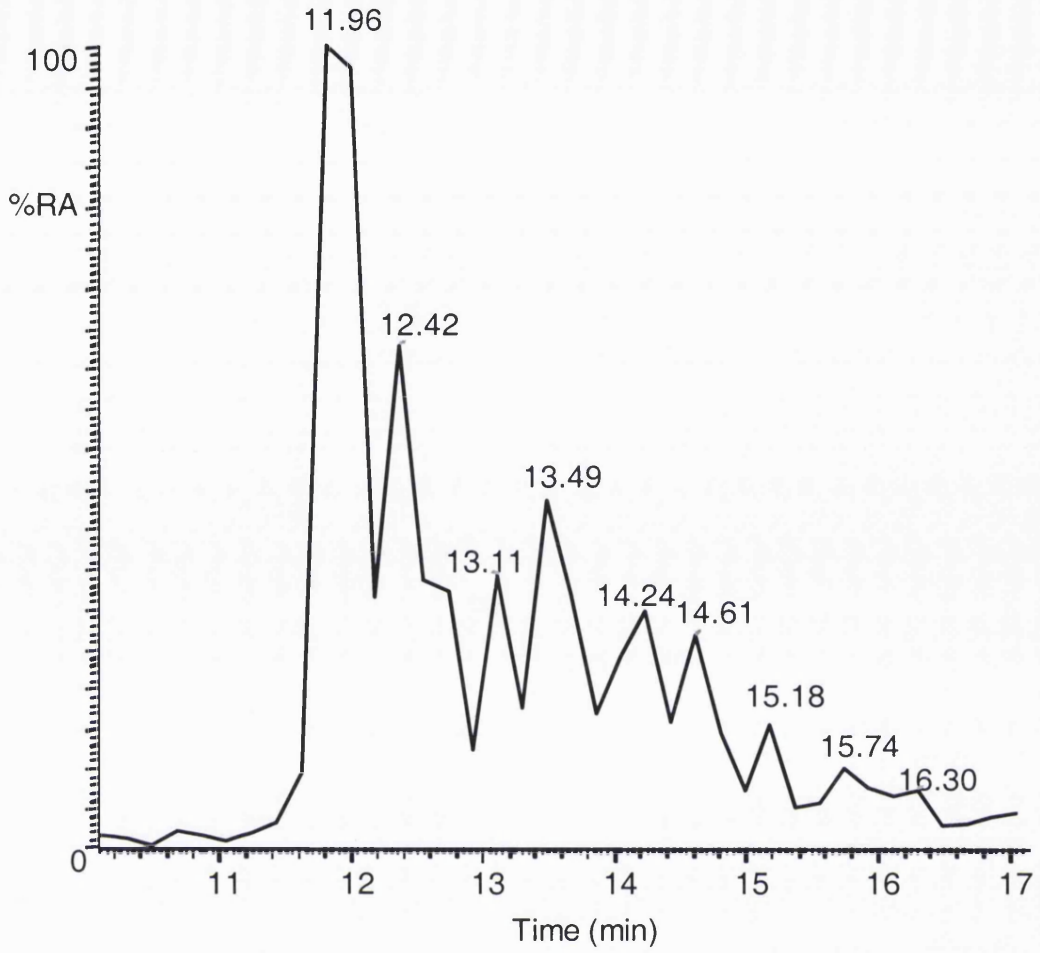

Figure 5.12 RIC for *m/z* 550 corresponding to oxidised/GP-derivatised dihydroxycholesterols extracted from rat brain. The oxysterol fraction U2A was prepared according to Figure 2.4. Chromatographic conditions are described in the experimental section 2.9.

Following oxidation/GP-derivatisation dihydroxycholesterols give a molecular ion, $[M]^+$, at *m/z* 550. Figure 5.12 shows the RIC generated for 550, as can be seen, seven distinct peaks are observed, and compared with that of 24S-hydroxycholesterol, are all of low abundance (RA<1%). The MS^2 (550→) and MS^3 (550→471→) spectra of the first eluting component at 11.96 min indicate a dihydroxy derivative of a 3-oxo-4-ene sterol. Figure 5.13a shows the MS^3 (550→471→) spectrum of the chromatographic peak eluting at 11.96 min. In the MS^3 spectrum the pattern of fragment ions at *m/z* 151(*b_1-12), 163(*b_3-C_2H_4) and 177(*b_2), confirms the 3-oxo-4-ene structure (derived from cholesterol oxidase treatment of the 3β-hydroxy-5-ene sterol). The presence of the significant fragment ion at *m/z* 353 ('*f) and *m/z* 367 ('*g) defines the location of one hydroxyl group at C-24

with the second necessarily on C-25 or C-27 (see example of the oxidised/GP-derivatised 24S-hydroxycholesterol in Figure 5.9a). In MS^2 and MS^3 spectra, the ratio of $[M-79-H_2O]^+$, $[M-107]^+$, $[M-79-2xH_2O]^+$, $[M-107-H_2O]^+$ (*m/z* 453, 443, 435, 425) fragment ions is 1.5:10:0.5:<0.5, and 10: 2.8: 1.5: 2.2, respectively. This shows the stability of the second group. Therefore, the second hydroxyl group is probably located to C-27, giving 24,27-dihydroxycholesterol.

The chromatographic peak eluting at 12.42 min from the capillary column also gave MS^2 and MS^3 spectra compatible with an oxidised/GP-derivatised dihydroxycholesterol, where one of the additional hydroxyl groups is on C-24 and the second on C-25 or C-27. A characteristic of MS^3 spectra of oxidised/GP-derivatised oxysterols with a 25-hydroxyl group is that the $[M-79-H_2O]^+$ ion (*m/z* 453) dominates the spectrum and all other fragment ions are of low relative abundances. Figure 5.13b shows the MS^3 spectrum of the chromatographic peak eluting at 12.42 min, the fragment ions at *m/z* 151($^*b_1$-12), 163($^*b_3$-C_2H_4) and 177($^*b_2$), and 353 ("f) are of lower abundances than in the spectrum of the 24,27-dihydroxy isomer, but the presence of a "h (*m/z* 381) suggests the location of the second hydroxyl group on C-25. Further evidence for the location of the ions of *m/z* 435, and 425 in the MS^2 spectrum 2.5:10.0:0.5:0.5. This is compatible with the enhanced lability of the C-25 hydroxyl group, as compared to that at C-27. This leads to the conclusion that the peak at 12.42 min corresponds to oxidised/derivatised 24,25-dihydroxycholesterol. The chromatographic peak at 13.11 min also gave MS^2 (550→) and MS^3 (550→471→) spectra compatible with an oxidised/GP-derivatised dihydroxycholesterol. In the MS^3 (550→471→) spectrum, the presence of a peak at *m/z* 325 ("e) indicate that both hydroxyl groups are on the C-17 side-chain (see Figure 5.14a). Further information is obtained from the ratio of ions of *m/z* 453, 443, 435, 425 in the MS^2 (550→) spectrum 2.5:10.0:<0.5:0.5. This suggests that the peak at 13.11 min corresponds to an oxidised/GP-derivatised 25,27-dihydroxycholesterol. Zhang *et al.* [24] have identified 25,27-dihydroxycholesterol in incubations of 27-hydroxycholesterol with rat

brain astrocytes, and 25,27-dihydroxycholesterol has been suggested to be an intermediate in cholesterol metabolism in astrocytes.

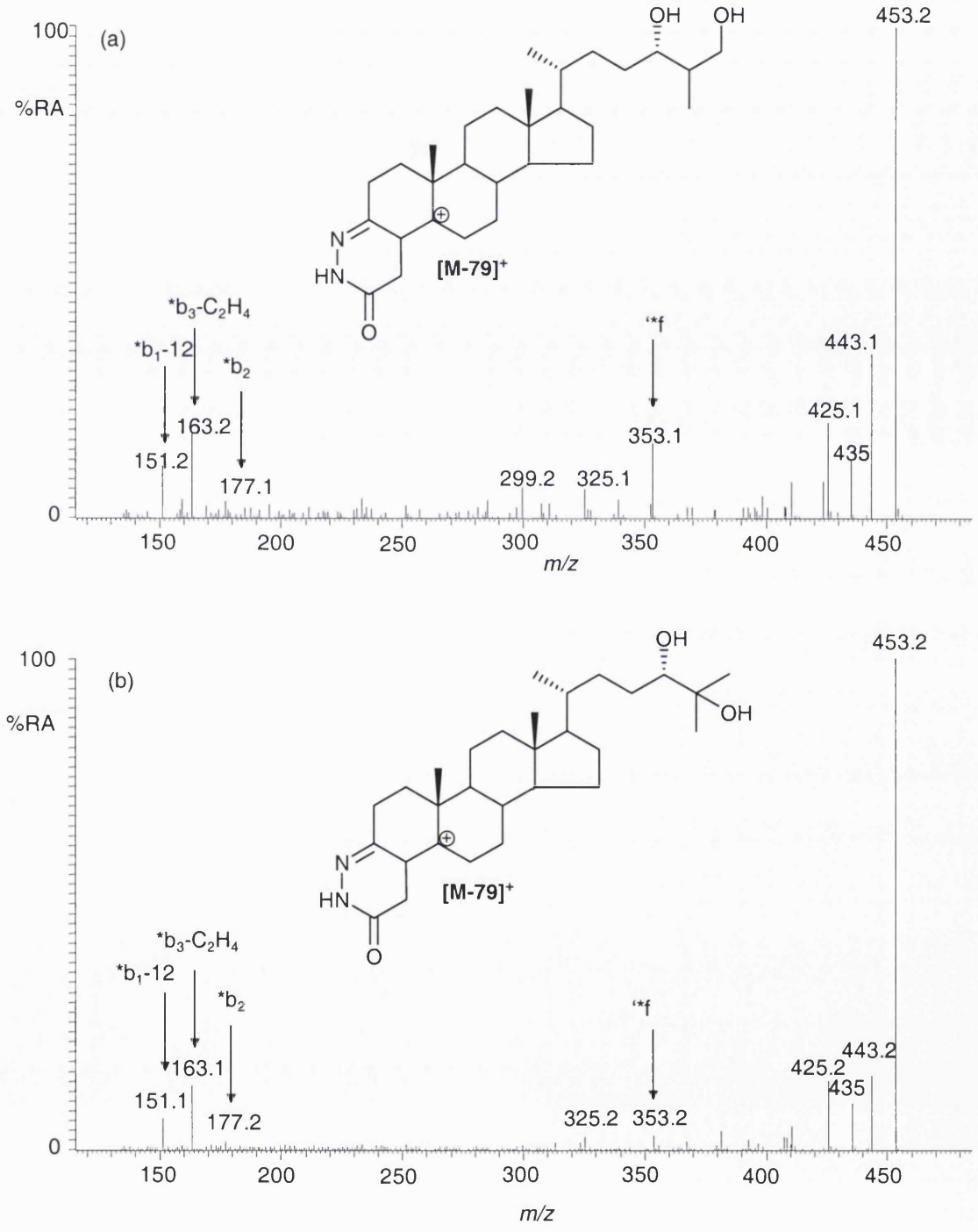

Figure 5.13 MS^3 (550→471→) spectra of chromatographic peaks eluting at (a) 11.96 min corresponding to 24,27-dihydroxycholesterol, (b) 12.42 min corresponding to 24,25-dihydroxycholesterol, refer to Figure 5.12.

The presence of a 6-hydroxyl group on the cholesterol skeleton alters the MS^3 spectrum of the oxidised/GP-derivative, in that instead of a triad of fragment ions at *m/z* 151, 163 and 177, only the ion at 177 is observed [68]. In the MS^3 (534→455→) spectrum of oxidised/GP-derivatised 6-hydroxycholesterol the $[M-107]^+$ ions are more abundant than $[M-79-H_2O]^+$ ions, also an intense ion is observed at *m/z* 383 corresponding to $[M-79-C_4H_8O]^+$ (see example for the GP-derivatised 6-hydroxycholest-4-ene-3-one in Figure 5.9c). The MS^3 (550→471→) spectrum of the peak eluting at 13.49 min gives a fragment ion at *m/z* 177, and the $[M-107]^+$ fragment is more abundant than the $[M-79-18]^+$ ion, signifying hydroxylation at C-6 (see Figure 5.14b). The presence of a fragment ion at 381 corresponding to $[M-79-18-C_4H_8O]^+$ provides further evidence for 6-hydroxylation. A fragment at *m/z* 341 ('*e) indicates that the second hydroxyl group is on the C-17 side-chain, and a fragment ion at *m/z* 369 ('*f) locates it to C-24. Therefore, the spectrum is compatible with that of oxidised/GP-derivatised 6,24-diydroxycholesterol. This is in agreement with studies by Mast *et al.* [22], who incubated 24-hydroxycholesterol with HEK293 cells transfected with CYP46A1, a dihydroxycholesterol with one hydroxyl group at C-24 and the second in the steroid nucleus was identified. Furthermore, CYP7B1, an enzyme with 6-hydroxylase activity, is expressed in brain [68,186,187]

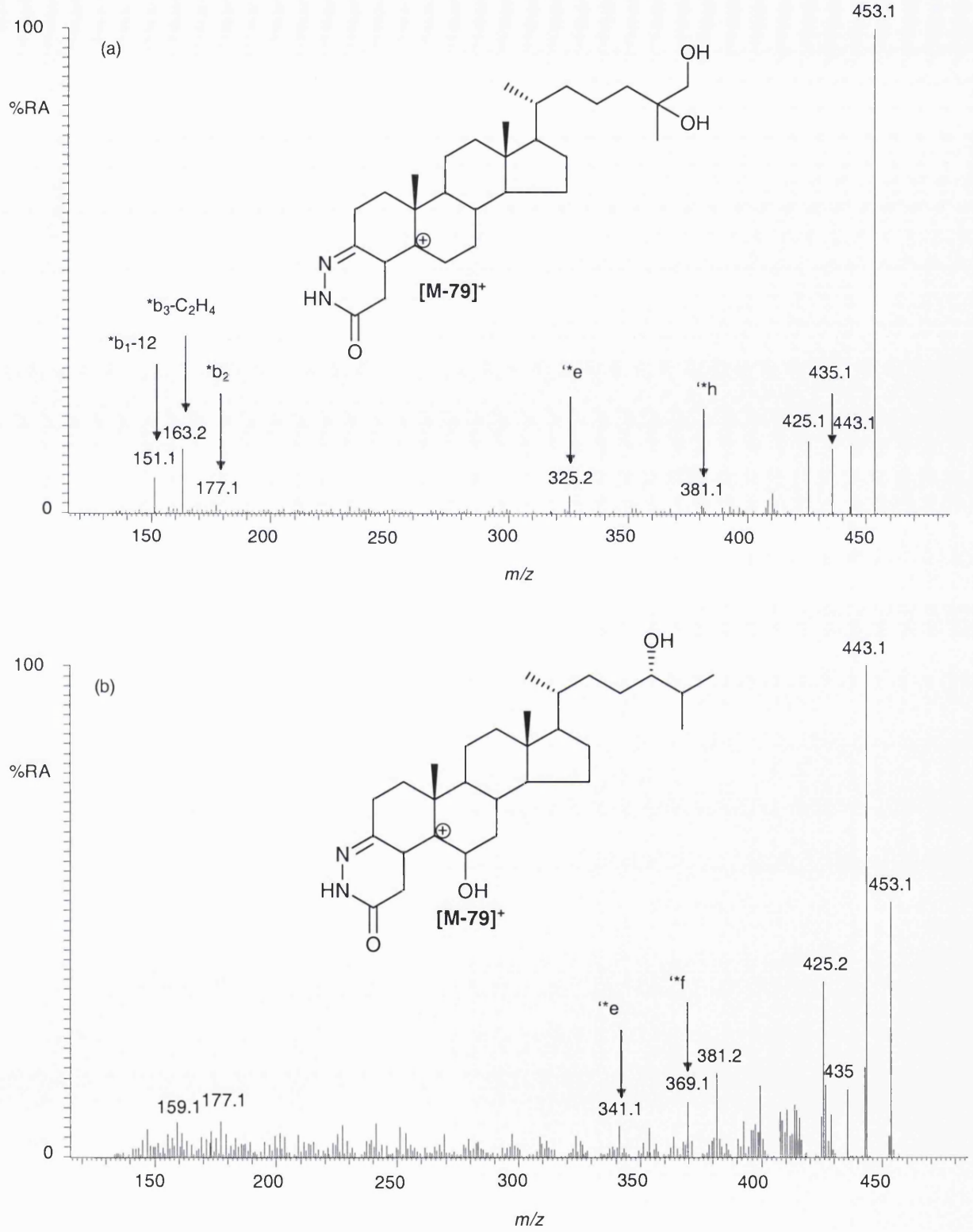

Figure 5.14 MS^3 (550→471→) spectra of chromatographic peaks eluting at (a) 13.11 min corresponding to 25,27-dihydroxycholesterol, (b) 13.49 min corresponding to 6,24-dihydroxycholesterol, refer to Figure 5.12.

The chromatographic peak at 14.24 min gives identical MS^2 (550→) and MS^3 (550→471→) spectra the authentic standard of oxidised/GP-derivatised 7α,25-dihydroxycholesterol. The 7-hydroxyl groups are characterised by fragment ions at *m/z* 151 and 179 in the MS^3 spectra, and their α- positioning is indicated by the abundance of fragment ion at *m/z* 231 (see Figure 5.15). The chromatographic peak eluting at 15.18 min gave MS^2 (550→) and MS^3 (550→471→) similar to that eluting at 14.24 min, and it is concluded that these are *syn* and *anti* conformers of the GP derivative of 7α,25-dihydroxycholesterol. The chromatographic peaks at 14.61 and 15.74 min give MS^2 (550→) and MS^3 (550→471→) spectra identical to those of the authentic standard of oxidised/GP-derivatised 7α,27-dihydroxycholesterol. Both 7α,25- and 7α,27-dihydroxycholesterol have been suggested as intermediates in the cholesterol metabolic pathways in rat brain [24].

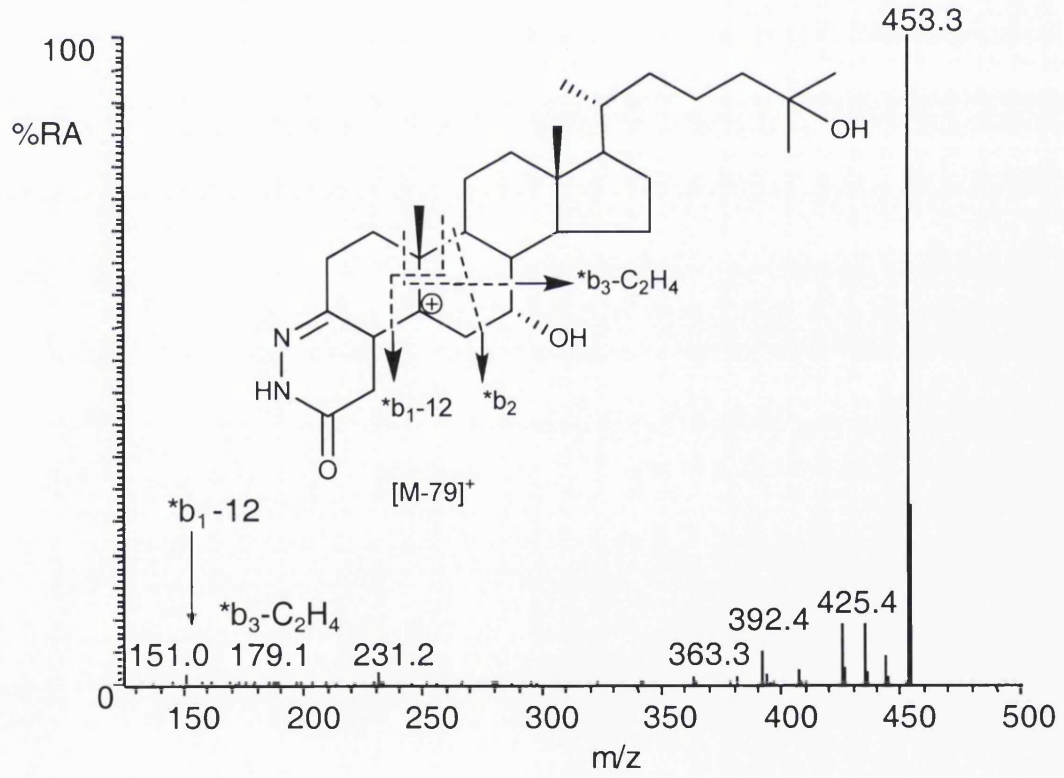

Figure 5.15 MS^3 (550→471→) spectrum of the chromatographic peak eluting at 14.24 min corresponding to 7α,25-dihydroxycholesterol (refer to Figure 5.12).

The oxidised/GP-derivatised oxysterol fraction U3A of rat brain (Figure 2.4)

The oxysterol fraction U3A was prepared in order to confirm that most oxysterols present in rat brain eluted in 10 mL ethyl acetate from the Unisil SPE column. The analytical procedure for obtaining the oxysterol fraction, U3A is shown in Figure 2.4. A second ethyl acetate fraction (10 mL) was collected, dried, treated with cholesterol oxidase and derivatised with GP reagent.

Cap-LC-MS^n analysis was performed on the fraction U3A, and the base peak chromatogram is shown in Figure 5.16. The chromatographic peak at 23.36 min (RRT 0.88) corresponded to monohydroxychlesterol, its MS^2 (534→) and MS^3 (534→455→) spectra were identical to the authentic 6-hydroxycholest-4-ene-3-one. 6-Hydroxycholest-4-ene-3-one is an autoxidation product of cholesterol. The major sterol in this fraction has a *m/z* 518 (RA 100%), and both the MS^2 (518→) and MS^3 (518→439→) spectra were identical to those from the authentic oxidised/GP-derivatised cholesterol.

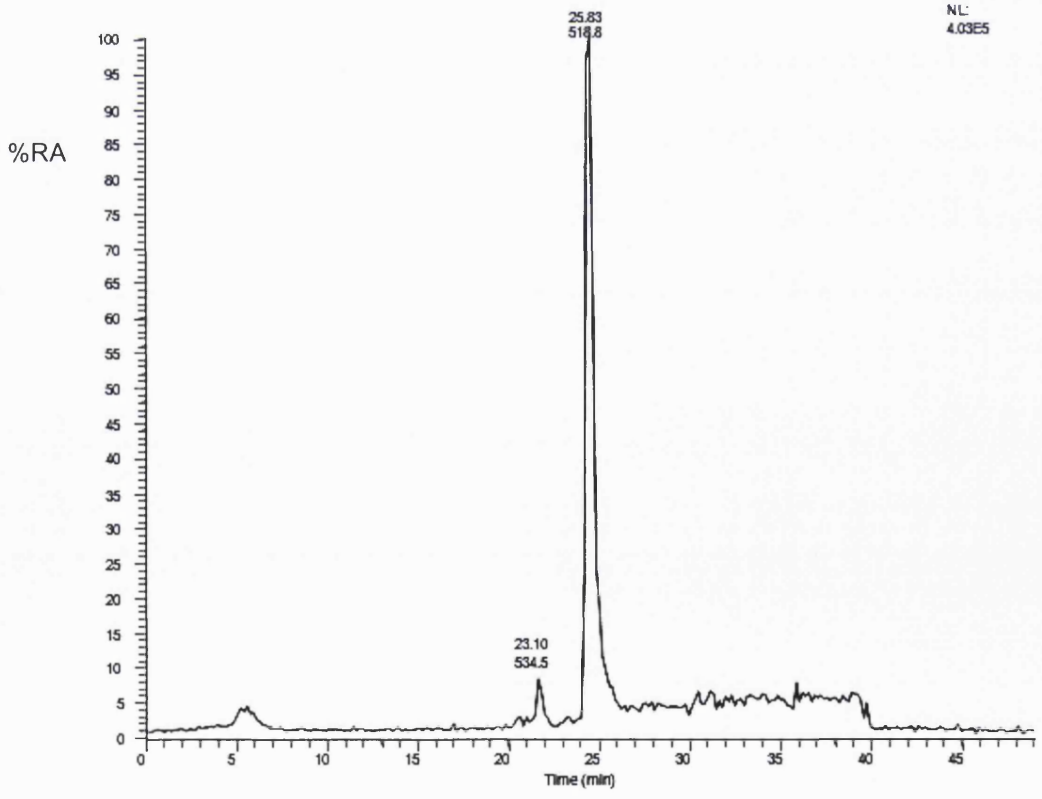

Figure 5.16 Base peak chromatogram of the fraction U3A. The analytical scheme for oxysterols isolation and analysis is shown in Figure 2.4, the route U3A.

In conclusion, there were no enzymatically formed oxysterols in this fraction signifying that an elution volume of 10 mL of ethyl acetate is sufficient for elution of most oxysterols present in rat brain from a Unisil SPE column. Cholesterol, however tails into this fraction.

The oxidised/GP-derivatised oxysterol fraction U2B of rat brain (Figure 2.4)

Naturally present oxysterols in the brain, possibly possess an oxo group, e.g. 7α,25-dihydroxycholest-4-ene-3-one, 7α,27-dihydroxy-cholest-4-ene-3-one [38]. Oxysterols containing a "natural" oxo group could be differentiated from their 3β-hydroxy-5-ene analogues, simply by performing a parallel experiment in the absence of cholesterol oxidase (see the analytical work-flow in Figure 2.4, the route U2B). Initially, RICs for the *m/z* values for all potential sterols were generated, and in a second cap-LC-MS run, MS^2 ($[M]^+\rightarrow$) and MS^3 ($[M]^+\rightarrow[M-79]^+\rightarrow$ and $[M-107]^+\rightarrow$) spectra were recorded for all potential oxysterols suggested to be present in the initial cap-LC-MS run. The TIC for the MS^3 transition 518→439→ generated one chromatographic peak at 25.83 min (Figure 5.17). The MS, MS^2 (518→), and MS^3 (518→439→) spectra of this chromatographic peak are identical to that from the reference GP-derivatised cholest-4-ene-3-one. Therefore, the rat brain contains cholest-4-ene-3-one (cholestenone).

The chromatographic peak at 14.61 min gives a MS spectrum corresponding to derivatised dihydroxycholest-4-ene-3-one (*m/z* 550). The characteristic fragment ions at *m/z* 151 and 179 suggest that the hydroxyl group at C-7 in the MS^3 (550→471→) spectrum, also the fragment ion at *m/z* 231 (RA 15%) indicates the α-positioning of C-7. The quality of spectrum was not sufficient to exactly locate the position of the second hydroxyl group. However, the spectrum strongly resembles that of 7α,27-hydroxycholesterol (Figure 5.18), and the RRT of 0.57 was identical to the authentic 7α,27-hydroxycholesterol. The TIC for the MS^3 transition 534→455→ generated one peak at 21.46 min corresponding to RRT of 0.83, but the quality of MS^3 spectrum was not sufficient to identify this oxysterol. Accordingly, the rat brain contains cholestenone, and 7α,x-dihydroxycholest-4-ene-3-one.

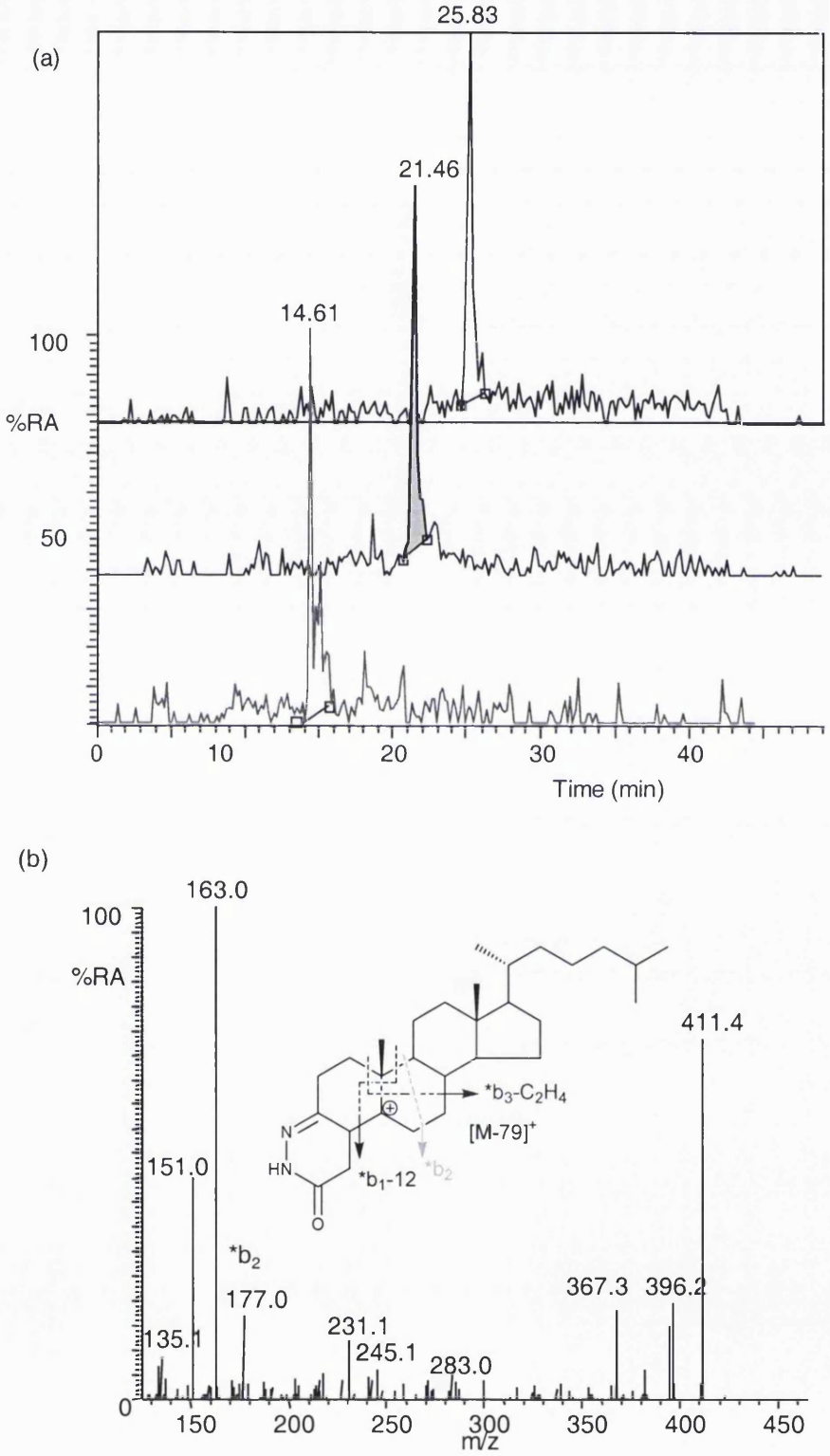

Figure 5.17 TICs for the MS^3 transition 518→439→ in black, 534→455→ in brown, and 550→471→ in green, from the oxysterol fraction U2B of rat brain (refer to Figure 2.4); (b) MS^3 (518→439→) spectrum of the chromatographic peak eluting at 25.83 min. The sample preparation work-flow is shown in Figure 2.4, the route U2B. Chromatographic conditions are described in section 2.9.

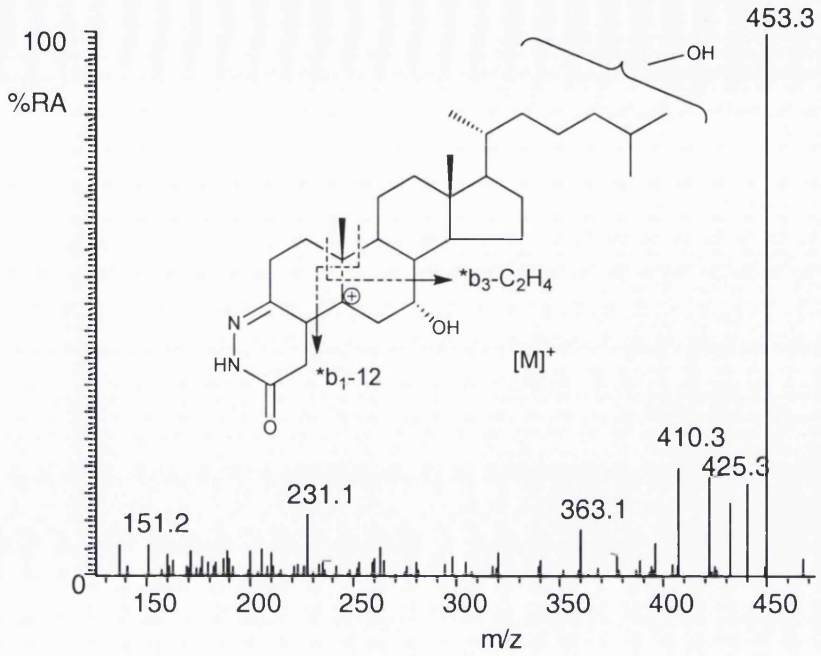

Figure 5.18 MS^3 (550→471→) spectrum of the chromatographic peak eluting at 14.61 min (7α,x-dihydroxycholest-4-ene-3-one) from the oxysterol fraction U2B of rat brain (refer to Figure 5.17).

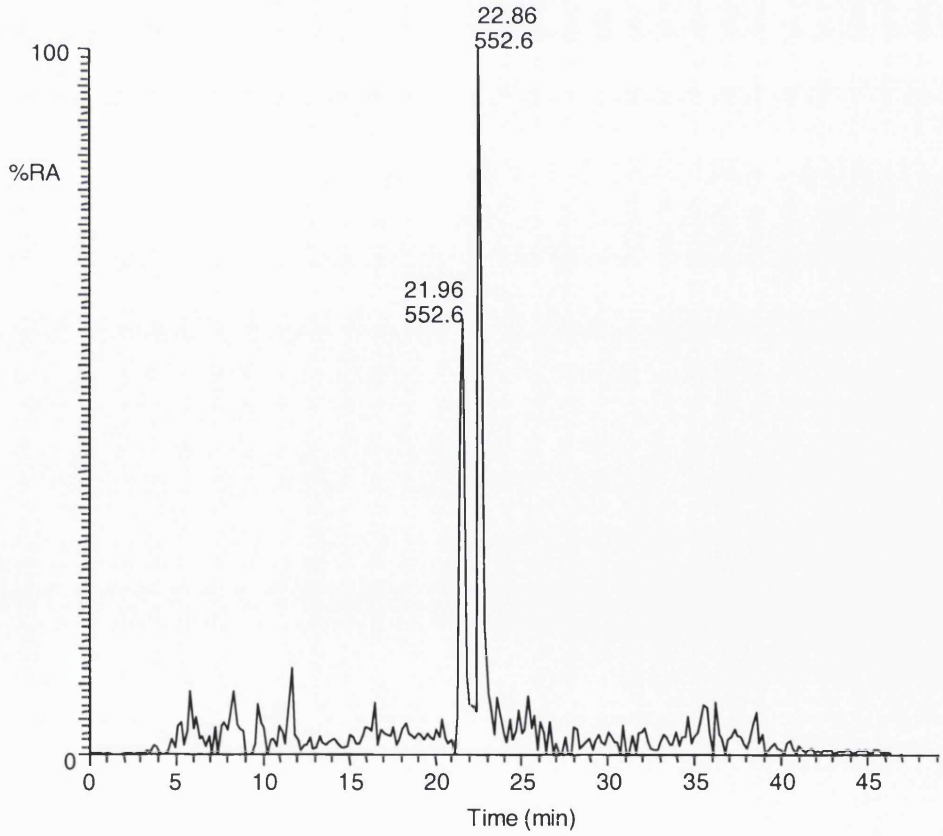

Figure 5.19 RIC for *m/z* 552 corresponding to GP-derivatised 3β-hydroxy-5-oxo-5,6-*seco*cholestan-6-al and 3,5-dihydroxy-B-norcholestane-6-carboxyaldehyde extracted from brain.

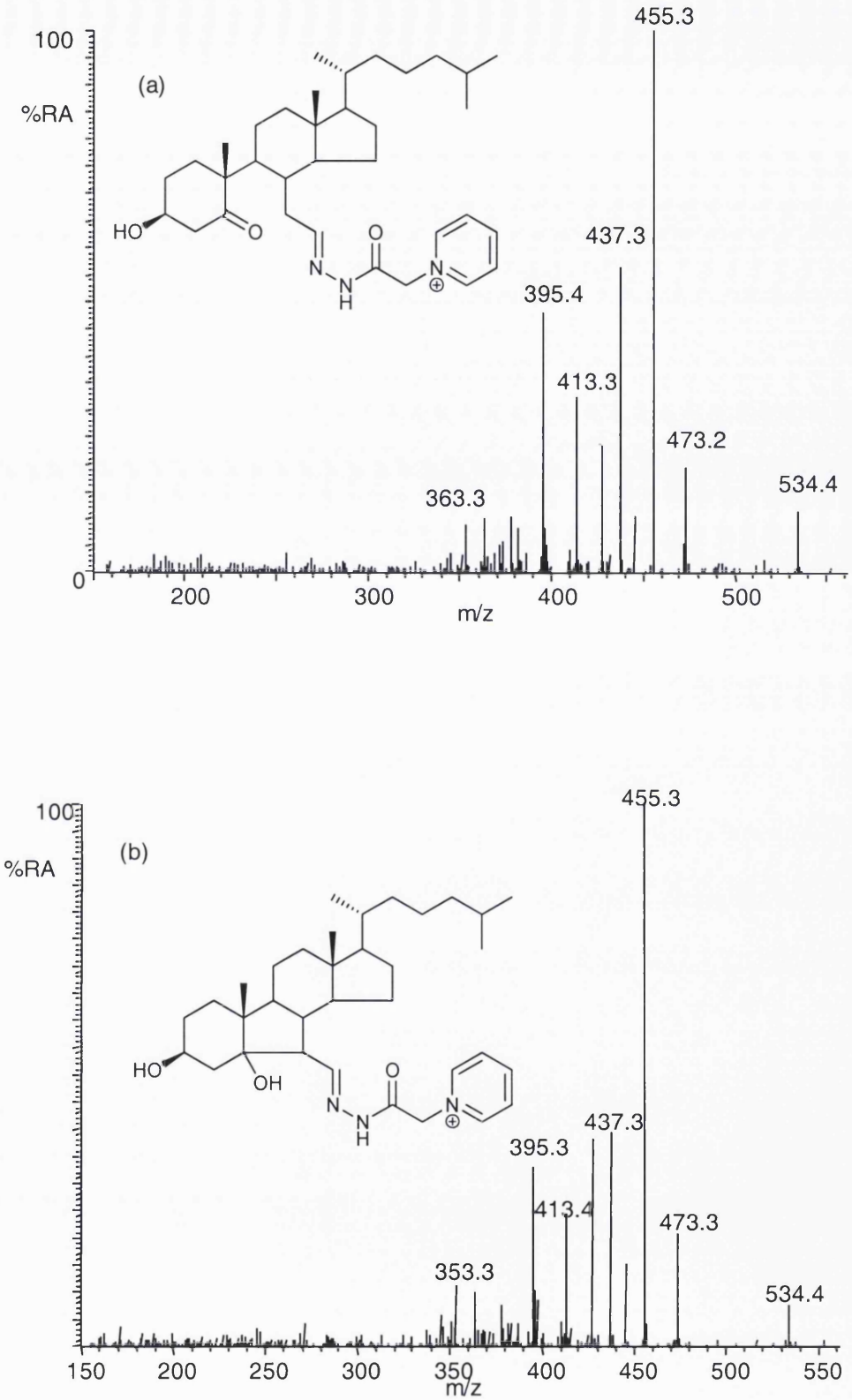

Figure 5.20 MS^2 (552→) spectra for chromatographic peaks eluting at (a) 21.96 min and (b) 22.86 min, refer to Figure 5.19.

It has recently been proposed that cholesterol 5,6-*seco*-sterol, 3β-hydroxy-5-oxo-5,6-*seco*cholestan-6-al, and its aldol, 3,5-dihydroxy-B-norcholestane-6-carboxyaldehyde have pro-atherogenic properties, and are present in atherosclerotic plaque material [94,95]. 5-*Seco*-sterol and its aldol both possess oxo groups, and are therefore also derivatised by the GP reagent. The RIC for their mass is shown in Figure 5.19. This chromatogram was recorded on the oxysterol fraction U2B isolated from rat brain according to the procedure described in Figure 2.4. The components of chromatographic peaks at 21.96 and 22.86 min, when subjected to MS^2 (552→) gave spectra identical to authentic standards of 3β-hydroxy-5-oxo-5,6-*seco*cholestan-6-al and 3,5-dihydroxy-B-norcholestane-6-carboxyaldehyde, respectively (Figures 5.20a,b), and the relative retention times of 0.85 and 0.88 also coincide with those of the corresponding authentic standards. This data confirms the presence of 5,6-*seco*-sterol and its aldol in rat brain. The abundance of these isomers was less than 2% that of 24S-hydroxycholesterol.

The oxidised/GP-derivatised cholesterol fraction U1A of rat brain (Figure 2.4)

The next experiment was designed to investigate whether there is some leakage of oxysterols into the fraction U1. The work-flow of this experiment is shown in Figure 2.4, the route UA1. The base peak chromatogram for the fraction U1A is shown in Figure 5.21a. The chromatographic peaks at 24.46 and 25.83 min were identified as oxidised/GP-derivatised desmosterol and cholesterol, respectively based on their RRT, MS, MS^2 ($[M]^+$→) and MS^3 ($[M]^+$→($[M-79]^+$→ and ($[M]^+$→($[M-107]^+$→) spectra. The oxidised/GP-derivatised cholesterol was present in high abundance (see the base peak chromatogram of the cholesterol fraction U1A, Figure 5.21a). RICs for all potential cholesterol metabolites were generated. Figure 5.21b-e shows RICs for *m/z* 516, 532, 534 and 550 corresponding to the $[M]^+$ ion of oxidised/GP-derivatised dehydroxycholesterol, oxocholesterols or dihydroxycholestadienes, monohydroxycholesterols, and dihydroxycholesterols, respectively. All chromatographic peaks were late eluting with RRT from 0.85 to 1.05. By recording MS^2 ($[M]^+$→) and MS^3 ($[M]^+$→$[M-79]^+$→) spectra of the late eluting peaks in the chromatogram,

oxidised/GP-derivatised 6-oxocholestenone *m/z* 532 (see supplementary material Figure S5.1), 5,6-epoxycholesterol *m/z* 534 (see supplementary material Figure S5.2), 6-hydroxycholest-4-ene-3-one *m/z* 534 (see supplementary material Figure S5.3), and campesterol *m/z* 548 (see Figure 5.21f) were identified by comparison of their RRT, MS^2 and MS^3 spectra with reference standards.

Table 5.2 also summarises the identified sterols/oxysterols in the cholesterol fraction U1A. 5,6-Epoxycholesterol and 6-oxocholestenone are autoxidation products as established in chapter 4. Further, 6-hydroxycholest-4-ene-3-one is formed as a side product of the oxidation/GP-derivatisation reactions of 3β,5α,6β-trihydroxycholestenane, which is also an autoxidation product.

RIC for *m/z* 550 generated only one chromatographic peak at 23.34 min corresponding to contaminant previously identified in chapter 4, section 4.1 (see Figure 5.21e; for a comparison with previously identified contaminant refer to Figure 4.3a). In summary, sterols and oxysterols are isolated by chromatography on a Unisil column into the cholesterol fraction U1, and the oxysterol fraction, U2. Although some oxysterols were identified in the fraction U1, they are autoxidation products of cholesterol, probably formed from cholesterol during storage and sample handling. No oxysterols formed by enzymatic processes were found in this fraction.

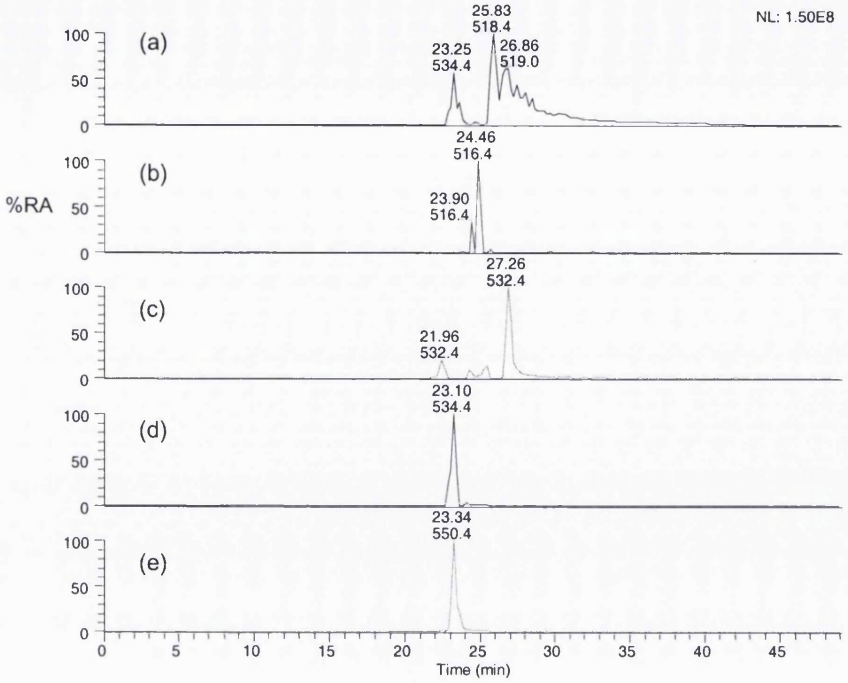

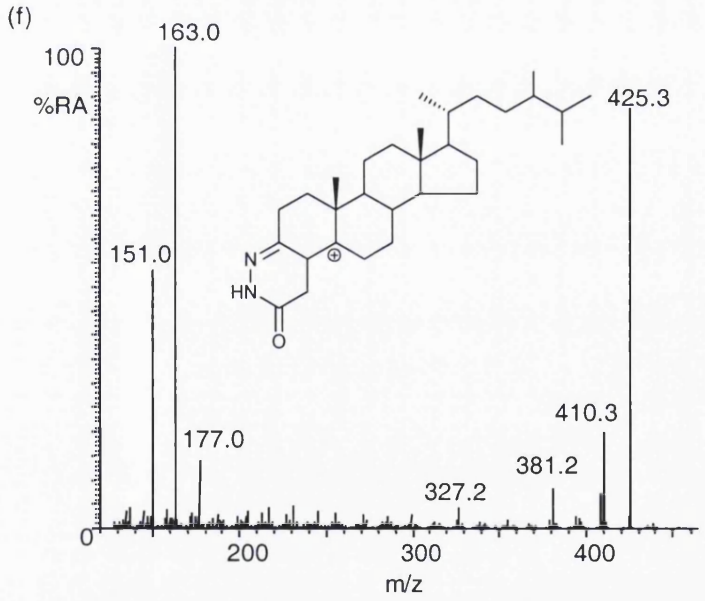

Figure 5.21 (a) Base peak chromatogram of the cholesterol fraction U1A from rat brain (refer to Figure 2.4, the route U1A), (b) RIC for oxidised/GP-derivatised sterol $[M]^+$ ions, *m/z* 516, (c) RIC for oxidised/GP-derivatised oxysterol $[M]^+$ ions, *m/z* 532, (d) RIC for oxidised/GP-derivatised monohydroxycholesterol $[M]^+$ ions, *m/z* 534, (e) RIC for oxidised/GP-derivatised dihydroxycholesterol $[M]^+$ ions, *m/z* 550, (f) MS^3 (534→455→) spectrum of chromatographic peak eluting at 27.26 min (campesterol) from rat brain sample. Chromatographic conditions are described in the method section 2.19. Shown in supplementary material Figures S5.1-5.3 are spectra of other oxysterols identified. See Table 5.2 for the identification of chromatographic peaks.

The oxidised/GP-derivatised oxysterol fraction U1B of rat brain (Figure 2.4)

In biological tissues cholesterol and oxysterols can exist as free alcohols or esterified to long-chain fatty acids. In order to analyse the sterol content of esters, the esterified sterols were hydrolysed. Fraction U1 was subjected to alkaline hydrolysis. After hydrolysis, the cholesterol fraction U1B (Figure 2.4, the route U1B) was passed twice through successive Unisil SPE columns, and the resulting oxysterol fraction was subjected to oxidation/GP-derivatisation protocols. A control rat brain sample was also prepared without the alkaline hydrolysis step (the sterol fraction U1A, Figure 2.4, the route U1A). The difference in the presence of oxysterols between the two factions U1A (without alkaline hydrolysis) and U1B (with alkaline hydrolysis) was taken as an indication of esterified oxysterols. No difference in sterol profile between these two samples was found, but the cholesterol level was approximately 100-fold lower in the oxysterol fraction U1B than in U1A (see Figure 5.22 for a comparison with the sterol fraction U1A refer to Figure 5.21). This finding is in agreement with results by Björkhem, Dietschy and Lütjohann [33,35,36,151,179]. They have reported that most cholesterol in the adult CNS is present in its free form, with only trace amounts of esterified cholesterol.

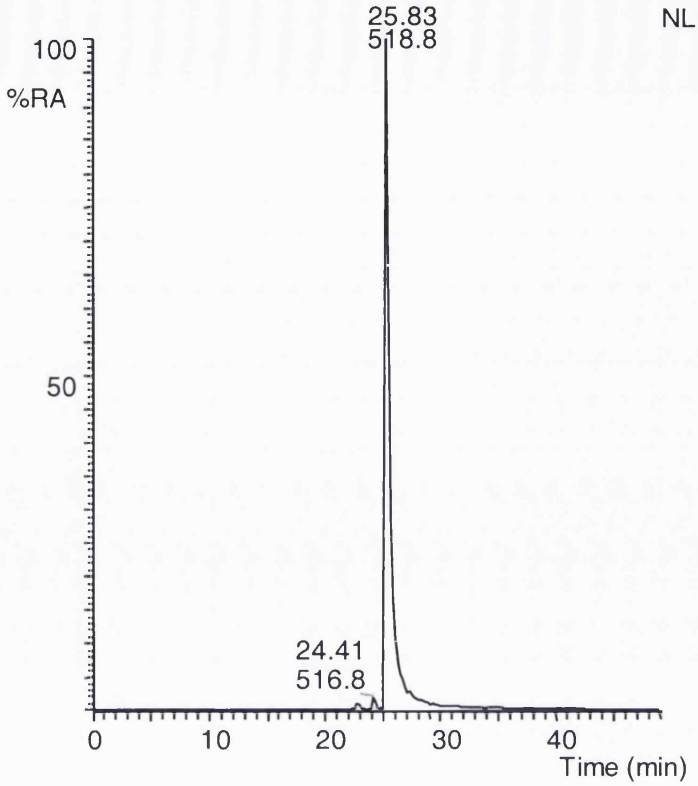

Figure 5.22 Base peak chromatogram of the fraction U1B. The rat brain (40 µg) was injected on-column. The chromatographic peaks eluting at 24.41 and 25.83 min were identified as the oxidised/GP-derivatised desmosterol and cholesterol, respectively.

Table 5.2 presents all identified sterols/oxysterols in the rat brain in this study.

Table 5.2 Summary of sterols and oxysterols identified in rat brain. Quantification is only for sterols found exclusively in Fraction U2A.

Sterol/oxysterol	Structure after oxidation with cholesterol oxidase	Formula of GP	Mass of GP	Retention time, min (RRT)	Identified in current work (concentration wet brain)	Identified by others in brain (concentration wet brain)
$C^{5,x}$-3β-ol	$C^{4,x}$-3-one	$C_{34}H_{50}N_3O^+$	516.4	24.46(0.95)	Desmosterol [a,e]	Rat (0.1% of total sterol)[g]
						Mouse (50 μg/g) [h]
				23.90 (0.93)	7-Dehydrocholesterol [e]	
C^4-3-one	C^4-3-one	$C_{34}H_{50}N_3O^+$	518.4	25.83(1.00)	Cholestenone [f]	
C^5-3β-ol	C^4-3-one	$C_{34}H_{52}N_3O^+$	518.4	25.83(1.00)	Cholesterol [a,e]	Human (7-8 mg/g) [i]
						Mouse (20 mg/g) [h]
C^5-24-methyl-3β-ol	C^4-24-methyl-3-one	$C_{34}H_{50}N_3O^+$	532.4	1.05(27.26)	Campesterol [a,e]	
C^5-3β-ol-x-one / $C^{5,x}$-3β,y-diol	C^4-3,x-dione/$C^{4,x}$-y-ol-3-one	$C_{34}H_{50}N_3O_2^+$	532.4	19.37(0.95)	24-Oxocholesterol (~0.5±0.2 μg/g) [d]	
				21.96(0.85)	6-Oxocholestenone [a,b,c,e]	
				22.41(0.87)		
			333.2	8.23(0.31)		
C^5-3β,x-diol	C^4-x-ol-3-one	$C_{34}H_{52}N_3O_2^+$	534.4	18.70(0.72)	24S-Hydroxycholesterol (20.3±3.4 μg/g) [d]	Human (5-15 μg/g) [j,m]
						Mouse (40-50 μg/g) [k,n]
				22.53(0.87)	7α-Hydroxycholesterol [a,e]	
				23.25(0.90)		
				19.14(0.74)	25-Hydroxycholesterol [a,e]	Rat astrocytes [l]
				21.31(0.82)	7β-Hydroxycholesterol [a,e]	
				21.95(0.85)		
				23.10(0.89)	6-Hydroxycholest-4-ene-3-one [a,e]	
				22.27(0.86)	5,6-Epoxycholesterol [a,e]	
C^5-3β,x-diol-y-one/ CA^5-3β-ol	C^4-x-ol-3,y-dione/ CA^4-3-one	$C_{34}H_{50}N_3O_3^+$	548.4	15.92(0.62)	24-Oxohydroxycholesterol (~125.1±2.5 ng/g) [d]	CYP46A1 [o]
					Not detected	Astrocytes [p]
C^5-3β,x,y-triol	C^4-x,y-diol-3-one	$C_{34}H_{52}N_3O_3^+$	550.4	12.42(0.48)	24,25-Dihydroxycholesterol (~75.3±4.6 ng/g) [d]	Astrocytes[p]/CYP46A1 [o]
				11.96(0.46)	24,27-Dihydroxycholesterol (~125.1±6.0 ng/g)[d]	CYP46A1 [o]
				13.11(0.51)	25,27-Dihydroxycholesterol (~45.0±1.3 ng/g) [d]	Astrocytes [p]
				13.49(0.51)	6,24-Dihydroxycholesterol (~56.8±1.1 ng/g) [d]	CYP46A1 [o]
				14.24(0.55)	7α,25-Dihydroxycholesterol (~32.0±0.7 ng/g) [d]	Astrocytes [p]
				14.61(0.57)	7α,27-Dihydroxycholesterol (~30±0.1 ng/g) [d]	Astrocytes [p]

C^5-x,y-diol-3-one	C^4-x,y-diol-3-one	$C_{34}H_{52}N_3O_3^+$	550.4	14.24(0.55) 15.18(0.59)	7α,25-Dihydroxycholest-4-en-3-one (~20.2±6.1 ng/g) [d]	Astrocytes [p]
5α-C-3β,x,y-triol/5,6-*Seco*-sterol Aldol	C-x,y-diol-3-one	$C_{34}H_{54}N_3O_3^+$	552.4	0.85(21.96) 0.88(22.86)	5,6-*seco*-sterol (~100.3 ±6.1 ng/g) [d] Aldol (~200.1±2.1 ng/g) [d]	Human (150 ng/g) [q]
C^5-x,y-epoxy-3β-ol	C^4-x-ol,y-methoxy-3-one	$C_{35}H_{54}N_3O_3^+$	564.4	0.65(16.75)	24S,25-Epoxycholesterol (~30.0 ±3.1 ng/g) [d]	
C^5-3β,x,y,z-tetraol	C^4-x,y,z-triol-3-one	$C_{34}H_{52}N_3O_4^+$	566.4	0.56(14.47)	Detected, not characterised	CYP46A1 [o]/Astrocytes [p]
5α-C-3β,x,y,z-tetraol	5α-C-x,y,z-triol-3-one	$C_{34}H_{54}N_3O_4^+$	568.4	0.47(12.16)	Detected, not characterised	

C, cholestane; CA, cholestanoic acid; 3β-hydroxy-5-oxo-5,6-*seco*cholestan-6-al (5,6-*seco*-sterol), 3,5-dihydroxy-B-norcholestane-6-carboxyaldehyde (aldol); GP, Girard P.

Superscripts indicate location of double bonds. See Figures 1.10, 1.12 and 1.13 for structures.

RRTs represent the relative retention times of the oxidised/GP-derivatised sterols/oxysterols to the oxidised/GP-derivatised cholesterol.

[a]Found in fraction U1 from Unisil column (refer to Figure 2.4).

[b]Both 3-GP and 6-GP derivatives formed.

[c]*Bis*-GP derivative formed.

[d]Mean ± standard deviation of triplicate assays (n=3)

[e]Found in fraction U2C from Unisil column (refer to Figure 2.4).

[f]Found in fraction U2B from Unisil column (refer to Figure 2.4).

[g]Other precursors of cholesterol, besides desmosterol, have been identified in rat brain [188,189]. Desmosterol concentration from ref. [188].

[h]From ref. [178].

[i]From ref. [165].

[j]From ref. [165].

[k]From ref. [178].

[l]Astrocytes show 25-hydroxylase activity when incubated with 27- and 24-hydroxycholesterol, and 7α-hydroxylase activity when incubated with 25- and 27-hydroxycholesterol [24].

[m]Other oxysterols identified in human brain include 27-hydroxycholesterol (1-3 ng/mg) [178], 22R-hydroxycholesterol (45-90 pg/mg) [158], 7-hydroxycholesterol (234-745 ng/mg, cerebellar cortex) [190], and 7-oxocholesterol (170-640 ng/mg cerebellar cortex) [190].

[n] Other oxysterols identified in mouse or rat brain include 27-hydroxycholesterol (5 ng/mg mouse) [178], 20S-hydroxycholesterol (50 pg/mg rat) [157].

[o]Recombinant CYP46A1 shows 25- and 27-hydroxylase activity when incubated with 24S-hydroxycholesterol. HEK293 cells transfected with CYP46A1 can also hydroxylate the steroid nucleus [22].

[p]Astrocytes show 25-hydroxylase activity when incubated with 27- and 24-hydroxycholesterol, and 7α-hydroxylase activity when incubated with 25- and 27-hydroxycholesterol [24], 25-hydroxycholesterol, 7α,25-dihydroxycholesterol, and 7α,25-dihydroxycholest-4-en-3-one are formed from endogenous precursors.

[q]Concentration of combined 5,6-seco-sterol and its aldol [94].

Discussion

The analytical method described here offers sensitivity, specificity and selectivity for the determination of oxysterols in brain. On-column detection limits were of the order of 0.8 pg, and at this level MS^2 and MS^3 spectra were sufficiently informative to allow structure determination. At this level of sensitivity, it was possible to identify novel oxysterols in the brain from only 30 μg of brain injected on-column. This will allow oxysterol analysis from distinct brain regions.

The most abundant oxysterol in rat brain is 24S-hydroxycholesterol, and its level was found to be between 17-23 μg/g. The identification of 24S-hydroxycholesterol in the brain is in agreement with the earlier study by Smith *et al.* in 1973 [191] and by Björkhem and colleagues [192] who have shown that in rat about 70% of the 24S-hydroxycholesterol in plasma is of cerebral origin. The conversion of cholesterol to 24S-hydroxycholesterol is the most quantitatively important mechanism for cholesterol elimination from the brain, with a net flux into the circulation [19]. The informative fragmentation (MS^3), of oxidised/GP-derivatised sterols has also allowed the identification of novel oxysterols in rat brain. This study provides the identification and approximate quantification of 24,25-, 24,27-, and 6,24-dihydroxycholesterols in rat brain (Table 5.2). Mast *et al.* [22] have incubated 24S-hydroxycholesterol with recombinant CYP46A1 or transfected cells and identified those sterols. Furthermore, the current study is the first to identify 24,25-, 25,27-, 7α,25- and 7α,27-dihydroxycholesterols in rat brain, although these oxysterols have been observed in incubations of 24-, 25- and 27-hydroxycholesterols with astrocytes [24,52,154]. The identification of novel oxysterols in brain and their low abundance (<2%) compared with 24S-hydroxycholesterol does not suggest that they act as transport forms of cholesterol from brain to liver. However, they may have biological activity acting as ligands for the liver X receptors e.g., LXR_β, which, like CYP46A1, is expressed in neurons, and interacting with other transcription factors such as sterol-regulatory element binding proteins (SREBRs) [68]. Additionally, 5,6-*seco*-sterol and its aldol were detected in rat brain. The presence of these two oxysterols in humans has been under debate [94,95,137], but their association

with neurodegenerative disease [94,95] indicates the importance of their analysis. The developed analytical methodology can be easily be used for oxysterol analysis in other tissues, as well as in nerve cells.

5.2 Oxysterols in the embryonic central nervous system

Oxysterols can cross the BBB unlike cholesterol, and are both exported from and imported to the brain [37]. In the adult, cholesterol is continuously synthesised throughout life and synthesis exceeds the need for structural cholesterol. This requires an export mechanism, which is provided by oxidation of cholesterol to 24S-hydroxycholesterol by CYP46A1. This oxysterol can pass the BBB [19]. CYP46A1 is expressed exclusively in the brain, in neurons [180], and in neonates appears to have low activity, which is greatly increase after birth, probably in response to increased cholesterol synthesis [193,194]. The enzyme CYP27A1 is responsible for 27-hydroxylation of cholesterol, and is expressed ubiquitously. In adults, 27-hydroxycholesterol is proven to be a net import product into the brain [195]. In developing brain, before the blood brain barrier (BBB) is fully developed cholesterol and its metabolites can be derived from the mother. However, after the barrier is sealed cholesterol must be synthesised *in situ.* Early in gestation, at E10-E11, upon formation of the BBB, the brain rapidly became the source of almost all of its own sterols (90% at birth). A recent study by Tint *et al.* [196] has confirmed *de novo* sterol synthesis in foetus brain beginning at approximately E10-11, when the BBB is formed. The early foetal brain also appears to conserve cholesterol by keeping CYP46A1 expression low until approximately E18 [196]. Therefore, the level of 24S-hydroxycholesterol in the brain depends on age [193,194].

In collaboration with scientists at Karolinska Institutet in Stockholm, the oxysterol content of embryonic (E11) mouse from different regions of the central nervous system (CNS) was investigated, and the current methodology was applied for their profiling, using the analysis scheme illustrated in Figure 2.5 [105]. This study was carried out on the whole CNS from E11 mouse, which was dissected into three regions:- ventral midbrain (VM), cortex (Ctx), and spinal cord (SC). GC-MS

analysis was performed on both sterol and oxysterol fractions isolated by chromatography on a Unisil column (fractions U1 and U2 respectively, see Figure 2.5) and derivatised to TMS ethers. Quantitative estimates of the most abundant sterols were made by analysing a known amount of lathosterol (5α-C^7-3β-ol) TMS ether in Karolinska Institutet, Sweden, and are summarised in Table 5.3. The amount of cholesterol (estimated 1.25 mg/g Ctx, 1.15 mg/g SC, and 0.48 mg/g VM wet weight) was appreciably lower than that reported in adult mouse (20 mg/g) [33,105,185]. However, this value was in good agreement with other data on E11-12 stage of development of mouse CNS (total sterols<1 mg/g) [196].

Lütjohann *et al.* [185] reported that in the adult mouse brain the ratio of desmosterol to cholesterol is of the order of 0.001. However, the cholesterol content significantly increases in CNS at birth and during early development and then declines sharply in more mature animals [33]. The current data give ratios of 0.03 (Ctx), 0.01 (SC), and 0.03 (VM) on E11 embryonic mouse CNS [105]. It is known that a desmosterol is a precursor of cholesterol and for this reason its elevated level relative to cholesterol indicates a high rate of cholesterol synthesis during this stage of development.

The limit of detection of the GC-MS instrument used was approximately 0.2 μg/g wet weight of tissue, which ruled out the identification of low abundance oxysterols [105]. Because of this, the samples were hydrolysed with HCl and sent to the School of Pharmacy, University of London for cap-LC-MS^n analysis. The work-flow of this experiment is shown in Figure 2.5. Capillary LC-MS^n analysis was performed on U2 oxysterol fractions. In this study the main goal is the identification of oxysterols in CNS. Therefore, the oxidation/GP-derivatisation and sample preparation methods have been optimised as described in chapters 3 and 4; and these methods were utilised for these compounds in this work. The oxidation reaction is only applicable to substrates with a 3β-hydroxy-5-ene or 3β-hydroxy-5α-hydrogen function, and reaction conditions have been tested so as to give quantitative conversion of 3β-hydroxy-5-ene oxysterols to their 3-oxo-4-ene analogues, also derivatisation reaction conditions have been used to give quantitative conversion of oxysterols to

their GP derivatives. The products of oxidation/GP-derivatisation were separated from unreacted GP hydrazine on a C_{18} SPE column and the methanol fractions (SPE-Fr1, -Fr2) subsequently analysed were those containing oxidised/GP-derivatised oxysterols. Less polar sterols tail into a final methanol-chloroform fraction (SPE-Fr3). It was observed that there was some tailing of the sterols from fraction U1 into the oxysterol fraction U2 due to the high level of sterols in the samples. However, oxysterols were found exclusively in fraction U2. It is noticeable that the chromatographic pattern for the three regions of mouse CNS is very similar (see Figure 5.23).

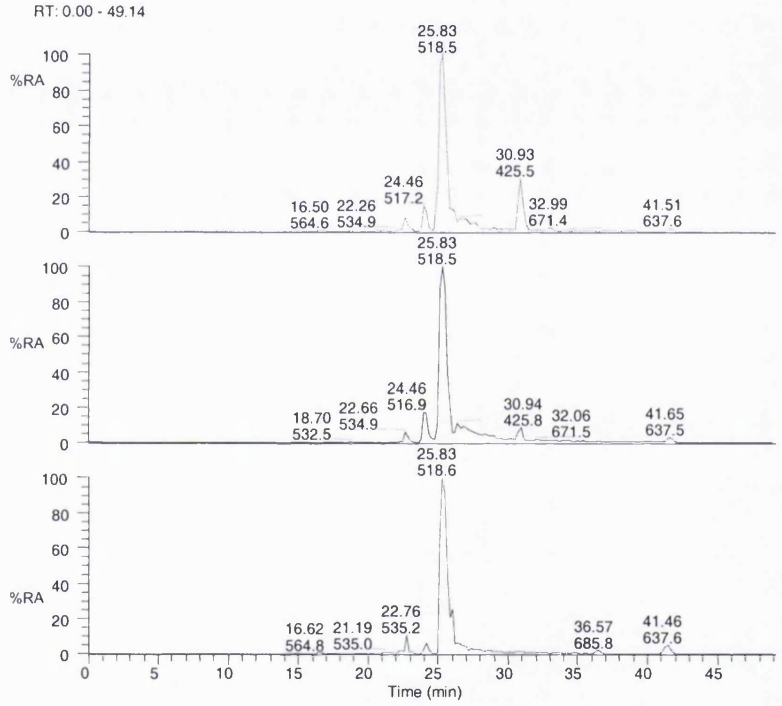

Figure 5.23 Base peak chromatograms are from the cortex, Ctx (upper trace), ventral midbrain, VM (middle trace), and spinal cord, SC (lower trace), 100 µg of the CNS extract from each section was injected on the capillary column. Chromatographic conditions as described in section 2.9. See Table 5.4 for the identification of chromatographic peaks.

By comparing analyte retention time, MS^2 ($[M]^+ \rightarrow$), and MS^3 ($[M]^+ \rightarrow [M-79]^+ \rightarrow$) spectra of components eluting from the reversed-phase column with authentic standards it was possible to identify the presence of desmosterol, cholesterol, campesterol, sitosterol, lathosterol, 6-, 7α-, 7β-, 24S-hydroxycholesterols, 24-oxocholesterol, 24,25-dihydroxycholesterol and 24,25-epoxycholesterol (see Table 5.3).

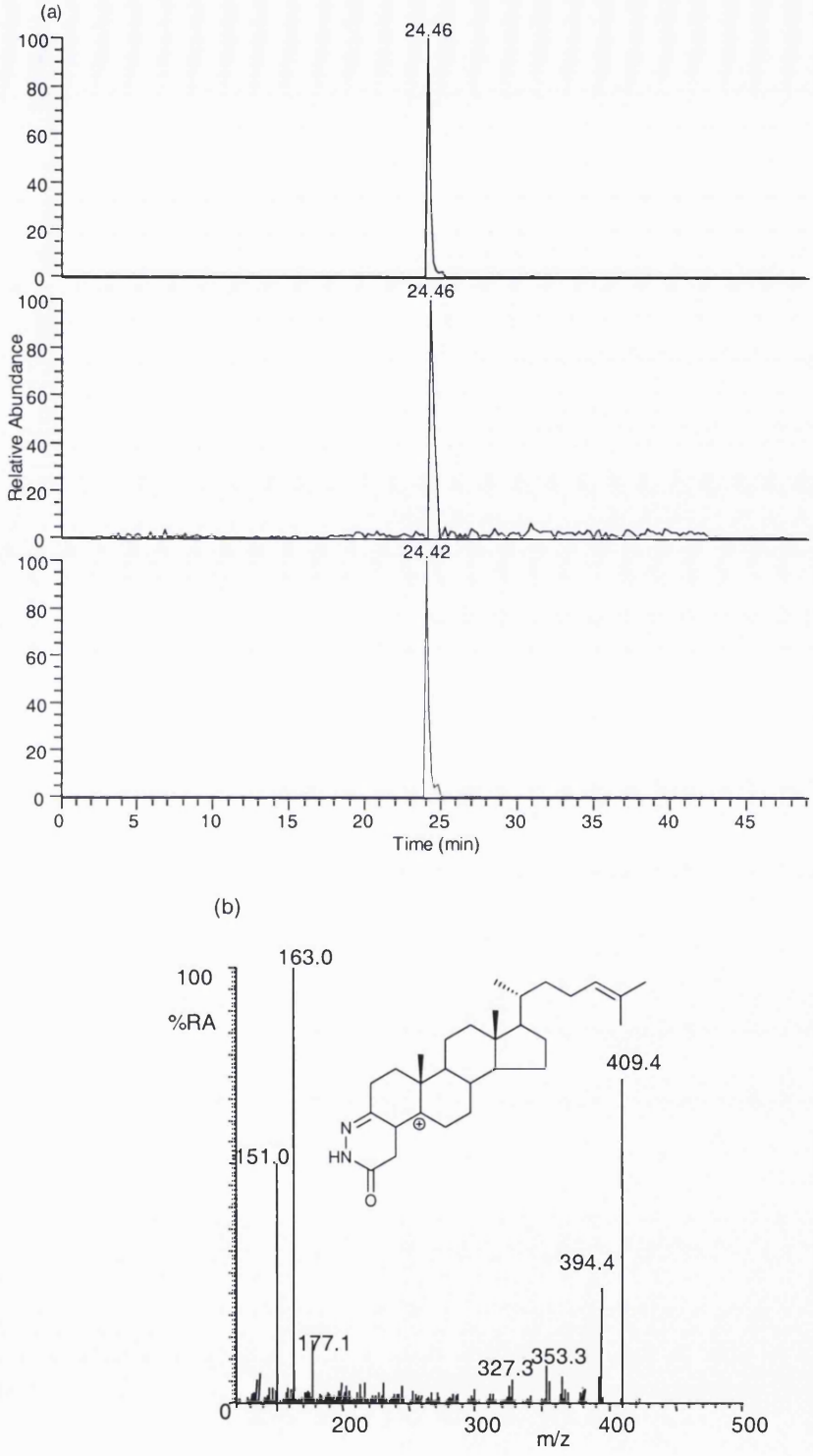

Figure 5.24 (a) TIC for the transition 516→437→ corresponding to the oxidised/GP-derivatised sterol $[M]^+$ ions, *m/z* 516 from the cortex, Ctx (upper trace), ventral midbrain, VM (middle trace), and spinal cord, Sc (lower trace). Chromatographic conditions are described in the experimental section. (b) MS^3 (516→437→) spectrum of chromatographic peak at 24.26 min from the cortex sample, and is identical to the authentic desmosterol standard.

For example, Figure 5.24a shows the TIC for the transition 516→437→ corresponding to oxidised/GP-derivatised 3β-hydroxy-cholestadiene. The RRT (0.95), MS^2 and MS^3 spectra of the chromatographic peak at 24.46 min are identical to the oxidised/GP-derivatised authentic desmosterol.

Figure 5.25 demonstrates the identification of 24,25-epoxycholesterol in the CNS, based on RRT, MS, MS^2 (564→) and MS^3 (564→485→) spectra. 24,25-Epoxycholesterol is labile to the oxidation/GP-derivatisation conditions employed in this study. As the derivatisation reaction proceeds in acidified 70% methanol, methanolysis can occur, which produces the 24-ol,25-methyl-ether (or 24-methyl-ether,25-ol). They both give $[M]^+$ ions at *m/z* 564. The TICs for the MS^3 transition 564→485→ from the cortex, ventral midbrain and spinal cord gave one chromatographic peak with retention time 16.73 min (RRT 0.65). The MS^2 (564→) and MS^3 (564→485→) spectra are equivalent to those derived from the 24S,25-epoxycholesterol standard.

Figure 5.26a shows TIC for the MS^3 transition 532→453→ corresponding to oxidised/GP-derivatised oxocholesterols, epoxycholestenols and dihydroxycholestadienes. The MS^2 (532→) and MS^3 (532→453→) spectra of the first eluting oxysterol (17.80 min, Ctx) suggest an epoxycholestenol rather than an oxoalcohol, and the MS^3 fragment ions at *m/z* 325, 353 and 367 (side-chain cleavage fragments '*e, '*f and '*g) indicate the additional functional groups are distal to C-24. Then MS^3 (532→453→) spectrum is identical to that of oxidised/GP-derivatised 24,25-epoxycholesterol (see Figure 5.26b). By recording MS^2 (532→) and MS^3 (532→453→) spectra of the later eluting peaks in the chromatograms 24-oxocholesterol (19.37 min), 6-oxocholestenone (21.96 and 22.41 min) and campesterol (26.99 min) were identified by comparison with reference standards. 6-Oxocholestenone is an autoxidation product of cholesterol as established in chapter 4. Figure 5.26c shows the MS^3 (532→453→) spectrum of the chromatographic peak at 26.99 min, which is identical to the oxidised/GP-derivatised authentic campesterol.

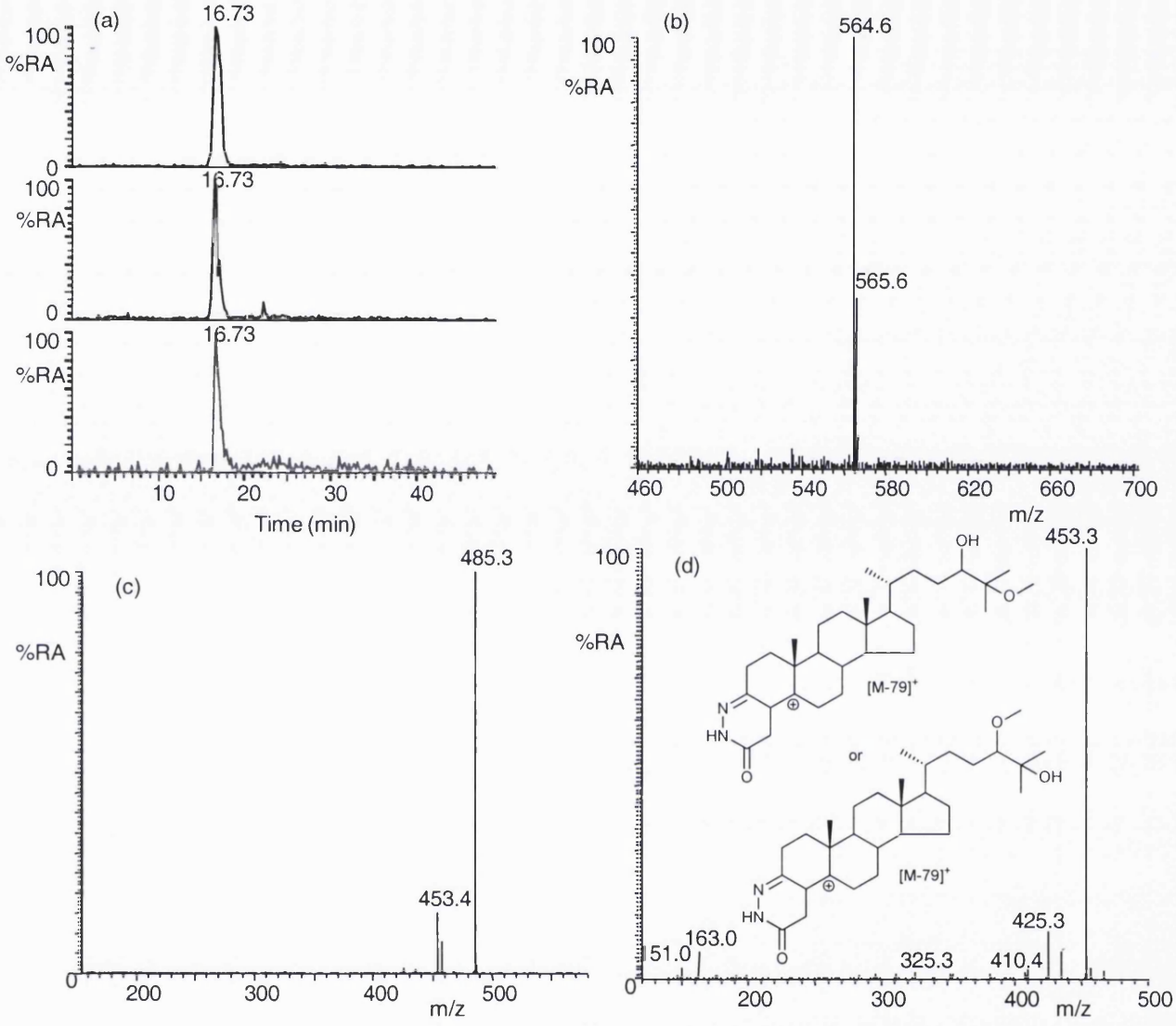

Figure 5.25 (a) TICs for the MS^3 transition 564→485→ of the oxidised/GP-derivatised oxysterol $[M]^+$ ions, *m/z* 564 from CNS regions cortex, Ctx (upper trace), ventral midbrain, VM (middle trace), and spinal cord, SC (lower trace). (b) MS, (c) MS^2 (564→), and (d) MS^3 (564→485→) spectra of the chromatographic peak eluting at 16.73 min (24-hydroxy,25-methoxycholesterol or 24-methoxy,25-hydroxycholesterol). Figures 38a,d,e in supplementary material show MS, MS^2 and MS^3 spectra of the oxidised/GP-derivatised 24,25-epoxycholesterol standard.

Following oxidation/GP-derivatisation monohydroxycholesterols give a precursor ion, $[M]^+$, at *m/z* 534. The RIC for *m/z* 534 from CNS region of cortex is shown in Figure 5.26a. The oxidised/GP-derivatised 24S-hydroxycholesterol was present in the CNS derived samples, and this compound eluted from the capillary column at 18.70 min, its MS^2 (534→), MS^3 (534→455→) spectra and RRT were identical to the oxidised/GP-derivatised authentic 24S-hydroxycholesterol standard.

Data from cap-LC-MS^n experiments indicates that the 24S-hydroxycholesterol level is low in embryonic (E11) mouse CNS.

The MS^2 (534→) and MS^3 (534→455→) spectra for the chromatographic peaks at retention times of 19.14 min (RRT 0.74) and 19.63 min (RRT 0.76) confirmed the presence of 25- and 27-hydroxycholesterols in the three regions of CNS (an example is shown for the cortex, Ctx, Figure 5.26a). Also evident in this figure is a peak with retention time 16.72 min equivalent to that of the oxidised/GP-derivatised 22R-hydroxycholesterol. Unfortunately, there was insufficient ion-current to record an MS^3 (534→455→) spectrum to confirm its identity. Additional monohydroxycholesterols were identified based on MS^2 (534→) and MS^3 (534→455→) spectra and RRT, 7β-hydroxycholesterol (21.31 min, RRT 0.82), 7α-hydroxycholesterol (22.53 min, RRT 0.87) and 6-hydroxycholest-4-ene-3-one (23.10 min, RRT 0.89) in the three regions of CNS. They are autoxidation products of cholesterol formed during the sample preparation, except for 7α-hydroxycholesterol, which is also formed by enzymatic reaction (see Chapter 4). 7α-Hydroxycholesterol was in high abundance (see Figure 5.26a, the oxidised/GP-derivatised 7α-hydroxycholesterol eluted from the capillary column at 22.53 min); this probably suggests that it has been formed by enzymatic and non-enzymatic processes.

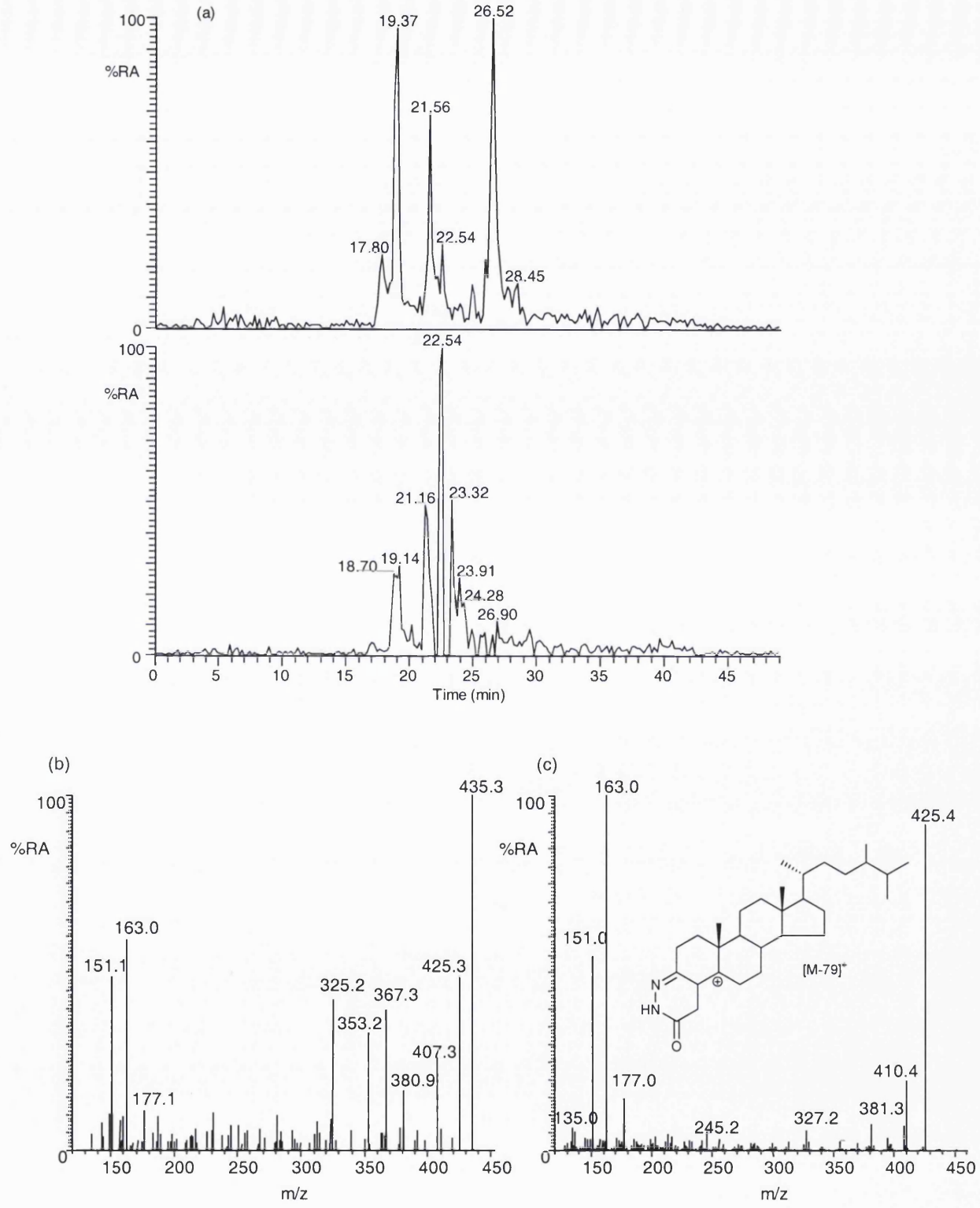

Figure 5.26 (a) RICs for oxidised/GP-derivatised oxysterol $[M]^+$ ions, *m/z* 532 (upper trace) and *m/z* 534 (lower trace) from the cortex of CNS. MS^3 (532→453→) spectra of the chromatographic peaks eluting at (b) 18.70 min (24,25-epoxycholesterol), (c) 26.99 min (campesterol) from the cortex sample.

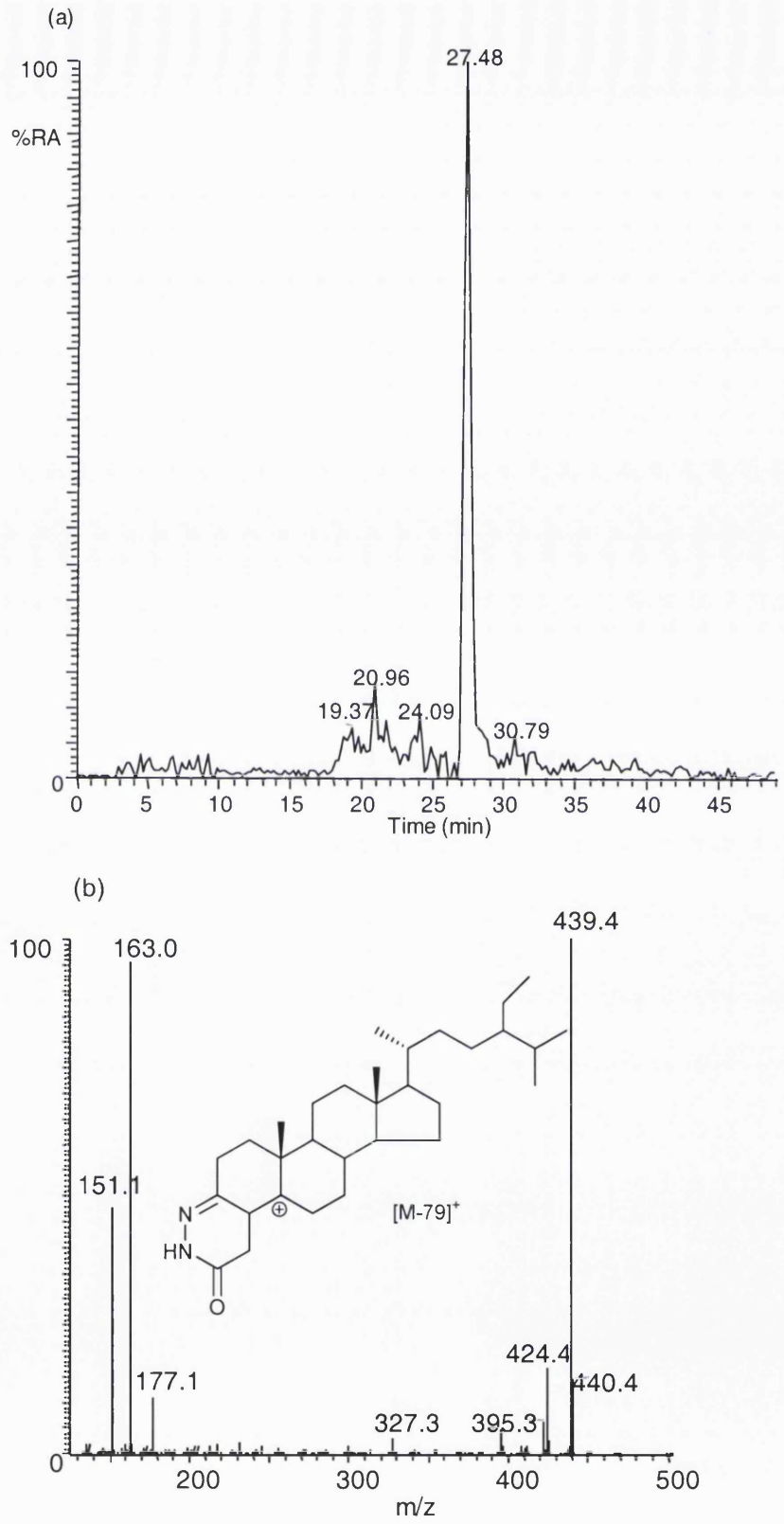

Figure 5.27 (a) RIC for the oxidised/GP-derivatised oxysterol $[M]^+$ ions, *m/z* 546 from the cortex of CNS. MS^3 (546→467→) spectrum of the chromatographic peaks eluting at (b) 28.15 min (sitosterol) from the cortex sample.

An additional sterol-like peak was identified in the RICs for *m/z* 546, generating one major peak at retention time 28.15 min (RRT 1.09), which gave MS^2 (546→) and MS^3 (546→467→) spectra corresponding to the oxidised/GP-derivatised sitosterol (Figure 5.27). Campesterol (C^5-24-Me-3β-ol) and sitosterol (C^5-24-Et-3β-ol) are plant sterols. Plant sterols are structurally related to cholesterol and differ in their chemical structure only due to the presence of an additional methyl (campesterol, C^5-24-Me-3β-ol) or ethyl (sitosterol, C^5-24-Et-3β-ol) group at the C-24 position of the side chain. These plant sterols may be present in the brain with a dietary origin [185], but also their detection may be a result of laboratory contamination of sample from rubber derived materials. The ratios of campesterol and sitosterol to cholesterol were 0.005 and 0.002, respectively in this work. Luthjöhann *et al.* in 2002 [185] determined that the ratios of campesterol and sitosterol to cholesterol in adult mouse were 0.001 and 0.0003, respectively.

Additionally, a number of oxysterol MS^3 ($[M]^+$→$[M-79]^+$→) spectra for $[M]^+$ ions, *m/z* 546, 548, 566, 568 were recorded, which did not correspond to available GP-derivatised standards, and their spectra were not readily interpretable. Table 5.3 lists all sterols and oxysterols identified in the embryonic (E11) mouse CNS in this work.

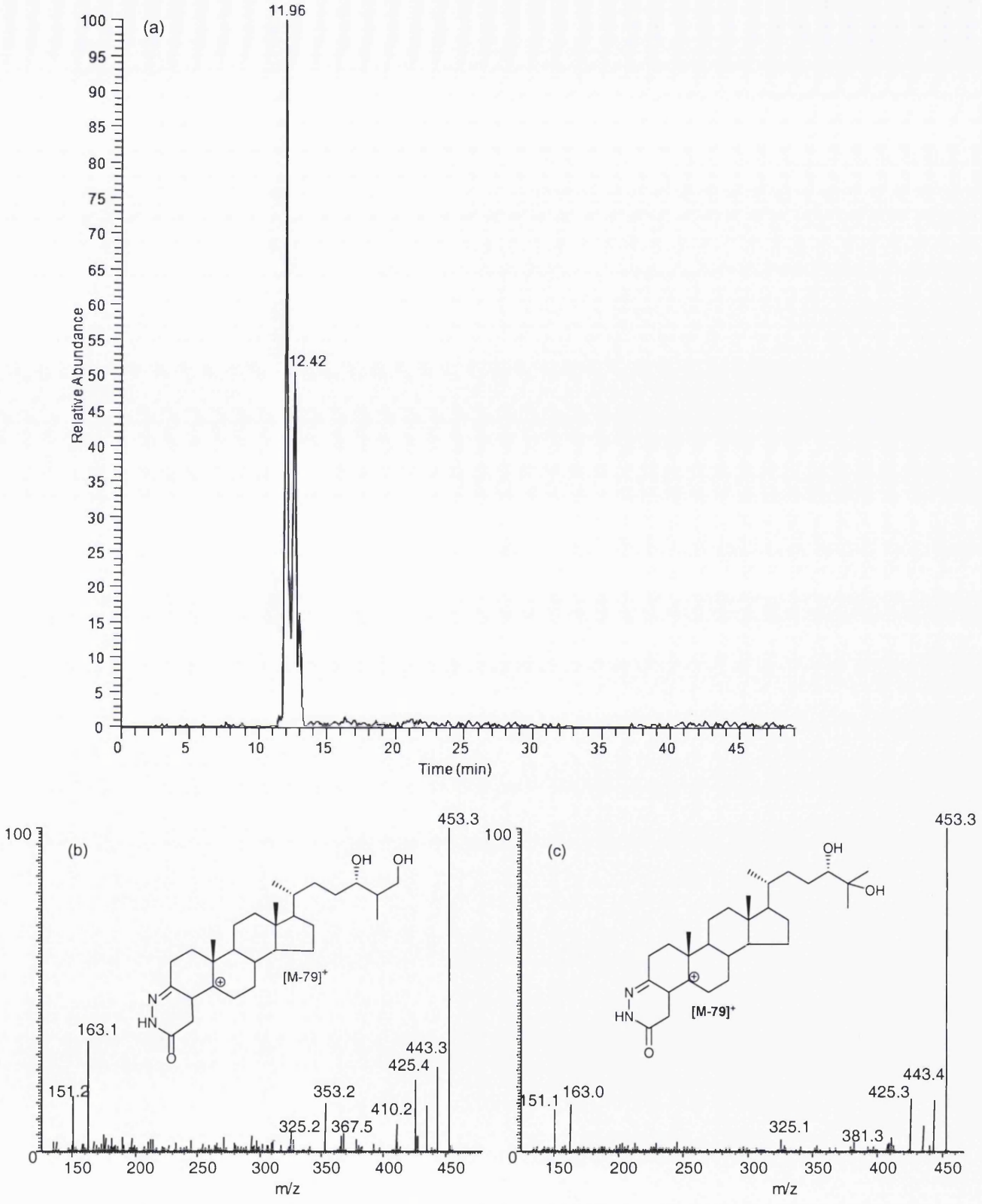

Figure 5.28 (a) RIC for the oxidised/GP-derivatised oxysterol $[M]^+$ ions, *m/z* 550 from the cortex of CNS. MS^3 (550→471→) spectrum of the chromatographic peak eluting at (b) 11.96 min (24,27-dihydroxycholesterol) and (c) 12.42 min (24,25-dihydroxycholesterol) from the cortex sample.

Monohydroxycholesterols can be converted by extrahepatic P450 (CYP) enzymes to dihydroxycholesterols [24,36,37,68,154]. Figure 5.28 shows RIC for *m/z* 550 corresponding to the $[M]^+$ ion of oxidised/GP-derivatised dihydroxycholesterols in the cortex region. The chromatographic peak eluting at 11.96 min (RRT 0.46) corresponds to possibly 24,27-dihydroxycholesterol. The location of one hydroxyl group on C-24 is indicated in the MS^3 (550→471→) spectrum by the fragment ion at *m/z* 353 ('*f), and the MS^2 (550→) and MS^3 (550→471→) spectra of this chromatographic peak were identical to previously the reported oxidised/GP-derivatised 24,27-dihydroxycholesterol in rat brain in this work. The second chromatographic peak eluting at 12.42 min (RRT 0.48) also corresponds to a dihydroxycholesterol with the additional hydroxyl group in the C17 side chain, The reduced abundance of the MS^3 (550→471→) fragment ions at *m/z* 151, 163, 177, and 353 (compare to 24,27-dihydroxycholesterol, Figure 5.28b) are indicative of the second additional hydroxyl group being located on C-25, giving 24,25-dihydroxycholesterol (Figure 5.28c).

The cholesterol 5,6-*seco*-sterol, 3β-hydroxy-5-oxo-5,6-*seco*cholestan-6-al, and its aldol, 3,5-dihydroxy-B-norcholestane-6-carboxyaldehyde have been found in rat brain in this study. Both molecules possess an oxo group reactive to GP hydrazine and give an $[M]^+$ ion at *m/z* 552. The RIC for *m/z* 552 revealed two chromatographic peaks eluted at 21.96 min (RRT 0.85) and 22.86 min (RRT 0.88) (Figure 5.29a), which are identical to retention times of the authentic 5,6-*seco*-sterol and its aldol standards. The MS^2 (552→) spectra recorded were identical to those of the authentic standards (Figure 5.29b). The presence of the 5,6-*seco*-sterol and its aldol was evident in three of the mouse CNS regions investigated in this study.

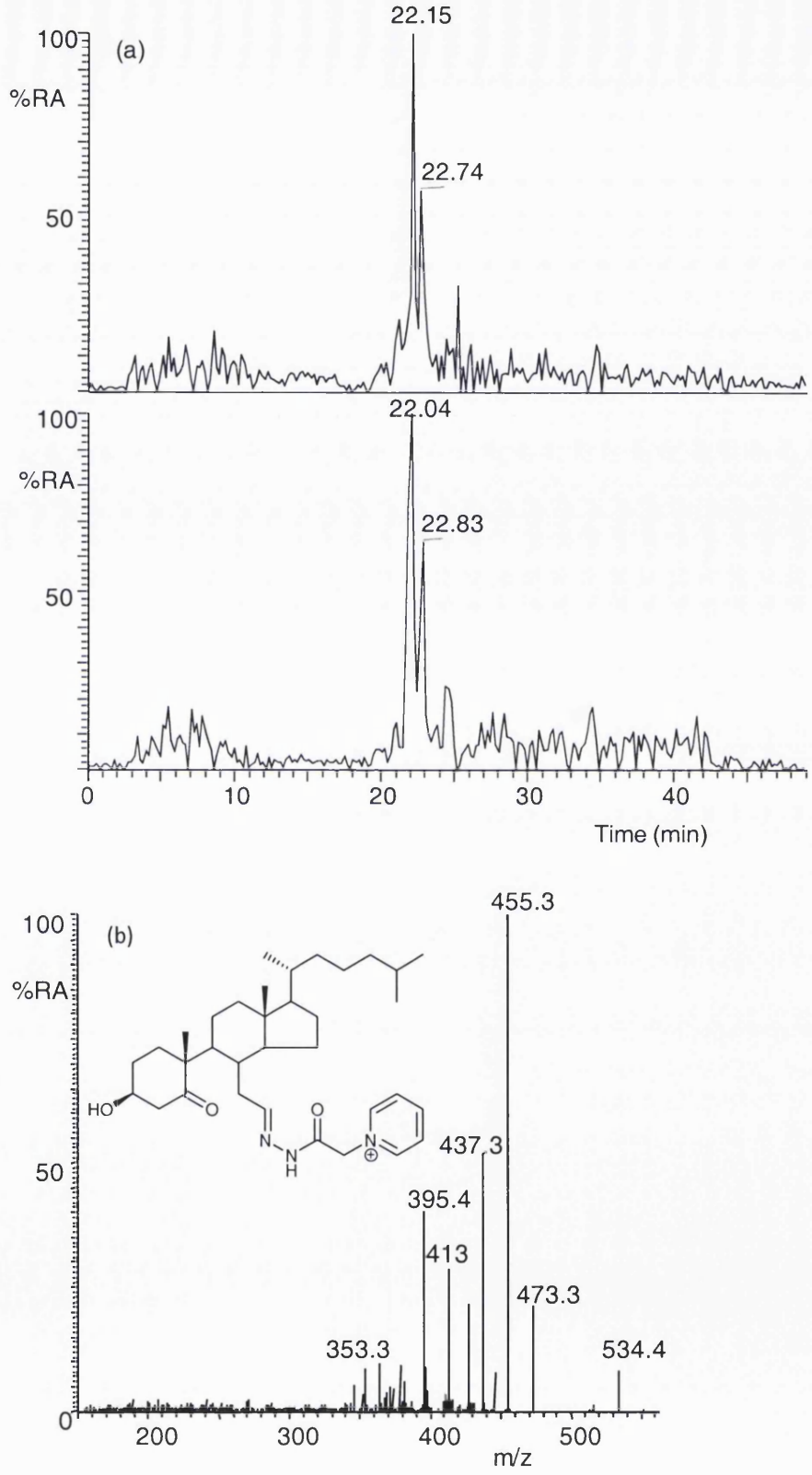

Figure 5.29 (a) RIC for the oxidised/GP-derivatised oxysterol $[M]^+$ ions, *m/z* 552 from the cortex (upper trace) and spinal cord (lower trace) regions of CNS. (b) MS^2 (552→) spectrum of the chromatographic peak eluting at 21.96 min (5,6-*seco*-sterol) from the cortex sample.

Table 5.3 Oxysterol/sterol content of foetal E11 mouse brain regions ventral midbrain (VM), cortex (Ctx) and spinal cord (SC) as determined by cap-LC-MS^n using the LCQ^{duo} mass spectrometer

Sterol/Oxysterol	$[M]^+$ (*m/z*)	Retention time, min (RRT)	Trivial name of sterol/oxysterol identified (concentration wet brain)
$C^{5,x}$-3β-ol	516.4	24.46 (0.95)	Desmosterol (37.5 μg/g[a]; 17 μg/g[b]; 34 μg/g[c])[d,h]
C^5-3β-ol	518.4	25.83 (1.00)	Cholesterol (1.2 mg/g[a,c]; 1.15 mg/g[b])[d,h]
5α-C-7-en-3β-ol	518.4	22.98 (0.89)	Lathosterol (14.1 μg/g[a]; 13.1 μg/g[b]; 6.2 μg/g[c])[d,h]
C^5-24-methyl-3β-ol	532.4	26.99 (1.05)	Campesterol (6.5 μg/g[a]; 4.2 μg/g[b]; 3.0 μg/g[c]) [d,h]
C^5-24-ethyl-3β-ol	546.4	28.15 (1.09)	Sitosterol (2.0 μg/g[a]; 1.6 μg/g[b]; 1.2 μg/g[c]) [d,h]
$C^{5,x}$-y,3β-diol	532.4	17.80 (0.70)	24S,25-Epoxycholesterol (10.1±2.2ng/g[a]; 5.1±1.1ng/g[b]; 18±1.0 ng/g[c]) [f,h]
C^5-3β-ol-x-one	532.4	19.37 (0.75)	24-Oxocholesterol (35.6±2.1ng/g[a]; 13.2±0.1ng/g[b]; 60.1±0.2ng/g[c]) [f,h]
C^4-3,6-dione	532.4	21.96 (0.85) 22.41 (0.87)	6-Oxocholestenone[e] (185.0±0.9ng/g[a]; 19.0±0.3ng/g[b]; 100.5±0.2 ng/g[c]) [f,g]
C^5-x,3β-diol	534.4	16.72 (0.65) 18.70 (0.72) 19.14 (0.74) 19.63 (0.76) 21.31 (0.82) 22.53 (0.87) 23.10 (0.89)	22R-Hydroxycholesterol (3.8±0.9ng/g, 2.3±0.8ng/g, 2.9±1.0ng/g[c]) [f] 24S-Hydroxycholesterol (26.3±0.8ng/g[a]; 13.3±0.1ng/g[b]; 10.9±0.3 ng/g[c]) [f,h] 25-Hydroxycholesterol (19.3±0.8ng/g[a]; 13.7±0.4ng/g[b]; 9.9±0.4 ng/g[c]) [f,h] 27-Hydroxycholesterol (9.7±0.3ng/g[a]; 8.9±0.4ng/g[b]; 7.3±0.5ng/g[c]) [f] 7β-Hydroxycholesterol (13.3±0.1ng/g[a]; 18.9±0.8ng/g[b]; 15.3±1.2 ng/g[c]) [f,g,h] 7α-Hydroxycholesterol (23.7±0.8ng/g[a]; 26.9±0.2ng/g[b]; 30.1±0.2 ng/g[c]) [f,g,h] 6β-Hydroxycholest-4-ene-3-one (568.9±9.8ng/g[a]; 109.2±10.1 ng/g[b]; 100.1±5.8ng/g[c]) [f,g,h]
C-x,y,z-triene-3β,x,y-triol	546.4	19.37 (0.75)	Detected, not characterised (2.0±0.8 ng/g[a,f]; 3.1±0.4 ng/g[b,f]; n/d)[h]
C- x,y,z -triene-3β,x,y-triol	546.4	20.96 (0.81)	Detected, not characterised (9.3±0.3 ng/g[a,f]; n/d; n/d)[h]
C-x,y-diene-3β,x,y-triol C-x,y-diene-3β,x,y-triol	548.4 548.4	11.78 (0.46) 21.76 (0.84)	Detected, not characterised (3.9 ±0.1 ng/g[a]; 1.9±0.8 ng/g[b]; 1.1±0.2 ng/g[c]) [f,h] Detected, not characterised (7.2±0.3ng/g[a]; 9.4±0.2 ng/g[b]; 2.1±0.2 ng/g[c]) [f,h]
C^5-24,25,3β-triol C^5-24,27,3β-triol	550.4 550.4	12.42 (0.48) 11.96 (0.46)	24,25-Dihydroxycholesterol (70.4±0.2ng/g[a]; 38.1±0.9ng/g[b]; 54.2±0.4 ng/g[c]) [f,h] 24,27-Dihydroxycholesterol (7.3±0.5 ng/g[a]; 6.2±0.4 ng/g[b]; 4.3±0.3 ng/g[c]) [f,h]
5,6-*Seco*-sterol/ Aldol	552.4 552.4	21.96 (0.85) 22.83 (0.88)	5,6-*seco*-sterol (60.3±0.2ng/g[a]; 30.2±0.4ng/g[b]; 10.1±0.3ng/g[c]) [f,h] Aldol (30.2±0.4 ng/g[a]; 21.2±0.6 ng/g[b]; 8.4 ±0.5 ng/g[c]) [f,h]
C^5-x,y-epoxy-3β-ol	564.4	16.73 (0.65)	24S,25-Epoxycholesterol (165.5±2.9ng/g[a]; 91.1±8.9ng/g[b]; 87.1±4.9ng/g[c]) [f,h]
C^5-3β,x,y,z-tetraol	566.4	14.47 (0.56)	Detected, not characterised[h]
5α-C-3β,x,y,z-tetraol	568.4	12.16 (0.47)	Detected, not characterised[h]

[a] An estimated quantity of oxysterol/sterol in the cortex (Ctx).

[b] An estimated quantity of oxysterol/sterol in the spinal cord (SC).

[c] An estimated quantity of oxysterol/sterol in the ventral midbrain (VM).

[d] As determined by GC-MS in Karolinska Institutet, Stockholm, Sweden.

[e]Both 3-GP and 6-GP derivatives formed.

[f]Mean ± standard deviation of triplicate injection (n=3).

[g]Potential autoxidation product as determined in Chapter 4.

[h]Found in the oxysterol fraction (U2) from Unisil column.

Discussion

In this study three regions of embryonic (E11) mouse CNS have been profiled for their sterol content using capillary LC and tandem mass spectrometry. The pattern of oxysterols in three regions of CNS was not significantly different, possibly because at this stage of development (E11) their origin is mainly from the dam rather than *de novo* brain biosynthesis. The level of cholesterol was significantly lower than that found in adult mouse brain, and the ratios of desmosterol and lathosterol, which are precursors of cholesterol, to cholesterol ~0.01 are greatly elevated when compared to the adult (0.001) [196,197]. This indicates that there is a high rate of cholesterol synthesis in CNS at this stage of development.

The levels of oxysterols identified in E11 CNS were extremely low (estimated 4-165 ng/g wet weight). The identified oxysterols include 7α-, 7β-, 24S-, 25-hydroxycholesterols, 24,25- and 24,27-dihydroxycholesterols, and 24S,25-epoxycholesterol. 24S-Hydroxycholesterol is biosynthesised exclusively in the brain by the action of cytochrome P450 enzyme CYP46A1 on preformed cholesterol, and is the most abundant oxysterol in adult brain [19,185,193]. This oxysterol is fluxed through the blood-brain barrier into the circulation. The level of 24S-hydroxycholesterol is between 40–50 μg/g in adult mouse brain [185], whereas the level of this oxysterol in the embryonic (E11) CNS was extremely low only between 10 - 26 ng/g. As a result, the current data suggests that the enzyme CYP46A1 required for hydroxylation of cholesterol to 24S-hydroxycholesterol in the brain is minimally active at the E11 stage of development. This finding is in accordance with a report by Tint and colleagues [196] who studied the Dhcr 7 knock out mouse. They have suggested that the blood brain barrier begins to form at E10 stage of foetus development and only after this is the brain required to biosynthesise essentially all of its own cholesterol. Before this stage of development mouse foetus receives most of its sterols from its mother, and this explains the low cholesterol level

and the high rate of synthesis at the E11 stage of development of the mouse CNS. Tint *et al.* [196] has detected that low levels of CYP46A1 at E11.5, and that its expression starts to increase after the E18-19 stage of development. However, maximal expression of this enzyme appears to occur only after about 3 weeks after birth when significant excretion of sterol from the CNS becomes necessary [196,198].

In contrast, the level of 24S,25-epoxycholesterol in the three CNS regions was between 87-165 ng/g, which is significantly higher than 24S-hydroxycholesterol. 24S,25-Epoxycholesterol is unique in that it is synthesised in a shunt in the mevalonate pathway, parallel to cholesterol and utilising the same enzymes required for cholesterol biosynthesis [153,160,161]. Consequently, 24S,25-epoxycholesterol is not a metabolite of cholesterol. Therefore, any cell type that can synthesise cholesterol should also have the capacity to generate 24S,25-epoxycholesterol, because 24S,25-epoxycholesterol is biosynthesised in the same pathway as cholesterol. Therefore, a comparatively high abundance of 24S,25-epoxycholesterol in the E11 mouse CNS may be a reflection of an active mevalonate pathway which simultaneously synthesises cholesterol at this stage of development.

In summary, this section of the thesis presents the first measurement of the oxysterol levels and their profile in the developing CNS. The data indicate that, at the E11 stage of development the oxysterol level of mouse CNS is low, while 24S,25-epoxycholesterol, a putative LXR ligand, is present at relatively high levels. These results, together with the finding the LXR receptors are expressed in the developing brain [199], suggest that 24S,25-epoxycholesterol may play a role during cortical and spinal cord development.

5.3 Oxysterols in primary cortical neurons derived from embryonic rat

Brain cholesterol metabolism is well balanced by a low rate of synthesis, elimination of excessive cholesterol after conversion into 24S-hydroxycholesterol and release into the systemic circulation. In the embryonic stage, neurons meet their cholesterol requirements by *de novo* synthesis [33,183]. The cholesterol synthesis rate and cholesterol content increase dramatically during

brain development. However, little is known concerning oxysterol content in cells of the CNS, and therefore, their specific roles and contribution to maintenance of cholesterol homeostasis. The majority of cholesterol present in the CNS resides in two different pools: (i) in the myelin sheath, (ii) in the plasma membrane of astrocytes and neurons [33,183]. Much of the cholesterol in the brain goes to make up the myelin sheaths coating axons. Neuronal cells contain only a small proportion of total brain cholesterol (~2%) [143]. The enzyme CYP46A1 is only expressed in neurons, indicating that the excretion of the cholesterol from the brain is initiated in neurons rather than in glial cells. It is evident that only a small pool of total brain cholesterol is available for CYP46A1 mediated cholesterol metabolism [143]. However, this pool of cholesterol has a high turnover rate in contrast to the bulk of cholesterol which is turned over more slowly. The half-life of brain cholesterol in adult rats is 2-4 months [19]. In neonates, CYP46A1 appears to have low activity, which greatly increases after birth, probably due to increased cholesterol availability [193].

The current study was further extended to the profiling of oxysterols in primary cortical neurons derived from embryonic rat at day 19 (E19). The analytical scheme used for oxysterol isolation from primary cortical neurons and their analysis is shown in Figure 2.6. Medium and cells were separated, and sterols were extracted, then cholesterol was separated from oxysterols by straight-phase chromatography, and the cholesterol U1 and oxysterol U2 fractions were oxidised with cholesterol oxidase, derivatised with Girard P (GP) hydrazine. The derivatised oxysterols were then separated on the reversed phase capillary column and analysed on the LCQ^{duo} mass spectrometer. Full scan MS, also MS^2 ($[M]^+ \rightarrow$) and MS^3 ($[M]^+ \rightarrow [M-79]^+ \rightarrow$) spectra were recorded for all potential sterols/oxysterols, again advantage was made of the neutral loss of -79 and -107 Da in MS^2 spectra. TICs were generated for all relevant sterol/oxysterol related MS^2 and MS^3 scans. The MS, MS^2 ($[M]^+ \rightarrow$) and MS^3 ($[M]^+ \rightarrow [M-79]^+ \rightarrow$ and $[M]^+ \rightarrow [M-107]^+ \rightarrow$) spectra derived from the resulting chromatographic peaks were assessed. The combined information allowed complete or partial identification of the compounds.

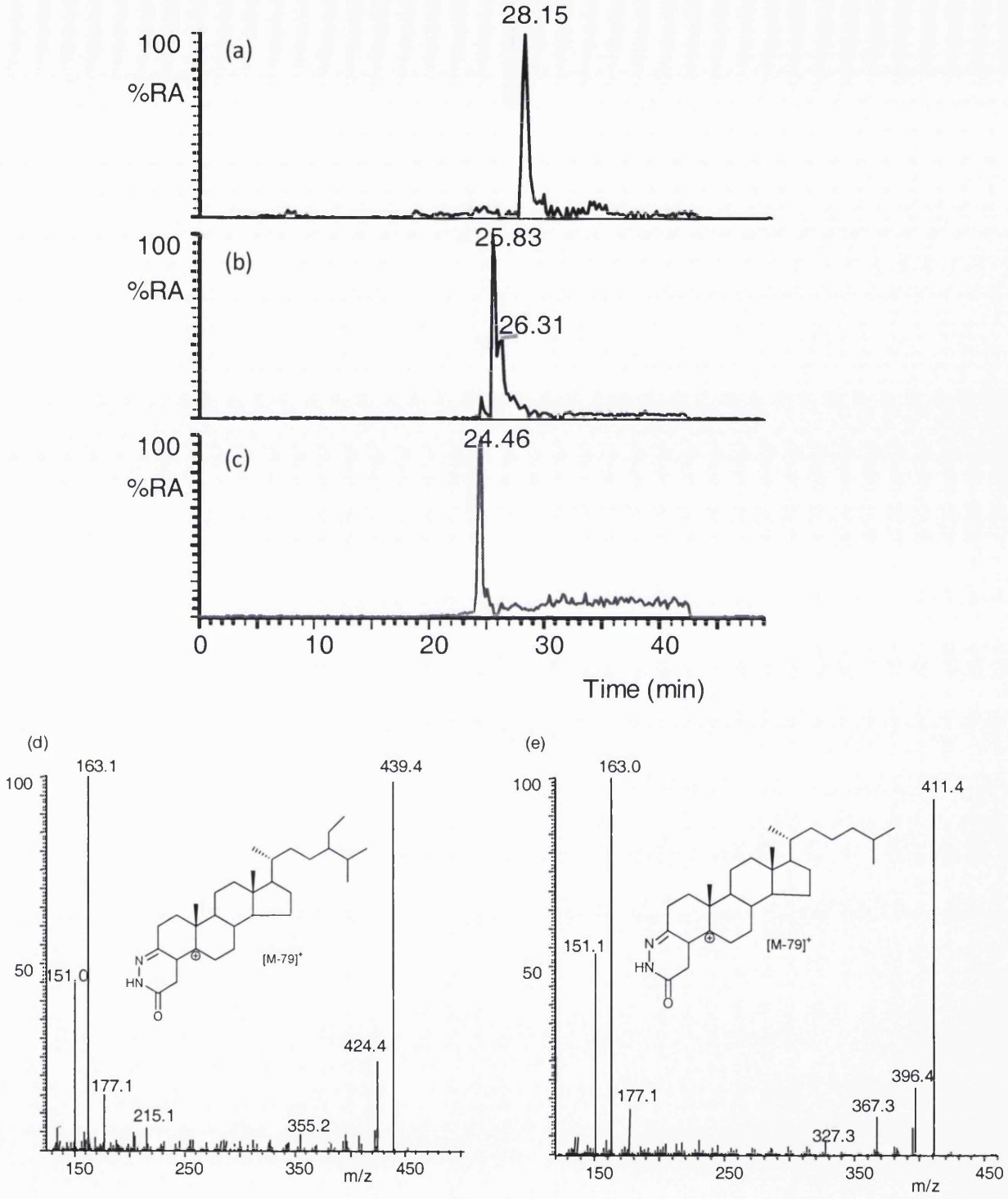

Figure 5.30 RICs for oxidised/GP-derivatised $[M]^+$ ions, *m/z* (a) 546, (b) 518, (c) 516. MS^3 ($[M]^+ \rightarrow [M\text{-}79]^+ \rightarrow$) spectra of the derivatised sterol, (d) eluting at 28.15 min (sitosterol), and (e) eluting at 25.83 min (cholesterol). Chromatographic conditions are described in section 2.9.

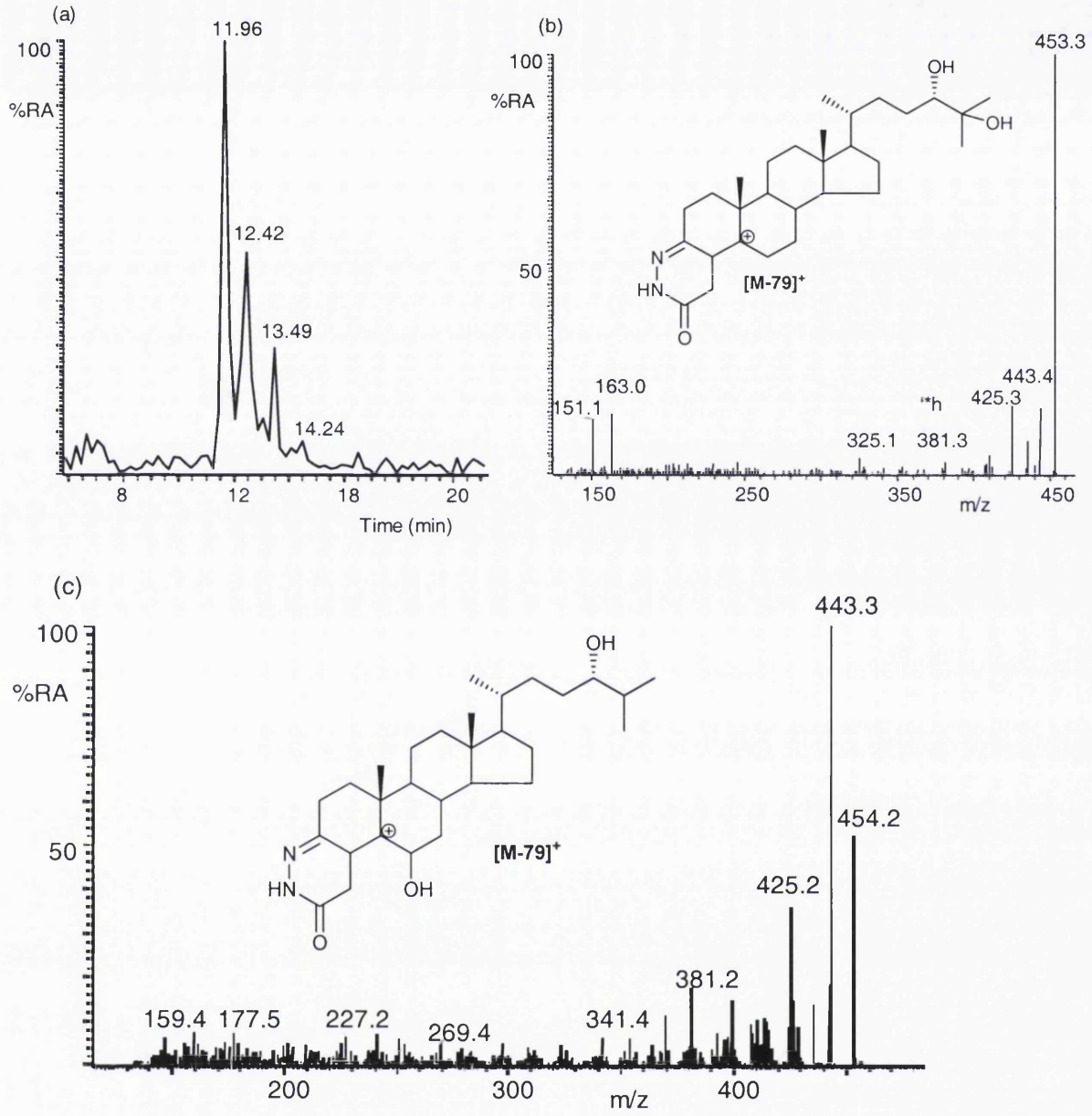

Figure 5.31 (a) RIC for oxidised/GP-derivatised dihydroxycholesterol $[M]^+$ ions, *m/z* 550. MS^3 (550→471→) spectrum of the chromatographic peak eluting at (b) 12.42 min (24,25-dihydroxycholesterol) and (c) 13 min (6,24-dihydroxycholesterol) from cortical neurons. Chromatographic conditions are described in section 2.9.

Using the methodology seventeen sterols/oxysterols were identified in the medium of primary cortical neurons (see Table 5.5). Oxysterols were in low abundance in the sample from cells, only approximately 3% in comparison to the sample from medium, and the identification of some oxysterols were not possible due to low quality of MS^3 spectra.

The RICs for *m/z* 518, 516 and 546 corresponding to the $[M]^+$ ion of the oxidised/GP-derivatised cholesterol, desmosterol, and sitosterol revealed chromatographic peaks at 28.15 (RRT 1.08), 25.83 (RRT 1.00), and 24.46 (RRT 0.95) min (Figure 5.30a-c). The identification of these three sterols was confirmed by recording their MS, MS^2, and MS^3 spectra and comparing their retention times and MS^n spectra to authentic standards (see Figure 5.30d-e).

Zhang and colleagues [24,154] have identified the presence of dihydroxycholesterols in rat glial cells. Figure 5.31a shows the RIC for *m/z* 550 corresponding to the $[M]^+$ of oxidised/GP-derivatised dihydroxycholesterols in cortical neurons. The chromatographic peak eluting at 11.96 min (RRT 0.46) corresponds to 24,27-dihydroxycholesterol, and its MS^2, and MS^3 spectra were identical to this authentic standard. The chromatographic peak at 12.42 min (RRT 0.48) corresponds to retention time of the authentic 24,25-dihydroxycholesterol. The location of one hydroxyl group on C-24 is indicated by the MS^3 fragment ion at *m/z* 353 ('*f), also the presence of a '*h (*m/z* 381) suggests the location of the second hydroxyl group on C-25, giving 24,25-hydroxycholesterol. The MS^2 (550→) and MS^3 (550→471→) spectra of the third chromatographic peak eluting at 13.49 min (RRT 0.52) suggest a dihydroxycholesterol with the additional group in the A/B rings. Earlier study with rat brain suggests that this is 6,24-dihydroxycholesterol. The chromatographic peak eluting at 14.24 min (RRT 0.55) corresponds to elution of 7α,25-dihydroxycholesterol, but the MS^2 (550→) and MS^3 (550→471→) were not of sufficient quality for the identification.

The RICs were generated for oxidised/GP-derivatised monohydroxycholesterols (*m/z* 534), oxocholesterols, epoxycholestenols and dihydroxycholestadienes (*m/z* 532), and also for *m/z* 544, 564. The compounds with those *m/z* values were identified by comparing their RRT, MS, MS^2 ($[M]^+$→) and MS^3 ($[M]^+$→$[M-79]^+$→) spectra to authentic standards, and their identities are summarised in Table 5.4. The presence of campesterol, 24S-, 27-, 6β-, 7α-, 7β-hydroxycholesterols, 24-oxocholesterol, and 24S,25-epoxycholesterol were identified in the cortical neurons. The TIC for the MS^3 transition 564→485→ is shown in Figure 5.32, and revealed only one

chromatographic peak corresponding to the retention time of the oxidised/GP-derivatised reference 24S,25-epoxycholesterol, and its MS^3 (564→485→) spectrum was identical to the MS^3 (564→485→) spectrum of the authentic 24S,25-epoxycholesterol. This study shows that 24S,25-epoxycholesterol is synthesised in neurons, and 24S,25-epoxycholesterol was recently established as a potent regulatory molecule of cellular cholesterol homeostasis [160,161]. However, its effects on cells in the CNS have yet to be described. 6β-, 7α-, 7β-Hydroxycholesterols, 6-oxocholestenone are autoxidation products of cholesterol as established in chapter 3.

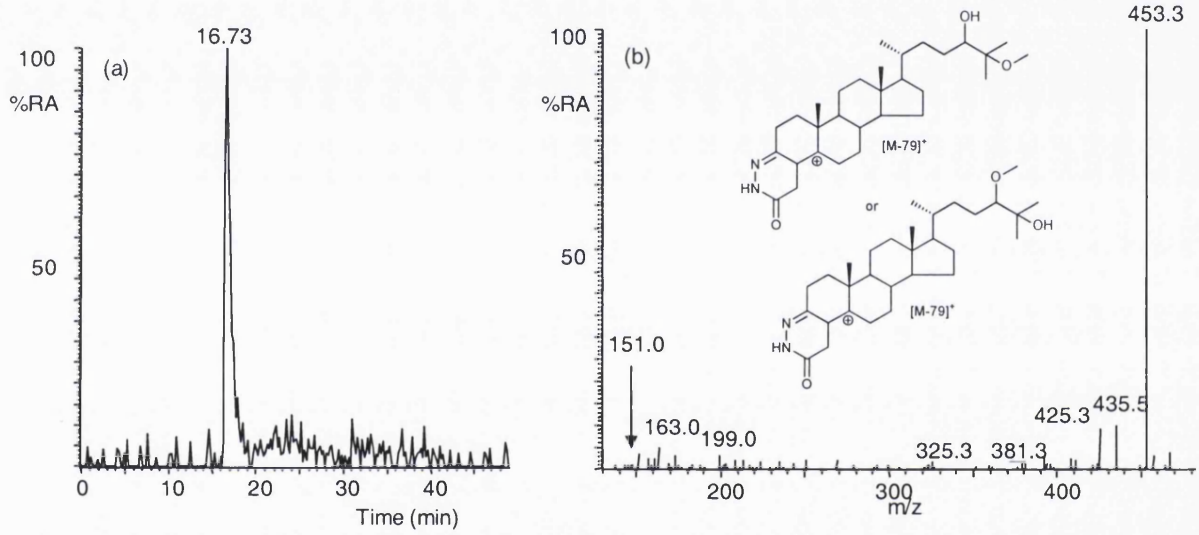

Figure 5.32 (a) TIC the MS^3 transition 564→485→ for oxidised/GP-derivatised oxysterol $[M]^+$ ions, *m/z* 564 for cortical neurons. (b) MS^3 (564→485→) spectrum of the chromatographic peak eluting at 16.73 min (24-hydroxy,25-methoxycholesterol or 24-methoxy,25-hydroxycholesterol) from cortical neurons. Chromatographic conditions are described in section 2.9.

It was possible to obtain semi-quantitative information, using the ion-trap mass spectrometer to record MS^2 ($[M]^+$→) spectra, and by generating RICs for MS^2 transitions $[M]^+$→$[M-79]^+$. The amount of identified sterols/oxysterol injected on the reversed phase column was calculated from the chromatographic peak area for the MS^2 transition $[M]^+$→$[M-79]^+$ using the external calibration plot generated for the oxidised/GP-derivatised authentic 24S-hydroxycholesterol and 25-hydroxycholesterol.

Table 5.4 Sterol/Oxysterols content of primary cortical neurons as determined by cap-LC-MS^n

Sterol	$[M]^+$ (*m/z*)	Retention time, min (Relative retention time)	Trivial name of sterol identified (ng per 10^8 cells)
$C^{5,x}$-3β-ol	516.4	24.46 (0.95)	Desmosterol[b,d]
C^5-3β-ol	518.4	25.83 (1.00)	Cholesterol[b,d]
C^5-24-methyl-3β-ol	532.4	27.05 (1.05)	Campesterol[b,d]
C^5-24-ethyl-3β-ol	546.4	27.12 (1.09)	Sitosterol[b,d]
$C^{5,22}$-24-ethyl-3β-ol	544.4	27.64 (1.07)	Stigmasterol[b,d]
C^5-3β-ol-x-one	532.4	19.37 (0.75)	24-Oxocholesterol (28.0±0.8 ng/10^8 cells) [c,d]
$C^{5,x}$-y,3β-diol	532.4	17.80 (0.70)	24,25-Epoxycholesterol (37.8±1.2 ng/10^8 cells) [c,d]
C^4-3,6-dione	532.4	21.96 (0.85) 22.41 (0.87)	6-Oxocholestenone[a] (100.2±1.8 ng/10^8 cells) [b,c,d,e]
C^5-x,3β-diol	534.4	18.70 (0.72) 19.63 (0.76) 21.31 (0.82) 22.53 (0.87) 23.10 (0.89)	24S-Hydroxycholesterol (87.9±0.9 ng/10^8 cells) [c,d] 27-Hydroxycholesterol (29.3±0.5 ng/10^8 cells) [c,d] 7β-Hydroxycholesterol (96.4 ±0.8 ng/10^8 cells) [b,c,d,e] 7α-Hydroxycholesterol (108.1±3.7 ng/10^8 cells) [c,d,e] 6β-Hydroxycholest-4-ene-3-one(143.6±3.4 ng/10^8 cells)[b,c,d,e]
C-x,y-diene-3β,x,y-triol	548.4	11.74 (0.46)	Detected, not characterised (30.2±0.6 ng/10^8 cells) [c,d]
C^4-3β-ol-x,y,z-trione	562.4	24.29 (0.95)	Detected, not characterised (20.3 ±1.7 ng/10^8 cells) [c,d]
C^4-w,x,y,z-tetraone	560.4	27.08 (1.06)	Detected, not characterised (87.7±1.2 ng/10^8 cells) [c,d]
C^5-24,25,3β-triol	550.4	12.42 (0.47)	24,25-Dihydroxycholesterol (65.3±1.1 ng/10^8 cells) [c,d]
C^5-24,27,3β-triol	550.4	11.91 (0.46)	24,27-Dihydroxycholesterol (59.9±0.3 ng/10^8 cells) [c,d]
C^5-6,24,3β-triol	550.4	13.49 (0.53)	6,24-Dihydroxycholesterol (56.5±0.5 ng/10^8 cells) [c,d]
C^5-7α,25,3β-triol	550.4	14.24 (0.55)	7α,25-Dihydroxycholesterol (35.2±0.1 ng/10^8 cells) [c,d]
C^5-x,y-epoxy-3β-ol	564.4	16.73 (0.65)	24,25-Epoxycholesterol (65.4±0.3 ng/10^8 cells) [c,d]

[a]Both 3-GP and 6-GP derivatives formed.

[b]Found in the cholesterol fraction (U1) from Unisil column.

[c]Mean ± standard deviation of triplicate assays (n=3).

[d]Found in the oxysterol fraction (U2) from Unisil column.

[e]Potential autoxidation products as determeined In chapter 4.

Discussion

In this section of the thesis primary cortical neurons have been profiled for their sterol content. The results demonstrate that embryonic neurons have the capacity to synthesise the essential molecule - cholesterol, and metabolise preformed cholesterol to oxysterols. It is known that cholesterol content and its synthesis rate increase drastically during brain development. Neurons appear to have a low rate of synthesis of cholesterol, in relation to glial cells probably because their primary function is the generation and propagation of electrical impulses [148]. The results presented in Table 5.4 demonstrate that oxysterols are in low abundance in cortical

neurons. 24S-Hydroxycholesterol was found at a level of 87 ng from 10^8 cells. This result is particularly relevant as CYP46A1 is expressed exclusively in the neurons [46,92,148,198]. 24S-Hydroxycholesterol is exclusively synthesised in these cells and its level is likely to reflect that of cholesterol itself. Furthermore, the pool of cholesterol in neurons has a high turnover rate in adult brain, which is in contrast to the bulk of brain cholesterol found in cells devoid of CYP46A1 [198]. Accordingly, 24S-hydroxycholesterol plays a key role in the removal of cholesterol from the brain.

This study has identified 24S,25-epoxycholesterol, which is present in neurons at approximately the same level as 24S-hydroxycholesterol. 24S,25-Epoxycholesterol is formed by the action of squalene epoxidase on 2,3-monoepoxysqualene (2,3-oxidosqualene) prior to cyclisation by oxidosqualene:lanosterol cyclase, resulting in a final 24S,25-epoxycholesterol rather than cholesterol (Figure 1.10). Therefore, 24S,25-epoxycholesterol synthesis parallels cholesterol synthesis. Our result is in agreement with the study by Wong *et al.* [160,161], who have shown that 24S,25-epoxycholesterol is synthesised in primary human brain cells, specifically astrocytes and neurons, and plays a likely role in brain cholesterol homeostasis.

Brain cells have also been found to metabolise oxysterols. Dihydroxycholesterols were identified as 24,25-, 24,27-, 6,24-, 7α,25-dihydroxycholesterols in cortical neurons, and their levels were between 23 – 45 ng per 10^8 cells. The data agrees well with that of Zhang *et al.* [24,154], who studied the metabolism of 24-, 25- and 27-hydroxycholesterols in rat brain microsomes and cultures of Schwann cells, astrocytes and neurons. They identified 7α,25- and 7α,27-dihydroxycholesterols. However, 24-hydroxycholesterol (C^5-3β,24-diol) was not found to be 7α-hydroxylated by brain microsomes, or cultures of Schwann cells, astrocytes, or neurons, and our data confirms this. Recently, Mast *et al.* [22] have shown that CYP46A1 is also responsible for the metabolism of 24S-hydroxycholesterol to 24,25- and 24,27-dihydroxycholesterols (C^5-3β,24S,25-triol and C^5-3β,24S,27-triol), in both cultures of HEK293 cells with human CYP46A1 cDNA, and an *in vitro* reconstituted system with recombinant enzyme, and our data confirms this.

Chapter 6

The potential of sterol analysis for the prenatal diagnosis of Smith-Lemli-Opitz syndrome by mass spectrometry

6. *Introduction*

Smith-Lemli-Opitz syndrome (SLOS) is a recessively inheritable metabolic disorder involving multiple malformations and mental retardation that is caused by an inborn error in the cholesterol synthesis pathway [200-203]. In 1993, Irons *et al.* [201,204] described a defect in cholesterol biosynthesis in patients with SLOS. Affected patients have difficulty forming cholesterol from its precursor 7-dehydrocholesterol (7-DHC) in the last steps of cholesterol biosynthesis (Figure 6.1). This block results in a characteristic pattern of low cholesterol concentrations and elevated levels of 7-DHC and its isomer 8-dehydrocholesterol (8-DHC) in body fluids and tissues [205-207]. This is due to a reduced activity of the enzyme catalysing the last step in the synthesis of cholesterol, 7-dehydrocholesterol-Δ^7-reductase [118,201,204,208]. In comparison to cholesterol, 7-DHC is present in control blood at very low levels, 7-dehydrocholesterol 100 ng/mL [202], and cholesterol 2 mg/mL [81,165], and in amniotic fluid, 7-dehydrocholesterol 1 ng/mL [202] and cholesterol 10-100 µg/mL [202,209]. This characteristic sterol pattern is used to biochemically confirm the diagnosis of SLOS in suspected patients [201,202,210]. Because cholesterol, 7-DHC and 8-DHC are present in all body fluids and tissues, diagnosis of affected patients can be carried out even in autopsy specimens [211]. It has been suggested that the syndrome could be diagnosed prenatally by identification of elevated levels of 7/8-DHC in amniotic fluid [206]. Kelley *et al.* have confirmed this hypothesis in 1994 [202,211]. They measured the level of dehydrocholesterols (DHCs) by gas chromatography – mass spectrometry (GC-MS) analysis of amniotic fluid, and therefore established a method for the prenatal diagnosis of SLOS [119,202,207,211,212]. Batta *et al.* [205] and Starck *et al.* [84] reported the diagnosis of SLOS in newborn blood spotted on filter paper by GC-MS technology making newborn screening using Guthrie blood spots possible. Most recently Johnson *et al.* [98] have described the use of the mono-(dimethylaminoethyl) succinyl ester as a derivative for sterols and analysed the derivatised sterols by ES tandem mass spectrometry. They measured the dehydrocholesterol to cholesterol ratio in plasma and plasma spotted onto filter paper for the diagnosis of SLOS. Zimmerman *et al.* [213] and

Seedorf *et al.* [214] used time-of-flight secondary ion mass spectrometry analysis for the measurement of DHC to cholesterol ratio in blood spots.

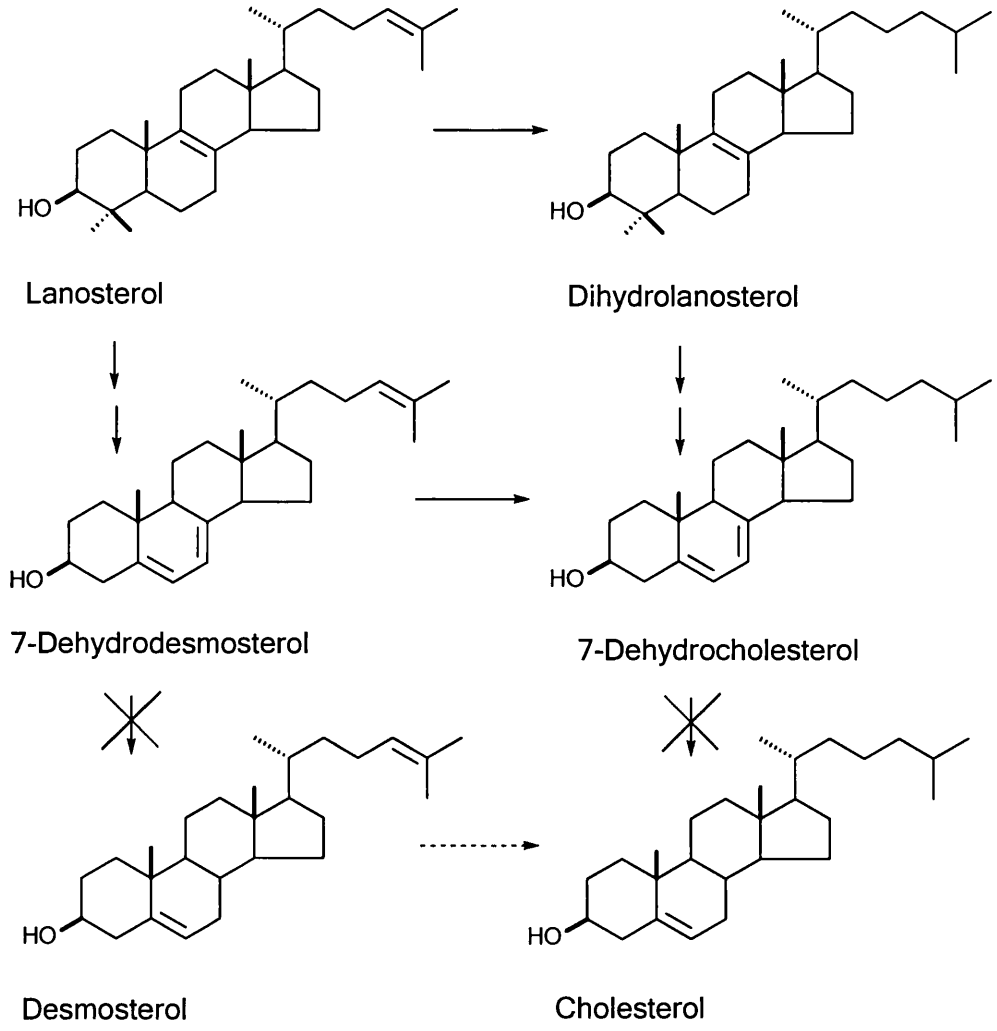

Figure 6.1 The latter part of the cholesterol biosynthesis pathway. Cholesterol can be biosynthesised from the intermediate lanosterol via intermediates which have a saturated side chain (right side) or from precursors which retain the C-24 double bond (left side). The symbol X represents the block in the SLOS.

This chapter describes the use of our derivatisation methodology for the analysis of sterols by capillary LC tandem mass spectrometry (MS^n) for the accurate prenatal diagnosis of SLOS through amniotic fluid analysis. Additionally, this methodology was applied for the diagnosis of SLOS from newborn blood spots. Briefly, in this method sterols are first oxidised by cholesterol oxidase, replacing the 3β-hydroxy-5-ene group with the 3-oxo-4-ene moiety, then derivatised with

Girard P (GP) reagent forming a GP hydrazone derivative (Figure 3.1), and finally analysed by nano-ES-MS^n and in the case of amniotic fluid samples by cap-LC-MS^n.

6.1 Results

It was previously demonstrated in section 3.4 that the oxidation/GP-derivatisation of sterols enhances electrospray ion current by two to three orders of magnitude. Therefore, the method is applicable directly to the amniotic fluid sample, without prior extraction of sterols from the amniotic fluid. The oxidation/GP-derivatisation reactions were performed in the same vial on 10 µL quantities of amniotic fluid, and as a result losses of analytes were minimised. Furthermore, the reactions progressed efficiently for both the 3β-hydroxy-5-ene and 3β-hydroxy-5,7-diene sterols giving 3-GP hydrazones of the 3-oxo sterols.

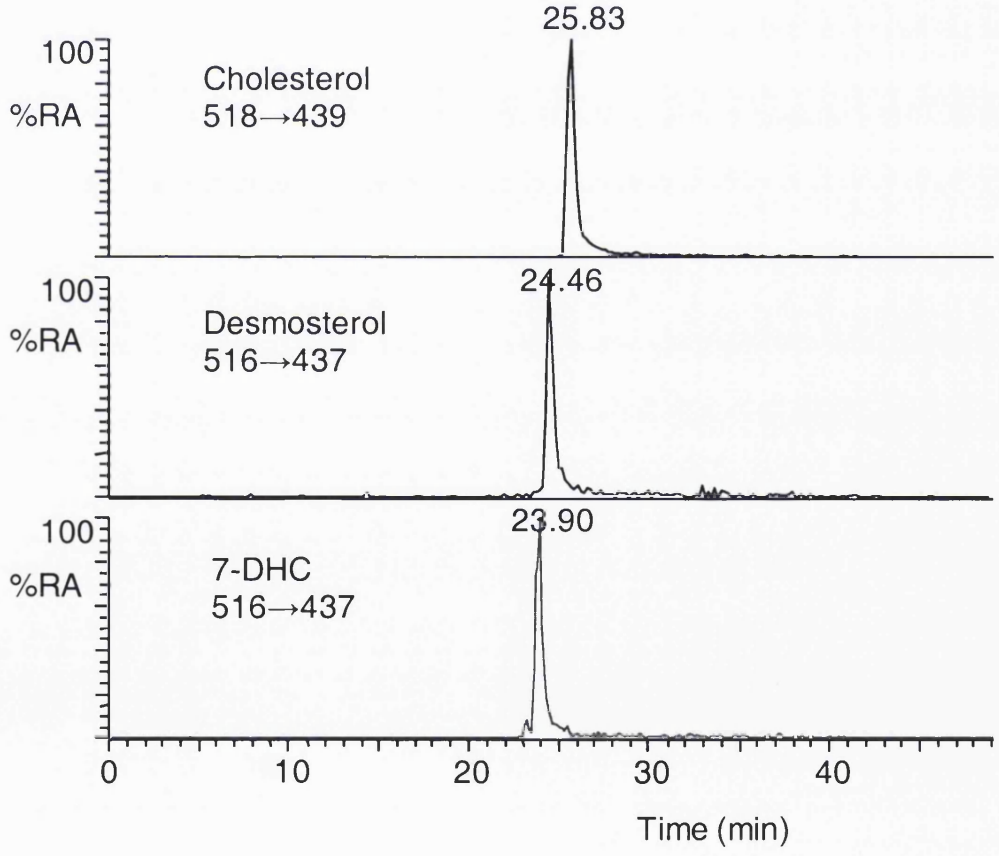

Figure 6.2 Analysis of oxidised/GP-derivatised cholesterol, 7-DHC and desmosterol standards by cap-LC-MS^n on the ion-trap mass spectrometer. RICs for the MS^2 transitions 518→439 (cholesterol, upper panel), 516→437 (desmosterol, central panel) and 516→437 (7-DHC, lower panel).

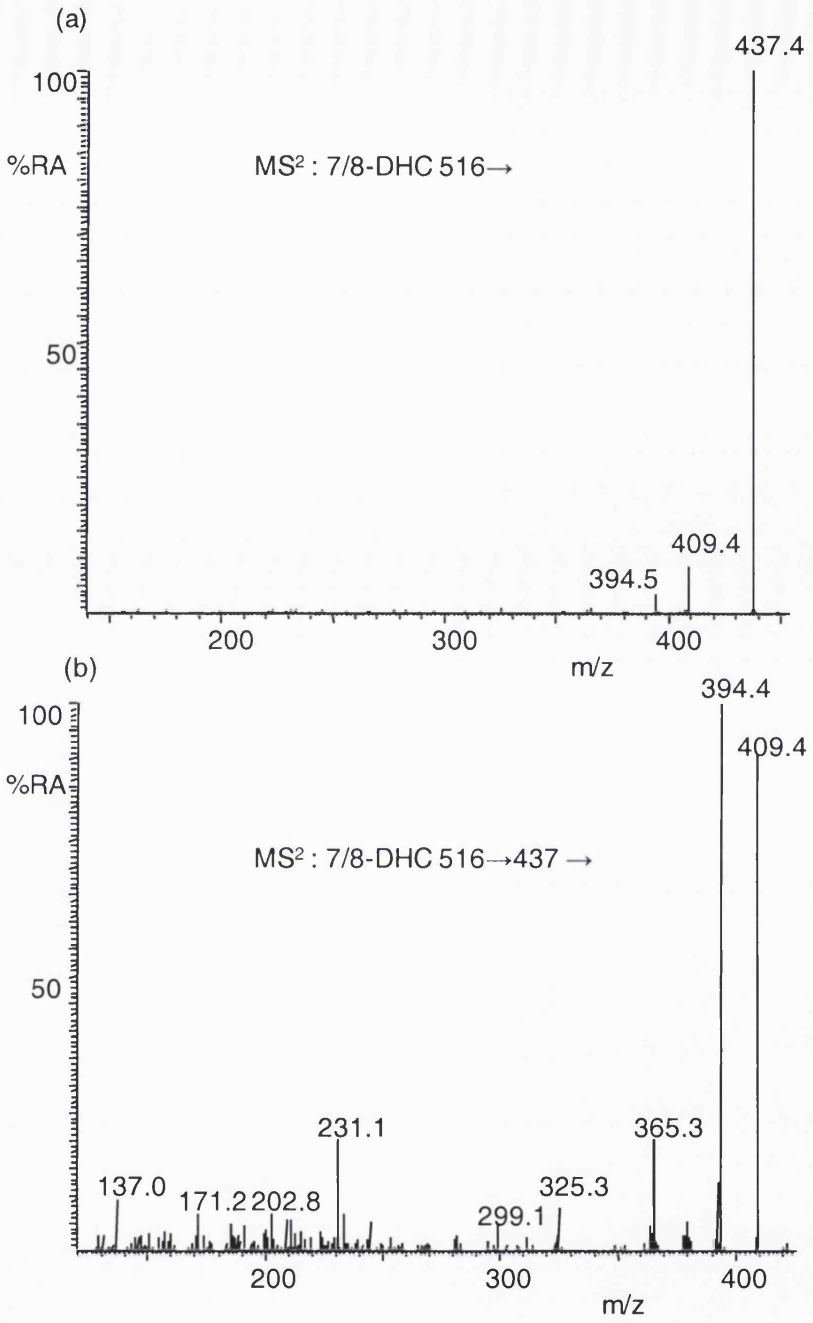

Figure 6.3 (a) MS^2 (516→), and (b) MS^3 (516→437→) spectra of the chromatographic peak eluting at 23.90 min corresponding to 7+8-DHC in the sample 31576.

Initially we evaluated the use of capillary LC combined with MS^n for the analysis of cholesterol and DHCs in amniotic fluid. The aim was to measure the ratio of DHC to cholesterol in control samples and those from SLOS pregnancies, and to evaluate whether this ratio could be used to allow the accurate prenatal diagnosis of SLOS. Cholesterol is the major sterol in control

amniotic fluid (10 - 100 µg/mL) [209]. Desmosterol is also a component of amniotic fluid, but only present at low level [212]. Both 7- and 8-dehydrocholesterol are found in amniotic fluid of SLOS patients [84,202,211]. There appears to be no disadvantage in measuring the summation of these isomeric forms for the diagnosis of SLOS.

It was established in chapter 3 that following oxidation/GP-derivatisation of 7-dehydrocholesterol, its B-ring isomer 8-dehydrocholesterol, and desmosterol give an $[M]^+$ ion of *m/z* 516 and cholesterol $[M]^+$ *m/z* 518. The oxidised/GP-derivatised cholesterol, desmosterol and 7-dehydrocholesterol are just resolved on the reversed-phase capillary column (see Figure 6.2), and 7-DHC elutes earlier than desmosterol, under the LC-MS conditions utilised in this study (see section 2.9). The oxidised/GP-derivatised 7-DHC is resolved from cholesterol and desmosterol, but it was not resolved from its isomer 8-DHC on the capillary reversed phase column, and therefore generates composite MS^2 (516→) and MS^3 (516→437→) spectra (Figure 6.3) [51]. As it is being chromatographically separated, oxidised/GP-derivatised cholesterol gives different fragment ions in its MS^2 (518→), MS^3 (518→439→) spectra to those generated by 7/8-DHC or desmosterol. An authentic standard of 8-DHC is not commercially available, nevertheless it is expected to give a similar MS^2 (516→) spectrum to 7-DHC in the ion-trap mass spectrometer. Figure 6.5a shows RIC for MS^2 transitions 518→439 and 516→437 corresponding to the oxidised/GP-derivatised cholesterol and 7/8-DHC in the sample 31576. Figure 6.3 illustrates MS^2 (516→) and MS^3 (516→437→) spectra corresponding to the chromatographic peak of 7/8-DHC in the sample 31576. Therefore, the following MS^2 transitions 518→439 and 516→437 could be generated for the determination of the relative abundance of cholesterol and 7/8-DHC (Figure 6.5).

Using the capillary LC-MS^2 analysis of authentic sterols, a five-point calibration plot for the relative quantification of 7-DHC to cholesterol was plotted for molar ratios between 0.02 and 1 against the corresponding area ratios, giving an R^2 of 1.00 (see Figure 6.4). This indicates that the oxidised/GP-derivatised sterols are suitable for the quantification of 7-DHC and cholesterol. The

sensitivity of the cap-LC-MS^n instrument allows the injection of as little as 0.01 µL of amniotic fluid on-column (i.e. containing <1 ng of sterol, as previously shown in section 3.10).

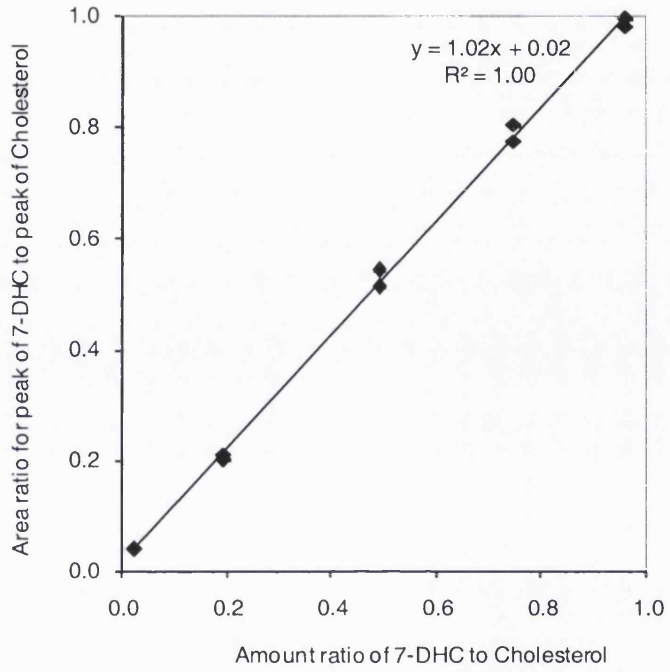

Figure 6.4 Calibration plot of area ratio of peak of 7-dehydrocholesterol to cholesterol against amount ratio of 7-dehydrocholesterol to cholesterol. Each calibrant was analysed by capillary LC-MS^n on a LCQ^{duo} ion trap instrument in duplicate.

Next, 18 blinded unknown specimens of amniotic fluid were obtained from normal pregnancies and pregnancies affected with SLOS. These were oxidised with cholesterol oxidase and derivatised with GP hydrazine and analysed by cap-LC-MS^n. Figure 6.5 shows the reconstructed ion chromatograms (RICs) for MS^2 transitions 518→439 and 516→437 corresponding to cholesterol and 7/8-DHC in the control and SLOS affected pregnancies.

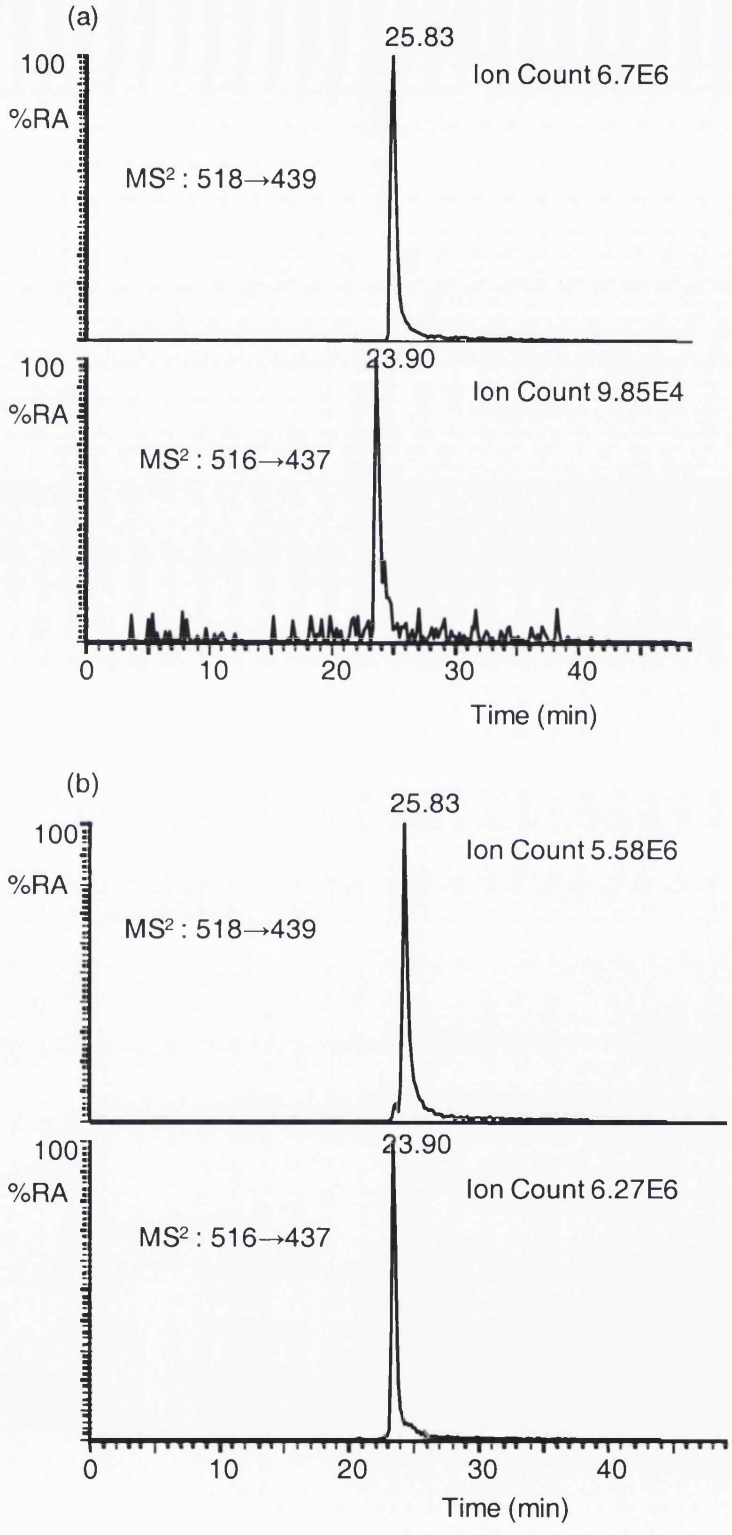

Figure 6.5 Analysis of oxidised/GP-derivatised 7+8-DHC and cholesterol from (a) control (sample 34090), and (b) SLOS affected (sample 31576), amniotic fluid by capillary-LC-MS^2 on the ion-trap mass spectrometer. Upper panels show RICs for the MS^2 transition 518→439 (cholesterol), and lower panels RICs for the MS^2 transition 516→437 (7/8-DHC).

Table 6.1 and Figure 6.6 summarise the 7/8-DHC to cholesterol ratios for the 18 samples analysed. It was determined that of the 18 amniotic fluid samples, six were from the SLOS-affected patients and twelve were from control samples (non-affected pregnancies). The 7/8-DHC to cholesterol ratio was found to lie below 0.02, within the range of 0.00 to 0.02 (mean ± standard deviation, 0.010 ± 0.006) in all control samples, whereas the 7/8-DHC to cholesterol ratio was found to be above 0.20, within the range of 0.20 to 1.13 (mean ± standard deviation, 0.79 ± 0.35) in the SLOS patients. The difference in the 7/8-DHC to cholesterol ratios between the two groups (control and SLOS-affected) is a factor of at least 10. There was no overlap between the 7/8-DHC to cholesterol ratio between pregnancies with affected and unaffected foetuses (0.2 – 1.13 vs. 0.00 – 0.02), and no instance of false-positive or negative results [51].

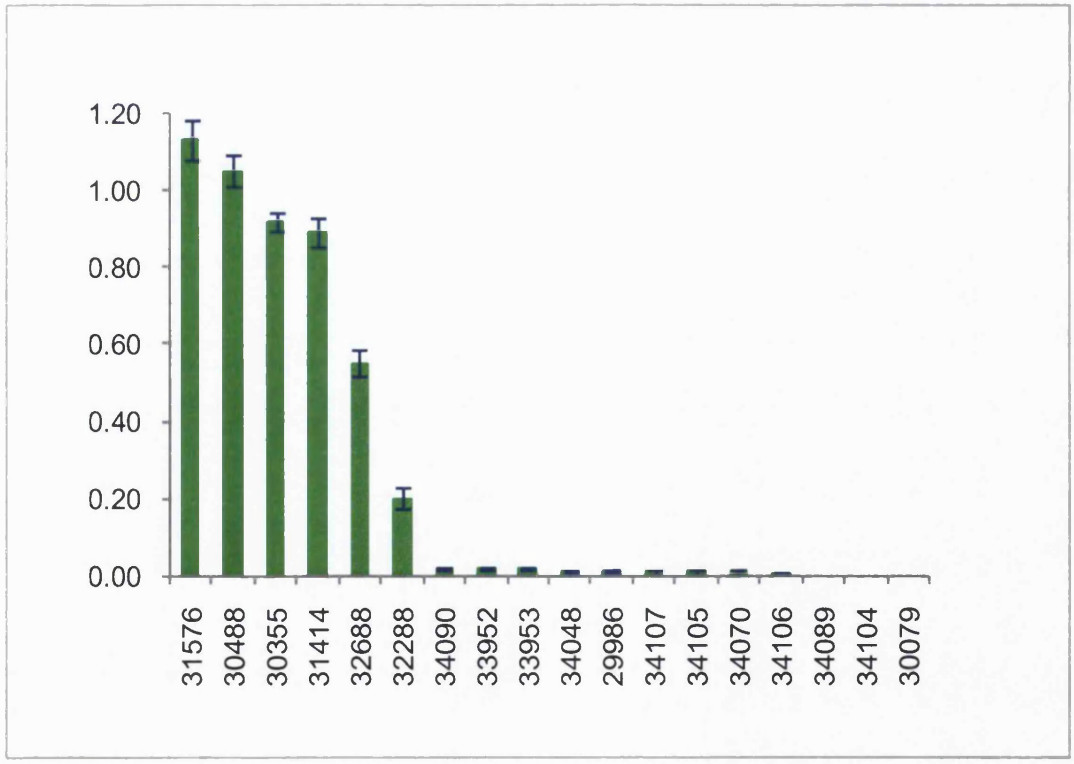

Figure 6.6 Mean ratio of 7/8-DHC to cholesterol for 18 amniotic fluids from SLOS-affected and non-affected pregnancies. Eighteen samples were subjected to oxidation/GP-derivatisation reactions in triplicate and were analysed by cap-LC-MS^n. Error bars show standard deviation of three measurements of the DHC to cholesterol ratio analysed by cap-LC-MS^2.

Table 6.1 Dehydrocholesterol to cholesterol ratio in amniotic fluid from eighteen SLOS-affected and non-affected pregnancies

Sample Assignment	Ratio of DHC/C[a]
Control Samples[b] (n=12)[d]	0.00 – 0.02
SLOS Patient 32288	0.20
SLOS Patient 32688	0.55
SLOS Patient 31414[c]	0.89
SLOS Patient 30355	0.92
SLOS Patient 30488	1.05
SLOS Patient 31576	1.13

[a]Ratio of 7+8-dehydrocholesterols to cholesterol

[b]Control (non-affected, 34106) sample intra-assay variation 5.91%; Control (34106) sample inter-assay variation 4.75%.

[c]SLOS (30355) patient intra-assay variation 4.56%; SLOS (30355) patient inter-assay variation 8.07%.

[d]Range of data from 12 control samples.

7-Dehydrocholesterol is unstable in the presence of oxygen and ultraviolet light, however, during the storage, extraction and processing of amniotic fluid samples, it was found that the loss of 7-dehydrocholesterol compared with other neutral sterols was negligible using simple precautions to avoid excessive exposure to light and processing samples rapidly.

Additionally, the methodology was equally applicable to the analysis of DHC to cholesterol ratio in blood spotted onto filter paper (as representative of Guthrie cards), with newborn screening in mind. Blood spots were analysed directly with no extractions or separations. A set of six samples, was subjected to the oxidation/GP-derivatisation reactions. Oxidised/GP-derivatised sterols were then separated from excess GP hydrazine by solid phase extraction on a C_{18} column. GP derivatives were eluted in 2 mL methanol (SPE-Fr1, -Fr2) as described in section 2.22, and the combined fractions were then infused directly through the nano-ES source into the LCQ^{duo} mass spectrometer. Figure 6.7 illustrates the nano-ES-MS spectrum of a sample from an SLOS patient. The peak at *m/z* 516 is about 8% of that at *m/z* 518, indicating a greatly elevated ratio of dehydrocholesterol to cholesterol. By recording the MS^2 ($[M]^+ \rightarrow$) and MS^3 ($[M]^+ \rightarrow [M-79]^+ \rightarrow$) spectra on the ion of *m/z* 516, it was confirmed that the major components at this *m/z* were oxidised/GP-

derivatised 7-dehydrocholesterol and possibly 8-dehydrocholesterol (Figure 6.2b,c). In conclusion, the results confirm the increased abundance of 7+8-DHC in the blood from a SLOS patient.

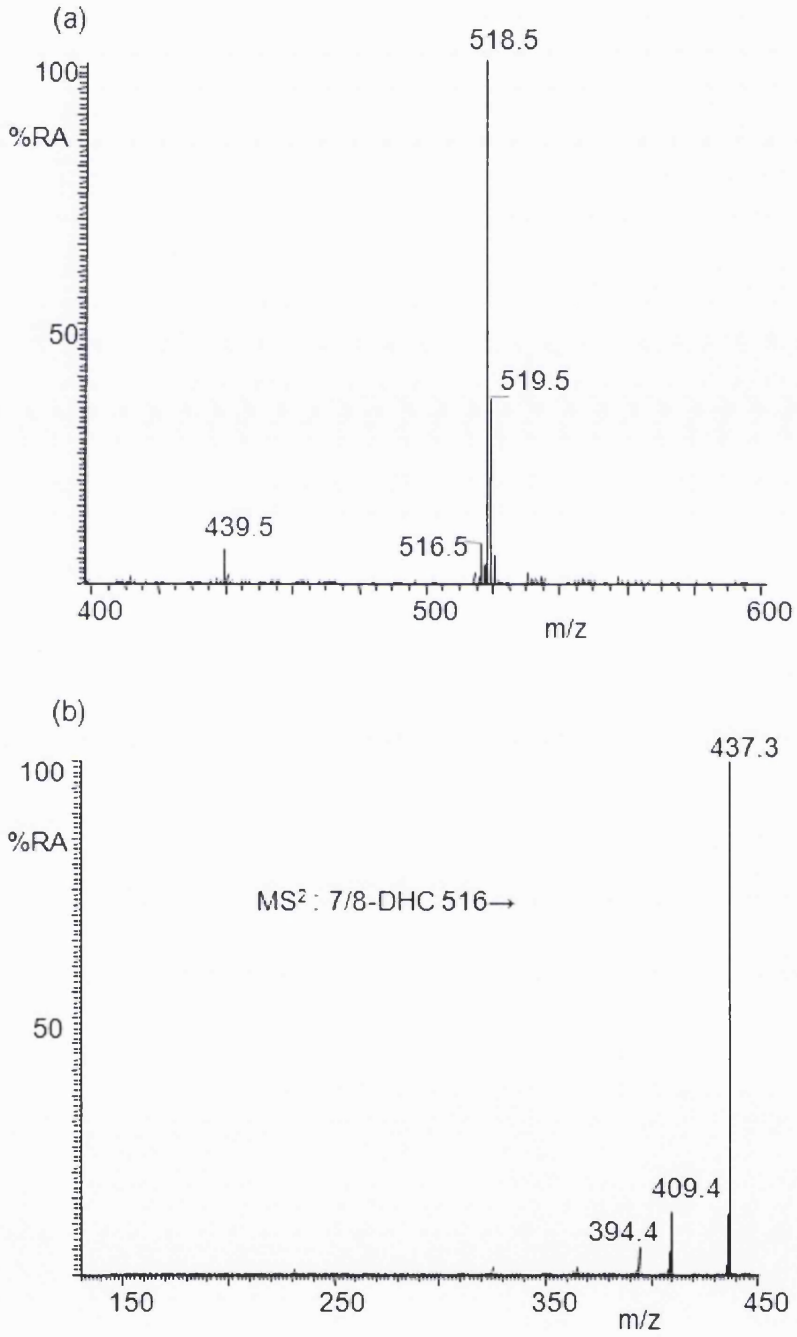

Figure 6.7 Analysis of oxidised/GP-derivatised 7/8-DHC from a blood spot from a SLOS patient by ES-MS^n on the ion trap mass spectrometer. (a) Mass spectrum of the oxidised/GP-derivatised sterols in the blood spot, (b) MS^2 spectrum of 7/8-DHC, (c) MS^3 (516→437→) spectrum of 7/8-DHC.

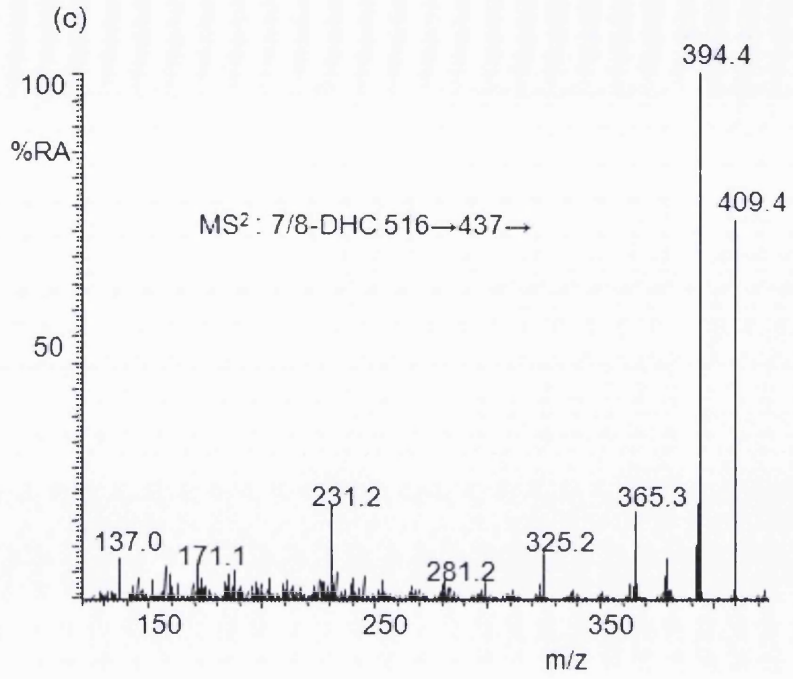

Figure 6.7 continued. Analysis of oxidised/GP-derivatised 7/8-DHC from a blood spot from a SLOS patient by ES-MS^n on the ion trap mass spectrometer. (c) MS^3 (516→437→) spectrum the oxidised/GP-derivatised of 7/8-DHC in the blood spot.

6.2 Discussion

The screening method described here is simple and reliable for the prenatal diagnosis of SLOS in amniotic fluid. The method avoids any pre-purification steps and the derivatisation of the sterols is carried out in the same vial with minimum losses. Further, it was demonstrated that the method is reproducible and due to the simplicity of the method it is highly suitable for routine screening of amniotic fluid. The method is sensitive and requires as little as 10 µL of amniotic fluid for oxidation/GP-derivatisation reactions, of which less than 0.01 µL is injected on the cap-LC-MS system. It is possible to chromatographically separate 7/8-DHC from desmosterol and cholesterol and to perform relative quantification using the transitions 516→437 for 7/8-DHC and 518→439 for cholesterol by utilising cap-LC-MS^n. However, the chromatographic run time of 50 min, along with the necessity of running at least one blank between biological samples, would make it difficult to implement for high throughput prenatal screening analysis. The derivatisation will certainly be necessary for analysis of sterols by mass spectrometry due to the non-polar nature of the analytes.

However, chromatography time can definitely be shortened and automated sample processing developed [51].

As an introduction to a possibly detailed study of blood spots we have tested the oxidation/GP-derivatisation chemistry and nano-ES-MS^n analysis on a trial set of six blood spots from SLOS patients. The results confirm the elevated abundance of 7/8-DHC in the blood from a SLOS patient.

In summary, the current cap-LC-MS^n method provides results of preliminary investigations toward a clinical method. The next requirement is optimisation of the chromatography. For instance, the utilisation of ultra small particle size (<1.7 μm) chromatography may allow rapid, less than 5 min, run time analysis of cholesterol and the DHCs. This chapter has demonstrated a suitable derivatisation technique for non-polar sterols and the MS^n fragmentations required for specific analysis of cholesterol and the DHCs.

Chapter 7

Summary

7. *Summary*

Following the mapping of the human genome and the continuing characterisation of the proteome, there is a great need for highly sensitive methods to identify biologically active sterols, confirm known sterols/oxysterols and characterise new structures and to analyse individual sterols and sterol profiles in cells, tissues and body fluids with high specificity [14]. Methods based on mass spectrometry with separating inlet interfaces are particulary well suited for this purpose. Mass spectrometry can provide information about molecular mass, elemental composition, functional groups and their location. In this study, mass spectrometry has been applied to the analysis of oxysterols, the oxygenated derivatives of cholesterol. Oxysterols are significant transport forms of cholesterol, important intermediates in bile acid synthesis, and substrates for steroid hormones. Their physiological importance as regulators of cholesterol homeostasis *in vivo* is still uncertain and based mainly on indirect evidence.

For the work described in this thesis the analysis is specifically targeted to the identification of oxysterols in biological tissues and fluids. In this regard, sterols with a 3β-hydroxy-5-ene group or 3β-hydroxy-5α-hydrogen structure were oxidised with cholesterol oxidase to 3-oxo-4-ene and 3-oxo analogues, respectively [102,166]. The oxo groups are subsequently derivatised with the Girard P reagent, so as introduce a quaternary nitrogen into the molecule. This strategy of oxidation with cholesterol oxidase, followed by derivatisation with GP hydrazine results in an improvement of ES current by a factor of 100 to 1000, and also adds specificity to the assay in that only compounds with a 3β-hydroxy group and a planar A/B-ring junction (i.e. 5,6-ene or 5α-H configuration) are prone to cholesterol oxidase activity.

The primary goal of this study was to establish reversed phase capillary chromatography and multi-stage fragmentation mass spectrometry methods for the separation, and characterisation of the oxidised/GP-derivatised reference oxysterols/sterols. Chapter 3 describes the optimisation of the capillary LC multi-stage tandem mass spectrometry method for the analysis of reference sterols/oxysterols. We established a sensitive, selective and specific capillary LC-MS^n method.

Forty reference oxysterols/sterols were oxidised with cholesterol oxidase and derivatised with GP hydrazine. In using multi-stage MS^2 the Girard-P derivatives of sterols give characteristic neutral losses of 79 Da and 107 Da, useful for high-specificity detection. The MS^3 spectra were recorded on the $[M-79]^+$ and $[M-107]^+$ fragment-ions to give structural information and molecular characterisation. It was established that the MS^2 spectra of isomeric oxidised/GP-derivatised oxysterols are similar; whereas their MS^3 spectra are different allowing isomer differentiation. Oxidised/GP-derivatised oxysterols/sterols were injected on a C_{18} capillary column, and ES-MS, -MS^2, and -MS^3 spectra recorded. Selectivity and specificity in detection helps to overcome interferences from other extracted compounds and matrix, which is a particularly important consideration in biological samples. A high sensitivity 0.8 pg on-column is necessary to minimise the amount of biological material that is required, to reduce the sample load on the analytical system, and to detect the low amounts of sterols/oxysterols present in biological samples. The reference database was created for oxidised/GP-derivatised oxysterols/sterols, which contains relative retention times for each oxysterol to cholesterol, and their MS, MS^2 $[M]^+\rightarrow$, MS^3 $[M]^+\rightarrow[M-79]^+\rightarrow$ and $[M-107]^+\rightarrow$ spectra. The identification of oxysterols/sterols from biological matrices was based on comparison of their relative retention times, MS, MS^2 and MS^3 spectra with reference sterols/oxysterols.

Oxysterols are present in very low concentrations in mammalian systems, always accompanied by high excess of cholesterol (10^3 to 10^5). It is therefore important to separate oxysterols from cholesterol early in the sample preparation, in order to prevent cholesterol autoxidation during the sample preparation and handling. This was achieved on a straight-phase Unisil SPE column, where cholesterol and more hydrophobic sterols elute with hexane-dichloromethane (Fraction U1), while oxysterols elute in ethyl acetate (Fraction U2). Oxysterols are then oxidised, derivatised and analysed by cap-LC-MS^n. These methods were applied to the identification and semi-quantification of oxysterols from the central nervous system. Chapter 4 describes the evaluation and assessment of the extent to which cholesterol is autoxidased during

the sample preparation. The addition of deuterium-labelled cholesterol to the rat brain permitted the detection of oxygenated oxysterols formed by autoxidation of cholesterol during processing of the samples. It was found that much of the autoxidation can be prevented by protecting samples from light, and completing the extraction and oxidation/GP-derivatisation rapidly. Ten cholesterol autoxidation products were identified when the spiked brain extract was passed once through the Unisil SPE column. The identified cholesterol autoxidation products were formed in negligible amounts in comparison to 24S-hydroxycholesterol in rat brain (less than 3%). The most common formed autoxidation products were 6-hydroxycholest-4-ene-3-one, cholestanetriol, and cholesterol-5,6-epoxide, which have been shown to be physiologically irrelevant. It was established that a double passage of the spiked brain extract through a Unisil SPE column results in nearly complete removal of cholesterol, and minimal cholesterol air-oxidation, as only four deuterium-labelled autoxidation products were identified. Of the four, two have previously been reported as the products of an enzymatic action, and cholesterol autoxidation, 7α- and 25-hydroxycholesterols.

Chapter 5 describes the use of the developed methodology of oxidation/Girard P derivatisation for the profiling of oxysterol content of rat brain. Twenty four oxysterols/sterols were identified in the rat brain. The oxysterols identified in rat brain were 24S-hydroxycholesterol, 24-oxocholesterol, 24,25-, 24,27-, 25,27-, 7α,25-, and 7α,27-dihydroxycholesterols. The most abundant oxysterol in rat brain was 24S-hydroxycholesterol and its level was between 17-24 μg/g. This is in agreement with the study by Smith *et al.* in 1973 [191] and Björkhem *et al.* [37]. To maintain the cholesterol balance in the brain, cholesterol becomes metabolised to 24S-hydroxycholesterol, a transport form of cholesterol that can pass through the blood-brain-barrier. In addition to acting as a transport form of cholesterol, oxysterols have biological activity, acting as ligands for the liver X receptors [68], and interacting with other transcription factors such as sterol regulatory-element binding proteins (SREBPs). The possibility exists that the above identified dihydroxycholesterols, due to their low abundance (<2%) compared with 24S-hydroxycholesterol, have this biological function. It has been suggested that ozone formed as a result of inflammation reacts with

cholesterol to form the oxysterol 3β-hydroxy-5-oxo-5,6-*seco*cholestan-6-al (5,6-seco-sterol) and its aldol, 3,5-dihydroxy-B-norcholestane-6-carboxylaldehyde, and that these sterols can initiate amylodogenesis of proteins and disease [94,131,135]. The presence of 5,6-*seco*-sterol and its aldol was confirmed in rat brain in this study. It is important to point out that the established analytical method allows the injection of only 30 µg to 40 µg of rat brain extract on the capillary reversed phase column, which will allow oxysterol analysis from distinct brain regions in future work.

The method was further extended to the analysis of oxysterols in three regions of embryonic (E11) mouse central nervous system: - ventral midbrain (VM), cortex (Ctx), and spinal cord (SC) (Chapter 5). For profiling the sterol content in CNS, fraction containing free oxysterols was isolated on a straight-phase Unisil SPE column, oxidised with cholesterol oxidase, and derivatised with GP hydrazine and analysed by cap-LC-MS^n. Using this methodology, nineteen oxysterols/sterols were identified in CNS. Low levels of oxysterols (estimated 4-165 ng/g wet weight) were measured in cortex (Ctx), ventral midbrain (VM), and spinal cord (Sc). The pattern of oxysterols in these three regions was similar, suggesting that at this stage of development (E11) their origin is mainly from the dam rather than *in situ* brain biosynthesis. The identified oxysterols include 7α-, 7β-, 22R-, 24S-, 25- and 27-hydroxycholesterol; 24,25- and 24,27-dihydroxycholesterol; and 24S,25-epoxycholesterol. Of these, 24S-hydroxycholesterol is biosynthesised exclusively in the brain. In comparison to adult mouse where the 24S-hydroxycholesterol level in the brain is about 40 µg/g [69,70,83,125], the level of 24S-hydroxycholesterol reported in this thesis (estimated 26 ng/g in Ctx, 13 ng/g in Sc, and 10 ng/g in VM) is extremely low. Therefore, the data suggests that the enzyme CYP46A1 necessary to hydroxylate cholesterol to 24S-hydroxycholesterol in brain is minimally active at the E11 stage of development. However, the level of 24S,25-epoxycholesterol in the three CNS regions (estimated 122 ng/g in Ctx, 69 ng/g in Sc, and 87 ng/g in VM) is significantly higher than the enzymatic hydroxycholesterols. 24,25-Epoxycholesterol is formed in parallel to cholesterol via a shunt of the mevalonate pathway, and its comparatively high level suggests that 24S,25-epoxucholesterol may play a role during cortical and spinal cord development. Levels of cholesterol

and its precursors were determined by CG-MS in the three CNS regions in the Karolinska Institutet, Sweden [105], and were also found to be significantly lower than those reported in the adult mouse CNS. This agrees with the concept that cholesterol levels in brain increase dramatically after birth [197]. In summary, the data on the oxysterol profile in developing CNS is presented for the first time. The data indicates that in early stages of development CYP46A1 has low activity.

The methods established in this thesis were further applied for the profiling of oxysterols in primary cortical neurons derived from embryonic (E19) rat brain. The methodology includes the enrichment of oxysterols using straight-phase chromatography, specific oxidation and derivatisation, and separation in their derivatised form by reversed-phase LC prior to multi-stage fragmentation mass spectrometry detection for their characterisation. Seventeen oxysterols/sterols were identified in the cortical neurons. 24S-Hydroxycholesterol was found at a level of 87 ng from 10^8 cells. The CYP46A1 enzyme responsible for generation of 24S-hydroxycholesterol from cholesterol is located exclusively in neurons [37,44,151], while neurons have a low rate of synthesis of cholesterol. This study has identified 24S,25-epoxycholesterol, and this cholesterol metabolite was present at a similar level to 24S-hydroxycholesterol. Dihydroxycholesterols were identified as 24,25-, 6,24-,24,27-, 7α,25-dihydroxycholesterols in cortical neurons, which agrees well with the data of Zhang *et al.* [24,154], who studied the metabolism of 24-, 25- and 27-hydroxycholesterols in rat brain microsomes and cultures of Schwann cells, astocytes and neurons. They found that only 25- and 27-hydroxycholesterols have undergone 7α-hydroxylation, but not 24-hydroxycholesterol, and our data confirms this. Mast *et al.* [22] have shown that CYP46A1 is also responsible for the conversion of 24S-hydroxycholesterol to 24,25- and 24,27-dihydroxycholesterols in both cultures of HEK293 cells with human CYP46A1 cDNA, and an *in vitro* reconstituted system with recombinant enzyme, which our data also confirms.

Chapter 6 describes a potential method for the accurate identification of Smith-Lemli-Opitz syndrome (SLOS) from amniotic fluid samples. The method is sensitive, requiring only 10 µL of amniotic fluid for oxidation/GP-derivatisation, of which only 0.01 µL or less is injected on the cap-

LC-MS^n system. The method includes the oxidation of 3β-hydroxysterols in amniotic fluid with cholesterol oxidase to their 3-ketones, which are then derivatised with Girard P hydrazine in a "one-reaction vessel". By utilising cap-LC-MS^n with the capillary reversed-phase column, it was possible chromatographically to separate 7/8-dehydrocholesterol from desmosterol and cholesterol, and to perform relative quantification using the specific transitions 516→437 for 7/8-dehydrocholesterol and 518→439 for cholesterol. In normal amniotic fluid the level of 7/8-dehydrocholesterol is less than 1% of that of cholesterol, while in SLOS it may exceed that of cholesterol. Therefore, by determining the 7/8-dehydrocholesterol to cholesterol ratio SLOS was accurately diagnosed. This methodology was also applied for the diagnosis of SLOS from blood spots samples from SLOS patients. The results confirm the elevated abundance of 7/8-dehydrocholesterol in the blood from a SLOS patient. The next requirement towards clinical method for the diagnosis of SLOS is improvement in the chromatographic time. The utilisation of ultra small particle size (<1.7 μm) chromatography may allow rapid (<5 min run time) and specific measurement of cholesterol and the 7/8-dehydrocholesterols. Chapter 6 demonstrated a suitable derivatisation technique for non-polar sterols, and the MS^2, MS^3 fragmentations needed for specific analysis of cholesterol and the dehydrocholesterols.

7.1 Conclusion and future directions

In this thesis we report the measurement of the oxysterol profile in rat brain and developing mouse CNS, which are present at very low levels pg/g – ng/g - μg/g. This thesis demonstrates that only a small amount of sample is required for analysis due to the sensitivity provided by capillary LC coupled to the LCQ^{duo} ion trap mass spectrometer instrument, when combined with derivatisation chemistry. This thesis also reports the first measurement of the oxysterol profile of cortical neurons. Although the data is only semi-quantitative it opens the possibility for future studies which can utilise absolute quantitative measurements based on isotope labelled reference standards. The challenge for future studies is to identify and quantify oxysterols in distinct brain regions and to investigate

how their levels change with age or stress, or in neurodegenerative disease. It is probable that novel sterols are still to be identified, and their biological effects of these and many already known sterols/oxysterols must be investigated.

References

1. Hamacher M., Meyer H. E., HUPO Brain Proteome Project: aims and needs in proteomics, *Expert Review of Proteomics*, **2005** Jan, 2(1), 1-3.

2. Tyers M., Mann M., From genomics to proteomics, *Nature*, **2003** Mar 13, 422(6928), 193-197.

3. Pearson H., Biologists initiate plan to map human proteome, *Nature*, **2008** Apr 24, 452(7190), 920-921.

4. Griffiths W. J., Karu K., Hornshaw M., Woffendin G., Wang Y., Metabolomics and metabolite profiling: past heroes and future developments, *European Journal of Lipid Science and Technology*, **2007**, 13(1), 45-50.

5. Oldiges M., Lutz S., Pflug S., Schroer K., Stein N., Wiendahl C., Metabolomics: current state and evolving methodologies and tools, *Applied Microbiology and Biotechnology*, **2007** Sep, 76(3), 495-511.

6. Lipid Metabolites And Pathways Strategy, *http://wwwlipidmapsorg/*, **2009**.

7. European Federation for the Science and Technology of Lipids, http://www.eurofedlipid.org/.

8. Japanese Conference on the Biochemistry of Lipids (JCBL), *http://lipidbankjp/*, **2009**.

9. Fahy E., Subramaniam S., Brown H. A., Glass C. K., Merrill A. H., Murphy R. C., Raetz C. R. H., Russell D. W., Seyama Y., Shaw W., Shimizu T., Spener F., Van Meer G., Vannieuwenhze M. S., White S. H., Witztum J. L., Dennis E. A., A comprehensive classification system for lipids, *Journal of Lipid Research*, **2005** May, 46(5), 839-861.

10. Watson A. D., Thematic review series: systems biology approaches to metabolic and cardiovascular disorders. Lipidomics: a global approach to lipid analysis in biological systems, *Journal of Lipid Research*, **2006** Oct, 47(10), 2101-2111.

11. Han X., Gross R. W., Global analyses of cellular lipidomes directly from crude extracts of biological samples by ESI mass spectrometry: a bridge to lipidomics, *Journal of Lipid Research*, **2003** Jun, 44(6), 1071-1079.

12. Siuzdak G., Scripps Center for Mass Spectrometry, *http://masspecscrippsedu/*, **2009**.

13. Makin H. L. J., Gower D. B., Kirk D. N., eds. Steroid Analysis, Glasgow: Blackie Academic & Professional 1995.

14. Griffiths W. J., Shackleton C., Sjövall J., Steroid analysis, In: Caprioli R., ed. *In Encyclopedia of Mass Spectrometry*, Oxford, UK, Elsevier, **2005**, 447-472.

15. Vandenheuvel W. J., Horning E. C., Gas chromatography of adrenal cortical steroid hormones, *Biochemical and Biophysical Research Communications* **1960** Oct, 3, 356-360.

16. Horning E. C., Vandenheuvel W. J., Creech B. G., Separation and Determination of Steroids by Gas Chromatography, *Methods of Biochemical Analysis*, **1963**, 11, 69-147.

17. Horning E. C., Vandenheuvel J. A., Gas Chromatography, *Annual review of biochemistry*, **1963**, 32, 709-754.

18. Shan H., Pang J. H., Li S. R., Chiang T. B., Wilson W. K., Schroepfer G. J., Chromatographic behavior of oxygenated derivatives of cholesterol, *Steroids*, **2003** Mar, 68(3), 221-233.

19. Bjorkhem I., Lutjohann D., Breuer O., Sakinis A., Wennmalm A., Importance of a novel oxidative mechanism for elimination of brain cholesterol - Turnover of cholesterol and 24(S)-hydroxycholesterol in rat brain as measured with O-18(2) techniques in vivo and in vitro, *Journal of Biological Chemistry*, **1997** Nov 28, 272(48), 30178-30184.

20. Bjorkhem I., Lutjohann D., Diczfalusy U., Stahle L., Ahlborg G., Wahren J., Cholesterol homeostasis in human brain: turnover of 24S-hydroxycholesterol and evidence for a cerebral origin of most of this oxysterol in the circulation, *J Lipid Res*, **1998** Aug, 39(8), 1594-1600.

21. Dzeletovic S., Breuer O., Lund E., Diczfalusy U., Determination of Cholesterol Oxidation-Products in Human Plasma by Isotope-Dilution Mass-Spectrometry, *Analytical Biochemistry*, **1995** Feb 10, 225(1), 73-80.

22. Mast N., Norcross R., Andersson U., Shou M. G., Nakayama K., Bjorkhem I., Pikuleva I. A., Broad substrate specificity of human cytochrome P450 46A1 which initiates cholesterol degradation in the brain, *Biochemistry*, **2003** Dec 9, 42(48), 14284-14292.

23. Schroepfer G. J., Jr., Oxysterols: modulators of cholesterol metabolism and other processes, *Physiological reviews*, **2000** Jan, 80(1), 361-554.

24. Zhang J., Akwa Y., Eletr M., Baulieu E. E., Sjovall J., Metabolism of 27-, 25- and 24-hydroxycholesterol in rat glial cells and neurons, *Biochemical Journal*, **1997** Feb 15, 322, 175-184.

25. Higashi T., Ninomiya Y., Iwaki N., Yamauchi A., Takayama N., Shimada K., Studies on neurosteroids XVIII - LC-MS analysis of changes in rat brain and serum testosterone levels induced by immobilization stress and ethanol administration, *Steroids*, **2006** Jul, 71(7), 609-617.

26. Higashi T., Takido N., Shimada K., Studies on neurosteroids XVII. Analysis of stress-induced changes in neurosteroid levels in rat brains using liquid chromatography-electron capture atmospheric pressure chemical ionization-mass spectrometry, *Steroids*, **2005** Jan, 70(1), 1-11.

27. Higashi T., Yamauchi A., Shimada K., Koh E., Mizokami A., Namiki M., Determination of prostatic androgens in 10 mg of tissue using liquid chromatography-tandem mass spectrometry with charged derivatization, *Analytical and Bioanalytical Chemistry*, **2005** Jun, 382(4), 1035-1043.

28. Higashi T., Yokoi H., Maekubo H., Honda A., Shimada K., Studies on neurosteroids XXIII. Analysis of tetrahydrocorticosterone isomers in the brain of rats exposed to immobilization using LC-MS, *Steroids*, **2007** Nov, 72(13), 865-874.

29. Higashi T., Yokoi H., Nagura Y., Nishio T., Shimada K., Studies on neurosteroids XXIV. Determination of neuroactive androgens, androsterone and 5 alpha-androstane-3 alpha,17 beta-diol, in rat brain and serum using liquid chromatography-tandem mass spectrometry, *Biomedical Chromatography*, **2008** Dec, 22(12), 1434-1441.

30. Honda A., Yamashita K., Miyazaki H., Shirai M., Ikegami T., Xu G. R., Numazawa M., Hara T., Matsuzaki Y., Highly sensitive analysis of sterol profiles in human serum by LC-ESI-MS/MS, *Journal of Lipid Research*, **2008** Sep, 49(9), 2063-2073.

31. Christie W. W., Lipid Chemistry, Biology and Analysis, *http://wwwlipidlibrarycouk/*, **2009**.

32. Wakelam M. J., Pettitt T. R., Postle A. D., Lipidomic analysis of signaling pathways, *Methods Enzymology*, **2007**, 432, 233-246.

33. Dietschy J. M., Turley S. D., Cholesterol metabolism in the central nervous system during early development and in the mature animal, *Journal of Lipid Research*, **2004** Aug, 45(8), 1375-1397.

34. Bodin K., Diczfalusy U., Analysis of cholesterol oxidation products in plasma, tissues and food, *European Journal of Lipid Science and Technology*, **2002** Jul, 104(7), 435-439.

35. Bjorkhem I., Diczfalusy U., Oxysterols - Friends, foes, or just fellow passengers?, *Arteriosclerosis Thrombosis and Vascular Biology*, **2002** May, 22(5), 734-742.

36. Bjorkhem I., Are side-chain oxidized oxysterols regulators also in vivo?, *Journal of Lipid Research*, **2008** Oct 23.

37. Bjorkhem I., Rediscovery of cerebrosterol, *Lipids*, **2007** Feb, 42(1), 5-14.

38. Griffiths W. J., Wang Y., Alvelius G., Liu S., Bodin K., Sjovall J., Analysis of oxysterols by electrospray tandem mass spectrometry, *Journal of The American Society for Mass Spectrometry*, **2006** Mar, 17(3), 341-362.

39. Folch J., Lees M., Sloane Stanley G. H., A simple method for the isolation and purification of total lipides from animal tissues, *Journal of Biological Chemistry*, **1957** May, 226(1), 497-509.

40. Bligh E. G., Dyer W. J., A rapid method of total lipid extraction and purification, *Canadian Journal of Biochemistry and Physiology*, **1959**, 37, 911 – 917.

41. Mcdonald J. G., Thompson B. M., Mccrum E. C., Russell D. W., Extraction and analysis of sterols in biological matrices by high performance liquid chromatography electrospray ionization mass spectrometry, *Lipidomics and Bioactive Lipids: Mass-Spectrometry-Based Lipid Analysis*, **2007**, 432, 145-170.

42. Gross R. W., Han X., Shotgun Lipidomics of Neutral Lipids as an Enabling Technology for Elucidation of Lipid-Related Diseases, *American Journal of Physiology - Endocrinology and Metabolism*, **2009** Jan 6.

43. Meaney S., *Studies on oxysterols : Origins, properties and roles,* Karolinska Institute, Stockholm: PhD thesis, **2003**.

44. Bjorkhem I., Lutjohann D., Diczfalusy U., Stahle L., Ahlborg G., Wahren J., Cholesterol homeostasis in human brain: turnover of 24S-hydroxycholesterol and evidence for a cerebral origin of most of this oxysterol in the circulation, *Journal of Lipid Research*, **1998** Aug, 39(8), 1594-1600.

45. Cazes J., Lipid Analysis by HPLC, *Encyclopedia of Chromatography*, Boca Raton, Florida, Marcel Dekker, Inc. **1993**, 476 - 480.

46. Worsfold P. T., A. Poole, C., *Encyclopedia of Analytical Science*, **2005**.

47. Griffiths W. J., Hornshaw M., Woffendin G., Baker S. F., Lockhart A., Heidelberger S., Gustafsson M., Sjovall J., Wang Y., Discovering oxysterols in plasma: a window on the metabolome, *Journal of Proteome Research*, **2008** Aug, 7(8), 3602-3612.

48. Liu S., Sjovall J., Griffiths W. J., Neurosteroids in rat brain: extraction, isolation, and analysis by nanoscale liquid chromatography-electrospray mass spectrometry, *Analytical Chemistry*, **2003** Nov 1, 75(21), 5835-5846.

49. Liere P., Pianos A., Eychenne B., Cambourg A., Liu S., Griffiths W., Schumacher M., Sjovall J., Baulieu E. E., Novel lipoidal derivatives of pregnenolone and dehydroepiandrosterone and absence of their sulfated counterparts in rodent brain, *Journal of Lipid Research*, **2004** Dec, 45(12), 2287-2302.

50. Schumacher M., Liere P., Akwa Y., Rajkowski K., Griffiths W., Bodin K., Sjovall J., Baulieu E. E., Pregnenolone sulfate in the brain: a controversial neurosteroid, *Neurochemistry International*, **2008** Mar-Apr, 52(4-5), 522-540.

51. Griffiths W. J., Wang Y., Karu K., Samuel E., Mcdonnell S., Hornshaw M., Shackleton C., Potential of sterol analysis by liquid chromatography-tandem mass spectrometry for the prenatal diagnosis of Smith-Lemli-Opitz syndrome, *Clinical Chemistry*, **2008** Aug, 54(8), 1317-1324.

52. Griffiths W. J., Milton D., Separation and identification of cholesterol metabolites in rat brain using LC-MSn, *Lc Gc Europe*, **2007** Dec, 26-26.

53. Lund E. G., Diczfalusy U., Quantitation of receptor ligands by mass spectrometry, *Methods Enzymology*, **2003**, 364, 24-37.

54. Dass C., *Fundamentals of contemporary mass spectrometry* John Wiley & Sons **2007**.

55. Wang Y., Griffiths W. J., Mass Spectrometry for Metabolite Identification In: Griffiths W. J., ed. *Metabolomics, Metabonomics and Metabolite Profiling* Cambridge, UK, The Royal Society of Chemistry **2008**, 1 - 43.

56. Aebersold R., Mann M., Mass spectrometry-based proteomics, *Nature*, **2003** Mar 13, 422(6928), 198-207.

57. Griffiths W. J., Liu S., Alvelius G., Sjovall J., Derivatisation for the characterisation of neutral oxosteroids by electrospray and matrix-assisted laser desorption/ionisation tandem mass spectrometry: the Girard P derivative, *Rapid Communications in Mass Spectrometry*, **2003**, 17(9), 924-935.

58. Lane C. S., Mass spectrometry-based proteomics in the life sciences, *Cellular and Molecular Life Sciences*, **2005** Apr, 62(7-8), 848-869.

59. Cole R. B., ed. Electrospray Ionisation Mass Spectrometry: Fundamentals, instrumentation and applications, New York: John Wiley and Sons 1997.

60. Kebarle P., A brief overview of the present status of the mechanisms involved in electrospray mass spectrometry, *Journal of Mass Spectrometry*, **2000** Jul, 35(7), 804-817.

61. Griffiths W. J., Jonsson A. P., Liu S., Rai D. K., Wang Y., Electrospray and tandem mass spectrometry in biochemistry, *Biochemical Journal*, **2001** May 1, 355(Pt 3), 545-561.

62. Cech N. B., Enke C. G., Practical implications of some recent studies in electrospray ionization fundamentals, *Mass Spectrometry Reviews*, **2001** Nov-Dec, 20(6), 362-387.

63. Kebarle P., Peschke M., On the mechanisms by which the charged droplets produced by electrospray lead to gas phase ions, *Analytica Chimica Acta*, **2000** Feb 1, 406(1), 11-35.

64. Rohner T., *Polymer nanospray interfaces for on-line electrochemically induced modifications application to protein mass spectrometry,* Lausanne University Switzerland: PhD thesis, **2003**.

65. Thermo Finnigan, *Hardware Manual for Finnigan LCQduo.* , **2001**.

66. Marzilli L. A., Fay L. B., Dionisi F., Vouros P., Structural characterization of triacylglycerols using electrospray ionization-MSn ion-trap MS, *Journal of the American Oil Chemists Society*, **2003** Mar, 80(3), 195-202.

67. Palmgren J. J., Toyras A., Mauriala T., Monkkonen J., Auriola S., Quantitative determination of cholesterol, sitosterol, and sitostanol in cultured Caco-2 cells by liquid chromatography-atmospheric

pressure chemical ionization mass spectrometry, *J Chromatogr B Analyt Technol Biomed Life Sci*, **2005** Jul 25, 821(2), 144-152.

68. Karu K., Hornshaw M., Woffendin G., Bodin K., Hamberg M., Alvelius G., Sjovall J., Turton J., Wang Y., Griffiths W. J., Liquid chromatography-mass spectrometry utilizing multi-stage fragmentation for the identification of oxysterols, *Journal of Lipid Research*, **2007** Apr, 48(4), 976-987.

69. Wang Y., Griffiths W. J., Capillary liquid chromatography combined with tandem mass spectrometry for the study of neurosteroids and oxysterols in brain, *Neurochemistry International*, **2008** Mar-Apr, 52(4-5), 506-521.

70. Wang Y., Karu K., Griffiths W. J., Analysis of neurosterols and neurosteroids by mass spectrometry, *Biochimie*, **2007** Feb, 89(2), 182-191.

71. Wang Y., Griffiths W. J., Capillary liquid chromatography combined with tandem mass spectrometry for the study of neurosteroids and oxysterols in brain, *Neurochemistry International*, **2008** Mar-Apr, 52(4-5), 506-521.

72. Wong P. S. H., Cooks G. R., Ion trap mass spectrometry *Current Separations*, **1997**, 16(3).

73. March R. E., An introduction to quadrupole ion trap mass spectrometry, *Journal of Mass Spectrometry*, **1997** Apr, 32(4), 351-369.

74. Bier M. E., Schwartz J. C., Electrospray-Ionisation Quadrupole Ion-Trap Mass Spectrometry In: Cole R. B., ed. *Electrospray Ionisation Mass Spectrometry: Fundamentals, instrumentation and applications*, New York, John Wiley and Sons **1997**, 235 - 270.

75. Stafford G., Jr., Ion trap mass spectrometry: a personal perspective, *Journal of The American Society for Mass Spectrometry*, **2002** Jun, 13(6), 589-596.

76. Wilm M. S., Mann M., Electrospray and Taylor-Cone Theory, Doles Beam of Macromolecules at Last, *International Journal of Mass Spectrometry and Ion Processes*, **1994** Sep 22, 136(2-3), 167-180.

77. Emmett M. R., Caprioli R. M., Micro-Electrospray Mass-Spectrometry - Ultra-High-Sensitivity Analysis of Peptides and Proteins, *Journal of The American Society for Mass Spectrometry*, **1994** Jul, 5(7), 605-613.

78. Abian J., Oosterkamp A. J., Gelpi E., Comparison of conventional, narrow-bore and capillary liquid chromatography mass spectrometry for electrospray ionization mass spectrometry: Practical considerations, *Journal of Mass Spectrometry*, **1999** Apr, 34(4), 244-254.

79. Voyksner R. D., Combining Liquid Chromatography with Electrospray Mass Spectrometry In: Cole R. B., ed. *Electrospray Ionisation Mass Spectrometry*, New York, John Wiley & Sons Inc. **1997**, 324 -342.

80. Abian J., The coupling of gas and liquid chromatography with mass spectrometry, *Journal of Mass Spectrometry*, **1999** Mar, 34(3), 157-170.

81. Wang Y., Griffiths W. J., Steroids, Sterols and the Nervous System, In: Griffiths W. J., ed. *Metabolomics, metabonomics and metabolite profiling*, Cambridge RSC Biomolecular Sciences Series **2008**, 71 - 115.

82. Griffiths W. J., Wang Y., The Importance of Steroidomics in the Study of Neurodegenerative Disease and Ageing, *Combinatorial Chemistry & High Throughput Screening*, **2009** Feb, 12(2), 212-228.

83. Griffiths W. J., Wang Y., Sterol lipidomics in health and disease: Methodologies and applications, *European Journal of Lipid Science and Technology*, **2009** Jan, 111(1), 14-38.

84. Starck L., Lovgren A., Diagnosis of Smith-Lemli-Opitz syndrome from stored filter paper blood specimens, *Archives of Disease in Childhood*, **2000** Jun, 82(6), 490-492.

85. Liu S., Griffiths W. J., Sjovall J., On-column electrochemical reactions accompanying the electrospray process, *Analytical Chemistry*, **2003** Feb 15, 75(4), 1022-1030.

86. Liu S., Griffiths W. J., Sjovall J., Capillary liquid chromatography/electrospray mass spectrometry for analysis of steroid sulfates in biological samples, *Analytical Chemistry*, **2003** Feb 15, 75(4), 791-797.

87. Jiang X., Ory D. S., Han X., Characterization of oxysterols by electrospray ionization tandem mass spectrometry after one-step derivatization with dimethylglycine, *Rapid Communication Mass Spectrometry*, **2007**, 21(2), 141-152.

88. Saldanha T., Sawaya A. C. H. F., Eberlin M. N., Bragagnolo N., HPLC separation and determination of 12 cholesterol oxidation products in fish: Comparative study of RI, UV, and APCI-MS detectors, *Journal of Agricultural and Food Chemistry*, **2006** Jun 14, 54(12), 4107-4113.

89. Burkard I., Rentsch K. M., Von Eckardstein A., Determination of 24S- and 27-hydroxycholesterol in plasma by high-performance liquid chromatography-mass spectrometry, *Journal of Lipid Research*, **2004** Apr, 45(4), 776-781.

90. Razzazi-Fazeli E., Kleineisen S., Luf W., Determination of cholesterol oxides in processed food using highperformance liquid chromatography-mass spectrometry with atmospheric pressure chemical ionisation, *Journal of Chromatography A*, **2000** Oct 27, 896(1-2), 321-334.

91. Yang C., Mcdonald J. G., Patel A., Zhang Y., Umetani M., Xu F., Westover E. J., Covey D. F., Mangelsdorf D. J., Cohen J. C., Hobbs H. H., Sterol intermediates from cholesterol biosynthetic pathway as liver X receptor ligands, *The Journal of biological chemistry*, **2006** Sep 22, 281(38), 27816-27826.

92. Bjorkhem I., Do oxysterols control cholesterol homeostasis?, *Journal of Clinical Investigation*, **2002** Sep, 110(6), 725-730.

93. Zhang Z., Li D. S., Blanchard D. E., Lear S. R., Erickson S. K., Spencer T. A., Key regulatory oxysterols in liver: analysis as Delta(4)-3-ketone derivatives by HPLC and response to physiological perturbations, *Journal of Lipid Research*, **2001** Apr, 42(4), 649-658.

94. Zhang Q. H., Powers E. T., Nieva J., Huff M. E., Dendle M. A., Bieschke J., Glabe C. G., Eschenmoser A., Wentworth P., Lerner R. A., Kelly J. W., Metabolite-initiated protein misfolding may trigger Alzheimer's disease, *Proceedings of the National Academy of Sciences of the United States of America*, **2004** Apr 6, 101(14), 4752-4757.

95. Bosco D. A., Fowler D. M., Zhang Q., Nieva J., Powers E. T., Wentworth P., Jr., Lerner R. A., Kelly J. W., Elevated levels of oxidized cholesterol metabolites in Lewy body disease brains accelerate alpha-synuclein fibrilization, *Nature chemical biology*, **2006** May, 2(5), 249-253.

96. Shackleton C. H. L., Chuang H., Kim J., Delatorre X., Segura J., Electrospray mass spectrometry of testosterone esters: Potential for use in doping control, *Steroids*, **1997** Jul, 62(7), 523-529.

97. Lai C. C., Tsai C. H., Tsai F. J., Lee C. C., Lin W. D., Rapid monitoring assay of congenital adrenal hyperplasia with microbore high-performance liquid chromatography/electrospray ionization tandem mass spectrometry from dried blood spots, *Rapid Communication in Mass Spectrometry*, **2001**, 15(22), 2145-2151.

98. Johnson D. W., Ten Brink H. J., Jakobs C., A rapid screening procedure for cholesterol and dehydrocholesterol by electrospray ionization tandem mass spectrometry, *Journal of Lipid Research*, **2001** Oct, 42(10), 1699-1705.

99. Johnson D. W., Ketosteroid profiling using Girard T derivatives and electrospray ionization tandem mass spectrometry: direct plasma analysis of androstenedione, 17-hydroxyprogesterone and cortisol, *Rapid Communications in Mass Spectrometry*, **2005**, 19(2), 193-200.

100. Sjovall J., Fifty years with bile acids and steroids in health and disease, *Lipids*, **2004** Aug, 39(8), 703-722.

101. Griffiths W. J., Alvelius G., Liu S., Sjovall J., High-energy collision-induced dissociation of oxosteroids derivatised to Girard hydrazones, *European Journal of Mass Spectrometry (EJMS)*, **2004**, 10(1), 63-88.

102. Brooks C. J. W., Cole W. J., Lawrie T. D. V., Maclachlan J., Borthwick J. H., Barrett G. M., Selective Reactions in the Analytical Characterization of Steroids by Gas-Chromatography Mass-Spectrometry, *Journal of Steroid Biochemistry and Molecular Biology*, **1983**, 19(1), 189-201.

103. Wang Y., Hornshaw M., Alvelius G., Bodin K., Liu S., Sjovall J., Griffiths W. J., Matrix-assisted laser desorption/ionization high-energy collision-induced dissociation of steroids: analysis of oxysterols in rat brain, *Analytical Chemistry*, **2006** Jan 1, 78(1), 164-173.

104. Kirk J. M., Tarbin J., Keely B. J., Analysis of androgenic steroid Girard P hydrazones using multistage tandem mass spectrometry, *Rapid Communication Mass Spectrometry*, **2006**, 20(8), 1247-1252.

105. Wang Y., Sousa K. M., Bodin M. S., Theofilopoulos S., Sacchetti P., Hornshaw M., Woffendin G., Karu K., Sjovall J., Arenas E., Griffiths W. J. Oxysterols in the Embryonic Central Nervous System: A Targeted Lipidomic Study. 2009.

106. Tian Q., Failla M. L., Bohn T., Schwartz S. J., High-performance liquid chromatography/atmospheric pressure chemical ionization tandem mass spectrometry determination of cholesterol uptake by Caco-2 cells, *Rapid Communication in Mass Spectrometry*, **2006**, 20(20), 3056-3060.

107. United States Enviromental Protection Agency, (Usepa), Determinative chromatographic separations *Method 8000C*, **2003**, http:/nlquery.epa.gov/.

108. Breuer O., Bjorkhem I., Simultaneous Quantification of Several Cholesterol Autoxidation and Monohydroxylation Products by Isotope-Dilution Mass-Spectrometry, *Steroids*, **1990** Apr, 55(4), 185-192.

109. Breuer O., Identification and Quantitation of Cholest-5-Ene-3-Beta,4-Beta-Diol in Rat-Liver and Human Plasma, *Journal of Lipid Research*, **1995** Nov, 36(11), 2275-2281.

110. Breuer O., Bjorkhem I., Use of an O-18(2) Inhalation Technique and Mass Isotopomer Distribution Analysis to Study Oxygenation of Cholesterol in Rat - Evidence for in-Vivo Formation of 7-Oxocholesterol, 7-Beta-Hydroxycholesterol, 24-Hydroxycholesterol, and 24-Hydroxycholesterol, *Journal of Biological Chemistry*, **1995** Sep 1, 270(35), 20278-20284.

111. Debarber A. E., Lutjohann D., Merkens L., Steiner R. D., Liquid chromatography-tandem mass spectrometry determination of plasma 24S-hydroxycholesterol with chromatographic separation of 25-hydroxycholesterol, *Analytical Biochemistry*, **2008** Oct 1, 381(1), 151-153.

112. Shan H., Pang J., Li S., Chiang T. B., Wilson W. K., Schroepfer G. J., Jr., Chromatographic behavior of oxygenated derivatives of cholesterol, *Steroids*, **2003** Mar, 68(3), 221-233.

113. Maxfield F. R., Tabas I., Role of cholesterol and lipid organization in disease, *Nature*, **2005** Dec 1, 438(7068), 612-621.

114. Liscum L., Cholesterol biosynthesis, In: Vance D. E.,Vance J. E., eds. *Biochemistry of Lipids, Lipoproteins, and Membranes*, Elsevier **2002**, 409 - 432.

115. Thompson G. R., Is good cholesterol always good?, *Bmj*, **2004** Aug 28, 329(7464), 471-472.

116. Clayton P. T., Disorders of cholesterol biosynthesis, *Archives of Disease in Childhood*, **1998** Feb, 78(2), 185-189.

117. Griffiths W. J., Why stereodomics in brain?, *European Journal of Lipid Science and Technology*, **2006**, 108, 707-708.

118. Tint G. S., Batta A. K., Xu G., Shefer S., Honda A., Irons M., Elias E. R., Salen G., The Smith-Lemli-Opitz syndrome: a potentially fatal birth defect caused by a block in the last enzymatic step in cholesterol biosynthesis, *Subcellular Biochemistry*, **1997**, 28, 117-144.

119. Dallaire L., Mitchell G., Giguere R., Lefebvre F., Melancon S. B., Lambert M., Prenatal-Diagnosis of Smith-Lemli-Opitz Syndrome Is Possible by Measurement of 7-Dehydrocholesterol in Amniotic-Fluid, *Prenatal diagnosis*, **1995** Sep, 15(9), 855-858.

120. Christenson L. K., Strauss Iii J. F., Cholesterol Metabolism in Steroidogenic Tissues, In: Mason J. I., ed. *Genetics of Steroid Biosynthesis and Function*, CRC Press, **2002**, 115 - 145.

121. Gill S., Chow R., Brown A. J., Sterol regulators of cholesterol homeostasis and beyond: The oxysterol hypothesis revisited and revised, *Progress in Lipid Research*, **2008** Nov, 47(6), 391-404.

122. Javitt N. B., Oxysterols: Novel biologic roles for the 21st century, *Steroids*, **2008** Feb, 73(2), 149-157.

123. Russell D. W., 50 years of advances in bile acid synthesis and metabolism, *Journal of Lipid Research*, **2008** Sep 24.

124. Russell D. W., The enzymes, regulation, and genetics of bile acid synthesis, *Annual review of biochemistry*, **2003**, 72, 137-174.

125. Griffiths W., Wang Y., Modern methods of bile acid analysis by mass spectrometry: a view into the metabolome, *Current Analytical Chemistry*, **2007**, 3, 103 -126

126. Brown A. J., Jessup W., Oxysterols and atherosclerosis, *Atherosclerosis*, **1999** Jan, 142(1), 1-28.

127. Bjorkhem I., Meaney S., Diczfalusy U., Oxysterols in human circulation: which role do they have?, *Current opinion in lipidology*, **2002** Jun, 13(3), 247-253.

128. Smith L. L., *Cholesterol autoxidation*, New York: Plenum Press **1981**.

129. Russell D. W., Oxysterol biosynthetic enzymes, *Biochimica et biophysica acta*, **2000** Dec 15, 1529(1-3), 126-135.

130. Bjorkhem I., Heverin M., Leoni V., Meaney S., Diczfalusy U., Oxysterols and Alzheimer's disease, *Acta Neurologica Scandinavica*, **2006**, 114, 43-49.

131. Wentworth P., Mcdunn J. E., Wentworth A. D., Takeuchi C., Nieva J., Jones T., Bautista C., Ruedi J. M., Gutierrez A., Janda K. D., Babior B. M., Eschenmoser A., Lerner R. A., Evidence for antibody-catalyzed ozone formation in bacterial killing and inflammation, *Science*, **2002** Dec 13, 298(5601), 2195-2199.

132. Pulfer M. K., Harrison K., Murphy R. C., Direct electrospray tandem mass spectrometry of the unstable hydroperoxy bishemiacetal product derived from cholesterol ozonolysis, *Journal of The American Society for Mass Spectrometry*, **2004** Feb, 15(2), 194-202.

133. Pulfer M. K., Murphy R. C., Formation of biologically active oxysterols during ozonolysis of cholesterol present in lung surfactant, *Journal of Biological Chemistry*, **2004** Jun 18, 279(25), 26331-26338.

134. Pulfer M. K., Taube C., Gelfand E., Murphy R. C., Ozone exposure in vivo and formation of biologically active oxysterols in the lung, *Journal of Pharmacology and Experimental Therapeutics*, **2005** Jan, 312(1), 256-264.

135. Wentworth P., Nieva J., Takeuchi C., Galve R., Wentworth A. D., Dilley R. B., Delaria G. A., Saven A., Babior B. M., Janda K. D., Eschenmoser A., Lerner R. A., Evidence for ozone formation in human atherosclerotic arteries, *Science*, **2003** Nov 7, 302(5647), 1053-1056.

136. Wang K., Bermudez E., Pryor W. A., The ozonation of cholesterol: separation and identification of 2,4-dinitrophenylhydrazine derivatization products of 3 beta-hydroxy-5-oxo-5,6-secocholestan-6-al, *Steroids*, **1993** May, 58(5), 225-229.

137. Smith L. L., Oxygen, oxysterols, ouabain, and ozone: A cautionary tale, *Free Radical Biology and Medicine*, **2004** Aug 1, 37(3), 318-324.

138. Kandutsch A. A., Chen H. W., Heiniger H. J., Biological activity of some oxygenated sterols, *Science*, **1978** Aug 11, 201(4355), 498-501.

139. Goldstein J. L., Debose-Boyd R. A., Brown M. S., Protein sensors for membrane sterols, *Cell*, **2006** Jan 13, 124(1), 35-46.

140. Horton J. D., Goldstein J. L., Brown M. S., SREBPs: activators of the complete program of cholesterol and fatty acid synthesis in the liver, *Journal of Clinical Investigation*, **2002** May, 109(9), 1125-1131.

141. Chawla A., Repa J. J., Evans R. M., Mangelsdorf D. J., Nuclear receptors and lipid physiology: Opening the X-files, *Science*, **2001** Nov 30, 294(5548), 1866-1870.

142. Janowski B. A., Willy P. J., Devi T. R., Falck J. R., Mangelsdorf D. J., An oxysterol signalling pathway mediated by the nuclear receptor LXR alpha, *Nature*, **1996** Oct 24, 383(6602), 728-731.

143. Wang Y. Q., Muneton S., Sjovall J., Jovanovic J. N., Griffiths W. J., The effect of 24S-hydroxycholesterol on cholesterol homeostasis in neurons: Quantitative changes to the cortical neuron proteome, *Journal of Proteome Research*, **2008** Apr, 7(4), 1606-1614.

144. Radhakrishnan A., Sun L. P., Kwon H. J., Brown M. S., Goldstein J. L., Direct binding of cholesterol to the purified membrane region of SCAP: Mechanism for a sterol-sensing domain, *Molecular Cell*, **2004** Jul 23, 15(2), 259-268.

145. Adams C. M., Reitz J., De Brabander J. K., Feramisco J. D., Li L., Brown M. S., Goldstein J. L., Cholesterol and 25-hydroxycholesterol inhibit activation of SREBPs by different mechanisms, both involving SCAP and Insigs, *Journal of Biological Chemistry*, **2004** Dec 10, 279(50), 52772-52780.

146. Song B. L., Javitt N. B., Debose-Boyd R. A., Insig-mediated degradation of HMG CoA reductase stimulated by lanosterol, an intermediate in the synthesis of cholesterol, *Cell Metabolism*, **2005** Mar, 1(3), 179-189.

147. Millatt L. J., Bocher V., Fruchart J. C., Staels B., Liver X receptors and the control of cholesterol homeostasis: potential therapeutic targets for the treatment of atherosclerosis, *Biochimica et biophysica acta*, **2003** Mar 17, 1631(2), 107-118.

148. Pfrieger F. W., Cholesterol homeostasis and function in neurons of the central nervous system, *Cellular and Molecular Life Sciences*, **2003** Jun, 60(6), 1158-1171.

149. Meaney S., Heverin M., Panzenboeck U., Ekstrom L., Axelsson M., Andersson U., Diczfalusy U., Pikuleva I., Wahren J., Sattler W., Bjorkhem I., Novel route for elimination of brain oxysterols across the blood-brain barrier: conversion into 7 alpha-hydroxy-3-oxo-4-cholestenoic acid, *Journal of Lipid Research*, **2007** Apr, 48(4), 944-951.

150. Xie C. L., Lund E. G., Turley S. D., Russell D. W., Dietschy J. M., Quantitation of two pathways for cholesterol excretion from the brain in normal mice and mice with neurodegeneration, *Journal of Lipid Research*, **2003** Sep, 44(9), 1780-1789.

151. Bjorkhem I., Crossing the barrier: oxysterols as cholesterol transporters and metabolic modulators in the brain, *Journal of Internal Medicine*, **2006** Dec, 260(6), 493-508.

152. Leoni V., Masterman T., Patel P., Meaney S., Diczfalusy U., Bjorkhem I., Side chain oxidized oxysterols in cerebrospinal fluid and the integrity of blood-brain and blood-cerebrospinal fluid barriers, *Journal of Lipid Research*, **2003** Apr, 44(4), 793-799.

153. Bjorkhem I., Diczfalusy U., 24(S),25-epoxycholesterol - A potential friend, *Arteriosclerosis Thrombosis and Vascular Biology*, **2004** Dec, 24(12), 2209-2210.

154. Zhang J., Akwa Y., Baulieu E. E., Sjovall J., 7-Alpha-Hydroxylation of 27-Hydroxycholesterol in Rat-Brain Microsomes, *Comptes Rendus De L Academie Des Sciences Serie Iii-Sciences De La Vie-Life Sciences*, **1995** Mar, 318(3), 345-349.

155. Zhang J., Larsson O., Sjovall J., 7-Alpha-Hydroxylation of 25-Hydroxycholesterol and 27-Hydroxycholesterol in Human Fibroblasts, *Biochimica Et Biophysica Acta-Lipids and Lipid Metabolism*, **1995** Jun 6, 1256(3), 353-359.

156. Mano N., Goto T., Uchida M., Nishimura K., Ando M., Kobayashi N., Goto J., Presence of protein-bound unconjugated bile acids in the cytoplasmic fraction of rat brain, *Journal of Lipid Research*, **2004** Feb, 45(2), 295-300.

157. Lin Y. Y., Welch M., Lieberman S., The detection of 20(S)-hydroxycholesterol in extracts of rat brains and human placenta by a gas chromatograph/mass spectrometry technique, *Journal of Steroid Biochemistry and Molecular Biology*, **2003** May, 85(1), 57-61.

158. Yao Z. X., Brown R. C., Teper G., Greeson J., Papadopoulos V., 22R-hydroxycholesterol protects neuronal cells from beta-amyloid-induced cytotoxicity by binding to beta-amyloid peptide, *Journal of Neurochemistry*, **2002** Dec, 83(5), 1110-1119.

159. Kudo K., Emmons G. T., Casserly E. W., Via D. P., Smith L. C., Pyrek J. S., Schroepfer G. J., Inhibitors of Sterol Synthesis - Chromatography of Acetate Derivatives of Oxygenated Sterols, *Journal of Lipid Research*, **1989** Jul, 30(7), 1097-1111.

160. Wong J., Quinn C. M., Guillemin G., Brown A. J., Primary human astrocytes produce 24(S),25-epoxycholesterol with implications for brain cholesterol homeostasis, *Journal of Neurochemistry*, **2007** Dec, 103(5), 1764-1773.

161. Wong J., Quinn C. M., Gelissen I. C., Brown A. J., Endogenous 24(S),25-epoxycholesterol fine-tunes acute control of cellular cholesterol homeostasis, *Journal of Biological Chemistry*, **2008** Jan 11, 283(2), 700-707.

162. Griffiths W. J., Tandem mass spectrometry in the study of fatty acids, bile acids, and steroids, *Mass Spectrometry Review*, **2003** Mar-Apr, 22(2), 81-152.

163. Liu S., Sjovall J., Griffiths W. J., Analysis of oxosteroids by nano-electrospray mass spectrometry of their oximes, *Rapid Communication Mass Spectrometry*, **2000**, 14(6), 390-400.

164. Lund E. G., Xie C. L., Kotti T., Turley S. D., Dietschy J. M., Russell D. W., Knockout of the cholesterol 24-hydroxylase gene in mice reveals a brain-specific mechanism of cholesterol turnover, *Journal of Biological Chemistry*, **2003** Jun 20, 278(25), 22980-22988.

165. Lutjohann D., Cholesterol metabolism in the brain: importance of 24S-hydroxylation, *Acta Neurologica Scandinavica*, **2006**, 114, 33-42.

166. Maclachlan J., Wotherspoon A. T. L., Ansell R. O., Brooks C. J. W., Cholesterol oxidase: sources, physical properties and analytical applications, *Journal of Steroid Biochemistry and Molecular Biology*, **2000** Apr, 72(5), 169-195.

167. Khan M. A., Wang Y., Heidelberger S., Alvelius G., Liu S., Sjovall J., Griffiths W. J., Analysis of derivatised steroids by matrix-assisted laser desorption/ionisation and post-source decay mass spectrometry, *Steroids*, **2006** Jan, 71(1), 42-53.

168. Myant N. B., *The biology of cholesterol and related steroids*, London, England: Heinemann Medical Books, **1981**.

169. Lane C. S., *The analysis of cytochrome P450 proteins by mass spectrometry,* The School of Pharmacy, University of London, London: PhD thesis, **2004**.

170. Smith L. L., Cholesterol Autoxidation 1981-1986, *Chemistry and Physics of Lipids*, **1987** Jul-Sep, 44(2-4), 87-125.

171. Murphy R. C., Johnson K. M., Cholesterol, reactive oxygen species, and the formation of biologically active mediators, *The Journal of biological chemistry*, **2008** Jun 6, 283(23), 15521-15525.

172. Smith W. L., Murphy R. C., Oxidized lipids formed non-enzymatically by reactive oxygen species, *The Journal of biological chemistry*, **2008** Jun 6, 283(23), 15513-15514.

173. Ansari G. A. S., Smith L. L., High-performance liquid chromatography of cholesterol autoxidation products *Journal of Chromatography*, **1979**, 175, 307 - 315.

174. Ansari G. A. S., Smith L. L., Assay of Cholesterol Autoxidation, *Oxygen Radicals in Biological Systems, Pt C*, **1994**, 233, 332-338.

175. Shoda J., Axelson M., Sjovall J., Synthesis of potential C27-intermediates in bile acid biosynthesis and their deuterium-labeled analogs, *Steroids*, **1993** Mar, 58(3), 119-125.

176. Toll A., Shoda J., Axelson M., Sjovall J., Wikvall K., 7 alpha-hydroxylation of 26-hydroxycholesterol, 3 beta-hydroxy-5-cholestenoic acid and 3 beta-hydroxy-5-cholenoic acid by cytochrome P-450 in pig liver microsomes, *FEBS Lett*, **1992** Jan 13, 296(1), 73-76.

177. Griffiths W. J., Liu S. Y., Yang Y., Purdy R. H., Sjovall J., Nano-electrospray tandem mass spectrometry for the analysis of neurosteroid sulphates, *Rapid Communications in Mass Spectrometry*, **1999**, 13(15), 1595-1610.

178. Heverin M., Bogdanovic N., Lutjohann D., Bayer T., Pikuleva I., Bretillon L., Diczfalusy U., Winblad B., Bjorkhem I., Changes in the levels of cerebral and extracerebral sterols in the brain of patients with Alzheimer's disease, *Journal of Lipid Research*, **2004** Jan, 45(1), 186-193.

179. Lutjohann D., Breuer O., Ahlborg G., Nennesmo I., Siden A., Diczfalusy U., Bjorkhem I., Cholesterol homeostasis in human brain: Evidence for an age-dependent flux of 24S-hydroxycholesterol from the brain into the circulation, *Proceedings of the National Academy of Sciences of the United States of America*, **1996** Sep 3, 93(18), 9799-9804.

180. Lund E. G., Guileyardo J. M., Russell D. W., cDNA cloning of cholesterol 24-hydroxylase, a mediator of cholesterol homeostasis in the brain, *Proceedings of the National Academy of Sciences of the United States of America*, **1999** Jun 22, 96(13), 7238-7243.

181. Wasilchuk B. A., Lequesne P. W., Vouros P., Monitoring Cholesterol Autoxidation Processes Using Multideuteriated Cholesterol, *Analytical Chemistry*, **1992** May 15, 64(10), 1077-1087.

182. Edmond J., Korsak R. A., Morrow J. W., Torokboth G., Catlin D. H., Dietary-Cholesterol and the Origin of Cholesterol in the Brain of Developing Rats, *Journal of Nutrition*, **1991** Sep, 121(9), 1323-1330.

183. Dietschy J. M., Turley S. D., Cholesterol metabolism in the brain, *Current opinion in lipidology*, **2001** Apr, 12(2), 105-112.

184. Fu X., Menke J. G., Chen Y., Zhou G., Macnaul K. L., Wright S. D., Sparrow C. P., Lund E. G., 27-hydroxycholesterol is an endogenous ligand for liver X receptor in cholesterol-loaded cells, *The Journal of biological chemistry*, **2001** Oct 19, 276(42), 38378-38387.

185. Lutjohann D., Brzezinka A., Barth E., Abramowski D., Staufenbiel M., Von Bergmann K., Beyreuther K., Multhaup G., Bayer T. A., Profile of cholesterol-related sterols in aged amyloid precursor protein transgenic mouse brain, *Journal of Lipid Research*, **2002** Jul, 43(7), 1078-1085.

186. Rose K., Allan A., Gauldie S., Stapleton G., Dobbie L., Dott K., Martin C., Wang L., Hedlund E., Seckl J. R., Gustafsson J. A., Lathe R., Neurosteroid hydroxylase CYP7B: vivid reporter activity in dentate gyrus of gene-targeted mice and abolition of a widespread pathway of steroid and oxysterol hydroxylation, *The Journal of biological chemistry*, **2001** Jun 29, 276(26), 23937-23944.

187. Stapleton G., Steel M., Richardson M., Mason J. O., Rose K. A., Morris R. G., Lathe R., A novel cytochrome P450 expressed primarily in brain, *The Journal of biological chemistry*, **1995** Dec 15, 270(50), 29739-29745.

188. Dorzewska J. A.-G., Z. , Patterns of free and esterified sterol fractions of the cerebral white matter in severe and moderate experimental hypoxia, *Medical Science Monitor*, **2000**, 6(2), 73 - 80

189. Wender M., Adamczewskagoncerzewicz Z., Doroszewska J., Transformation of Sterols Pattern in Course of Late Development of Rat-Brain, *Folia Neuropathologica*, **1995**, 33(1), 31-34.

190. Miyajima H., Adachi J., Kohno S., Takahashi Y., Ueno Y., Naito T., Increased oxysterols associated with iron accumulation in the brains and visceral organs of acaeruloplasminaemia patients, *Qjm*, **2001** Aug, 94(8), 417-422.

191. Dhar A. K., Teng J. I., Smith L. L., Sterol Metabolism .19. Biosynthesis of Cholest-5-Ene-3beta, 24-Diol (Cerebrosterol) by Bovine Cerebral Cortical Microsomes, *Journal of Neurochemistry*, **1973**, 21(1), 51-60.

192. Meaney S., Babiker A., Lutjohann D., Diczfalusy U., Axelson M., Bjorkhem I., On the origin of the cholestenoic acids in human circulation, *Steroids*, **2003** Sep, 68(7-8), 595-601.

193. Lutjohann D., Bjorkhem I., Locatelli S., Dame C., Schmolling J., Von Bergmann K., Fahnenstich H., Cholesterol dynamics in the foetal and neonatal brain as reflected by circulatory levels of 24S-hydroxycholesterol, *Acta Paediatrica*, **2001** Jun, 90(6), 652-657.

194. Quan G., Xie C. L., Dietschy J. M., Turley S. D., Ontogenesis and regulation of cholesterol metabolism in the central nervous system of the mouse, *Developmental Brain Research*, **2003** Dec 19, 146(1-2), 87-98.

195. Heverin M., Meaney S., Lutjohann D., Diczfalusy U., Wahren J., Bjorkhem I., Crossing the barrier: net flux of 27-hydroxycholesterol into the human brain, *Journal of Lipid Research*, **2005** May, 46(5), 1047-1052.

196. Tint G. S., Yu H. W., Shang Q., Xu G. R., Patel S. B., The use of the Dhcr7 knockout mouse to accurately determine the origin of fetal sterols, *Journal of Lipid Research*, **2006** Jul, 47(7), 1535-1541.

197. Jurevics H. A., Kidwai F. Z., Morell P., Sources of cholesterol during development of the rat fetus and fetal organs, *Journal of Lipid Research*, **1997** Apr, 38(4), 723-733.

198. Ohyama Y., Meaney S., Heverin M., Ekstrom L., Brafman A., Shafir M., Andersson U., Olin M., Eggertsen G., Diczfalusy U., Feinstein E., Bjorkhem I., Studies on the transcriptional regulation of cholesterol 24-hydroxylase (CYP46A1) - Marked insensitivity toward different regulatory axes, *Journal of Biological Chemistry*, **2006** Feb 17, 281(7), 3810-3820.

199. Wang L., Schuster G. U., Hultenby K., Zhang Q., Andersson S., Gustafsson J. A., Liver X receptors in the central nervous system: from lipid homeostasis to neuronal degeneration, *Proceedings of the National Academy of Sciences of the United States of America*, **2002** Oct 15, 99(21), 13878-13883.

200. Elias E. R., Irons M., Abnormal cholesterol metabolism in Smith-Lemli-Opitz syndrome, *Current opinion in pediatrics*, **1995** Dec, 7(6), 710-714.

201. Irons M., Elias E. R., Tint G. S., Salen G., Frieden R., Buie T. M., Ampola M., Abnormal Cholesterol-Metabolism in the Smith-Lemli-Opitz Syndrome - Report of Clinical and Biochemical Findings in 4 Patients and Treatment in One Patient, *American Journal of Medical Genetics*, **1994** May 1, 50(4), 347-352.

202. Kelley R. I., Diagnosis of Smith-Lemli-Opitz Syndrome by Gas-Chromatography Mass-Spectrometry of 7-Dehydrocholesterol in Plasma, Amniotic-Fluid and Cultured Skin Fibroblasts, *Clinica Chimica Acta*, **1995** Apr 30, 236(1), 45-58.

203. Salen G., Shefer S., Batta A. K., Tint G. S., Xu G., Honda A., Irons M., Elias E. R., Abnormal cholesterol biosynthesis in the Smith-Lemli-Opitz syndrome, *Journal of Lipid Research*, **1996** Jun, 37(6), 1169-1180.

204. Irons M., Elias E. R., Salen G., Tint G. S., Batta A. K., Defective cholesterol biosynthesis in Smith-Lemli-Opitz syndrome, *Lancet*, **1993** May 29, 341(8857), 1414.

205. Batta A. K., Tint G. S., Shefer S., Abuelo D., Salen G., Identification of 8-Dehydrocholesterol (Cholesta-5,8-Dien-3-Beta-Ol) in Patients with Smith-Lemli-Opitz Syndrome, *Journal of Lipid Research*, **1995** Apr, 36(4), 705-713.

206. Irons M. B., Tint G. S., Prenatal diagnosis of Smith-Lemli-Opitz syndrome, *Prenatal diagnosis*, **1998** Apr, 18(4), 369-372.

207. Sharp P., Haan E., Fletcher J. M., Khong T. Y., Carey W. F., First-trimester diagnosis of Smith-Lemli-Opitz syndrome, *Prenatal diagnosis*, **1997** Apr, 17(4), 355-361.

208. Tint G. S., Salen G., Batta A. K., Shefer S., Irons M., Ampola M., Frieden R., Abnormal Cholesterol and Bile-Acid Synthesis in an Infant with a Defect in 7dehydrocholesterol(7dhc)-Delta-7 Reductase, *Gastroenterology*, **1993** Apr, 104(4), A1008-A1008.

209. Chevy F., Humbert L., Wolf C., Sterol profiling of amniotic fluid: a routine method for the detection of distal cholesterol synthesis deficit, *Prenatal diagnosis*, **2005** Nov, 25(11), 1000-1006.

210. Tint G. S. I., M. Elias, E. R. Batta, A. K. Frieden, R. Chen, T. S. Salen, G. , Defective cholesterol biosynthesis associated with the Smith-Lemli-Opitz syndrome, *The New England Journal of Medicine*, **1994**, 330, 369 - 372.

211. Abuelo D. N., Tint G. S., Kelley R., Batta A. K., Shefer S., Salen G., Prenatal Detection of the Cholesterol Biosynthetic Defect in the Smith-Lemli-Opitz Syndrome by the Analysis of Amniotic Liquid Sterols, *American Journal of Medical Genetics*, **1995** Apr 10, 56(3), 281-285.

212. Tint G. S., Abuelo D., Till M., Cordier M. P., Batta A. K., Shefer S., Honda A., Honda M., Xu G. R., Irons M., Elias E. R., Salen G., Fetal Smith-Lemli-Opitz syndrome can be detected accurately and reliably by measuring amniotic fluid dehydrocholesterols, *Prenatal diagnosis*, **1998** Jul, 18(7), 651-658.

213. Zimmerman P. A., Hercules D. M., Naylor E. W., Direct analysis of filter paper blood specimens for identification of Smith-Lemli-Opitz syndrome using time-of-flight secondary ion mass spectrometry, *American Journal of Medical Genetics*, **1997** Jan 31, 68(3), 300-304.

214. Seedorf U., Fobker M., Voss R., Meyer K., Kannenberg F., Meschede D., Ullrich K., Horst J., Benninghoven A., Assmann G., Smith-Lemli-Opitz Syndrome Diagnosed by Using Time-of-Flight Secondary-Ion Mass-Spectrometry, *Clinical Chemistry*, **1995** Apr, 41(4), 548-552.

Appendix A Publications

1. Y. Wang, K. M. Sousa, K. Bodin, S.Theofilopoulos, P.Sacchetti, M. Hornshaw, G. Woffendin, K. Karu, J. Sjövall, E. Arenas, W. J. Griffiths, Oxysterols in the Embryonic Central Nervous System: A Targeted Lipidomic Study, *Molecular Biology Systems, in preparation.*
2. W. J. Griffiths, Y. Wang, K. Karu, E. Samuel, S. McDonnell, M. Hornshaw, C. Shackleton, Potential of sterol analysis by liquid chromatography - tandem mass spectrometry for the prenatal diagnosis of Smith-Lemli-Opitz syndrome, *Clinical Chemistry,* August 2008, Vol. 54, Issue 7, 1317-1324.
3. K. Karu, M. Hornshaw, G. Woffendin, K. Bodin, M. Hamberg, G. Alvelius, J. Sjövall, J. Turton, Y. Wang and W.J. Griffiths, Liquid Chromatography Combined with Mass Spectrometry Utilising High-Resolution, Exact Mass, and Multi-Stage Fragmentation for the Identification of Oxysterols in Rat Brain, *Journal of Lipid Research*, April 2007, Vol. 48, Issue 4, 976- 987.
4. W.J. Griffiths, K. Karu, M. Hornshaw, G. Woffendin, Y. Wang, Metabolomics and metabolite profiling: past heroes and future developments, *European Journal Mass Spectrometry*, 2007, 13, 45-50.
5. Y. Wang, K. Karu and W. J. Griffiths, Analysis of neurosterols and neurosteroids by mass spectrometry, *Biochemie*, February 2007, Vol. 89, Issue 2, 182-191.
6. M. Harrison, M. Hornshaw, K. Karu, J. Sjöval, Y. Wang, W. J. Griffiths, High Resolution and High Mass Accuracy in the Study of Oxysterols present in Cortical Neurons, In: '*Abstracts of the 17th IMSC 2006 International Mass Spectrometry Meeting of the International Mass Spectrometry Society*', p. 86, Prague, Czech Republic, September 2006.
7. K. Karu, G. Alvelius, K. Bodin, J. Sjövall, Y. Wang, W. J. Griffiths, Capillary-LC-MS^n for the Analysis of Oxysterols Brain, '*Abstracts of the 17th IMSC 2006 International Mass*

Spectrometry Meeting of the International Mass Spectrometry Society', p 87, Prague, Czech Republic, September 2006.

8. S. Heilderberger, K. Karu, Y. Wang, W. J. Grifffiths, Proteomics Strategies for the Analysis of Proteins involved in Steroid Synthesis, Metabolism and Transport, '*Abstracts of the 17th IMSC 2006 International Mass Spectrometry Meeting of the International Mass Spectrometry Society*', p 81, Prague, Czech Republic, September 2006.
9. K. Karu, W. J. Griffiths, Analysis of oxysterols in rat brain utilising capillary LC tandem mass spectrometry, In: *'Abstracts of the 28th Annual Meeting of the British Mass Spectrometry Society*', p 201, University of York, September 2005.
10. K. Karu, W. J. Griffiths, L. H. Patterson, The metabolism of DesCI MI: a potential anticancer prodrug, In: *'Abstracts of the 28th Annual Meeting of the British Mass Spectrometry Society*', p 199, University of York, September 2005.
11. C. Lane, K. Karu, C. Seibert, W.J. Griffiths, L.H. Patterson, 2005, *Molecular Cell Proteomics*, 4, (Suppl. 8), 5481.
12. N. Ortuzar Kerr, S. S. Grewel, B. Garcia-Ochoa Martin, K. Karu, L. H. Patterson, M. Searcey, Design and synthesis of bio-oxidatively activated prodrugs based upon the duocarmycins: Routes to Boc-CI and CI-MI prodrugs, *229th ACS National Meeting*, San Diego, CA, March 13-15, 2005, Abstract.
13. M. Searcey, K. Karu, S. S. Grewal, N. Ortuzar Kerr, W. Griffith, L. H. Patterson, Prodrug analogs of the duocarmycins activated by CYP-oxidation. *229th ACS National Meeting*, San Diego, CA, March 15-17, 2005, Abstract.
14. K. Karu, W. J. Griffiths, Differentiation of 2- and 4-hydroxy-estradiol by tandem mass spectrometry, In: '*Abstracts of the 27th Annual Meeting of the British Mass Spectrometry Society*', p. 152, University of Derby, September 2004.

Appendix B Accompanying CD

The accompanying CD contains data referred to in the text.

The data is available as Pdf.file and word.file

Chapters 2 and 3

Supplementary Material, Table 1. Sterols/oxysterols analysed in the present study.

Supplementary Material, Figures 1 to 40. The oxidised/GP-derivativased sterols/oxysterols analysed in this study.

Chapter 4

Supplementary Material, Figures S4.1 to S4.3.

Figure S4.1 (a) Base peak chromatogram of the oxidised/GP-derivatised cholestane-3β,5α,6β-triol. **(b & c)** MS^3 (534→455→) spectra of chromatographic peaks eluting at (b) 21.70 min, and (c) 22.90 min.

Figure S4.2 (a) RIC for oxidised/GP-derivatised oxysterol $[M]^+$ ions, *m/z* 541 (upper trace), *m/z* 534 (lower trace) from the rat brain. (b) MS^3 (516→437→) spectra of chromatographic peaks eluting at 25.01 min, and (c) MS^3 (523→444→) spectra of chromatographic peaks eluting at 25.31 min.

Chapter 5

Supplementary Material, Figures S5.1 to S5.3.

Figure S5.1 MS^3 (532→453→) spectra of chromatographic peaks eluting at 22.73 min and 22.99 min.

Figure S5.2 MS^3 (534→455→) spectrum of chromatographic peak eluting at 22.21 min.

Figure S5.3 MS^3 (534→455→) spectrum of chromatographic peak eluting at 21.96 min.